

THESIS

HYDRAULIC MODELING ANALYSIS OF THE MIDDLE RIO GRANDE
- ESCONDIDA REACH, NEW MEXICO

Submitted by

Amanda K. Larsen

Department of Civil Engineering

In partial fulfillment of the requirements

For the degree Master of Science

Colorado State University

Fort Collins, CO

Spring 2007

COLORADO STATE UNIVERSITY

February 21, 2007

WE HERBY RECOMMEND THAT THE THESIS PREPARED UNDER OUR SUPERVISION BY AMANDA KELLI LARSEN ENTITLED **HYDRAULIC MODELING ANALYSIS OF THE MIDDLE RIO GRANDE – ESCONDIDA REACH, NEW MEXICO** BE ACCEPTED AS FULFILLING IN PART REQUIREMENTS FOR THE DEGREE OF MASTER OF SCIENCE.

Committee on Graduate Work

Advisor

Department Head

ABSTRACT OF THESIS

HYDRAULIC MODELING ANALYSIS OF THE MIDDLE RIO GRANDE - ESCONDIDA REACH, NEW MEXICO

Human influence on the Middle Rio Grande has resulted in major changes throughout the Middle Rio Grande region in central New Mexico, including problems with erosion and sedimentation. Hydraulic modeling analyses have been performed on the Middle Rio Grande to determine changes in channel morphology and other important parameters. Important changes occurring in the Escondida reach between 1918 and 2005 were analyzed for this study.

The Escondida reach covers 17.7 miles from the Escondida Bridge to the US Highway 380 Bridge. Spatial and temporal trends in channel geometry, discharge, and sediment have been analyzed. In addition, historic bedform data were analyzed and potential equilibrium conditions were predicted. This study will help facilitate better management of restoration, irrigation, and flood protection efforts.

Aerial photographs, GIS active channel planforms, cross-section surveys, hydraulic model analysis and channel classification methods were used to analyze spatial and temporal trends in channel geometry and morphology. Narrowing of the channel was observed from GIS active channel planforms between 1918 and 2005, with the upstream section of the channel showing the greatest narrowing. Fluctuations were observed in nearly all channel geometry properties. These fluctuations may be caused by a complex

response to past channel changes. In addition, the mean bed grain diameter increased slightly from 0.15 mm to 0.31 mm between 1962 and 2002.

Field observations of bedforms were compiled and compared to the bedforms predicted by van Rijn and by Simons and Richardson. Both methods produced acceptable results, but a large amount of scatter was observed in the data. Wide variability across a single cross section may be the source of the scatter.

Analyses of trends in sediment and water discharge shows a dry period between 1949 and 1979, a wet period between 1979 and 2000, and a dry period between 2000 and 2005. By contrast, the mean daily suspended sediment discharge remained nearly constant. Difference mass curves showed aggradation and degradation that approximately correlated with changes in mean bed elevation.

A variety of approaches were used to predict future equilibrium width and slope conditions. The approaches used include hydraulic geometry equations, hyperbolic and exponential regressions, stable channel geometry, and sediment transport relationships. Several methods predicted an equilibrium width around 300 ft, and Julien-Wargadalam and SAM analysis predicted equilibrium slopes between 0.00065 and 0.00139. Both the equilibrium slope and width predictions seem to provide reasonable estimates of future conditions.

Amanda K. Larsen
Department of Civil Engineering
Colorado State University
Fort Collins, CO 80523
Spring 2007

ACKNOWLEDGEMENTS

I would first like to thank the U.S. Bureau of Reclamation in Albuquerque for providing me with this project. I would especially like to thank Robert Padilla, Tamera Massong, and Drew Baird for their insights about the river and for the wonderful field visit. Thanks also to my advisor, Dr. Pierre Julien for his guidance and support throughout the project.

Many, many thanks to Seema for believing in me from beginning to end. Thank you for your patience and understanding, and thank you for helping me get acquainted with CSU and Fort Collins. I don't know what I would have done without you! Also, thanks to the YABS for being my weekly retreat from the academic world. Your support and friendship have been very important.

Finally, thank you to my family. Mom and Dad, you have always known that I can do whatever I put my mind to. Thank you for encouraging me to follow my dreams and giving me the love and support I needed to take the first steps. Matthew, thanks for being the best little brother I could have asked for. You always make me smile, and you remind me that I shouldn't take life too seriously. Dale, Kathy and Hannah, I am so thankful that I have gotten to spend the last year with you. Thank you for giving me a place to go when I needed to get away. Chris, thank you for your unconditional love. Thank you for the hours on the phone talking, the many visits, and for all your help with the wedding. I love you and can't wait to be your wife.

TABLE OF CONTENTS

ABSTRACT OF THESIS.....	iii
ACKNOWLEDGEMENTS.....	v
TABLE OF CONTENTS.....	vi
LIST OF FIGURES.....	ix
LIST OF TABLES.....	xiv
LIST OF SYMBOLS.....	xvi
CHAPTER 1: INTRODUCTION.....	1
CHAPTER 2: LITERATURE REVIEW.....	4
2.1 REACH DESCRIPTION.....	4
2.2 MIDDLE RIO GRANDE HISTORY.....	6
2.3 HYDROLOGY, GEOLOGY AND CLIMATE OF THE MIDDLE RIO GRANDE.....	8
2.4 PREVIOUS STUDIES OF THE MIDDLE RIO GRANDE.....	9
2.5 PLANFORM CLASSIFICATION METHODS.....	13
2.6 BEDFORM CLASSIFICATION METHODS.....	15
CHAPTER 3: GEOMORPHIC CHARACTERIZATION.....	16
3.1 SITE DESCRIPTION AND BACKGROUND.....	16
3.1.1 <i>Subreach Definition</i>	20
3.1.2 <i>Available Data</i>	22
Water and Suspended Sediment Data.....	22
Bed Material.....	24
Survey Lines and Dates.....	24
3.1.3 <i>Channel Forming Discharge</i>	28
Effective Flow.....	28
Recurrence Interval.....	29
Bankfull Measurements.....	32
3.2 CLASSIFICATION, LONGITUDINAL PROFILE, CHANNEL GEOMETRY AND SEDIMENT.....	32
3.2.1 <i>Channel Planform Methods</i>	32
Slope-Discharge Methods.....	33
Channel Morphology Methods.....	35
Stream Power Methods.....	36
3.2.2 <i>Channel Planform Results</i>	37
3.2.3 <i>Sinuosity Methods</i>	46
3.2.4 <i>Sinuosity Results</i>	46
3.2.5 <i>Longitudinal Profile Methods</i>	48

Thalweg Elevation.....	48
Mean Bed Elevation.....	48
Energy Grade Slope.....	49
Water Surface Slope.....	49
3.2.6 <i>Longitudinal Profile Results</i>	50
Thalweg Elevation.....	50
Mean Bed Elevation.....	53
Energy Grade Slope.....	55
Water Surface Slope.....	56
3.2.7 <i>Channel Geometry Methods</i>	57
3.2.8 <i>Channel Geometry Results</i>	58
3.2.9 <i>Bend Migration Methods</i>	60
3.2.10 <i>Bend Migration Results</i>	60
3.2.11 <i>Bed Material Analysis Methods</i>	65
3.2.12 <i>Bed Material Analysis Results</i>	66
3.3 SUSPENDED SEDIMENT AND WATER HISTORY.....	68
3.3.1 <i>Methods</i>	68
3.3.2 <i>Results</i>	69
Single Mass Curves.....	69
Double Mass Curve.....	72
Difference Mass Curve.....	73
3.4 FLOODPLAIN ANALYSIS.....	74
3.4.1 <i>Methods</i>	75
3.4.2 <i>Results</i>	75
3.5 BEDFORM ANALYSIS.....	76
3.5.1 <i>Methods</i>	76
3.5.2 <i>Results</i>	80
3.6 SUMMARY.....	84
CHAPTER 4: EQUILIBRIUM STATE PREDICTORS.....	89
4.1 HYDRAULIC GEOMETRY.....	89
4.1.1 <i>Methods</i>	89
4.1.2 <i>Results</i>	95
4.2 WIDTH REGRESSION MODELS.....	99
4.2.1 <i>Method</i>	99
Hyperbolic Model.....	99
Exponential Model.....	100
4.2.2 <i>Results</i>	102
4.3 SEDIMENT TRANSPORT.....	105
4.3.1 <i>Methods</i>	105
4.3.2 <i>Results</i>	107
4.4 SAM.....	110
4.4.1 <i>Methods</i>	110
4.4.2 <i>Results</i>	111
4.5 SCHUMM'S (1969) RIVER METAMORPHOSIS MODEL.....	112
4.6 LANE'S (1955) BALANCE.....	114

4.7 SUMMARY.....	116
4.7.1 <i>Equilibrium Width</i>	116
4.7.2 <i>Equilibrium Slope</i>	117
CHAPTER 5: SUMMARY AND CONCLUSIONS.....	119
REFERENCES.....	122
APPENDIX A.....	126
APPENDIX B.....	144
APPENDIX C.....	146
APPENDIX D.....	180
APPENDIX E.....	185
APPENDIX F.....	197
APPENDIX G.....	206

LIST OF FIGURES

Figure 2.1 Location Map and Topographic Map of the Escondida Reach.....	5
Figure 2.2 Hydrograph for San Acacia and San Marcial Gauges.....	8
Figure 2.3 Location of Previous Studies.....	12
Figure 3.1 2005 Aerial Photo of Subreach 1.....	17
Figure 3.2 2005 Aerial Photo of Subreach 2.....	18
Figure 3.3 2005 Aerial Photo of Subreach 3.....	19
Figure 3.4 Subreach Definitions and Agg/Deg Location.....	21
Figure 3.5 Annual Suspended Sediment yield at San Acacia and San Marcial gauges..	23
Figure 3.6 Socorro Range Line Locations.....	27
Figure 3.7 Annual Peak Flow at San Acacia Gauge.....	30
Figure 3.8 Annual Peak Flow at San Marcial Gauge.....	30
Figure 3.9 Comparisons of Annual Peak Flows.....	31
Figure 3.10 Rosgen Channel Classification Key (Rosgen 1996).....	35
Figure 3.11 Chang's Stream Classification Method Diagram.....	37
Figure 3.12 Historical Planforms of Subreach 1.....	39
Figure 3.13 Historical Planforms of Subreach 2.....	40
Figure 3.14 Historical Planforms of Subreach 3.....	41
Figure 3.15 Sinuosity.....	47
Figure 3.16 Change in Thalweg Elevation by SO-line.....	51
Figure 3.17 Thalweg Elevation Profile.....	52
Figure 3.18 Reach Averaged Mean Bed Elevation.....	53
Figure 3.19 Change in Mean Bed Elevation Between 1962 and 1985.....	54

Figure 3.20 Change in Mean Bed Elevation Between 1985 and 2002.....	54
Figure 3.21 Energy Grade Line Slope.....	55
Figure 3.22 Water Surface Elevation Slope.....	56
Figure 3.23 Channel Geometry Properties.....	59
Figure 3.24 Bend Migration at Agg/Deg 1326.....	62
Figure 3.25 Bend Migration at Agg/Deg 1378-1386.....	63
Figure 3.26 Bend Migration at Agg/Deg 1419-1426.....	64
Figure 3.27 Grain Size Classification (Julien 1998).....	65
Figure 3.28 Bed Material Mean Grain Size.....	66
Figure 3.29 Bed Material Particle Size Distributions.....	67
Figure 3.30 Water Discharge Single Mass Curve.....	70
Figure 3.31 Suspended Sediment Discharge Single Mass Curve.....	71
Figure 3.32 Suspended Sediment Concentration Double Mass Curve.....	72
Figure 3.33 Suspended Sediment Difference Mass Curve.....	73
Figure 3.34 Top Width vs. Discharge for Agg/Deg 1406-1418.....	75
Figure 3.35 Top Width vs. Discharge for Agg/Deg 1456-1476.....	76
Figure 3.36 Bedform Classification by Simons and Richardson (from Julien 1998)....	77
Figure 3.37 Bedform Classification by van Rijn (1984, from Julien 1998).....	79
Figure 3.38 Observed Ripples Plotted on Graphs from Simons and Richardson (L) and van Rijn (R) (after Julien 1998).....	80
Figure 3.39 Observed Dunes Plotted on Graphs from Simons and Richardson (L) and van Rijn (R) (after Julien 1998).....	81
Figure 3.40 Observed Transition Bedforms Plotted on Graphs from Simons and Richardson (L) and van Rijn (R) (after Julien 1998)	81

Figure 3.41 Observed Antidunes/Plan Bed Plotted on Graphs from Simons and Richardson (L) and van Rijn (R) (after Julien 1998).....	82
Figure 3.42 Typical Cross-Section with Bedforms.....	83
Figure 4.1 Variation of Wetted Perimeter P with Discharge Q and Type of Channel (after Simons and Alberston 1963).....	91
Figure 4.2 Variation of Average Width W with Wetted Perimeter P (after Simons and Alberston 1963).....	91
Figure 4.3 Escondida Empirical Width-Discharge Relationships.....	98
Figure 4.4 Hyperbolic and Exponential Regressions – Subreach 1.....	102
Figure 4.5 Hyperbolic and Exponential Regressions – Subreach 2.....	102
Figure 4.6 Hyperbolic and Exponential Regressions – Subreach 3.....	103
Figure 4.7 Hyperbolic and Exponential Regressions – Total Reach.....	103
Figure 4.8 Total Load Rating Curves from BORAMEP and Psands.....	108
Figure 4.9 Results from SAM for 2002 conditions at $Q = 5000 \text{ cfs}$	111
Figure 4.10 Lane's Balance (1955).....	114
Figure A.1 Cross-section survey at SO-line 1313.....	128
Figure A.2 Cross-section survey at SO-line 1314.....	128
Figure A.3 Cross-section survey at SO-line 1316.....	129
Figure A.4 Cross-section survey at SO-line 1320.....	129
Figure A.5 Cross-section survey at SO-line 1327.....	130
Figure A.6 Cross-section survey at SO-line 1339.....	130
Figure A.7 Cross-section survey at SO-line 1342.5.....	131
Figure A.8 Cross-section survey at SO-line 1346.....	131
Figure A.9 Cross-section survey at SO-line 1349.....	132
Figure A.10 Cross-section survey at SO-line 1352.....	132

Figure A.11 Cross-section survey at SO-line 1360.....	133
Figure A.12 Cross-section survey at SO-line 1371.....	133
Figure A.13 Cross-section survey at SO-line 1380.....	134
Figure A.14 Cross-section survey at SO-line 1394.....	134
Figure A.15 Cross-section survey at SO-line 1396.5.....	135
Figure A.16 Cross-section survey at SO-line 1398.....	135
Figure A.17 Cross-section survey at SO-line 1401.....	136
Figure A.18 Cross-section survey at SO-line 1410.....	136
Figure A.19 Cross-section survey at SO-line 1414.....	137
Figure A.20 Cross-section survey at SO-line 1420.....	137
Figure A.21 Cross-section survey at SO-line 1428.....	138
Figure A.22 Cross-section survey at SO-line 1437.9.....	138
Figure A.23 Cross-section survey at SO-line 1443.....	139
Figure A.24 Cross-section survey at SO-line 1450.....	139
Figure A.25 Cross-section survey at SO-line 1456.....	140
Figure A.26 Cross-section survey at SO-line 1462.....	140
Figure A.27 Cross-section survey at SO-line 1464.5.....	141
Figure A.28 Cross-section survey at SO-line 1469.5.....	141
Figure A.29 Cross-section survey at SO-line 1470.5.....	142
Figure A.30 Cross-section survey at SO-line 1471.2.....	142
Figure A.31 Cross-section survey at SO-line 1472.....	143
Figure D.1 Bed Material Grain Size Distribution (subreach 1).....	181
Figure D.2 Bed Material Grain Size Distribution (subreach 2).....	182

Figure D.3 Bed Material Grain Size Distribution (subreach 3).....	183
Figure E.1 Field Notes for Example Cross-section (pg.1).....	186
Figure E.2 Field Notes for Example Cross-section (pg.2).....	187
Figure E.3 Field Notes for Example Cross-section (pg.3).....	188
Figure E.4 Cross-section 1380 (surveyed 9/12/1990, Q = 70 cfs).....	189
Figure E.5 Cross-section 1360 (surveyed 4/23/1991, Q = 2300 cfs).....	189
Figure E.6 Cross-section 11414 (surveyed 5/23/1992, Q = 3800 cfs).....	190
Figure E.7 Cross-section 1450 (surveyed 5/27/1993, Q = 5000 cfs).....	190

LIST OF TABLES

Table 3.1 Available Daily Discharge Data.....	22
Table 3.2 Available Suspended Sediment Data.....	23
Table 3.3 Available Bed Material Data at SO-Lines.....	24
Table 3.4 Socorro Range Line Survey Dates.....	26
Table 3.5 GeoTool Inputs.....	29
Table 3.6 Recurrence Interval.....	31
Table 3.7 Channel Classification Inputs.....	42
Table 3.8 Channel Classification Results.....	45
Table 3.9 Sinuosity Changes.....	47
Table 3.10 Bend Migration.....	61
Table 3.11 Bed Material Type.....	67
Table 3.12 Water Discharge.....	70
Table 3.13 Suspended Sediment Discharge.....	71
Table 3.14 Suspended Sediment Concentration.....	73
Table 3.15 Channel Geometry Changes.....	86
Table 4.1 Hydraulic Geometry Calculation Inputs.....	94
Table 4.2 Escondida Empirical Width-Discharge Inputs.....	95
Table 4.3 Predicted Equilibrium Widths from Hydraulic Geometry Equations with Q = 5000 cfs.....	96
Table 4.4 Equilibrium Slope Predictions with Q = 5000 cfs.....	97
Table 4.5 Escondida Empirical Width-Discharge Results.....	98
Table 4.6 Hyperbolic and Exponential Regression Input.....	101
Table 4.7 Hyperbolic Regression Equations and Predicted Widths.....	104

Table 4.8 Exponential Regression Equations and Predicted Widths.....	105
Table 4.9 Total Load and Bed Load Calculations.....	107
Table 4.10 Equilibrium Slope Determined from Transport Capacity Equations.....	109
Table 4.11 Current Conditions and Equilibrium Slope and Width from SAM.....	112
Table 4.12 Schumm's (1969) Channel Metamorphosis Model.....	113
Table 4.13 Observed Channel Changes at Q = 5000 cfs.....	113
Table 4.14 Change in Channel Characteristics for Lane's Balance.....	115
Table B.1 Aerial photography survey dates and information.....	145
Table C.1 HEC-RAS output for 1962 geometry.....	147
Table C.2 HEC-RAS output for 1972 geometry.....	153
Table C.3 HEC-RAS output for 1985 geometry.....	160
Table C.4 HEC-RAS output for 1992 geometry.....	166
Table C.5 HEC-RAS output for 2002 geometry.....	173
Table D.1 Grain Size Distribution (subreach 1).....	181
Table D.2 Grain Size Distribution (subreach 2).....	182
Table D.3 Grain Size Distribution (subreach 3).....	183
Table D.4 Grain Size Distribution (Escondida reach).....	184
Table E.1 Summary of Bedform Observations.....	191
Table F.1 BORAMEP Input – General Information.....	198
Table F.2 BORAMEP Input – Suspended Sediment Percent in Range.....	199
Table F.3 BORAMEP Input – Bed Material Percent in Range.....	200
Table F.4 BORAMEP Output.....	201

LIST OF SYMBOLS

A	channel cross-section area
c	sediment concentration
C_1	empirical coefficient
C_2	empirical coefficient
D	hydraulic depth (A/W)
D_{\max}	maximum depth in channel
d^*	dimensionless grain diameter
d_{50}	effective size (particle diameter corresponding to 50% finer)
d_{84}	effective size (particle diameter corresponding to 85% finer)
d_s	mean grain size
F	width to depth ratio (W/h)
F_r	Froude number
F_s	side factor
G	specific gravity
g	gravitational acceleration
h	average depth
k	decay constant
L	meander wavelength
m	Julien-Wargadalam exponent
n	Manning's roughness coefficient
P	sinuosity
P_w	channel wetted perimeter
Q	water discharge
Q_{50}	peak water discharge for a 50 year return period
Q_b	bed material load
Q_s	sediment discharge
Q_t	percent of the total load that is sand or bed material load
R_h	hydraulic radius
S	channel slope
S_v	valley slope
T	transport-stage parameter
t	time
V	flow velocity
W	channel top width
W_e	equilibrium width
W_i	initial width
W_t	width at time t
Y	relative change in channel width
γ	specific weight of water
κ	slope-discharge threshold value
ν_m	kinematic viscosity
τ^*	grain Shield's parameter
τ_{*c}	critical Shield's parameter
ω	specific stream power

Chapter 1: Introduction

The Middle Rio Grande covers about 170 miles of central New Mexico from Cochiti Dam to Elephant Butte Reservoir (Tetra Tech, Inc. 2002). The river has been greatly influenced by humans beginning as early as 10,000 years ago (Scurlock 1998). More recently, the Middle Rio Grande Conservancy District, the Bureau of Reclamation and the Army Corps of Engineers have undertaken numerous projects along the Middle Rio Grande to combat floods and sedimentation problems (MRGCD 2004).

The cumulative effect of centuries of human influence on the Middle Rio Grande is a dramatic change in the habitat of many native species, leading to a decrease in their presence along the river. Dams constructed for flood control purposes have regulated the flow of the river, virtually eliminating the seasonal flooding essential to the reproduction of the Rio Grande Silvery Minnow and many native trees such as the cottonwood (Bogan et al. 2006, Earick 1999). As a result, aging cottonwoods are being replaced by Russian olive and tamarisk, and the Rio Grande Silvery Minnow, once found from Espanola, NM to the Gulf of Mexico, is now present in only five percent of its former range (Earick 1999, MRGESACP 2006a). Today, about ninety-five percent of the Rio Grande Silvery Minnow population is concentrated in the San Acacia reach (below the San Acacia diversion dam) of the Middle Rio Grande (MGRCD v. Norton 2002). In addition, habitat

reduction has threatened the Southwestern Willow Flycatcher. In 1994 and 1995 the Rio Grande Silvery Minnow and the Southwestern Willow Flycatcher, respectively, were placed on the endangered species list in response to their dwindling numbers (MRGESACP 2006b, MRGCD v. Norton 2002).

The Escondida Reach stretches 17.7 miles from the upstream extent at the Escondida Bridge to the downstream extent at the US Highway 380 Bridge near San Antonio. Historically, this section of the river has been an aggrading, sand-bed channel showing a mostly braided pattern. However, narrowing of the channel has occurred both before and after the channelization projects completed in the 1950's (Porter and Massong 2004).

The objectives of this study of the Escondida Reach include:

- Identifying spatial and temporal trends in channel geometry and morphology. Visual observations of aerial photographs and GIS active channel planforms, cross-section surveys, hydraulic modeling using HEC-RAS, and channel classification methods will be used to identify trends. In addition, changes in bed material were observed from cross-section data.
- Determining the ability of bedform prediction equations to match bedform observations. Field observations of bedforms will be compared with the bedforms predicted by van Rijn and Simons & Richardson.
- Analyzing trends in water and sediment discharge. Mass curves developed from USGS gauge data will be used to show changes in the relevant parameters.
- Providing estimates of potential equilibrium slope and width conditions. Conditions will be predicted using hydraulic geometry equations, hyperbolic and

exponential regressions, stable channel geometry, and sediment transport relationships.

The information presented in this thesis is divided into five chapters. An introduction to the Escondida reach and the Middle Rio Grande, along with the purpose and objectives of the study, is included in Chapter 1. Chapter 2 includes a literature review of studies relevant to the study for the Escondida reach. This chapter also covers the site description, historical background of the study area, as well as information about the climate, hydrology, and geology of the area of study. Chapter 3 includes a study of the geomorphic and river characteristics, suspended sediment and water history, analysis of the active floodplain, and an assessment of historic bedform data. Chapter 4 includes an investigation of equilibrium predictors for the study reach. A summary of the study results and conclusions are included in Chapter 5. Appendices A-E include tables and plots relevant to the morphological assessment of the reach, including hydraulic model output, bed material gradations, and bedform classification. Appendices F and G include model output and other information used in the equilibrium predictor methods.

Chapter 2: Literature Review

2.1 Reach Description

The Rio Grande River originates in southwestern Colorado in the San Juan Mountains. It continues south through Colorado, and into New Mexico and along the Texas – Mexico border before reaching its confluence in the Gulf of Mexico. The Middle Rio Grande, located in central New Mexico, stretches from the Cochiti Dam to the Elephant Butte Reservoir and covers about 170 miles (Tetra Tech, Inc. 2002).

The Escondida reach will be analyzed in this study. The reach is located near Socorro, NM, about 65 miles south of Albuquerque, NM. The Escondida Bridge marks the upstream extent of the reach, while the US Highway 380 Bridge marks the downstream extent. Figure 2.1 shows a location map of the study reach.

Eight small tributaries enter the Middle Rio Grande in the Escondida reach. The majority of these tributaries are arroyos. The arroyos entering the river include the Arroyo de lo Pinos, Arroyo de Tio Bartolo, Arroyo de la Presilla, Arroyo de Tajo, Arroyo de las Canas, and Brown Arroyo. In addition, the Escondida Drain and the North Socorro diversion channel also outfall in the Escondida reach.

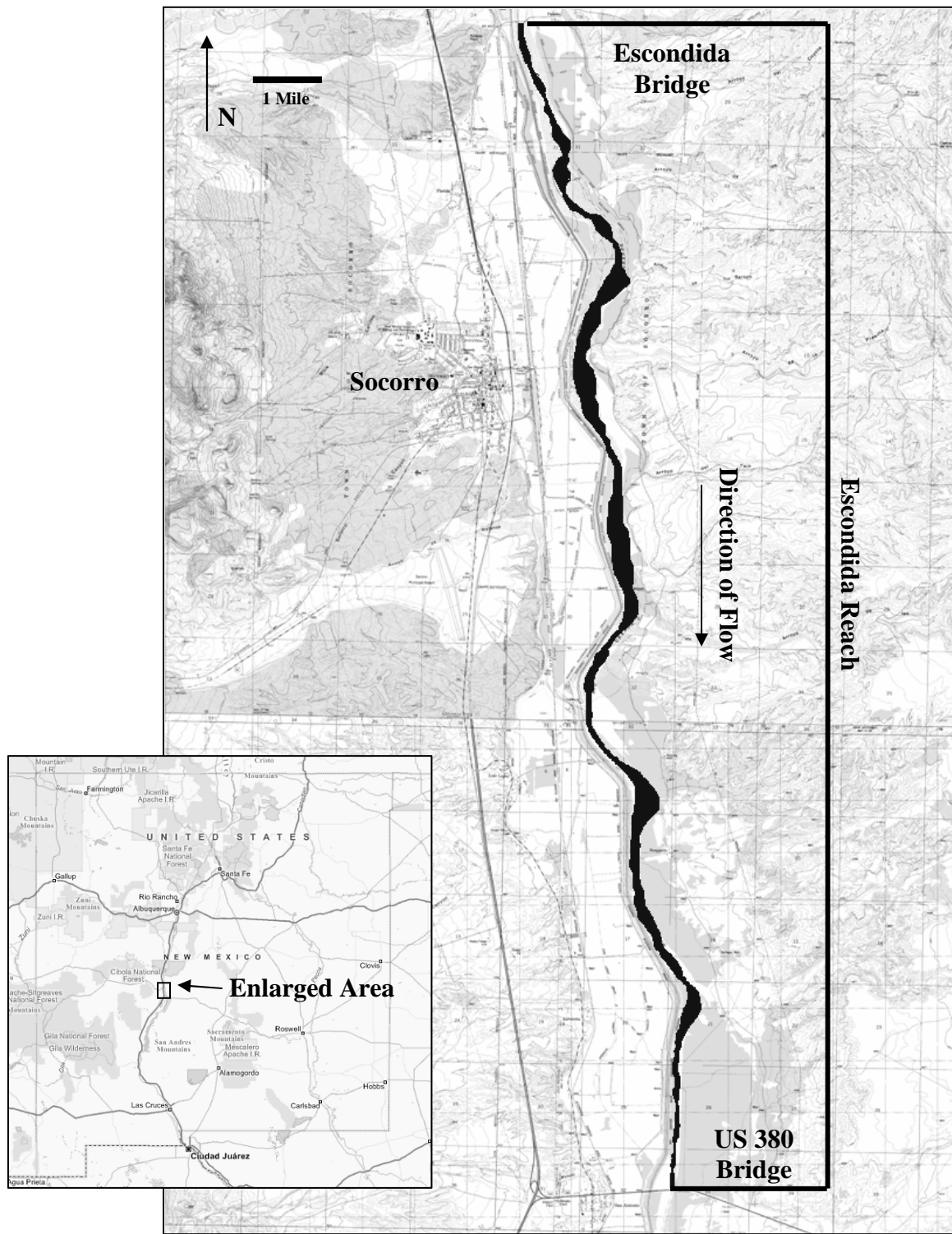


Figure 2.1 Location Map and Topographic Map of the Escondida Reach

The role of arroyos in the Middle Rio Grande River is as a primary source of sediment. The arroyos contribute most of the gravel-sized material present in the reach and contribute most of their sediment during high-intensity summer thunderstorms (Reclamation 2003). The material contributed by each tributary varies. For example, the Arroyo de las Canas typically contributes gravel-sized material, while the North Socorro diversion channel contributes mostly sand-sized material (Porter and Massong 2004).

2.2 Middle Rio Grande History

Since the arrival of the first humans along on the Middle Rio Grande River over 10,000 years ago, their activities have had a significant impact on the river as well as on the natural areas surrounding the river. Early Pueblo inhabitants cleared areas of the Bosque to make way for farmland. Later, Spanish settlers introduced grazing livestock to the area and continued to clear native riparian forests for both farming and new settlements to accommodate their ever-increasing population. In addition to introducing livestock to the area, Spanish settlers also introduced many exotic plant species that invaded the habitat of native plants. These human impacts, coupled with natural events such as droughts, led to changes in vegetation types as well as increased soil erosion along much of the Middle Rio Grande (Scurlock 1998).

By the beginning of the 20th century, significant changes had occurred in the Middle Rio Grande Valley. Increased mining, logging, and grazing had destroyed much of the vegetation, resulting in dramatic erosion and a subsequent increase in the sediment load in the river (Scurlock 1998). In addition to problems caused by local forces, increased irrigation by farmers in Colorado reduced the quality and quantity of the water

reaching the Middle Rio Grande region. Reduced flows, pollutants, and increased sediment load from Colorado farmers further exacerbated the problems faced by the inhabitants of the land along the river (Herford 1984).

The increased erosion and sediment load had caused a loss of about 13 percent of the capacity of Elephant Butte Reservoir by the mid 1930's (Clark 1987). The increased sediment load also led to severe aggregation along the River. Between 1880 and 1924, the bed of the river rose 9 feet at San Marcial (Scurlock 1998).

To combat the many problems facing the River, the Middle Rio Grande Conservancy District (MRGCD) was formed in 1923. The purpose of the MRGCD was to "provide flood protection from the Rio Grande, and make the surrounding area hospitable for urbanization and agriculture." Between 1923 and 1935 one storage dam and four diversion dams, as well as 817 miles of drainage and irrigation channels, had been constructed by the MRGCD (MRGCD 2006). The dams included the El Vado Dam on the Rio Chama, Angostura Dam, Isleta Dam, San Acacia Dam, and Cochiti Dam (Lagasse 1980).

The MRGCD's efforts were an initial success. Following the Congressional Flood Control Acts in 1948 and 1950, the Bureau of Reclamation and the Army Corps of Engineers repaired and updated the structures originally installed by the MRGCD. Additional structures were also constructed to combat flooding and sedimentation problems along the river (MRGCD 2006).

2.3 Hydrology, Geology and Climate of the Middle Rio Grande

The hydrology of the region is dominated by a spring snowmelt period and a summer thunderstorm period. Figure 2.2 shows a typical annual hydrograph based on data from the San Acacia and San Marcial gauges, located upstream and downstream of the reach, respectively. The first, longer peak seen between April and June is a result of snowmelt in the Rio Grande headwaters. The second, shorter peak seen in August is the result of an intense summer thunderstorm characteristic of the Middle Rio Grande River.

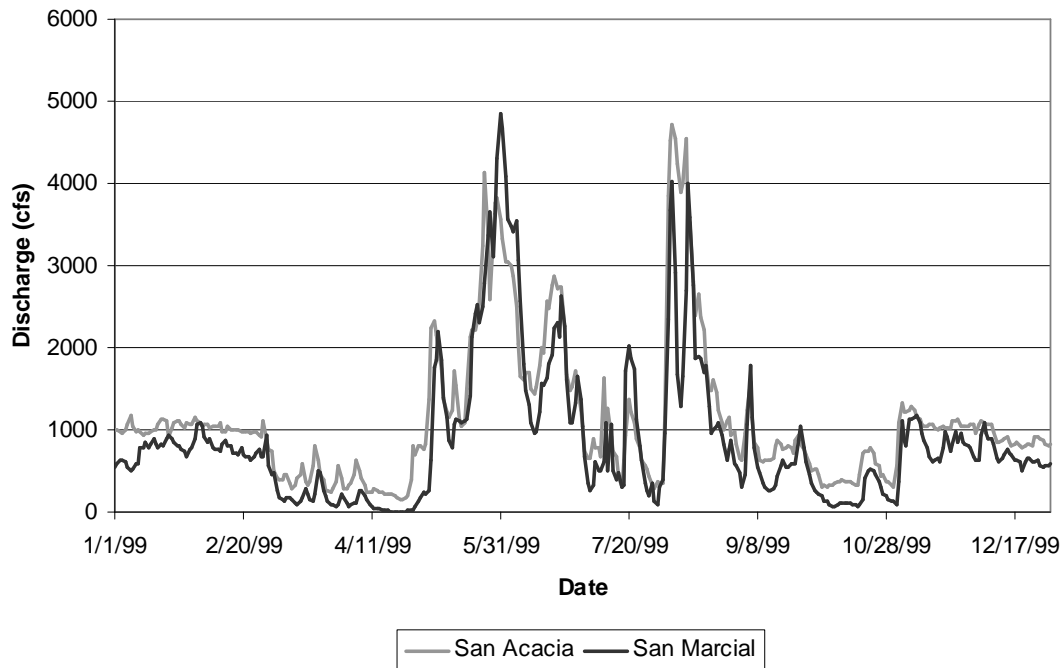


Figure 2.2 *Hydrograph for San Acacia and San Marcial Gauges*

The valley through which the Middle Rio Grande River runs was formed by the Rio Grande Rift rather than by the river, as is common in some river systems. The rift was formed by tectonic forces slowly pulling and stretching the Earth's crust, while at the same time, pushing up rock on either side of the rift. Over time, the aggrading nature of the Middle Rio Grande has helped fill the rift by depositing as much as 20,000 feet of sediment in some areas and about 5,000 feet in the Socorro area (Earick 1999, Hawley

1987). Another of the Earth's geological phenomenon is also changing the face of the Middle Rio Grande Valley. The Socorro Magma Body, centered about 12.5 miles upstream of the study reach, is causing an uplift of the valley (Larsen and Reilinger 1983, Ouchi 1983). The center was estimated to have risen at a rate of 1.3 to 2.3mm/yr between 1951 and 1980. The uplift is causing an increase in slope downstream of the center and a decrease in the slope upstream of the center (Reclamation 2003).

The Escondida reach is located in a semi-arid region of the United States. Analysis of precipitation trends at Socorro, NM and Bernardo, NM by Reclamation indication that the current average annual precipitation is about 10 inches. Historically, the average annual precipitation was about 10 inches before 1940. Between 1940 and 1970, the average annual precipitation in the region was reduced to about 8 inches (Reclamation 2003).

2.4 Previous Studies of the Middle Rio Grande

Documentation of changes along the Middle Rio Grande has been taking place for long periods of time. The Middle Rio Grande currently stands as one of the most documented rivers in the United States (Graf 1994). The studies performed have attempted to document and estimate the changes in river planform, channel geometry, bed material composition, and equilibrium state conditions. The effects of human influences such as agriculture, channelization works, dams, and channel restoration efforts have also been studied along the Middle Rio Grande.

Extensive studies have been done in the upper portion of the Middle Rio Grande from Cochiti Dam to Corrales, NM. The Bosque del Apache, located downstream of the

Escondida reach, has also been extensively studied as part of a localized restoration effort. Most of the studies in the upper portion of the river focus on the effects of the Cochiti Dam. It was estimated that Abiquiu, Jemez, Galisteo, and Cochiti Dams would reduce the sediment flow at Bernalillo by as much as 75 percent in the 20 years following dam construction. The degradation caused by the reduced sediment supply was estimated to progress as far downstream as the Rio Puerco (Woodson and Martin 1962). Other studies analyzed changes in bed material gradation downstream of the Cochiti Dam. Dewey et al. (1979) noted the formation of gravel bars as far downstream as Albuquerque.

Studies on the river as a whole have also been conducted. Graf (1994) documented changes between 1940 and 1980 based on aerial photos and topographical maps. Before 1940, the river planform was wide, shallow and braided. Following channelization, flood control, and restoration efforts along the river, the channel narrowed throughout most of the Middle Rio Grande. At this time the river also transitioned from a braided to a single-thread channel (Bauer 2000). The channel also became more laterally mobile as the narrowing channel became increasingly unstable. Graf (1994) observed migration of the main channel to be as high as 1 km (0.6 miles) in some areas between 1940 and 1980.

Compared to the extensive studies performed on the upstream reaches of the Middle Rio Grande, the Escondida reach has received relatively little attention. However, some important insights have been gained from the studies performed. The sources of sediment in the river were assessed by Albert (2004). This study revealed that 65% of the total sediment recorded at the Albuquerque and Bernardo gauges, located in

the upper portion of the river, was contributed by bed degradation. In reaches downstream of the Rio Puerco, however, only about 8% of the total sediment was contributed by bed degradation. Much of the rest of the sediment is contributed by the Rio Puerco, which contributes twice as much sediment to the river as passes through the river at Albuquerque (Bauer 2000).

The US Bureau of Reclamation (Reclamation) has funded several studies of the morphology of the Middle Rio Grande. These studies were performed at Colorado State University (CSU) under the direction of Dr. P.Y. Julien. Figure 2.3 shows the locations of the studies conducted by CSU. The reaches that have been studied as of 2006 include:

- Rio Puerco (Richard et al. 2001), updated by Vensel et al. (2005). This reach covers 10 miles from the mouth of the Rio Puerco (Agg/Deg 1101, river mile 126) to the San Acacia Diversion Dam (Agg/Deg 1206, river mile 116.2). This reach is the downstream most reach that has been previously studied by CSU.
- Corrales (Leon and Julien, 2001a), updated by Albert et al. (2003). This reach covers 10.3 miles from the Corrales Flood Channel (Agg/Deg 351, river mile 196) to the Montano Bridge (Agg/Deg 462, river mile 188).
- Bernalillo Bridge (Leon and Julien 2001b), updated by Sixta et al. (2003a). This reach covers 5.1 miles from New Mexico Highway 44 (Agg/Deg 298, river mile 203.8) to cross-section CO-33 (Agg/Deg 351, river mile 198.2).
- San Felipe (Sixta et al. 2003b). This reach covers 6.2 miles from the mouth of Arroyo Tonque (Agg/Deg 174, river mile 217) to the Angostura Diversion Dam (Agg/Deg 236, river mile 209.7).

- Cochiti Dam (Novak and Julien 2005). This reach covers 8.2 miles from the outlet of Cochiti Dam (Agg/Deg 17, river mile 232.6) to the mouth of Galisteo Creek (Agg/Deg 97, river mile 224.4).

The extensive amount of data and corresponding research performed by CSU under Dr. P.Y. Juilen has been organized into the Middle Rio Grande Database. All data, analysis, and literature related to the studies as well as all theses, dissertations, and Reclamation reports, are included in the database (Novak 2006).

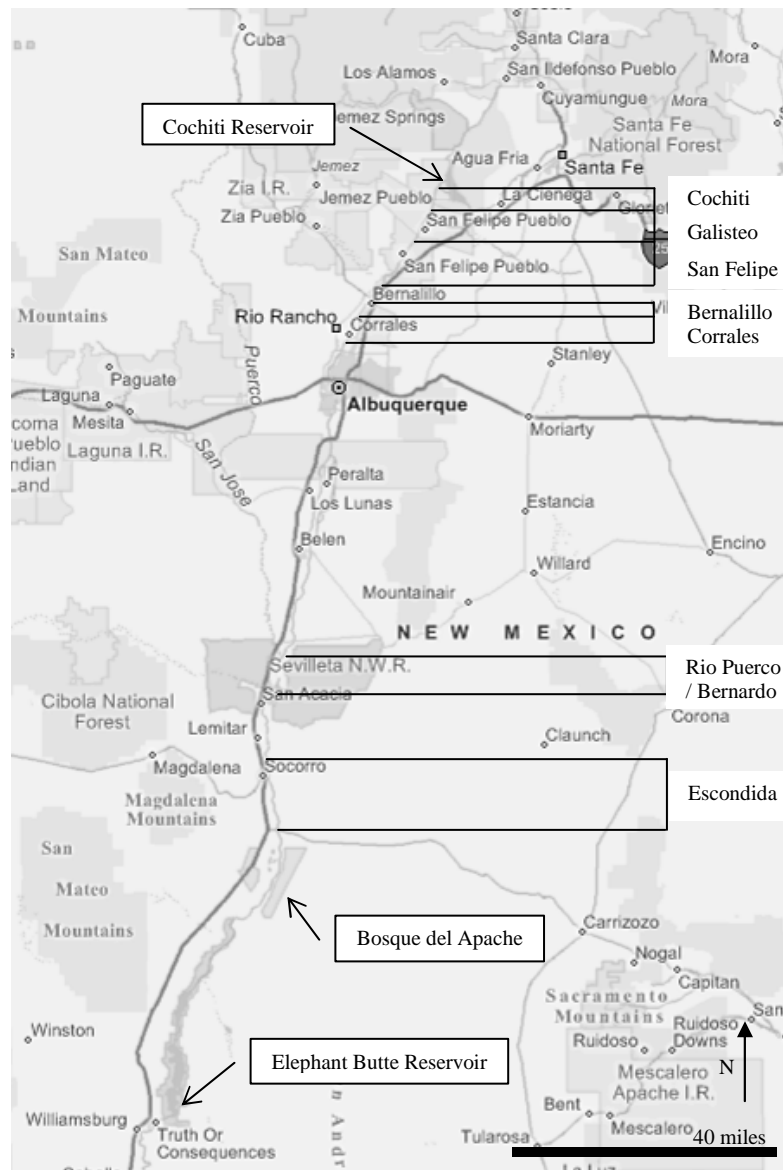


Figure 2.3 Location of Previous Studies

2.5 Channel Planform Classification Methods

Ten channel planform classification methods were investigated for applicability to the Escondida reach. Each method is discussed below.

Leopold and Wolman (1957) analyzed a large amount of data from streams with bed material sizes ranging from coarse sand to small boulders. These channels had discharges between 10 and 10,000 cfs. Their classification includes three designations, straight, meandering and braided. The designations are divided by a critical slope value calculated based on the discharge in the channel.

Lane (from Richardson et al. 2001) developed classifications for sand bed channels. This classification is also based on the slope and discharge in the channel, but includes designations for meandering, intermediate, and braided channels.

Henderson's (1966) method is based on the data set compiled by Leopold and Wolman (1957). Therefore, it encompasses the same large range of both bed material sizes and discharge values. Henderson included median grain diameter in addition to the slope and discharge parameters developed by Leopold and Wolman (1957).

Schumm and Khan (1972) performed laboratory flume experiments in sand to develop their relationship. They determined a critical valley slope at which channels become straight, braided, or have a meandering thalweg.

Rosgen (1996) developed a detailed classification system that encompasses nearly all bed material sizes, channel slopes, and sinuosity values. The method also allows for single and multi-thread channels. Although the classification includes a wide range of values, classification can be difficult in channels that have been altered by humans as this method was developed for natural streams.

Parker (1976) performed tests in alluvial systems in the laboratory setting. Observations of natural channels were also included in the development of the classification. The primary division developed by Parker was between braided and meandering channels with a transitional zone between the two classifications.

Nanson and Croke (1992) classified channels based primarily on their floodplains. Three primary classifications and twelve sub-classes were developed for a wide range of stream power values as well as for bed material from silts to boulders.

Chang (1979) compiled data from numerous sources including both canals and rivers to develop a classification method based on stream power. This classification is developed for channels with bed material between 0.1mm and 1 mm, discharges between 100 cfs and 1 million cfs, and valley slopes between 0.00001 and 0.01.

Ackers and Chalton (1970, from Ackers 1982) developed classification methods for gravel bed streams. Their classification finds a critical slope value based on the channel discharge in a manner similar to Leopold and Wolman (1957).

van den Berg (1995) developed a classification method based on analysis of wide alluvial floodplains. This method is applicable for channels with a mean annual discharge greater than 35 cfs, bed material between 0.1 mm and 100 mm, and a sinuosity greater than 1.3. In addition, the channel must be in dynamic equilibrium with no incising or rapid incision.

The methods selected for use in the analysis are explained in more detail in Chapter 3.

2.6 Bedform Classification Methods

Bedform classification methods were developed by Simons and Richardson (from Julien 1998) and van Rijn (1984). The method devised by Simons and Richardson is based on a comparison of stream power and median grain size based on a large number of laboratory experiments. Good results were achieved with this method in shallow streams, but it was not as reliable in deeper streams. The method is applicable in channels with a sand grain diameter up to 1 mm and for values of stream power between 0.001 ft/lb-s and about 2.5 ft/lb-s (Julien 1998).

van Rijn (1984) developed a classification method based on the dimensionless grain diameter, d_* , and the transport-stage parameter, T . The classification was developed primarily to describe lower regime bedforms as these are most commonly observed in the field. Unlike many bedform classification methods, van Rijn's method uses a considerable amount of field data as well as laboratory data. The use of field data in developing the model makes this method more reliable when compared to channels in the field (van Rijn 1984).

Chapter 3: Geomorphic Characterization

3.1 Site Description and Background

The 17.7-mile-long Escondida Reach is the subject of this report. The upstream extent of the reach is the Escondida Bridge (River Mile 104.8) north-west of the town of Escondida, NM. The downstream extent is the US Highway 380 Bridge (River Mile 87.1) located directly west of the town of San Antonio, NM. Historically, this reach has been an aggrading, sand-bed channel with a primarily braided planform, but the channel has narrowed due to human influences and natural processes (Porter and Massong 2004). Figures 3.1 – 3.3 show 2005 aerial photographs of the study reach. Notice the abundance of arroyos entering the reach in subreach 1 and the very straight, narrow planform of subreach 3. Also, notice how the river runs nearly parallel to the low-flow conveyance channel located on the west bank of the river, indicating that the levees protecting the conveyance channel may be influencing the path of the river.

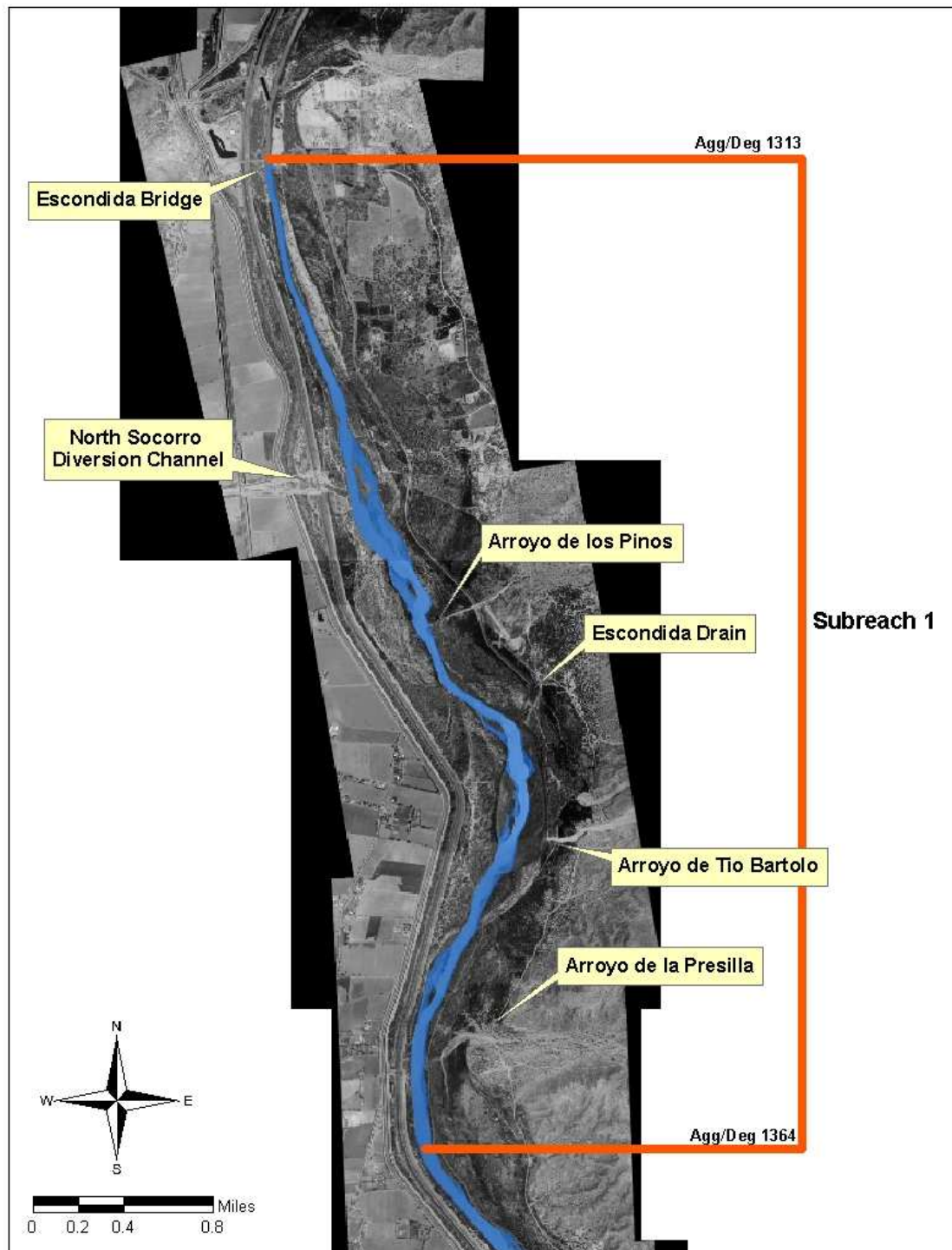


Figure 3.1 2005 Aerial Photo of Subreach 1

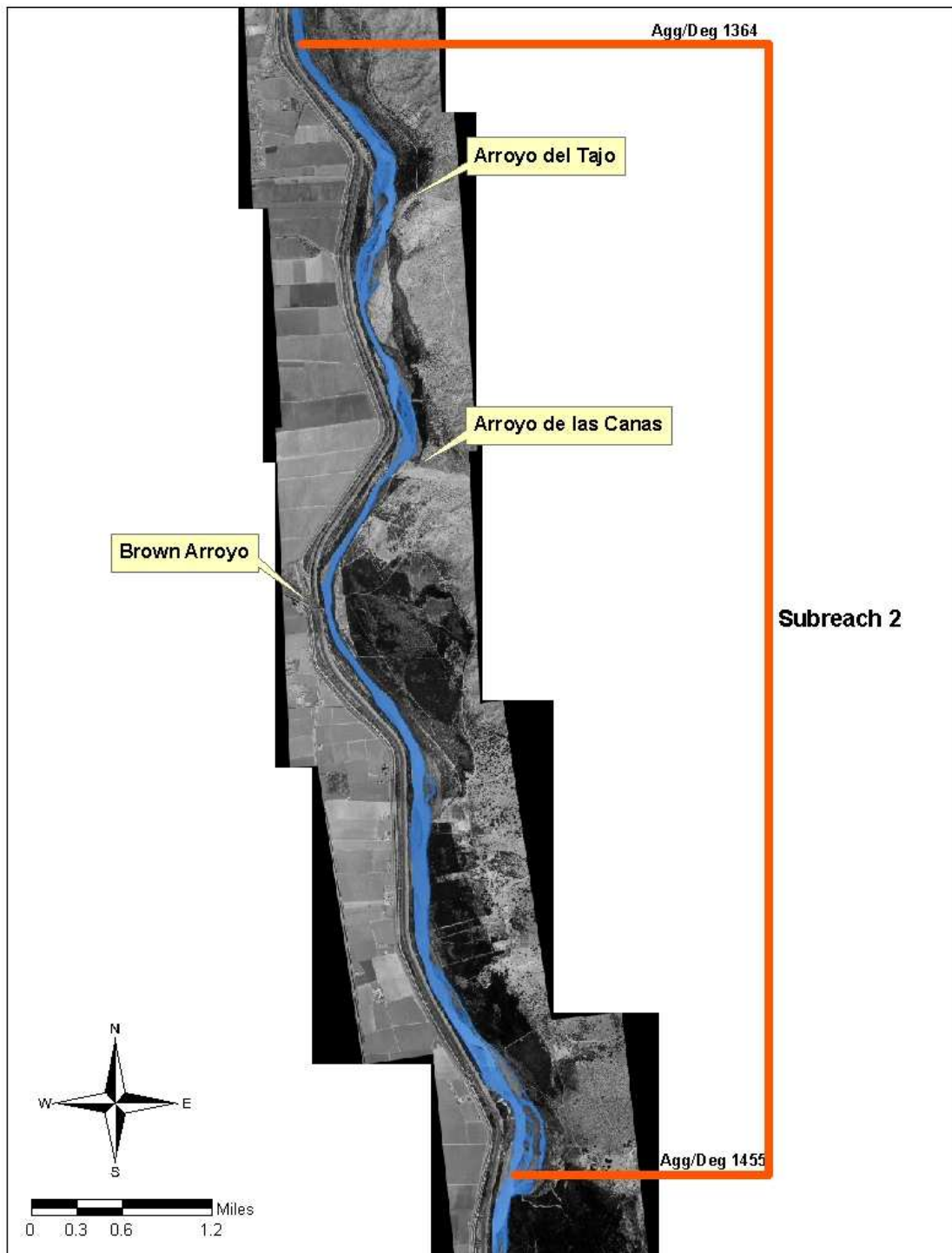


Figure 3.2 2005 Aerial Photo of Subreach 2

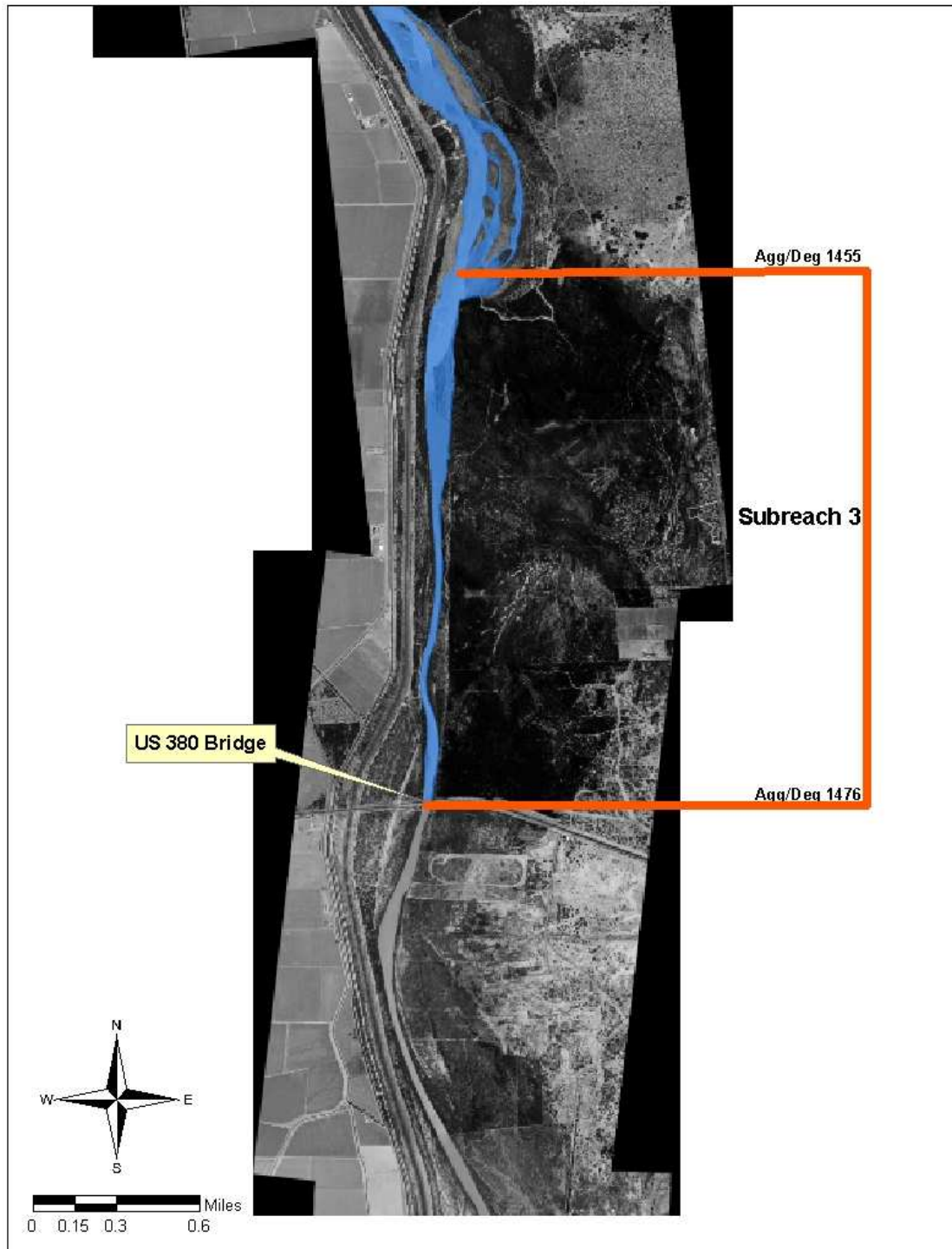


Figure 3.3 2005 Aerial Photo of Subreach 3

3.1.1 Subreach Definition

In an effort to better assess the historic changes in the Escondida reach, as well as to make better predictions of possible future conditions, the reach was divided into three subreaches. The subreach definitions were determined by initial assessments of the channel width and planform from GIS aerial photos. In addition, aggradation and degradation based on the minimum channel elevations also helped determine the final delineations. The location of the subreach delineations and locations of Agg/Deg cross-section surveys can be seen in Figure 3.4. Subreach 1 stretches from the Escondida Bridge to Agg/Deg line 1346, located between Arroyo de la Presilla and Arroyo del Tajo. Subreach 2 stretches from Agg/Deg line 1364 to Agg/Deg 1455. Finally, Subreach 3 stretches from Agg/Deg 1455 to the US Highway 380 Bridge.

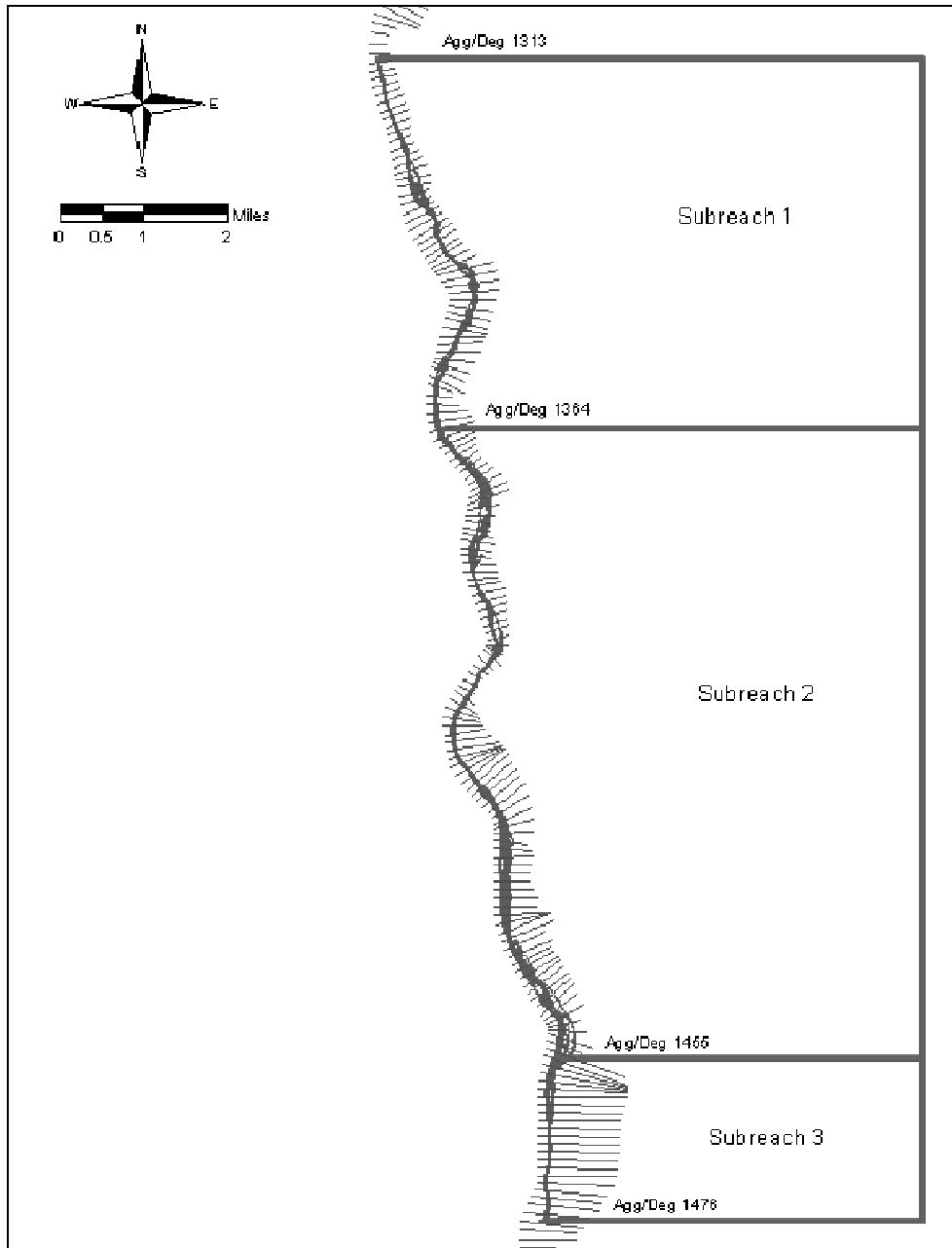


Figure 3.4 Subreach Definitions and Agg/Deg Location

3.1.2 Available Data

The data used in this study were retrieved from a number of different agencies including Reclamation, the United States Geological Survey (USGS), the National Oceanic and Atmospheric Administration (NOAA), and the Middle Rio Grande database compiled at Colorado State University for Reclamation.

Water and Suspended Sediment Data

Historical mean daily discharge data were obtained from two USGS gauges; the San Acacia gauge (08354900), located approximately 11 miles upstream of the study reach, and the San Marcial gauge (08358400), located approximately 18 miles downstream of the study reach. The dates of available discharge data are shown in Table 3.1.

Table 3.1 Available Daily Discharge Data

USGS Gauging Station	Dates
RG at San Acacia	1958-2005
RG at San Marcial	1949-2005

Two additional gauges are located at the bridges on the upstream and downstream boundaries of the study reach but are only able to record real-time discharge data, not the historical data necessary for this study.

In addition, daily suspended sediment data were also available at the San Acacia and San Marcial gauges. Figure 3.5 shows the annual suspended sediment load at each gauge. A blank year indicates that complete sediment data were not available for that year.

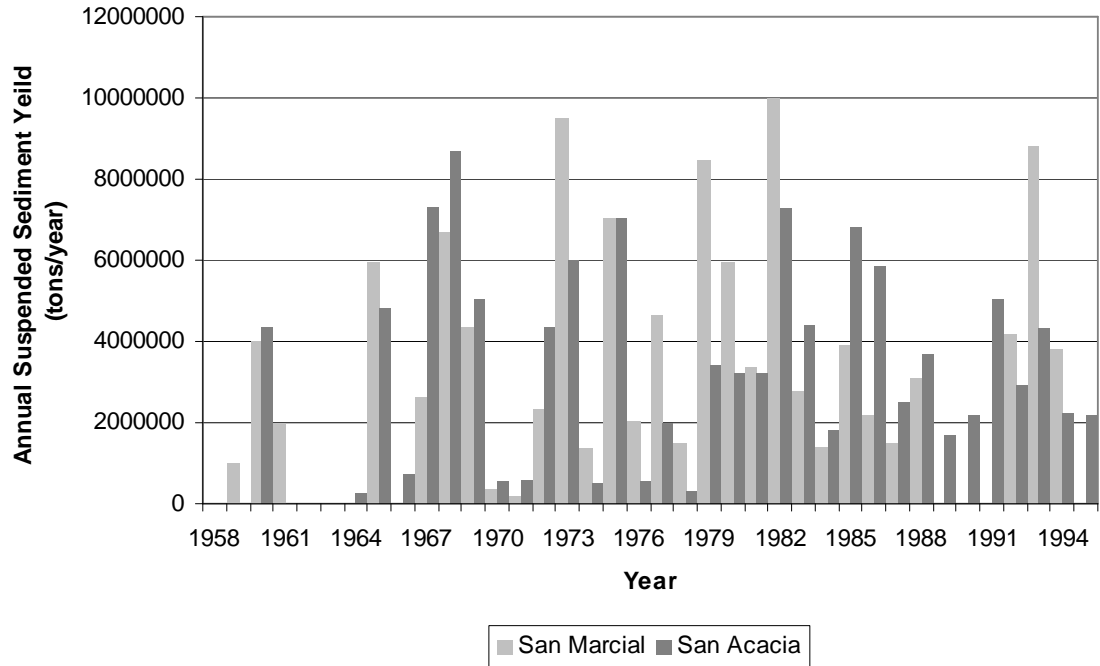


Figure 3.5 Annual Suspended Sediment Yield at San Acacia and San Marcial Gauges

Continuous suspended sediment data were not always available for all parameters at all gauges. Table 3.2 gives the dates of continuous, viable data at each gauge.

Table 3.2 Available Suspended Sediment Data

USGS Gauging Station	Dates
RG at San Marcial	Oct. 1956 - July 1962
	Sep. 1962 - Aug. 1966
	Oct. 1966 – Sep. 1989
	Oct. 1991 – Sep. 1995
RG at San Acacia	Jan 1959 – Sep. 1959
	Jan 1960 – Sep. 1961
	July 1961
	April 1962 - July 1962
	Aug 1962 - Sep. 1962
	March 1963 - Sep. 1996

Bed Material

Bed material data were collected at Socorro range lines (SO-lines) by Reclamation from 1990-2005 (see Figure 3.6). The surveys include grain-size

distributions for each sample. The dates and locations of the material collected are displayed in Table 3.3.

Table 3.3 Available Bed Material Data at SO-Lines

Years	SO Line Number									
	1313	1316	1346	1371	1380	1401	1414	1437.9	1450	1470.5
1990								x	x	x
1991					x	x			x	x
1992							x	x		x
1993							x	x		x
1994							x	x		x
1995							x	x		x
1996		x		x			x	x	x	x
1997		x	x	x			x	x	x	x
1998							x	x		x
1999	x	x	x	x			x	x		x
2002							x			
2005							x			x

Additional bed material data were also obtained from the USGS gauging stations at San Acacia and San Marcial. Data were sporadically available from 1966-2004 at the San Acacia gauge and from 1968-2004 at the San Marcial gauge. The information from the gauging stations was only used in analysis when appropriate bed material data were not available from the SO-line surveys.

Survey Lines and Dates

Cross-section information was collected by Reclamation using two methods. Agg/Deg lines were surveyed using aerial photography and do not provide detailed information about the channel in any location covered by water at the time of the survey. However, they do provide information about the topography of a large area of the floodplain not covered by the detailed on-ground surveys. Agg/Deg lines 1313-1476 were used in the hydraulic analysis (see Figure 3.4). This includes one cross-section

upstream of the study reach and one cross-section downstream of the study reach.

Because the extent of the Agg/Deg lines used does not exactly match the limits of study, the length of the reach used for hydraulic analysis is slightly longer than the actual study reach. Agg/Deg lines are spaced about 500 feet apart and were surveyed in 1962, 1972, 1985, 1992, and 2002.

SO range lines were surveyed by Reclamation beginning in 1987. These surveys provide detailed information about the channel cross-section that is not available from the aerial photographs. Thirty-three SO-lines are located in the reach. Figure 3.6 shows the location of the SO-lines and Table 3.4 shows the dates of available survey data at each SO-line. Appendix A contains cross-section plots of the SO-line data.

Table 3.4 Socorro Range Line Survey Dates

SO - Line	Year														
	1987	1989	1990	1991	1992	1993	1994	1995	1996	1997	1998	1999	2002	2004	2005
1313							X		X		X			X	
1314							X		X		X			X	X
1316							X		X		X				
1320					X		X		X		X				X
1327								X	X		X	X			X
1339					X				X		X	X			X
1342.5												X			
1346					X			X	X		X	X			X
1349												X			
1352												X			X
1360					X			X	X		X	X			X
1371					X				X		X	X			X
1380			X		X			X	X		X	X			X
1392															X
1394			X		X				X		X	X			X
1396.5												X			
1398												X			
1401			X		X			X	X		X	X			X
1410			X		X	X	X	X	X	X		X	X		X
1414			X		X	X	X	X	X	X		X	X		X
1420			X		X	X	X	X	X	X		X	X		X
1428			X		X	X		X	X	X		X	X		X
1437.9	X	X	X	X	X	X		X	X	X		X			X
1443			X		X	X		X	X	X		X	X		X
1450	X	X	X	X	X	X		X	X	X		X	X		X
1456			X		X	X		X	X	X		X	X		X
1462			X		X	X		X	X	X		X	X		X
1464.5												X			
1469.5		X													
1470.5		X	X	X	X	X	X	X	X	X	X	X	X		X
1471.2		X													
1472	X	X													

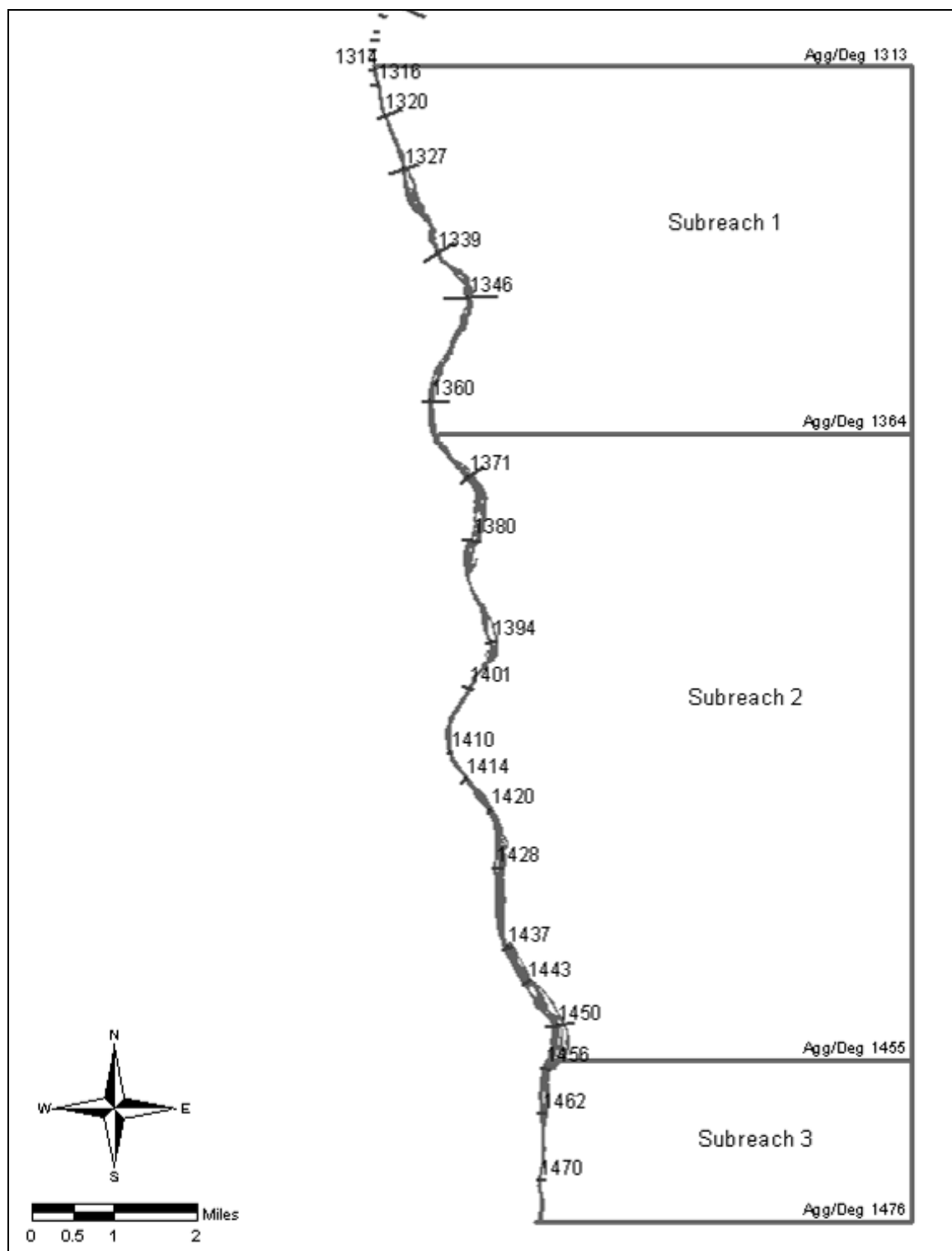


Figure 3.6 Socorro Range Line Locations

3.1.3 Channel Forming Discharge

Effective Flow

The effective flow in the channel was determined using GeoTool. This program uses discharge data and sediment data to determine the discharge at which the majority of the sediment in the channel is transported. The program was run twice. One run used the daily discharge data collected at the San Acacia gauge; the second run used the daily discharge data from the San Marcial gauge. Both sets of data were determined to have a lognormal distribution. Slope and width information was obtained from HEC-RAS runs using discharges near the expected effective flow. The bed material diameter information was taken from bed material data collected at the SO-lines throughout the reach.

Yang's Sand equation was used to calculate the sediment transport rate. Of the methods available, Yang's Sand equations was both applicable and required input information that was easily obtained from available data. The energy slope was estimated from HEC-RAS runs in the same manner as the slope and width information. Temperature and bed material data were obtained from SO-line surveys.

An empirical relationship between discharge and hydraulic radius was developed by running HEC-RAS at a wide range of flows and using regression analysis to determine the relationship. The final input data for the effective flow calculations are shown Table 3.5.

Table 3.5 GeoTool Inputs

Input Parameters	
Slope (ft/ft)	0.00079
d ₅₀ (mm)	0.25
d ₈₄ (mm)	0.62
Characteristic Width (ft)	1044
Yang's Sand Method	
Energy Slope (ft/ft)	0.0093
d ₅₀ (mm)	0.25
Temp (°F)	60
Effective Width (ft)	1044
Regression Equation	R _h = 0.11Q ^{0.37}
Manning's n	0.022

The GeoTool analysis resulted in effective discharges ranging from about 3000 cfs to 5000 cfs depending upon the number of bins data were divided into. The ideal number of bins is the largest number of bins with a minimum number of empty bins (Brown 2006). The effective discharge corresponding to the ideal number of bins was determined to be 4600 cfs for both the San Acacia and San Marcial gauges.

Recurrence Interval

The 2, 5, 7, and 10 year flows were calculated from the annual peak flow information obtained from the San Acacia and San Marcial gauges. Figures 3.7 and 3.8 show the annual peak flows at San Acacia and San Marcial. Figure 3.9 displays a comparison of the peak flows at the two gauges.

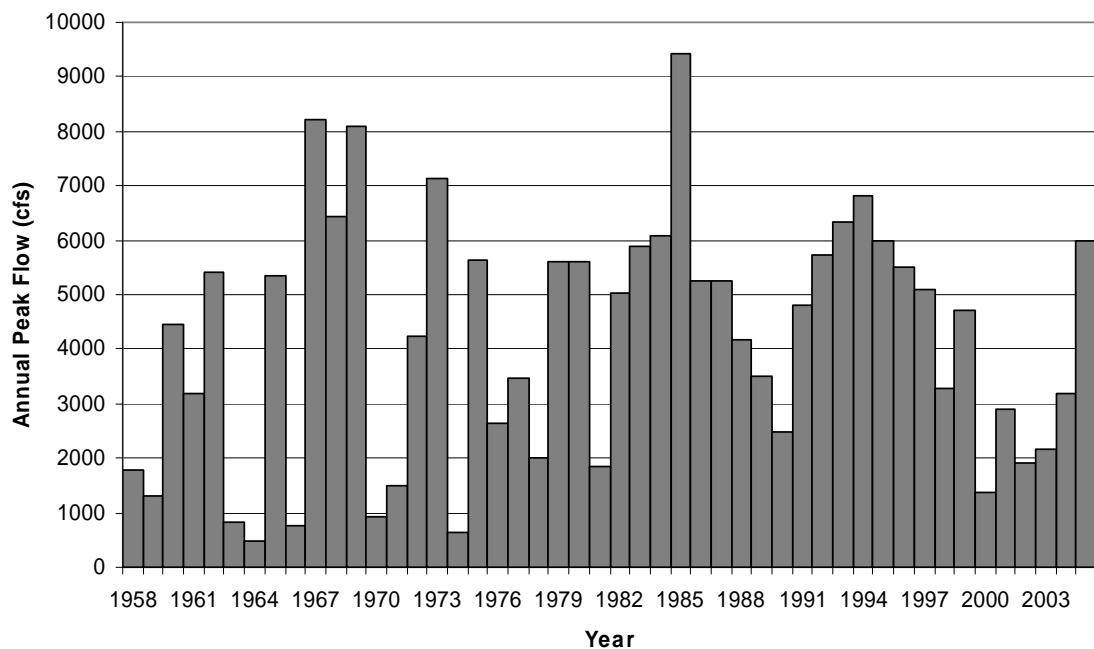


Figure 3.7 Annual peak flow at San Acacia gauge

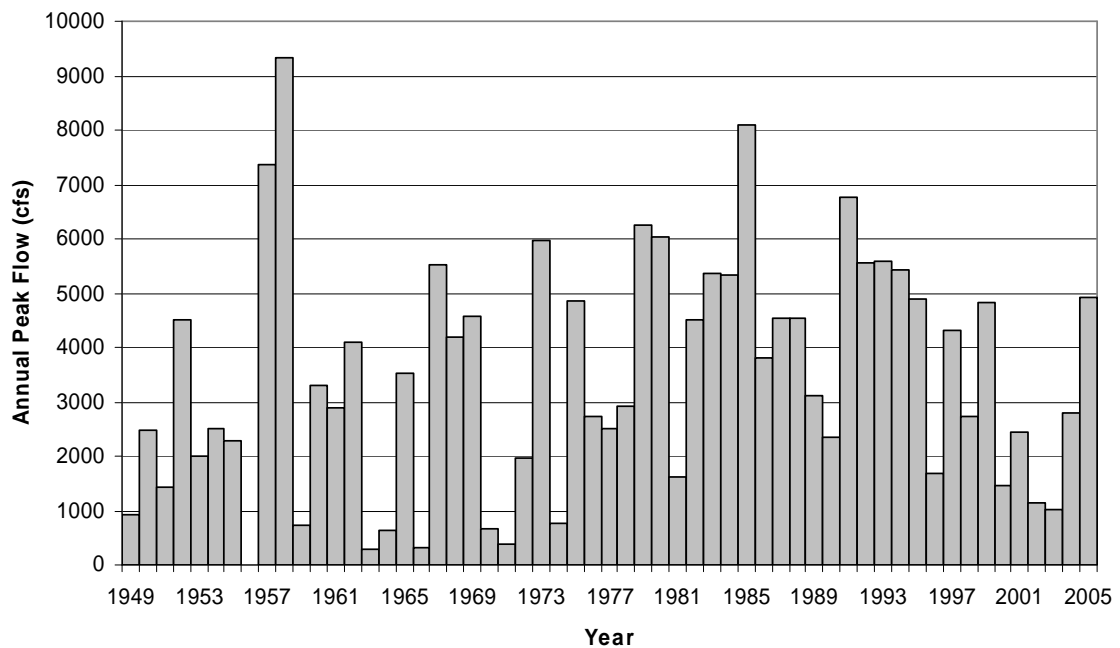


Figure 3.8 Annual peak flow at San Marcial gauge

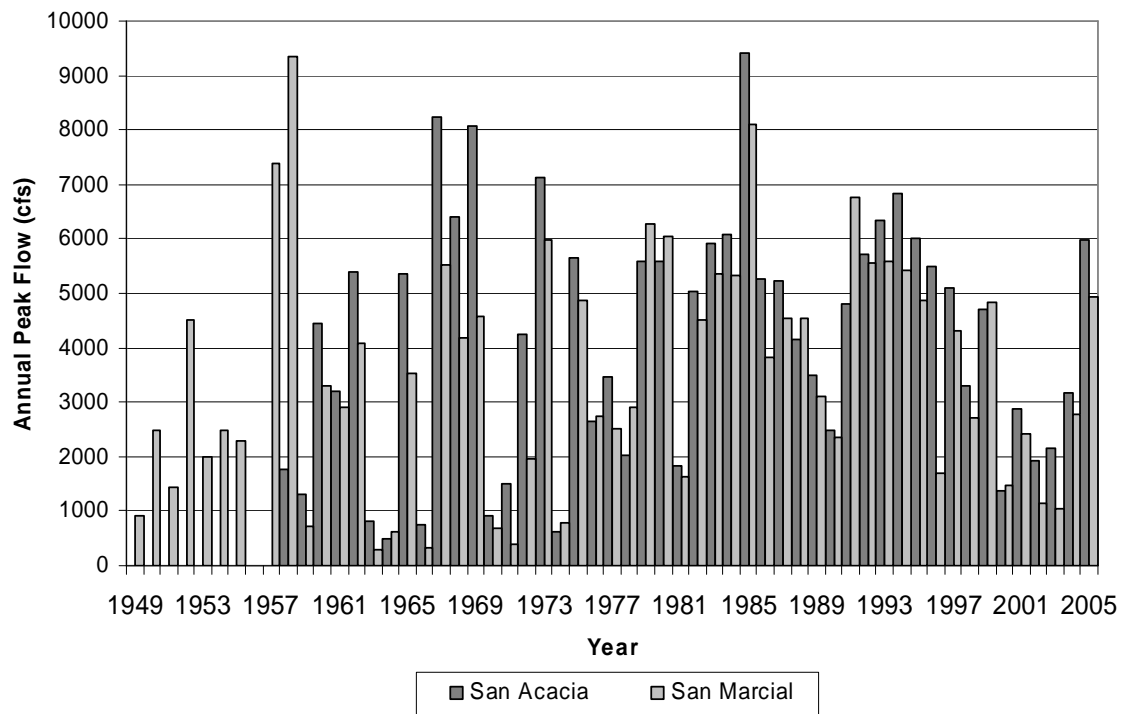


Figure 3.9 Comparisons of Annual Peak Flows

The recurrence intervals calculated from the actual annual peak flows and corresponding discharges can be seen in Table 3.6.

Table 3.6 Recurrence Interval

Recurrence Interval (years)	Discharge (cfs)	
	San Acacia	San Marcial
10	6,846	6,095
7	6,350	5,584
5	5,984	5,384
2	4,587	3,100

Based on the recurrence interval analysis, the effective discharge is in the approximate range of a 2-year storm event.

Bankfull Measurements

Bankfull flow was not calculated directly for the Escondida reach, but a near-bankfull discharge of 5000 cfs was observed by Reclamation in August, 1999 in the San Acacia reach located just upstream of the Escondida reach. In addition, calculations performed by Reclamation in the San Acacia reach estimated the bankfull discharge of 5000 cfs with a recurrence interval between 1.5 and 2.5 years (Reclamation 2003). The recurrence interval calculated by Reclamation corresponds well with the recurrence interval calculated above. Because the reaches are located immediately adjacent to one another, and the recurrence intervals match well, the 5000 cfs bankfull discharge determined by Reclamation will be used in the hydraulic analysis of the Escondida reach.

3.2 Classification, Longitudinal Profile, Channel Geometry, and Sediment

3.2.1 Channel Planform Methods

A number of quantitative channel classification methods were investigated to determine the methods most applicable to the Escondida reach. A qualitative classification of the channel was also made based on observations of aerial photographs and GIS channel planforms.

The channel was classified based on slope-discharge relationships including Leopold and Wolman (1957), Lane (1957, from Richardson, et. al 2001), Henderson (1984), and Schumm and Khan (1972). Channel morphology methods by Rosgen (1994) and Parker (1976) were also used, along with stream power relationships developed by Nanson and Croke (1992) and Chang (1979).

Two additional methods were also investigated, but found to be inapplicable to the Escondida reach. These methods include Ackers and Charlton (1970, from Ackers 1982) and van den Berg (1995). Ackers and Charlton (1970, from Ackers 1982) was developed for gravel-bed rivers and van den Berg (1995) was developed for channels with a sinuosity greater than 1.3.

Slope-Discharge Methods

Leopold and Wolman (1957) determined a critical slope value, based on discharge, which separates braided from meandering planforms. The following equation shows the slope-discharge relationship:

$$S = 0.6Q^{-0.44}$$

Where S is the critical slope and Q is the channel discharge (cfs). Channels with slopes greater than the critical slope will have a braided planform, while channels with slopes less than the critical slope will have a meandering planform. Straight channels may fall on either side of the critical slope. Leopold and Wolman identified channels with a sinuosity greater than 1.5 as meandering and channels with a sinuosity less than 1.5 as straight. Using the slope-discharge relationship and the critical sinuosity value, channels can be divided into straight, meandering, braided, or straight/braided channels.

Lane (from Richardson et. al 2001) developed a slope-discharge threshold value, κ , calculated by this equation:

$$\kappa = SQ^{0.25}$$

Where S is the channel slope and Q is the channel discharge (cfs). The classification of the stream is based on the value of κ as shown below:

Meandering:	$\kappa \leq 0.0017$
Intermediate:	$0.010 > \kappa > 0.0017$
Braided:	$\kappa \geq 0.010$

These threshold values assume the use of English units. Values of κ are also available for SI units.

Henderson (1984) developed a slope-discharge method that also accounts for the median bed size by plotting the critical slope as defined by Leopold and Wolman against the median bed size. The following equation resulted:

$$S = 0.64d_s^{1.14}Q^{-0.44}$$

Where S is the critical slope, d is the median grain size (ft), and Q is the discharge (cfs). For slope values that plot close to this line, the channel planform is expected to be straight or meandering. Braided channels plot well above this line.

Schumm and Khan (1972) developed empirical relationships between valley slope and channel planform based on flume experiments. Thresholds were determined for each channel classification as follows:

Straight:	$S_v < 0.0026$
Meandering Thalweg:	$0.0026 < S_v < 0.016$
Braided:	$0.016 < S_v$

Channel Morphology Methods

Rosgen (1994) developed a channel classification method based on entrenchment ratio, width/depth ratio, sinuosity, slope, and bed material. Using these channel characteristics, Rosgen developed eight major classifications and a number of sub-classifications. Figure 3.10 shows Rosgen's method for stream classification.

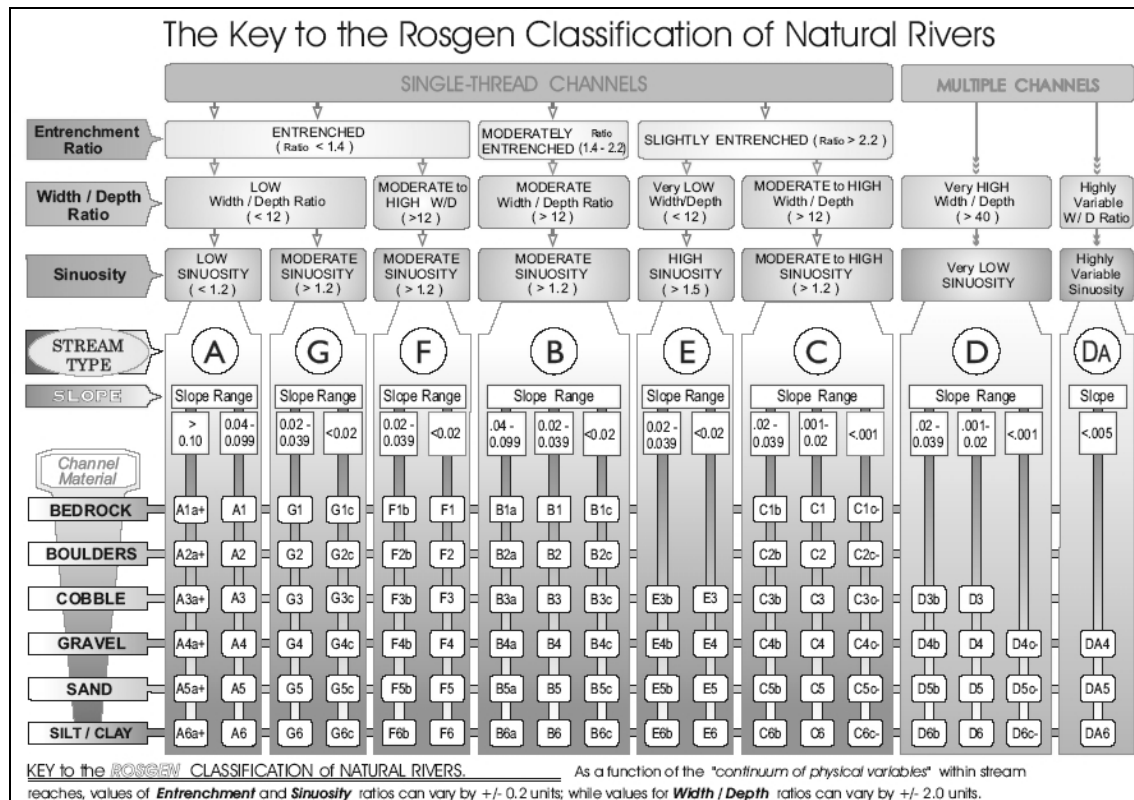


Figure 3.10 Rosgen Channel Classification Key (Rosgen 1996)

Parker (1976) considered the relationship between slope, Froude number, and width to depth ratio. Experiments in laboratory flumes and observations of natural channels lead to the following channel planform classifications:

Meandering:	$S/F \ll W/h$
Transitional:	$S/F \sim W/h$
Braided:	$S/F >> W/h$

Where S is the channel slope, F is the Froude number, and W/h represents the width to depth ratio.

Stream Power methods

Nanson and Croke (1992) used specific stream power and sediment characteristics to differentiate between types of channel planforms. The equation used to determine specific stream power is as follows:

$$\omega = \gamma Q S / W$$

Where ω is specific stream power (W/m^2), γ is the specific weight of water (N/m^3), S is channel slope, and W is channel width (m). Three main classes and twelve sub-classes were developed by Nanson and Croke. Three classifications of interest in this reach, along with the corresponding specific stream power and expected sediment type, are shown below:

- Braided-river floodplains (braided):
 - $\omega = 50-300$
 - gravels, sand, and occasional silt
- Meandering river, lateral migration floodplains (meandering):
 - $\omega = 10-60$
 - gravels, sands, and silts
- Laterally stable, single-channel floodplains (straight):
 - $\omega < 10$
 - silts and clays

Chang (1979) used data from numerous rivers and canals to develop channel classifications based on stream power. The classifications are presented in terms of valley slope and discharge. Figure 3.11 shows the four classification regions defined by Chang for sand streams.

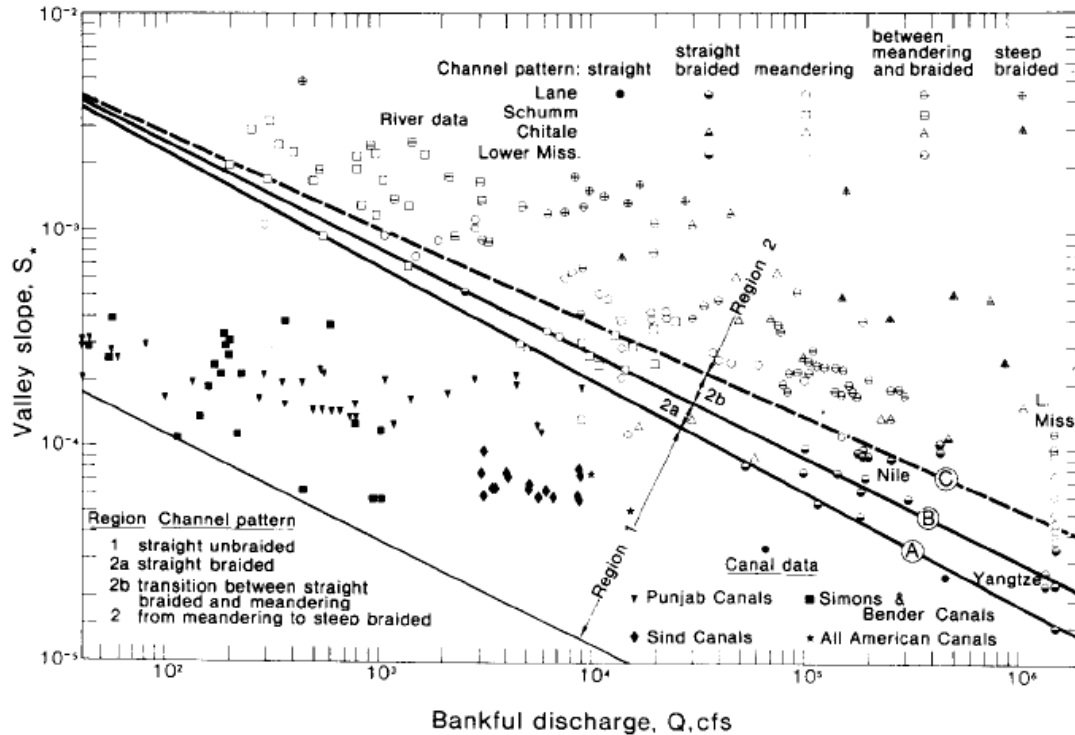


Figure 3.11 *Chang's Stream Classification Method Diagram*

Chang found that at low valley slopes, rivers will have a straight planform. With constant discharge, an increase in valley slope will cause the channel to transform to a braided or meandering planform.

3.2.2 Channel Planform Results

Visual, qualitative characterization of the channel was performed using channel planforms delineated from aerial photographs using GIS in 1918, 1935, 1949, 1962,

1972, 2001, 2002, 2004, and 2005. See Appendix B for information about the aerial photographs. Aerial photographs for 1985 were not available, so a planform delineation was obtained from the Reclamation database. Figures 3.12 – 3.14 show the historical planforms for the Escondida reach.

Based on visual observations, the historical channel was somewhat sinuous, but recent planforms show a relatively straight, narrow channel. Some planforms indicate a tendency toward areas of braiding, especially at low flow. The upstream and downstream extents of the reach have seen the most dramatic shift toward a very straight, non-braided channel. This change may be due to the flow being forced into a confined area under the bridges at the upstream and downstream extents of the reach.

Two of the largest shifts can be seen at the upstream and downstream extents of the reach. Between 1935 and 1949, the channel was shortened slightly on the downstream end of the reach. The bridge at this location was moved upstream. In addition, between 1949 and 1962, the upstream extent of the channel was moved considerably. These channel shifts were not caused by natural channel migration, but by bridge construction and maintenance projects.

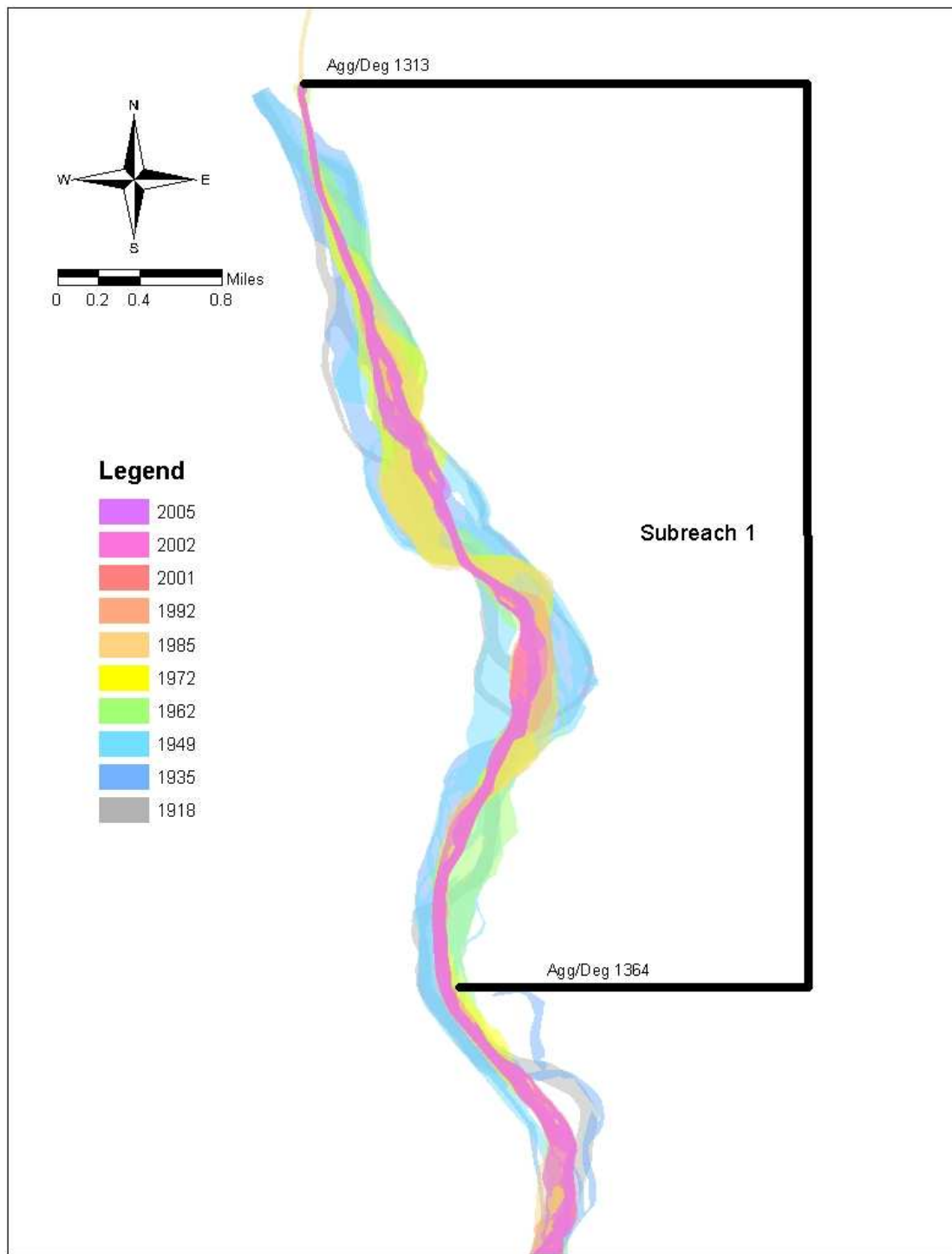


Figure 3.12 Historical planforms of Subreach 1

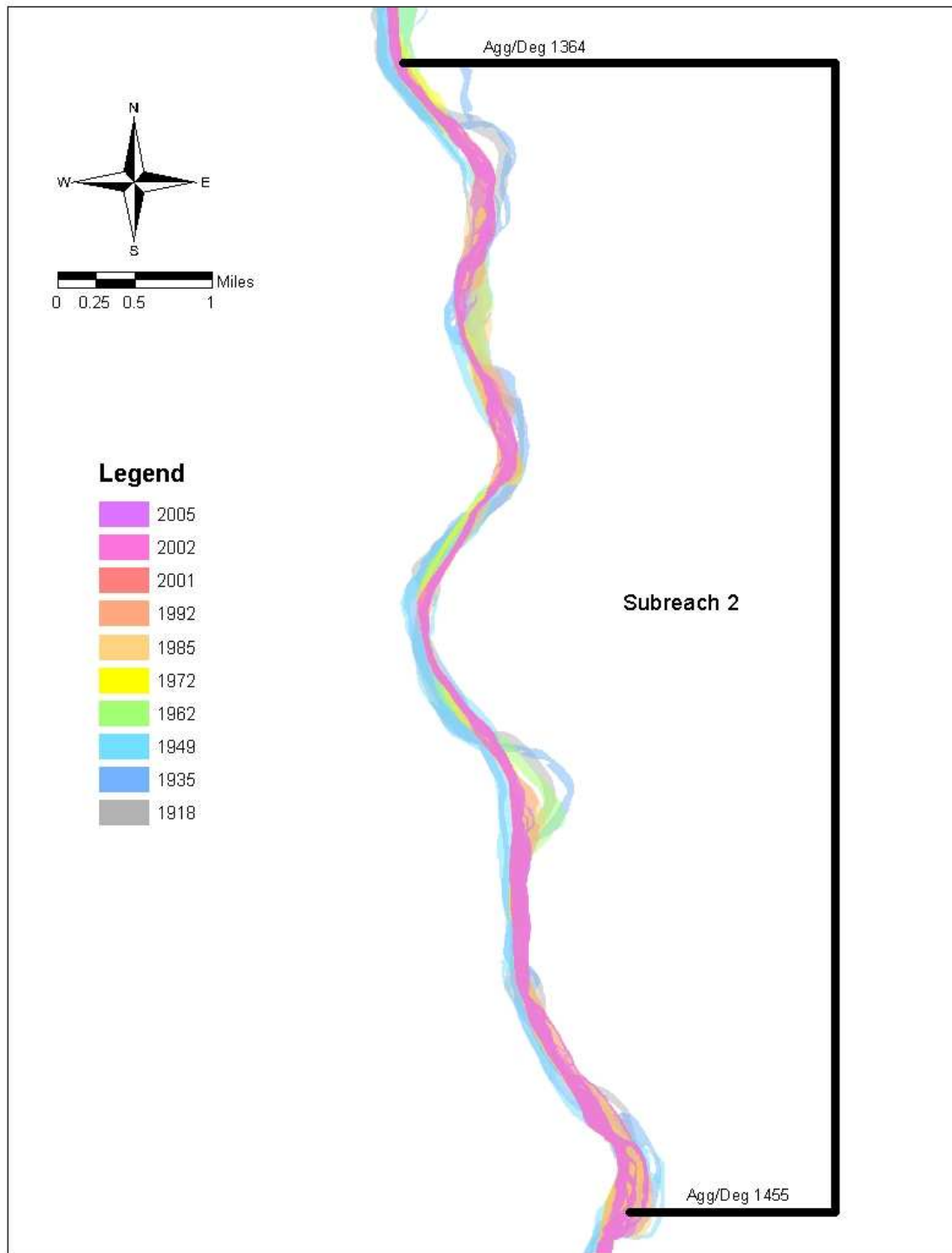


Figure 3.13 Historical planforms of Subreach 2

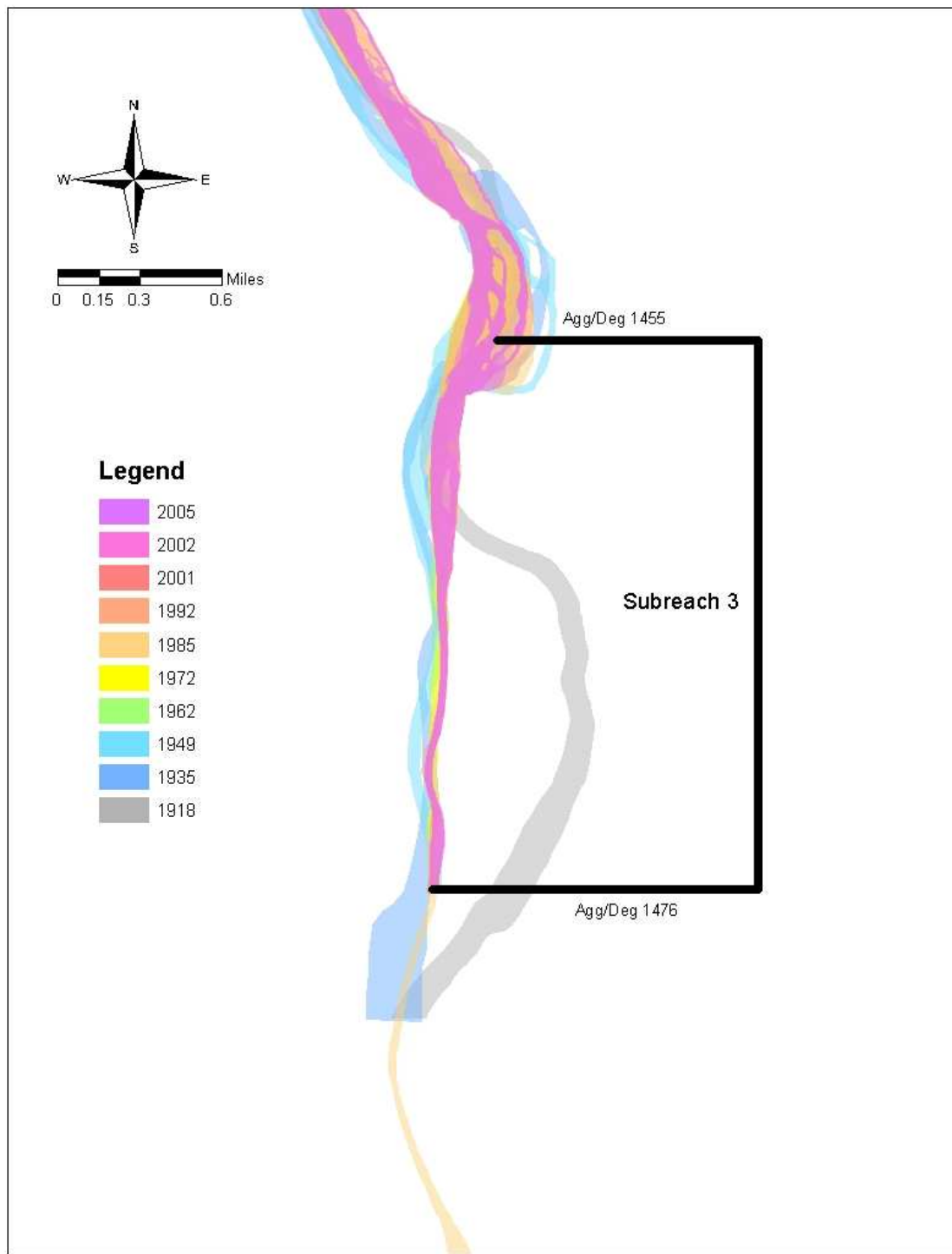


Figure 3.14 Historical planforms of Subreach 3

To obtain the values needed in the quantitative channel classification methods, a HEC-RAS model of the reach was run at the bankfull discharge of 5000 cfs. The model

was run in years that Agg/Deg survey information was available. Because the channel bed is not clearly defined in the Agg/Deg surveys, available SO survey line information was added to the models to increase detail. Measurements of the channel and valley lengths were obtained from aerial photos in GIS. Table 3.7 shows the input values obtained from HEC-RAS and GIS. Channel characteristics were averaged for each subreach and the overall reach using weighted averages based on half the distance to the next upstream and downstream cross-sections.

Table 3.7 Channel Classification Inputs

	Q (cfs)	Channel Slope (ft/ft)	Valley Slope (ft/ft)	d ₅₀ (mm)	Bankfull Width (ft)	Flood Prone Width (ft)	Depth (ft)	Fr	EG Slope (ft/ft)
1962									
1	5,000	0.00094	0.0010	0.15	1417	2387	1.54	0.39	0.0011
2	5,000	0.00078	0.0009	0.15	774	2344	2.37	0.42	0.0008
3	5,000	0.00055	0.0006	0.15	3234	5247	2.82	0.33	0.0010
Total	5,000	0.00080	0.0009	0.15	1291	2713	2.16	0.39	0.0009
1972									
1	5,000	0.00089	0.0010	0.11	1416	2113	1.86	0.39	0.0010
2	5,000	0.00080	0.0009	0.11	1296	2077	2.51	0.43	0.0008
3	5,000	0.00070	0.0007	0.11	3156	5500	2.86	0.36	0.0009
Total	5,000	0.00082	0.0009	0.11	1572	2503	2.34	0.40	0.0009
1985									
1	5,000	0.00082	0.0009	0.15	1417	2393	2.51	0.40	0.0012
2	5,000	0.00086	0.0009	0.13	774	2407	1.96	0.42	0.0010
3	5,000	0.00052	0.0005	0.10	3239	5535	2.75	0.28	0.0004
Total	5,000	0.00081	0.0009	0.13	1295	2781	2.24	0.40	0.0010
1992									
1	5,000	0.00076	0.0008	0.22	468	2082	3.41	0.41	0.0009
2	5,000	0.00081	0.0009	0.27	881	2593	2.23	0.43	0.0010
3	5,000	0.00072	0.0007	0.25	1287	5203	3.20	0.39	0.0007
Total	5,000	0.00078	0.0009	0.23	796	2739	2.74	0.42	0.0009
2002									
1	5,000	0.00078	0.0009	0.37	505	1775	3.04	0.46	0.0010
2	5,000	0.00077	0.0009	0.30	1024	2518	2.15	0.42	0.0009
3	5,000	0.00076	0.0008	0.24	2000	4867	2.37	0.36	0.0006
Total	5,000	0.00077	0.0009	0.31	982	2572	2.46	0.42	0.0009

The channel classification for each subreach and the overall reach in the five years analyzed are given in Table 3.8. The table shows that none of the methods shows a distinct change in the channel planform over time. The channel morphology methods by Parker (1976) and Rosgen (1994) are the only methods that show variation over time and/or between the subreaches in a given year. Leopold and Wolman (1957), Schumm and Khan (1972), and Nanson and Croke (1992) all indicated a straight planform for all subreaches in all years, which is true because the sinuosity in all cases is below 1.5. However, this generalization does not clearly explain the river's situation. Lane (1957, from Richardson et. al, 2001) and Parker (1976) both classify the channel as in a transitional state between meandering and braided. Parker (1976) indicates an overall tendency toward braiding from 1962-1985 and a tendency toward meandering in 1992 and 2002. Rosgen (1994) classifies the channel as B5c from 1962 to 1985 and as C5c from 1992 to 2002. The B5c classification indicates a channel that is moderately entrenched, with a slope of less than 0.02 and a large width to depth ratio. The C5c classification is similar to the B5c classification except that C5c channels are only slightly entrenched and have well developed floodplains. Henderson (1984) shows a braided classification for all years and subreaches, while Chang (1979) gives a meandering or steep braided classification.

When compared with the observations from the aerial photographs, the methods that indicate a straight or braided channel classification provide the best representation of the actual channel characteristics. Because braiding is only seen in large sections of the channel at low flows, the straight classification given by Leopold and Wolman (1957), Schumm and Khan (1972), and Nanson and Croke (1992) is the most accurate for the

bankfull discharge of 5000 cfs. Because each of Rosgen's (1994) classifications is very specific, this method also results in a reasonable description of the study reach. The sinuosity of the reach is the only property that is not accurately described. Both the C5c and B5c classifications indicate that the channel should have a sinuosity greater than 1.2. The sinuosity in the reach may be less than the required 1.2 because the levees placed along the channel have forced the channel into a confined space.

Table 3.8 Channel Classification Results

	D ₅₀ type	Slope-discharge			Channel Morphology		Stream Power		
		Leopold and Wolman	Lane	Henderson	Schumm & Khan	Rosgen	Parker	Nanson & Croke	Chang
1962									
1	Fine Sand	Straight	Intermediate	Braided	Straight	B5c	Braiding / Transitional	Straight	Meandering to Steep Braided
2	Fine Sand	Straight	Intermediate	Braided	Straight	C5c	Meandering / Transitional	Straight	Meandering to Steep Braided
3	Fine Sand	Straight	Intermediate	Braided	Straight	B5c	Braiding / Transitional	Straight	Meandering to Steep Braided
Total	Fine Sand	Straight	Intermediate	Braided	Straight	B5c	Braiding / Transitional	Straight	Meandering to Steep Braided
1972									
1	Very Fine Sand	Straight	Intermediate	Braided	Straight	B5c	Braiding / Transitional	Straight	Meandering to Steep Braided
2	Very Fine Sand	Straight	Intermediate	Braided	Straight	B5c	Meandering / Transitional	Straight	Meandering to Steep Braided
3	Very Fine Sand	Straight	Intermediate	Braided	Straight	B5c	Braiding / Transitional	Straight	Meandering to Steep Braided
Total	Very Fine Sand	Straight	Intermediate	Braided	Straight	B5c	Braiding / Transitional	Straight	Meandering to Steep Braided
1985									
1	Fine Sand	Straight	Intermediate	Braided	Straight	B5c	Braiding / Transitional	Straight	Meandering to Steep Braided
2	Fine Sand	Straight	Intermediate	Braided	Straight	C5c	Meandering / Transitional	Straight	Meandering to Steep Braided
3	Very Fine Sand	Straight	Intermediate	Braided	Straight	B5c	Braiding / Transitional	Straight	Meandering to Steep Braided
Total	Fine Sand	Straight	Intermediate	Braided	Straight	B5c	Braiding / Transitional	Straight	Meandering to Steep Braided
1992									
1	Fine Sand	Straight	Intermediate	Braided	Straight	C5c	Meandering / Transitional	Straight	Meandering to Steep Braided
2	Medium Sand	Straight	Intermediate	Braided	Straight	C5c	Meandering / Transitional	Straight	Meandering to Steep Braided
3	Fine Sand	Straight	Intermediate	Braided	Straight	C5c	Meandering / Transitional	Straight	Meandering to Steep Braided
Total	Fine Sand	Straight	Intermediate	Braided	Straight	C5c	Meandering / Transitional	Straight	Meandering to Steep Braided
2002									
1	Medium Sand	Straight	Intermediate	Braided	Straight	C5c	Meandering / Transitional	Straight	Meandering to Steep Braided
2	Medium Sand	Straight	Intermediate	Braided	Straight	C5c	Meandering / Transitional	Straight	Meandering to Steep Braided
3	Fine Sand	Straight	Intermediate	Braided	Straight	C5c	Braiding / Transitional	Straight	Meandering to Steep Braided
Total	Medium Sand	Straight	Intermediate	Braided	Straight	C5c	Meandering / Transitional	Straight	Meandering to Steep Braided

3.2.3 Sinuosity Methods

The sinuosity of the Escondida reach, as well as the sinuosity of the three sub-reaches, was measured in GIS from aerial photographs of the reach. The valley length was measured for the entire reach and for each subreach as the straight-line distance between the upstream and downstream extents of the reach. The channel length was measured by estimating the location of the river thalweg based on the aerial photographs and planform delineations. The channel length was divided by the valley length to calculate the sinuosity.

Some difficulty was encountered when estimating the river thalweg due to varying quality of aerial photographs. In addition, aerial photographs were unavailable for 1985, so Reclamation's channel planform was used to estimate the channel and valley lengths for that year. The upstream and downstream extents of the Escondida reach were both relocated during the period of study. The downstream extent was relocated between 1935 and 1949, and the upstream extent was relocated between 1949 and 1962. This resulted in a valley length that was not identical for all years measured.

3.2.4 Sinuosity Results

As seen in Table 3.9, the overall sinuosity decreased from 1.19 to 1.09 between 1918 and 2005. Although the trend was toward a decreasing sinuosity, there were increases in the total channel sinuosity in 1972, 1992, and 2002. Figure 3.15 shows how the sinuosity changed in each subreach and in the entire reach over time.

Table 3.9 Sinuosity Changes

	1918	1935	1949	1962	1972	1985	1992	2001	2002	2005
Subreach 1	1.13	1.15	1.12	1.10	1.16	1.10	1.09	1.09	1.10	1.09
Subreach 2	1.21	1.14	1.12	1.12	1.11	1.09	1.13	1.12	1.12	1.10
Subreach 3	1.22	1.06	1.04	1.01	1.01	1.02	1.02	1.03	1.04	1.02
Total	1.19	1.13	1.11	1.10	1.12	1.08	1.10	1.10	1.11	1.09

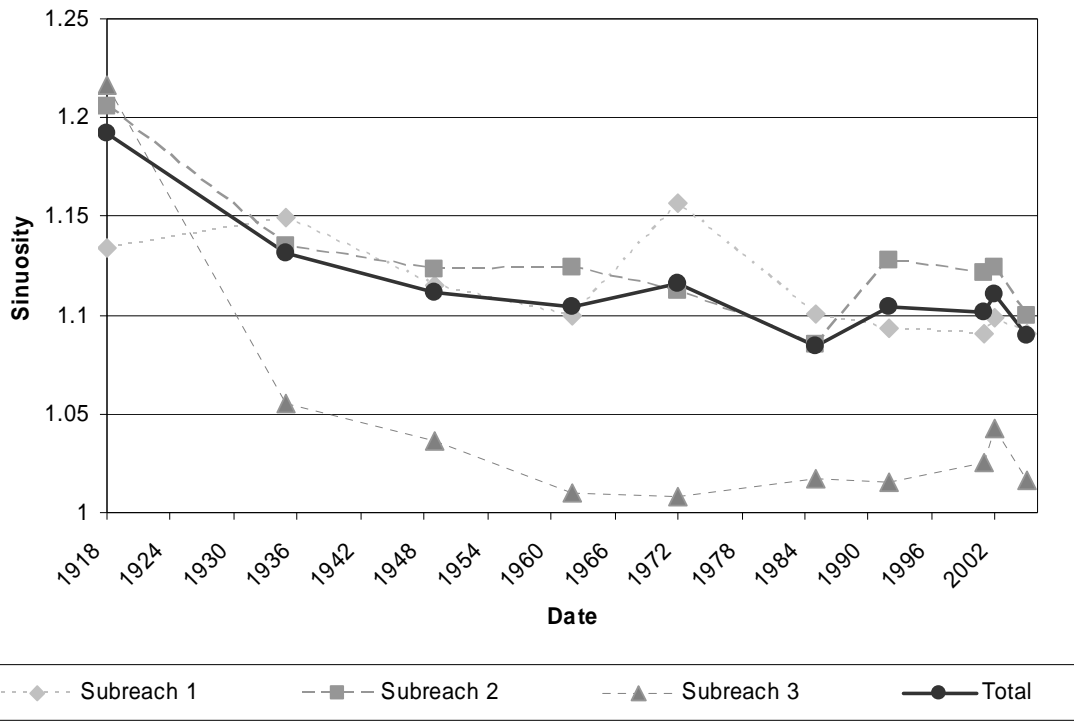


Figure 3.15 Sinuosity

Subreach 3 showed a significant decrease between 1918 and 1935. The sinuosity of this reach continued a steady decrease until 1985 when the sinuosity began to increase. This increase lasted until 2002, when sinuosity decreased again to its current form. Subreach 2 also began with a trend toward decreasing sinuosity. The sinuosity of subreach 2 followed that of subreach three with the exception of a slight increase seen in 1962. The sinuosity of subreach 1 alternated between increasing and decreasing more than the other reaches. An increase in sinuosity was seen between 1918 and 1935,

followed by a decreasing trend that continued until 1962. A sharp increase in 1972 was followed by a steady decrease in sinuosity until 2002. In 2002, as in the other reaches, the sinuosity increased, only to decrease again in 2005.

In 1918, the sinuosity of subreach 3 was slightly higher than the other reaches, but following 1935, it remained far less sinuous than the other reaches. Subreach 1 and subreach 2 tended to have sinuosity values close to each other and close to the overall sinuosity. This may be due to the straightening seen at the downstream extent of the reach extending far into subreach 3. Although pronounced straightening also occurred at the upstream extent, it had less of an effect on the sinuosity of subreach 1 because it is much longer than subreach 3.

3.2.5 Longitudinal Profile Methods

Thalweg Elevation

The thalweg elevation was calculated as the lowest point in the channel based on the SO-line surveys. Because the SO-line surveys offer more detailed cross section information, they were used instead of the Agg/Deg surveys. SO-line data were only available from 1987-2005.

Mean Bed Elevation

Trends in mean bed elevation were evaluated using the Agg/Deg survey data. The method used to generate the Agg/Deg surveys from aerial photographs results in the mean bed elevation being displayed as the elevation of the cross-section anywhere water was present in the survey. This elevation was used to show the changes in mean bed

elevation through time. Because the SO-lines usually fall at the same location as the Agg/Deg lines, only the Agg/Deg lines were used to analyze the mean bed elevation. The change in mean bed elevation at each cross-section was evaluated, along with the changes in the average mean bed elevation by subreach. The averages calculated for the subreaches are based on weighted averages derived from half the distance between next upstream and downstream Agg/Deg line.

Energy Grade Slope

The energy grade line (EGL) slope for the reach was obtained from HEC-RAS models run at the bankfull discharge of 5000 cfs. The average EGL slope for each subreach and the entire reach was calculated in the same manner as the average mean bed elevation.

Water Surface Slope

The water surface slope between cross-sections was calculated from the water surface elevation at each cross section determined by HEC-RAS and distance between cross-sections. Because the water surface slope was computed as a property of the area between two cross-sections rather than a property of the cross-section itself, the weighting scheme used to calculate the subreach averages was based on the distance to the next downstream cross section.

3.2.6 Longitudinal Profile Results

Thalweg Elevation

Figure 3.16 shows the change of the thalweg elevation at each SO-line over time. Only SO-lines with enough years of sample data to provide useful information about trends were plotted. The cross-sections in subreach 1, SO-lines 1313-1360 (shown in shades of orange) decrease as much as 5 feet and then increase several feet. In subreach 2 (shown in shades of green), SO-lines 1380-1414 have a steadily decreasing trend with an overall degradation of around 5 feet. The thalweg elevation in subreach 2, SO-lines 1420-1450, alternates between increasing and decreasing with nearly every sample, resulting in little long-term change. The general trend at the only SO-line in subreach 3 (shown in blue) is one of an initial degradation of about 5 feet over 7 years, followed by a generally increasing trend for the next 5 years. Two of the data points in this cross-section do not seem reasonable as they indicate one-year aggradation and degradation of more than 10 feet. Surveying error is a likely explanation for these discrepancies. In addition, the data sampled in 2005 indicate an increase of between 10 and 15 feet in just one year. This is an unlikely scenario, and the data at these points were not considered in the above discussion.

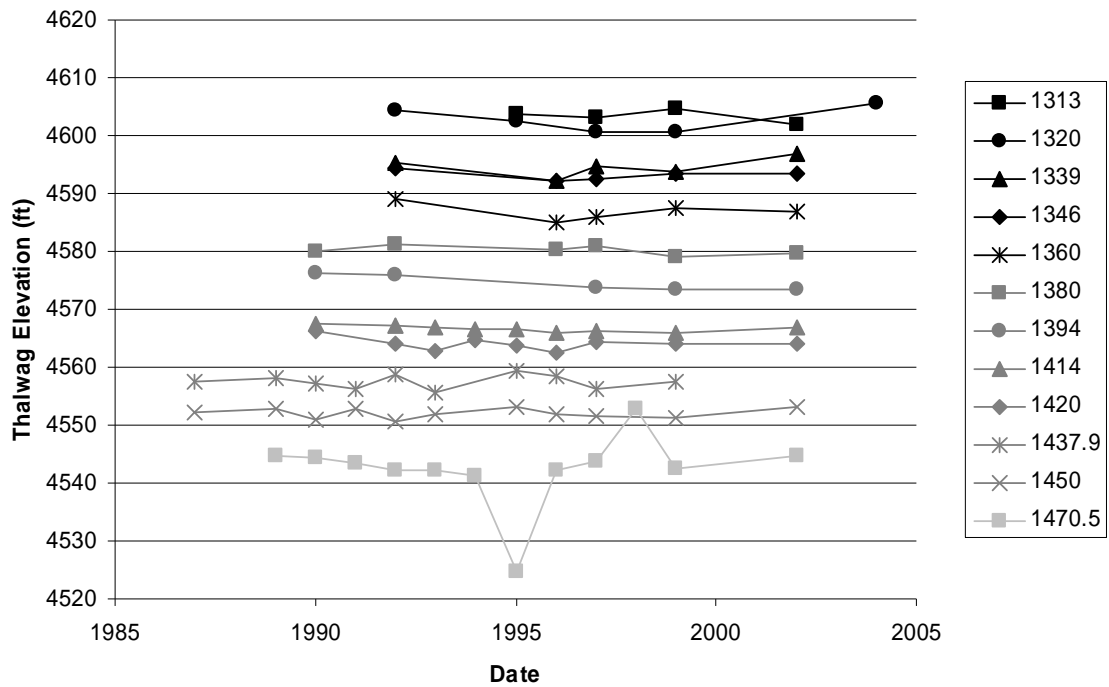


Figure 3.16 Change in thalweg elevation by SO-line

The marked increase in thalweg elevation in 2005 can be more clearly seen in Figure 3.17. This figure shows the thalweg elevation profile of the entire reach. Subreach 3 has had the most change in since 1987, while subreach 2 seems to have been the most stable in recent years. Subreach 1 has seen some recent degradation of the thalweg elevation, but the changes are not as large as those seen in subreach 3.

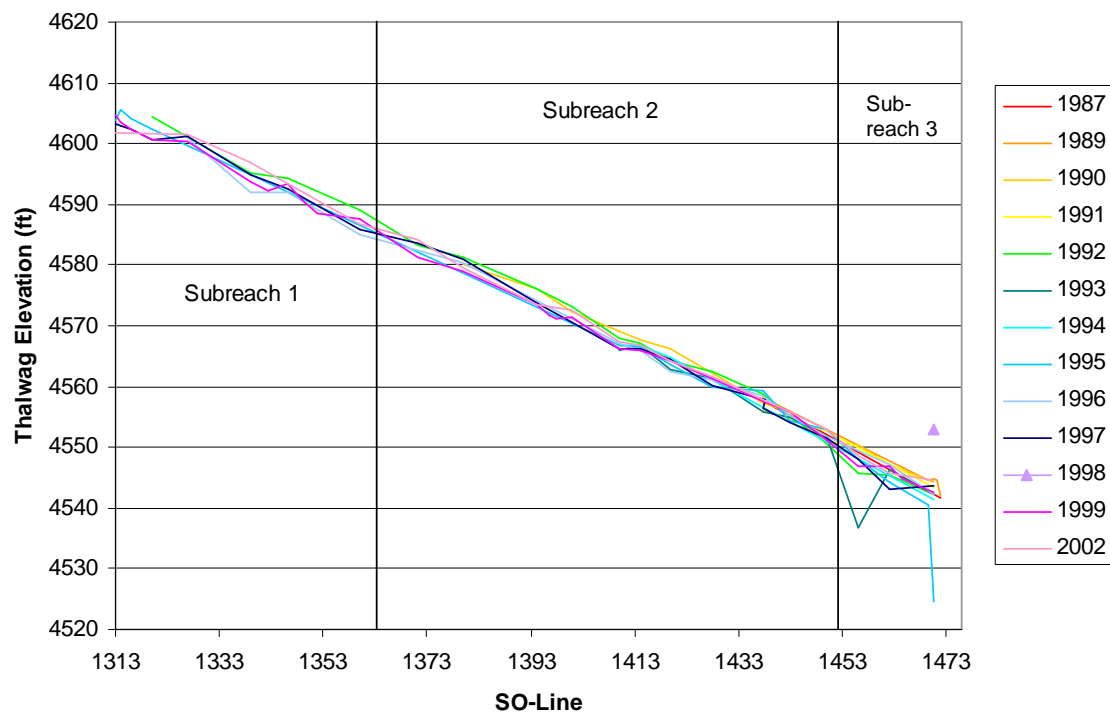


Figure 3.17 Thalweg elevation profile

Mean Bed Elevation

Changes in mean bed elevation over time are shown in Figure 3.18 for each subreach and for the entire reach.

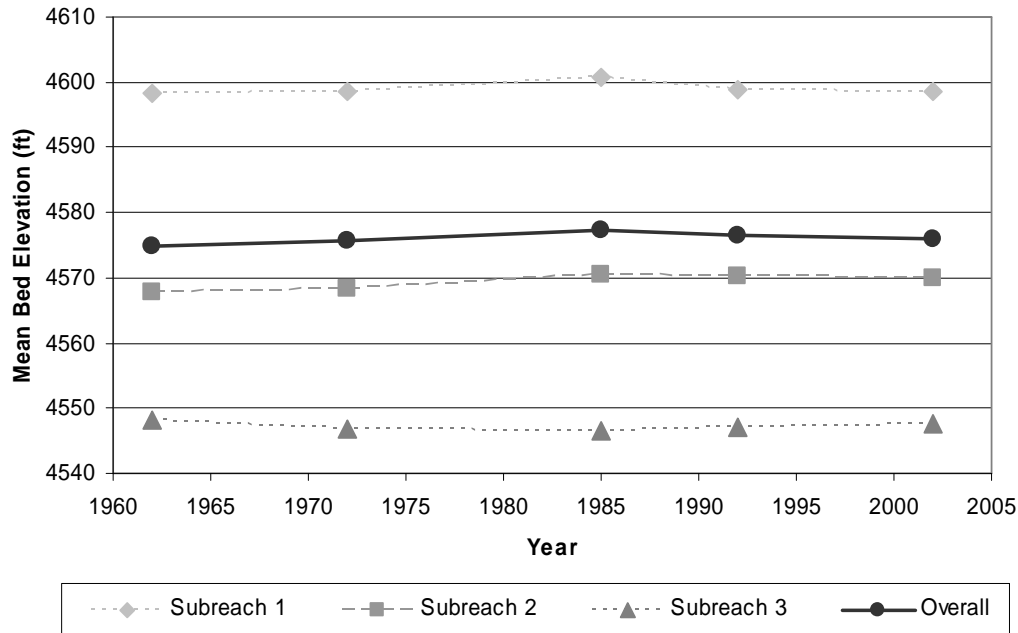


Figure 3.18 Reach averaged mean bed elevation

Subreach 1 and subreach 2 show an average increase of about 2 feet between 1962 and 1985. The mean bed elevation in these two subreaches then decreases between 1985 and 2002. Subreach 3 follows an opposite trend of first decreasing and then increasing.

The change in mean bed elevation at each Agg/Deg line can be seen in Figures 3.19 and 3.20. Degradation was seen at the upstream and downstream extents of the reach between 1962 and 1985, with aggradation in the rest of the reach. The maximum change in mean bed elevation took place at Agg/Deg line number 1343 with almost 7 feet of aggradation. This is opposite of the degradational trend observed in an upstream reach during the same time period (Bauer 2000).

Severe degradation took place at many cross-sections in subreach 1 between 1985 and 2002, with a maximum degradation of nearly 5 feet at Agg/Deg 1337. Degradation also dominated subreach 2 during this time period, but the changes were not as severe as in subreach 1. The cross-sections in subreach 3 aggraded as much as 3 feet at Agg/Deg 1469 between 1985 and 2002.

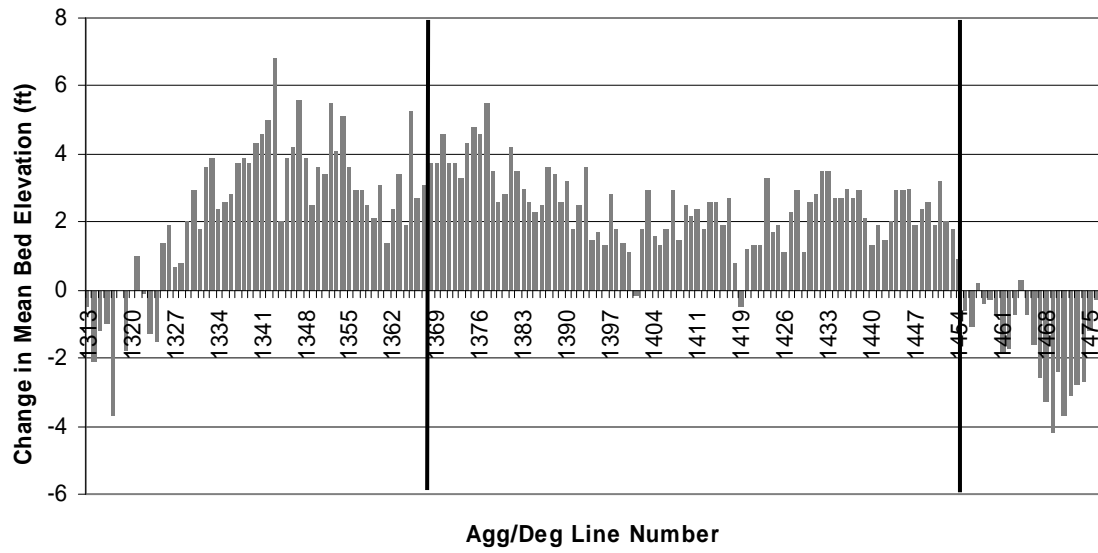


Figure 3.19 Change in mean bed elevation between 1962 and 1985

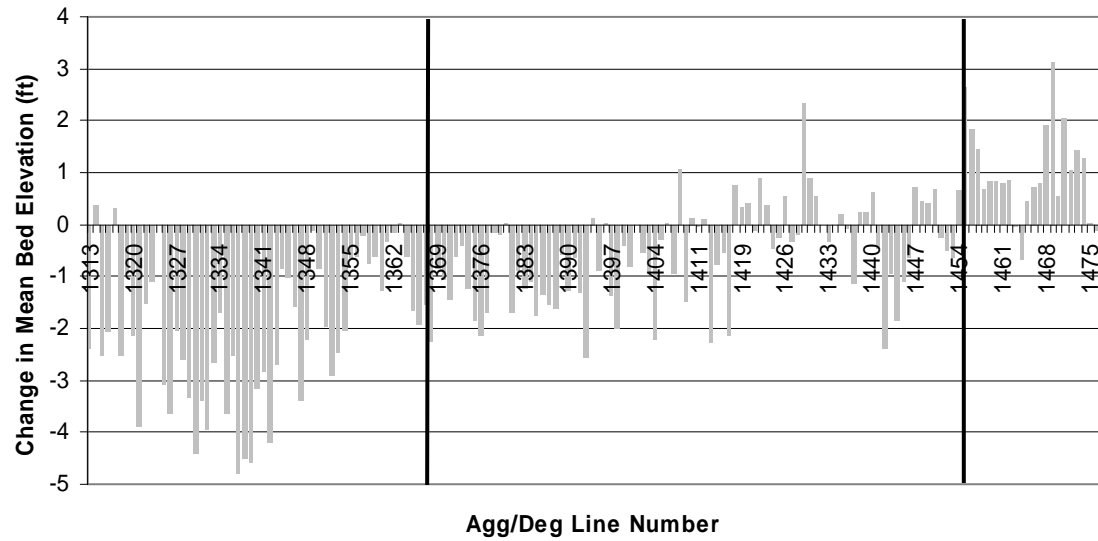


Figure 3.20 Change in mean bed elevation between 1985 and 2002

Energy Grade Slope

Figure 3.21 shows the change in EGL slope with time for each subreach and the entire reach.

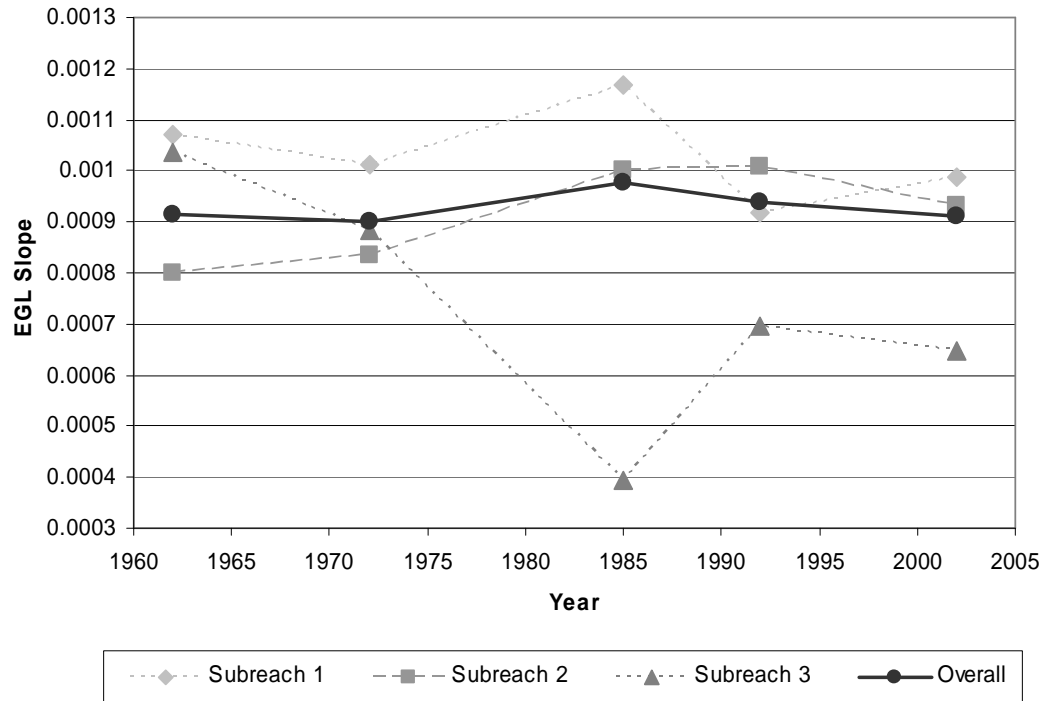


Figure 3.21 Energy grade line slope

In 1962 and 1972, the EGL slope for all three subreaches was within 0.0003 ft/ft of one another. In 1985, however, the EGL slope of subreach 3 decreased significantly, but subreaches one and two increased at approximately the same rate. By 2002, subreach 1 and subreach 2 had similar EGL slopes, while the EGL slope for subreach 3 was still far lower.

Water Surface Slope

The average water surface slope by subreach and for the entire reach is shown in Figure 3.22.

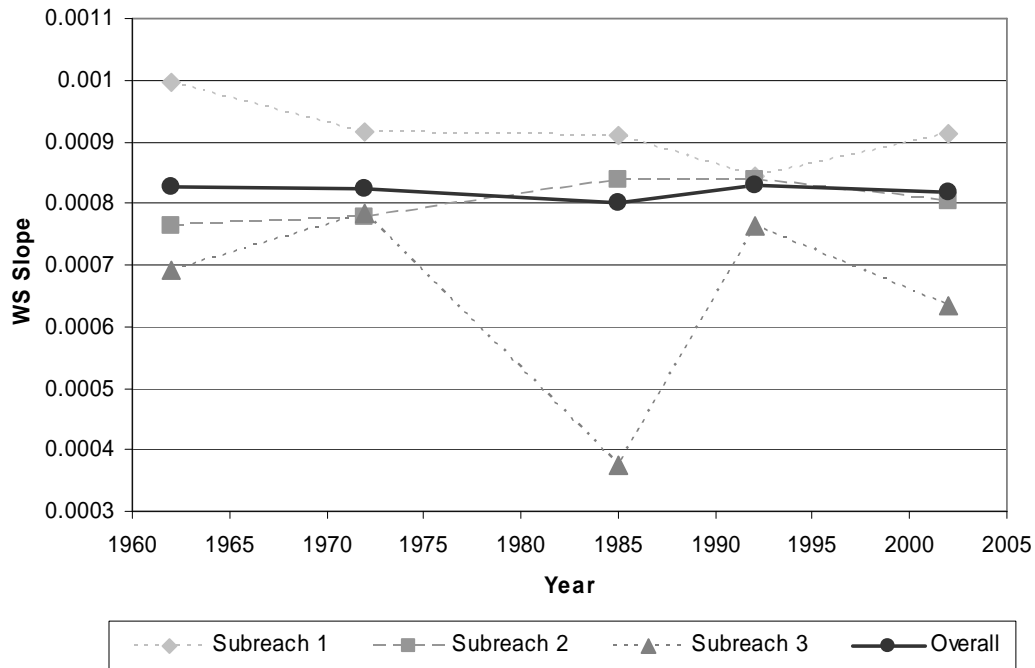


Figure 3.22 Water surface elevation slope

The water surface slope of subreach 1 showed a decreasing trend from 1962 to 1992 with an increase occurring between 1992 and 2002. Subreach 2 showed an opposite trend with an increase in water surface slope between 1962 and 1985, little change between 1985 and 1992, and a decrease between 1992 and 2002. The water surface slope of subreach 3 was highly variable. This reach showed an increase from 1962 to 1972 followed by a dramatic decrease in 1985. In 1992, the water surface slope increased again to near 1972 levels before falling again in 2002.

3.2.7 Channel Geometry Methods

Trends in geometric properties were analyzed from HEC-RAS model runs using the bankfull discharge of 5000 cfs. The HEC-RAS geometry files were available from Reclamation for 1962, 1972, 1985, 1992, and 2002. Each model used 162 cross-sections at a spacing of approximately 500 feet. A Manning's n value of 0.02-0.024 was used for the main channel and a Manning's value of 0.1 was used for the overbank area. Manning's n values, bank station and levee locations, and downstream reach lengths were originally determined by Reclamation. Each geometry file was evaluated and compared to GIS aerial photography for the corresponding year. Adjustments to the bank stations, levee locations, and reach lengths were made based on engineering judgment to best represent the actual channel conditions.

Channel geometry parameters calculated at each cross section by HEC-RAS include:

Cross-Sectional Area	A
Top Width	W
Wetted Perimeter	P _w
Hydraulic Depth	D
Velocity	V
Froude Number	F _r

The numerical results from the HEC-RAS output can be found in Appendix C. The above geometric parameters and other properties available from HEC-RAS were used to calculate two additional channel geometry properties. These properties include:

Max Depth
 $D_{max} = \text{Water Surface Elevation} - \text{Minimum Channel Elevation}$
Width/Depth Ratio
 $W/D = \text{Top width} / \text{Hydraulic Depth}$

The average values of the eight channel properties were calculated using the same weighting factors as the EGL slope calculations.

3.2.8 Channel Geometry Results

Figure 3.23 shows the trends in the average cross-sectional area, top width, wetted perimeter, hydraulic depth, maximum depth, channel velocity, Froude number, and width/depth ratio in each subreach and in the overall reach.

Top width, cross-sectional area, and wetted perimeter all follow similar trends. The cross-sectional area and wetted perimeter show nearly identical trends. This is reasonable because the two parameters are a function of the width and depth. The top width and wetted perimeter not only have similar trends; they also have similar magnitudes. This indicates that the channel is very wide compared to the depth.

The trends in the width to depth ratio indicate a general trend toward a deeper, narrower channel until 1992, and a slightly wider, shallower channel in 2002. In addition, the high values of the width to depth ratio further reinforce the idea that the channel is very wide compared to its depth.

The hydraulic depth and the maximum depth are also closely related. The hydraulic depth is the depth of a rectangular channel which, when divided by the top width of the channel, gives the cross-sectional area of the channel. The maximum depth is the maximum depth found in the channel. The overall trend for both parameters is very similar. Both parameters show an increase in 1992, followed by a decrease in 2002. This correlates well with the decrease in width in 1992 and the subsequent increase in 2002, because as the channel becomes deeper, it must also narrow to maintain continuity.

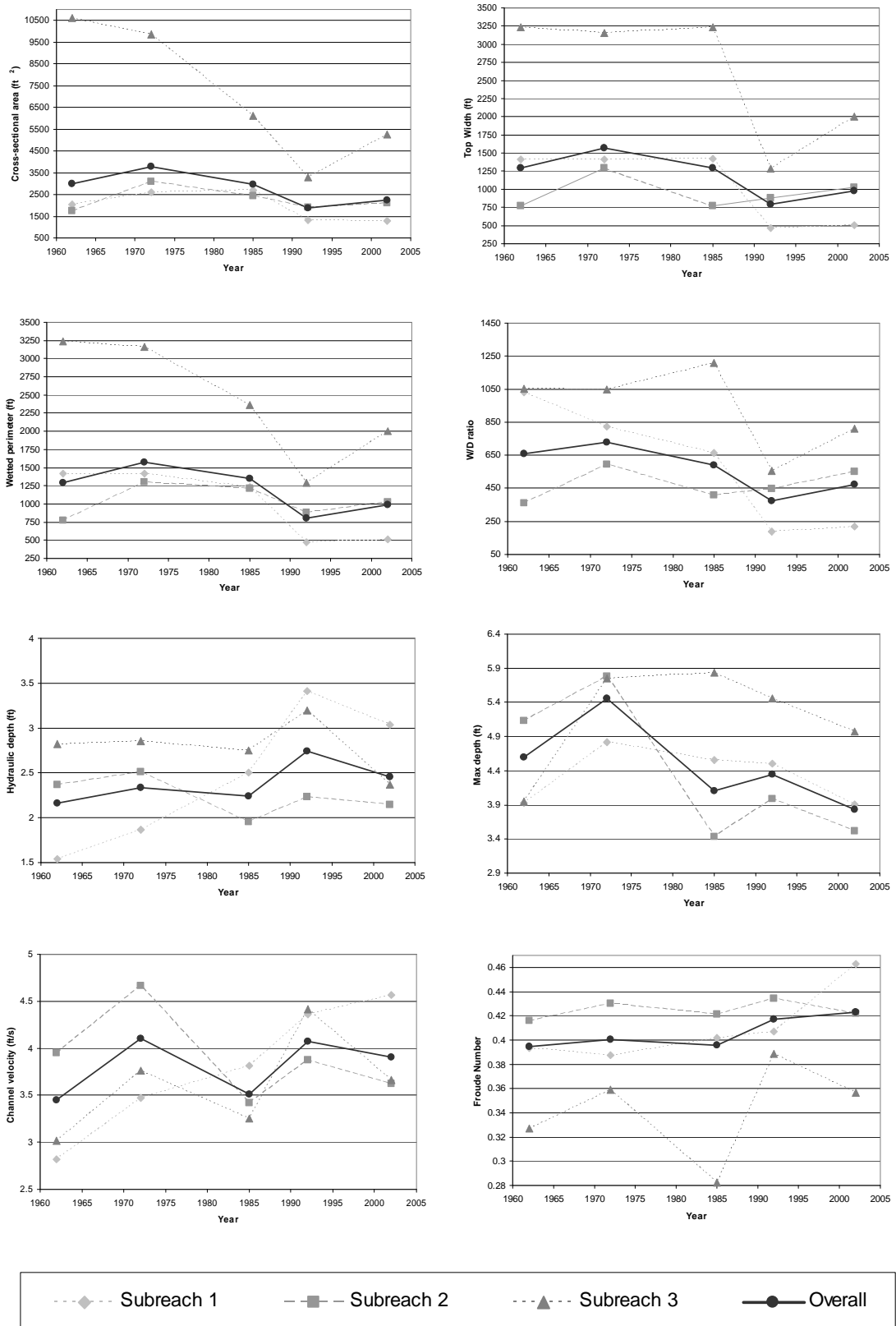


Figure 3.23 Channel Geometry Properties

The trends in velocity are generally opposite the trends observed in the width to depth ratio. This suggests that as the channel becomes narrower, the velocity in the channel increases. The opposite correlation can also be true. An increased channel velocity may scour the channel bed causing increased depth and decreased width.

The average Froude number in the channel in all subbreaches and in all years is well below one, indicating that the flow in the channel is generally in the sub-critical regime. This is expected because super-critical flow would be very difficult to maintain in a sand-bed channel. In addition, the general trends seen in the channel velocity are similar to those seen in the Froude number.

3.2.9 Bend Migration Methods

General observations of the bend migration in the reach were performed using aerial photographs and channel planform delineations in GIS. Areas of movement were identified visually. The changes at the locations of movement were then measured and further analyzed using GIS.

3.2.10 Bend Migration Results

Observations made of recent bend migration indicate that since 1992, very little movement has occurred in the reach. However, observation of bend migrations since 1962 indicates that movement has occurred between 1962 and 1992. Table 3.10 shows the locations of significant movement for each time period analyzed. The magnitude and direction of the movement are also included.

Table 3.10 Bed Migration

Year	Agg/Deg Number	Movement	
		Magnitude (ft)	Direction
1985-1992			
	1326-1332	330	R
	1333	120	L
	1352	100	R
	1376	220	L
	1471	150	R
1972-1985			
	1326	200	L
	1363	240	R
	1397-1405	300	L
	1413	120	L
	1421	100	R
	1467	100	L
1962-1972			
	1326	390	R
	1343	295	L
	1347	335	R
	1355	215	R
	1375	250	L
	1378-1386	590	R
	1419-1426	850	R

A few locations showed either very large movement in a single observation period or continued movement over several observation periods. Figure 3.24 shows the progressive channel location near Agg/Deg 1326, Figure 3.25 shows the 590 foot movement observed between Agg/Deg 1378 and Agg/Deg 1386 between 1962 and 1972, and Figure 3.26 shows the 850 foot migration of Agg/Deg 1419-1426 between 1962 and 1972.

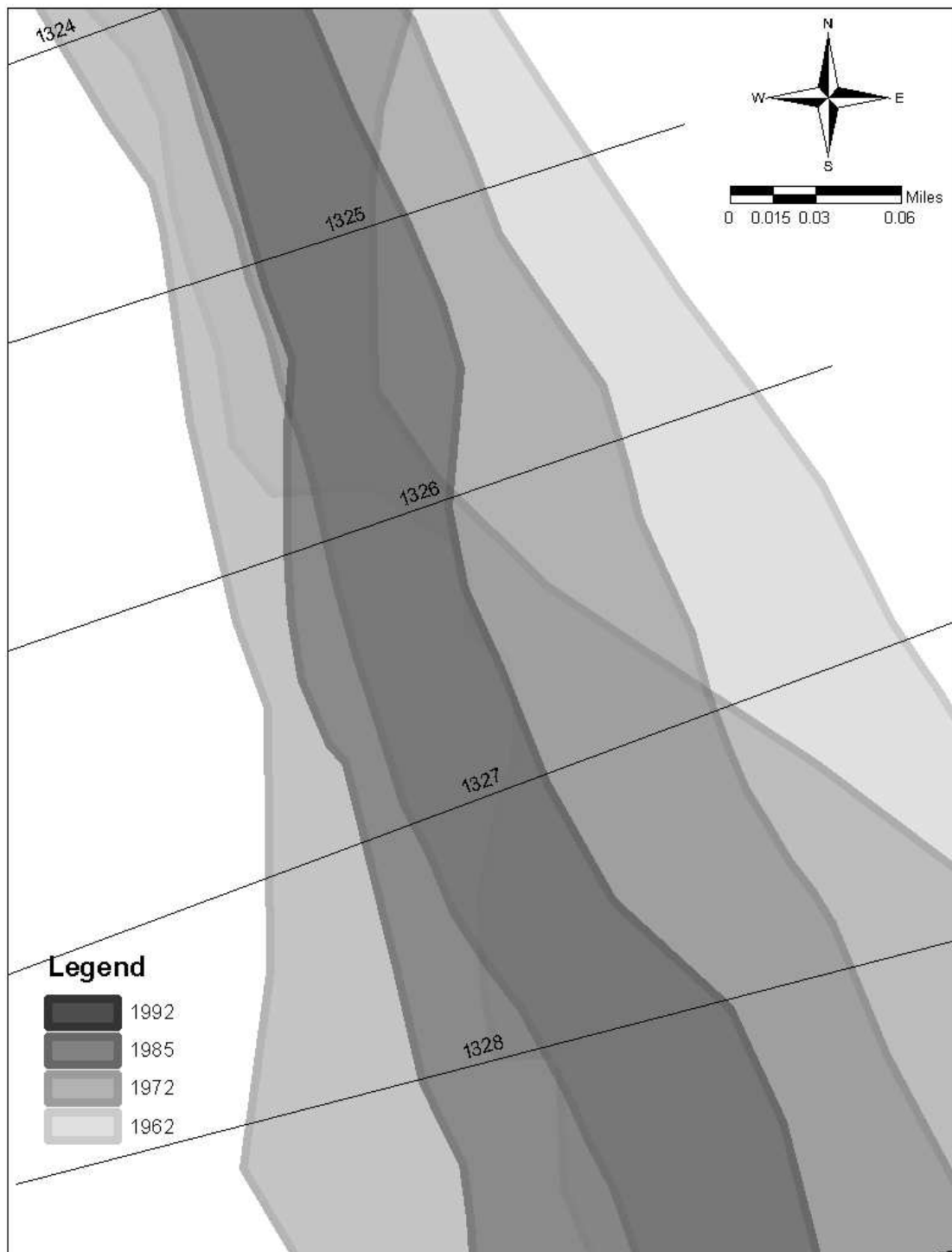


Figure 3.24 Bend migration at Agg/Deg 1326

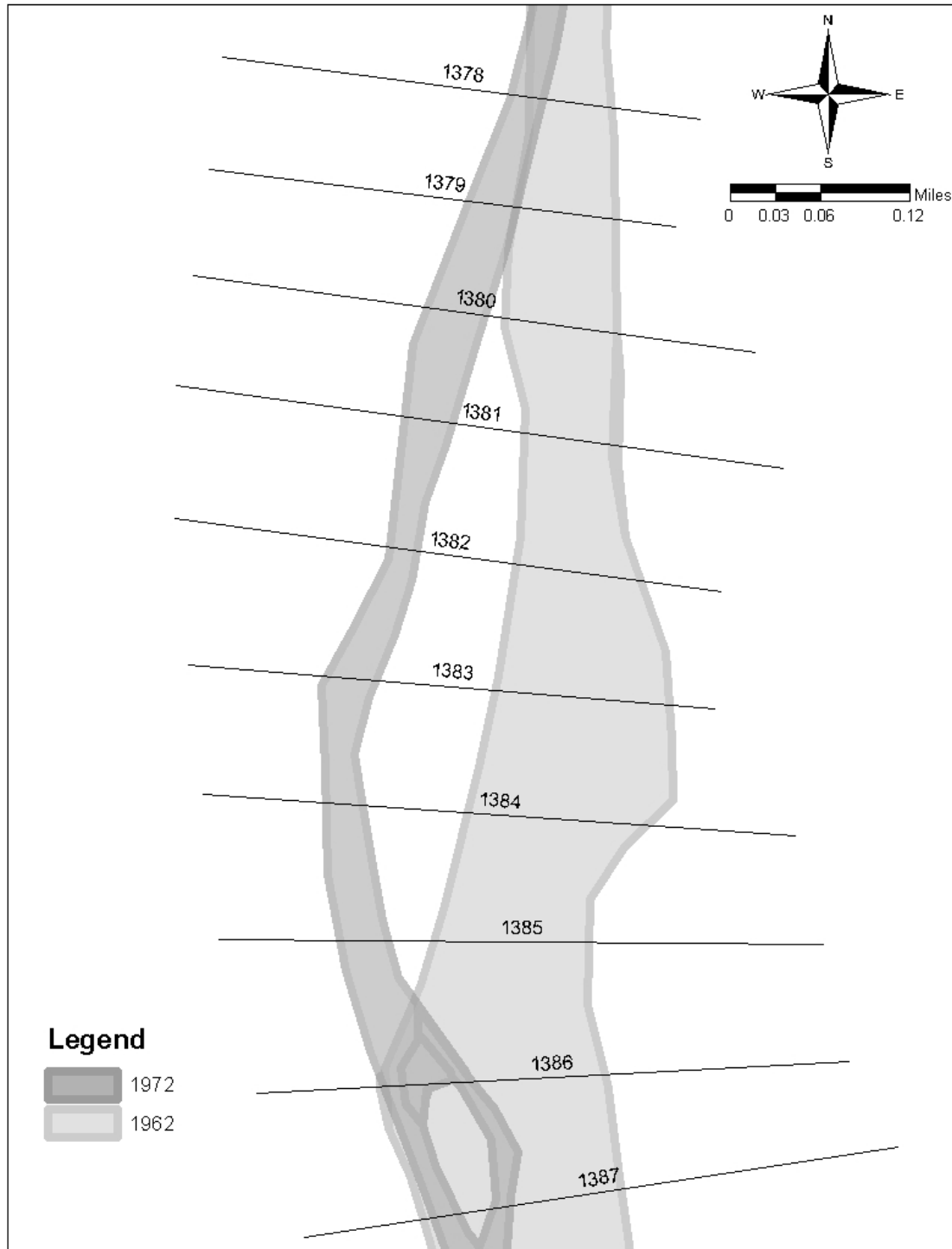


Figure 3.25 Bend migration at Agg/Deg 1378-1386

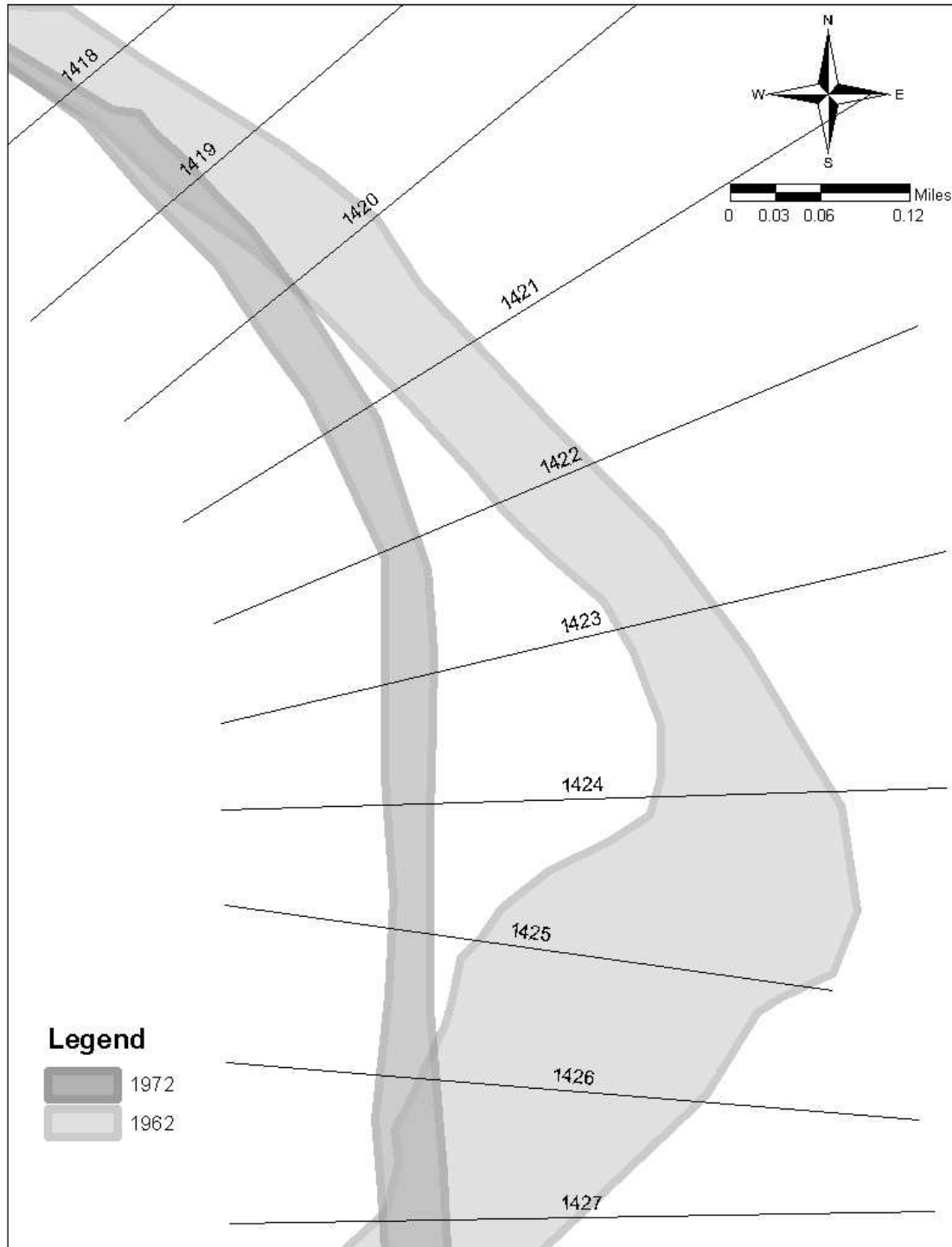


Figure 3.26 Bend migration at Agg/Deg 1419-1426

3.2.11 Bed Material Analysis Methods

The bed material surveys taken at SO-lines were used to determine the median bed grain size for each subreach. When appropriate data were not available at the SO-lines, bed material from the San Acacia and San Marcial gauges was used. In both 1962 and 1972, bed material data were not available, so the grain sizes from the closest available years were used. When SO-line data were used, the median grain size for the subreach was calculated using a weighted average based on the distance between SO-lines. The gauge data that were most similar to the available SO-line data were used in the absence of SO-line data. Grain size classification was determined using Figure 3.27 from Julien (1998).

Class name	Size range	
	mm	in.
<i>Boulder</i>		
Very large	4,096–2,048	160–80
Large	2,048–1,024	80–40
Medium	1,024–512	40–20
Small	512–256	20–10
<i>Cobble</i>		
Large	256–128	10–5
Small	128–64	5–2.5
<i>Gravel</i>		
Very coarse	64–32	2.5–1.3
Coarse	32–16	1.3–0.6
Medium	16–8	0.6–0.3
Fine	8–4	0.3–0.16
Very fine	4–2	0.16–0.08
<i>Sand</i>		
Very coarse	2,000–1,000	
Coarse	1,000–0,500	
Medium	0,500–0,250	
Fine	0,250–0,125	
Very fine	0,125–0,062	
<i>Silt</i>		
Coarse	0,062–0,031	
Medium	0,031–0,016	
Fine	0,016–0,008	
Very fine	0,008–0,004	
<i>Clay</i>		
Coarse	0,004–0,0020	
Medium	0,0020–0,0010	
Fine	0,0010–0,0005	
Very fine	0,0005–0,00024	

Figure 3.27 Grain size classification (Julien 1998)

3.2.12 Bed Material Analysis Results

Figure 3.28 shows the change in grain size in each subreach. While the entire reach remains in the range of grain sizes for sand, there has been an overall increase in grain size in recent years.

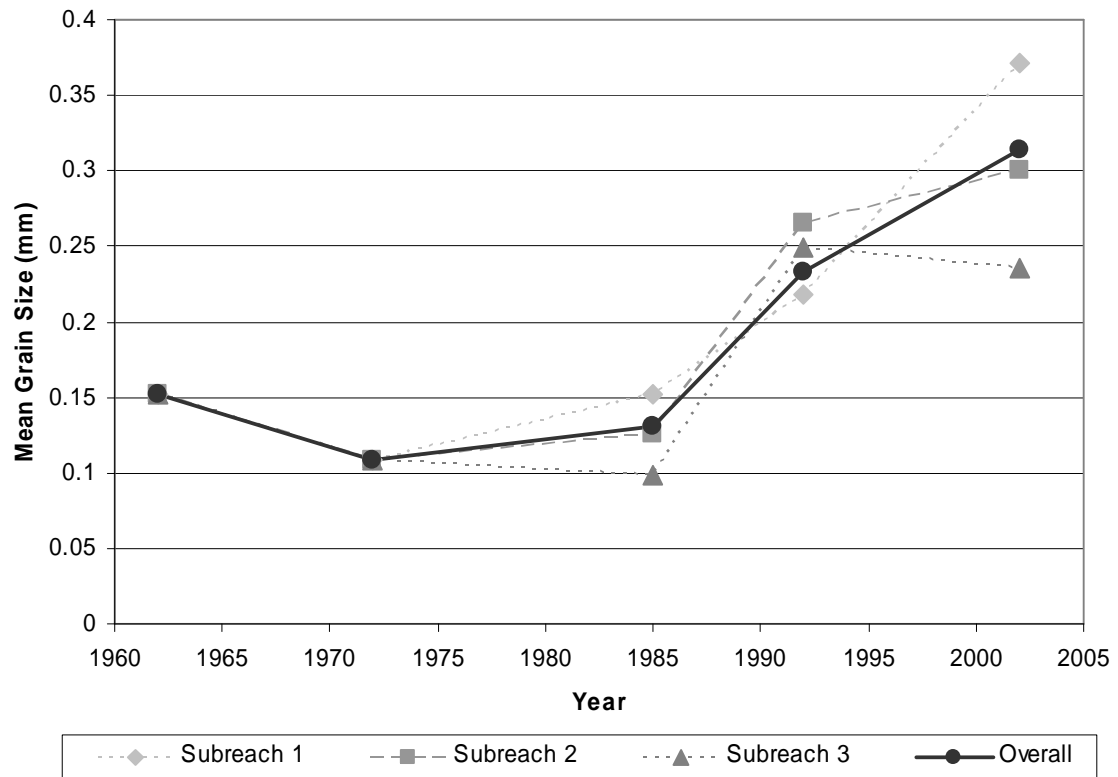


Figure 3.28 Bed material mean grain size

The bed material types are summarized in Table 3.11. The bed material size was obtained from SO-line surveys where available. When SO-line surveys were not available, San Acacia gauge data were used for subreach 1, San Marcial gauge data were used for subreach 3, and an average of San Acacia and San Marcial gauge data were used for subreach 2.

Table 3.11 Bed material type

Subreach	1962	1972	1985	1992	2002
1	Fine Sand	Very Fine Sand	Fine Sand	Fine Sand	Medium Sand
2	Fine Sand	Very Fine Sand	Fine Sand	Medium Sand	Medium Sand
3	Fine Sand	Very Fine Sand	Very Fine Sand	Fine Sand	Fine Sand
Total	Fine Sand	Very Fine Sand	Very Fine Sand	Fine Sand	Medium Sand

The bed material classification has increased from very fine sand in 1972 to medium sand in 2002. Average particle size distributions for each year are shown in Figure 3.29. The particle size distribution also indicates a recent trend toward increasing grain size. Particle-size distributions for each year and subreach are shown in Appendix D.

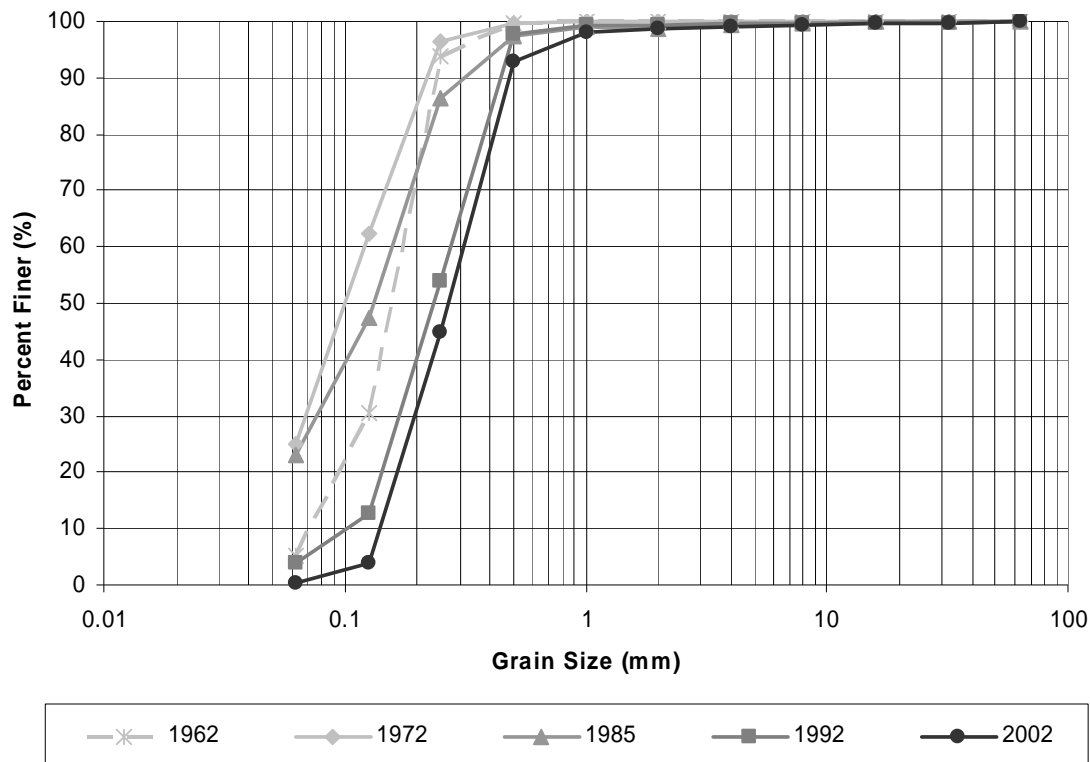


Figure 3.29 Bed material particle size distributions

3.3 Suspended Sediment and Water History

Single and double mass curves were used to show trends in water discharge, suspended sediment discharge, and suspended sediment concentration. A difference mass curve was developed to show trends in suspended sediment continuity. Suspended sediment continuity compares the amount of sediment entering the reach versus the amount of sediment leaving the reach. Discharge and suspended sediment data were compiled from the USGS gauging stations at San Acacia and San Marcial. There were some large gaps in available data. When data were not available for one or both of the elements under consideration, the date was excluded from the cumulative analysis.

3.3.1 Methods

Trends in water and suspended sediment discharge were displayed in single mass curves for each gauge. These graphs show cumulative discharge versus time and cumulative suspended sediment discharge versus time. Suspended sediment discharge versus water discharge was graphed in a double mass curve to show the trends in suspended sediment concentration for both the San Acacia and San Marcial gauges.

To develop the difference mass curve for the suspended sediment continuity analysis, the cumulative difference between the San Acacia gauge, located upstream of the study reach, and the San Marcial gauge, located downstream of the study reach, was plotted versus time. A negative slope shows that more suspended sediment is leaving the reach than entering the reach. A positive slope shows that more suspended sediment is entering the reach than leaving the reach. The contributions of arroyos along the reach were not accounted for, so more sediment may have entered the reach than was recorded

by the San Acacia gauge. In addition, because both gauges are located a considerable distance from the study reach, the suspended sediment readings taken at the gauges may not represent the true amount of suspended sediment entering and leaving the reach.

3.3.2 Results

Single Mass Curves

The single mass curve for water discharge is shown in Figure 3.30. Both the San Acacia (SA) and San Marcial (SM) gauges have similar flow trends. Both curves show breaks around 1979 and 2000. In about 1979, the discharge increased from approximately 600 cfs to over 2000 cfs. A similar increase in discharge was observed in the San Filipe, Cochiti, and Rio Pureco reaches (Bauer 2000, Novak 2006, Vensel et al 2005). However, the increase in discharge was not as great as in the Escondida reach. At the break around the year 2000, the gauge at San Acacia decreased from 2900 cfs to 1000 cfs, and the gauge at San Marcial decreased from 2200 cfs to 750 cfs. Table 3.12 shows the average discharge for each period displayed on the graph.

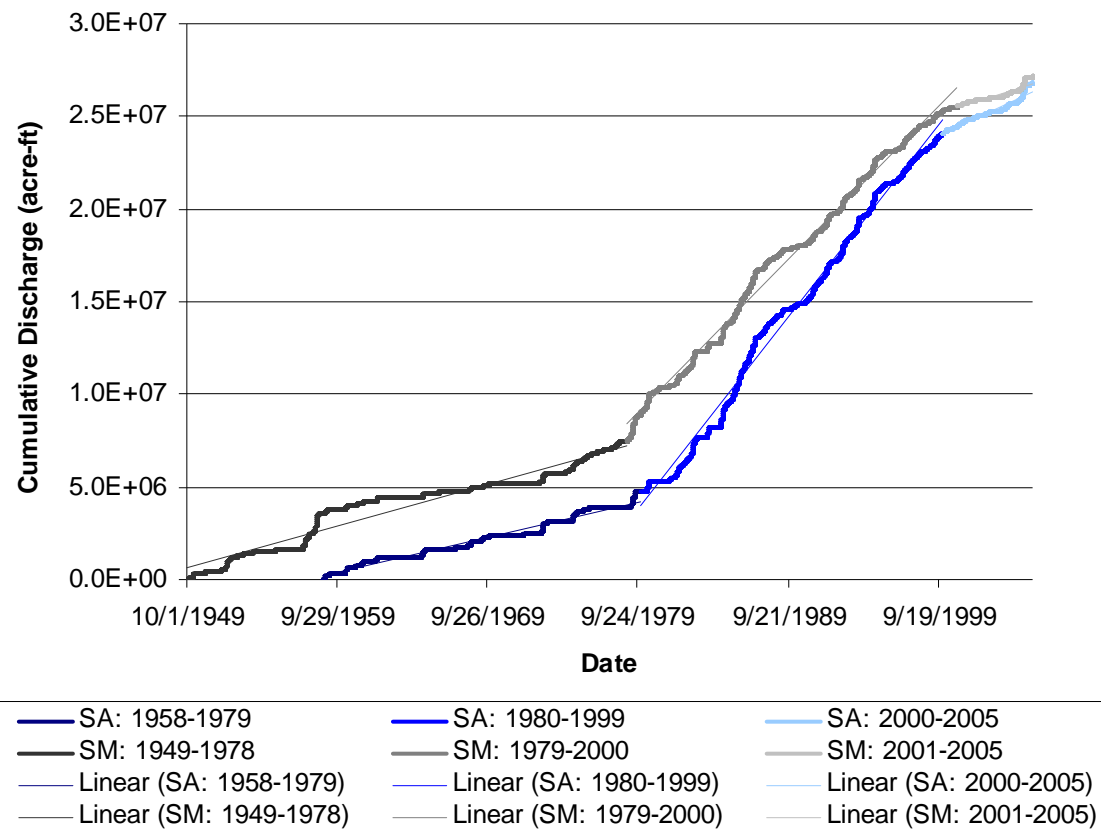


Figure 3.30 Water Discharge Single Mass Curve

Table 3.12 Water Discharge

Gauge	Years	acre-ft/day	R ² value
San Acacia			
	1958-1979	522	0.98
	1980-1999	2856	0.99
	2000-2005	1055	0.93
San Marcial			
	1949-1978	621	0.94
	1979-2000	2263	0.99
	2001-2005	740	0.84

Figure 3.31 shows the single mass curve for suspended sediment discharge at the San Acacia and San Marcial gauges. The suspended sediment discharge at the two gauges does not correlate as well as the water discharge. The San Marcial gauge has a much higher suspended sediment discharge than the San Acacia gauge from 1956 until

about 1968. From 1968 to 1991, the two gauges both have a suspended sediment discharge of about 10000 tons/day. From 1991 to 1996, the San Marcial gauge again shows a much higher suspended sediment discharge.

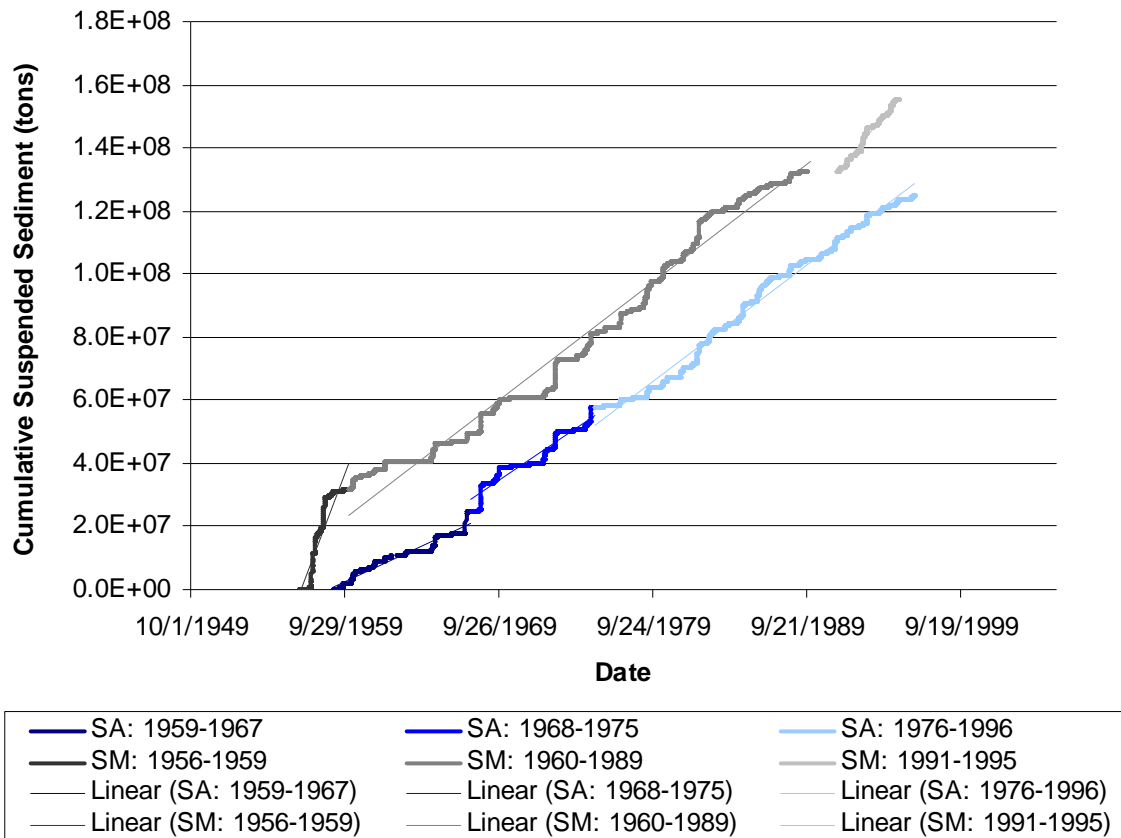


Figure 3.31 Suspended Sediment Discharge Single Mass Curve

Table 3.13 shows the average suspended sediment discharge for the periods shown on the graph. The R^2 value for each trend line is also shown.

Table 3.13 Suspended Sediment Discharge

Gauge	Years	tons/day	R^2 value
San Acacia	1959-1967	6062	0.94
	1968-1975	9172	0.92
	1976-1996	10066	0.99
San Marcial	1956-1959	35276	0.88
	1960-1989	10232	0.98
	1992-1995	16707	0.98

Double Mass Curves

A double mass curve was developed at each gauge to show the changes in suspended sediment concentration over time. Figure 3.32 shows the two double mass curves.

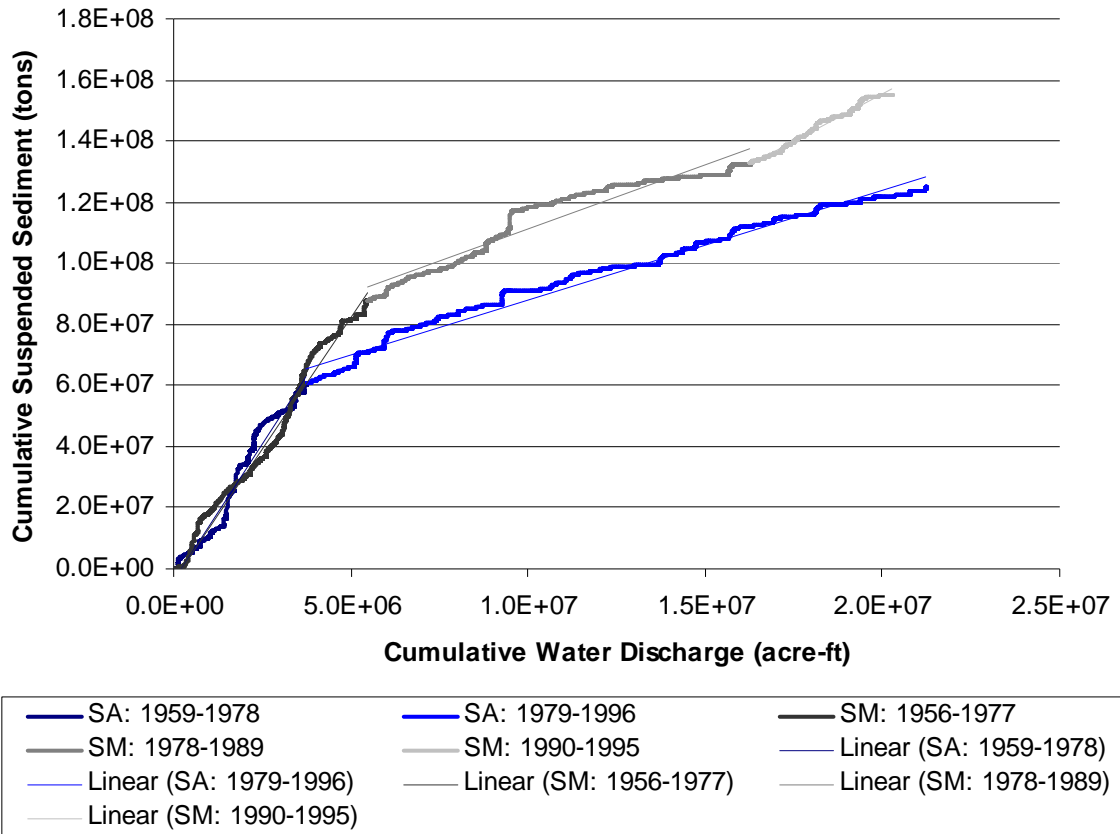


Figure 3.32 Suspended Sediment Concentration Double Mass Curve

From 1959 to 1978, the two curves are very similar, with an average suspended sediment concentration around 13,000 mg/L. Around 1978, both curves break, and the suspended sediment concentration drops to about 3000 mg/L. The concentration at the San Acacia gauge remains at about 3000 mg/L through the end of the available data. The San Marcial gauge, however, shows an increase in suspended sediment concentration from 3000 mg/L to 4500 mg/L around 1990. The decrease in suspended sediment

concentration corresponds with the increase in water discharge. The suspended sediment discharge changes little through time, so an increase in water discharge must cause a decrease in suspended sediment concentration. Table 3.14 shows the average concentration as well as the R^2 values for each segment of the graph.

Table 3.14 Suspended Sediment Concentration

Gauge	Years	tons/acre-ft	mg/L	R^2 value
San Acacia				
	1959-1978	17.9	13165	0.97
	1979-1996	3.58	2633	0.98
San Marcial				
	1956-1977	17.21	12657	0.97
	1978-1989	4.16	3060	0.92
	1990-1995	6.2	4560	0.98

Difference Mass Curve

The difference mass curve in Figure 3.33 shows the increases and decreases in the suspended sediment volume present in the reach over time.

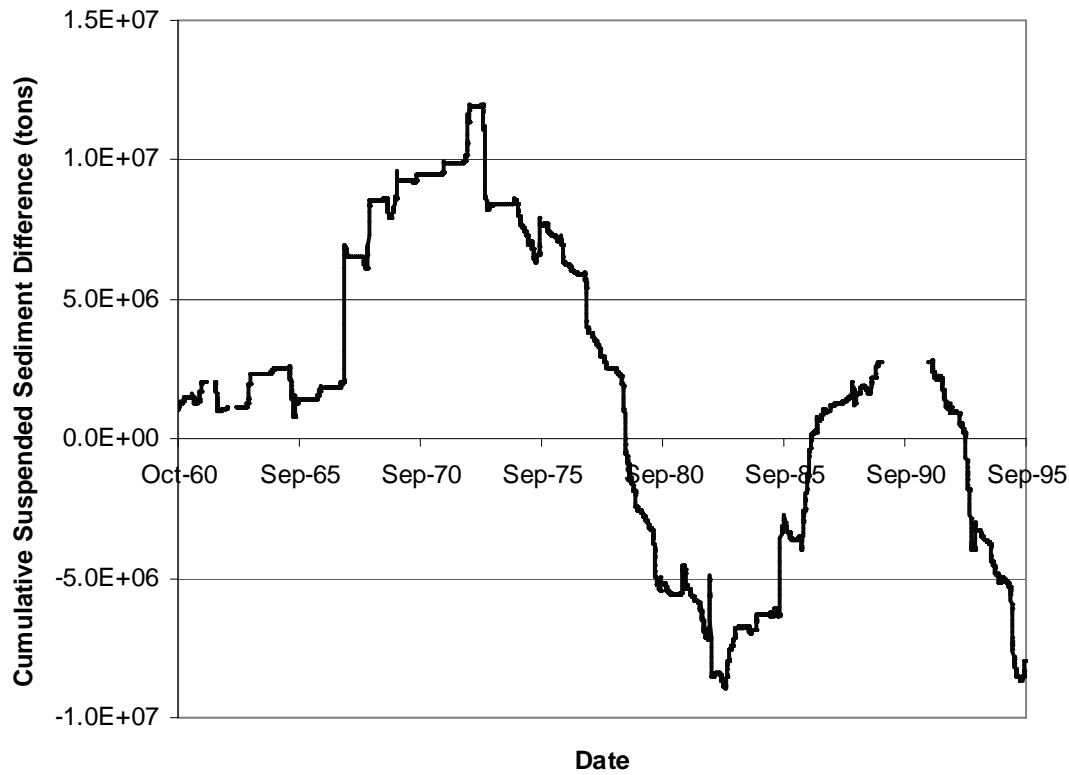


Figure 3.33 Suspended Sediment Difference Mass Curve

When more sediment is entering the reach than leaving the reach, aggradation is expected to occur because the sediment inflow that does not exit the reach must remain in the reach. Conversely, when more sediment is leaving the reach than entering, degradation of the channel is expected because the extra sediment leaving the reach is probably being eroded from the channel bed. While arroyos could contribute some of the extra sediment, much of it is probably being degraded from the bed.

The graph shows that from 1960 to 1973, more sediment was entering the reach than was leaving the reach, indicating a trend toward aggradation. This trend reversed from 1973 to 1983, with more suspended sediment leaving the reach than entering the reach, indicating a trend toward degradation. The trend toward degradation reversed from 1983 to 1989, and again from 1989 to 1995.

Based on the maximum sediment accumulation in the reach, the river should have aggraded by about 10 feet between 1960 and 1973, degraded by 6 feet between 1973 and 1983, aggraded by about less than a foot between 1983 and 1989, and finally degraded by about 7 feet between 1989 and 1995. These amounts of aggradation and degradation are much higher than the amounts of aggradation and degradation actually observed in the cross-section surveys. The average observed values of aggradation and degradation were between 2 feet and 4 feet.

3.4 Floodplain Analysis

Observations by Reclamation indicate that an extended floodplain becomes active in the lower portion of the Escondida reach. The extent of the floodplain and the discharge at which the floodplain becomes inundated were investigated.

3.4.1 Methods

HEC-RAS was used to determine the top width at each cross-section at a series of discharges ranging from 1000 cfs to 6000 cfs. Initial observations from the HEC-RAS data showed two distinct regions of significant floodplain inundation. The average top width in each area was plotted versus discharge for each year of cross-section data to determine the discharge at which the floodplain becomes active. The floodplain becomes active when the top width becomes much greater with a small increase in discharge.

3.4.2 Results

The first area of interest stretches from about Agg/Deg 1406 to Agg/Deg 1418. The second area of interest stretches from about Agg/Deg 1456 to Agg/Deg 1476. Figures 3.34 and 3.35 show the top width vs. discharge for the two areas of interest.

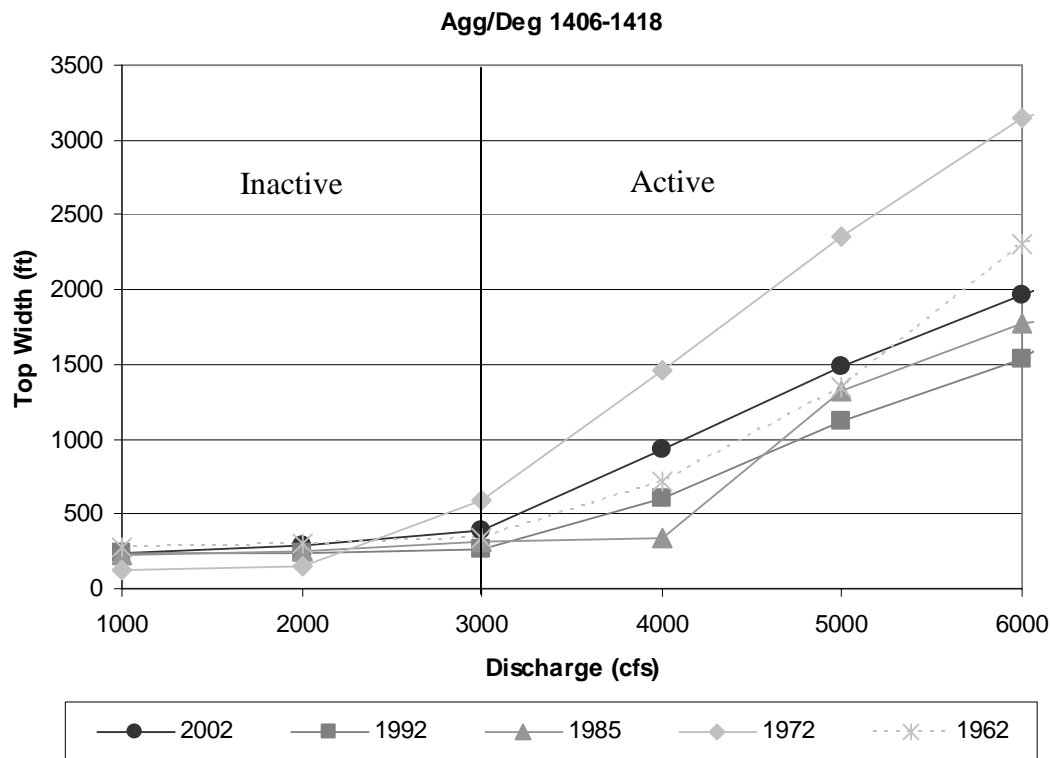


Figure 3.34 Top width vs. discharge for Agg/Deg 1406-1418

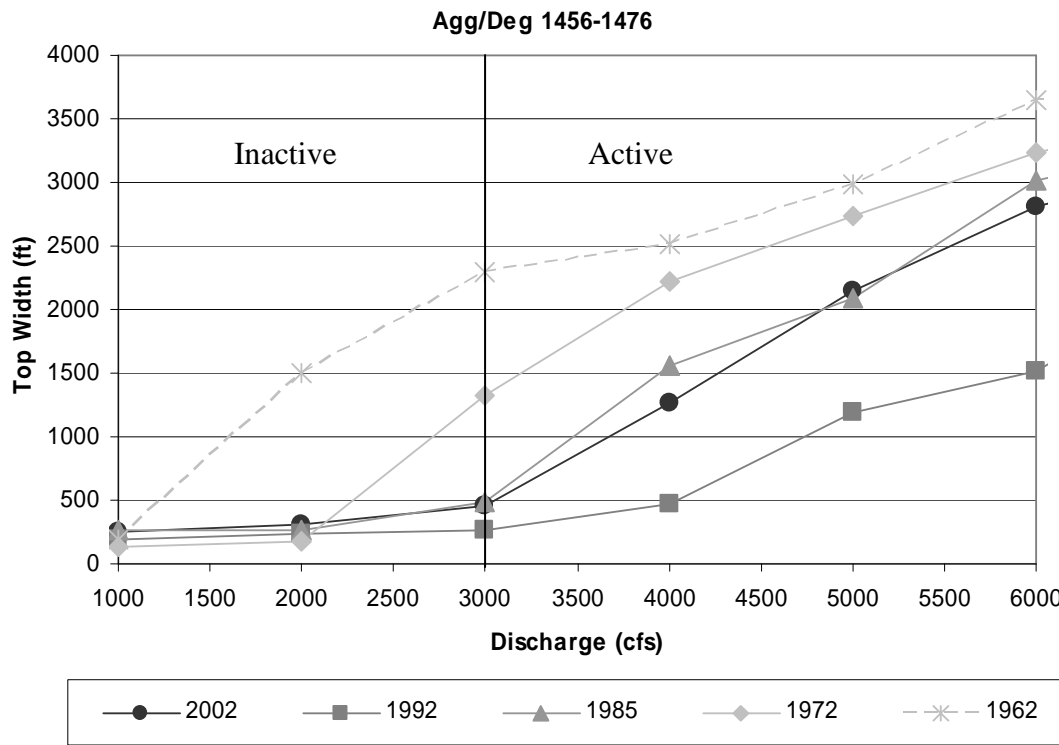


Figure 3.35 Top width vs. discharge for Agg/Deg 1456-1476

Both graphs show that the top width increases sharply around 3000 cfs, indicating that the floodplain becomes active in both areas of interest at about 3000 cfs. A discharge of 3000 cfs has a recurrence interval of less than 2 years. Based on this information, the floodplain is frequently inundated.

3.5 Bedform Analysis

3.5.1 Methods

Two methods for predicting bedforms were selected for use in this analysis. The methods were developed by Simons and Richardson (1963, from Julien 1998) and van Rijn (1984).

Simons and Richardson (1963, from *Julien 1998*) performed laboratory experiments to develop a bedform prediction method based on stream power and median grain size diameter.

$$\text{Stream power: } \tau_0 V = \gamma q S$$

Where τ_0 (lb/ft²) is shear stress, V (ft/s) is velocity, γ (lb/ft²) is the specific weight of water, q (ft²/s) is unit discharge and S is channel slope. Figure 3.36 shows the region where each bedform is expected based on the observations from Simons and Richardson's experiments.

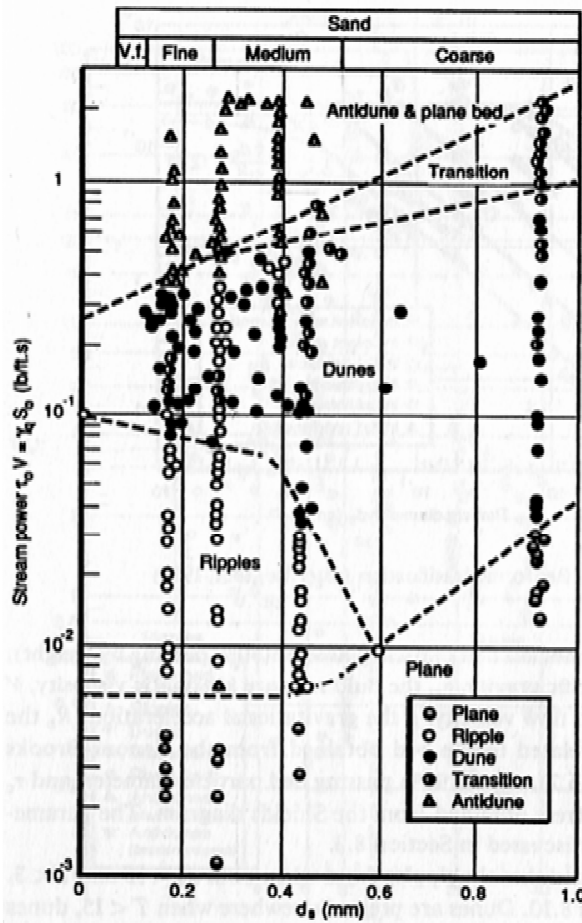


Figure 3.36 Bedform classification by Simons and Richardson (from Julien 1998)

van Rijn (1984) developed a bedform prediction method based on the dimensionless grain diameter and transport-stage parameter.

$$\text{Dimensionless grain diameter: } d_* = d_{50} \left[\frac{(G-1)g}{v_m^2} \right]^{1/3}$$

Where d_* is the dimensionless grain diameter, d_{50} (ft) is the median grain diameter, G is the specific gravity of the sediment and v ($\text{lb}^* \text{s}/\text{ft}^2$) is the kinematic viscosity of water.

$$\text{Transport-stage parameter: } T = \frac{\tau_* - \tau_{*c}}{\tau_{*c}}$$

Where T is the transport-stage parameter, τ^* is the grain Shield's parameter, and τ_{*c} is the critical Shield's parameter. Figure 3.37 shows the bedforms expected based on van Rijn's method.

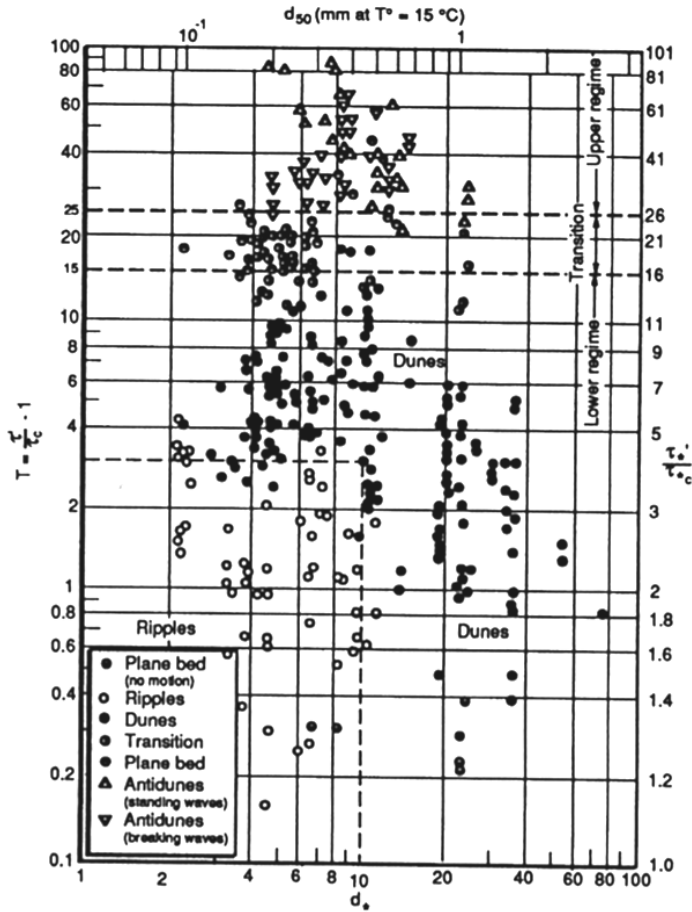


Figure 3.37 Bedform classification by van Rijn (1984, from Julien 1998)

Bedform data were collected by Reclamation at a number of SO-lines between 1990 and 1995. The dominant bedform was selected from the actual field notes as the bedform that covered the largest portion of the main flow area in a cross-section. The expected bedforms at each location were calculated using HEC-RAS, the discharge recorded at the San Acacia and San Marcial gauges on the dates the bedform data were collected, and bed material data. When possible, bed material samples taken at the same time as the bedform observations were used in the calculations. When this information was not available, bed material samples from the nearest SO-line were used. The predicted bedforms were then compared with the dominant bedform at each cross-section.

to determine the ability of the methods to correctly predict bedforms on the Middle Rio Grande.

3.5.2 Results

The bedform type observed at each location was plotted on the charts developed by Simons and Richardson and van Rijn based on the calculations performed for each method. Figures 3.38 – 3.41 show each of the four bedform types plotted on both graphs.

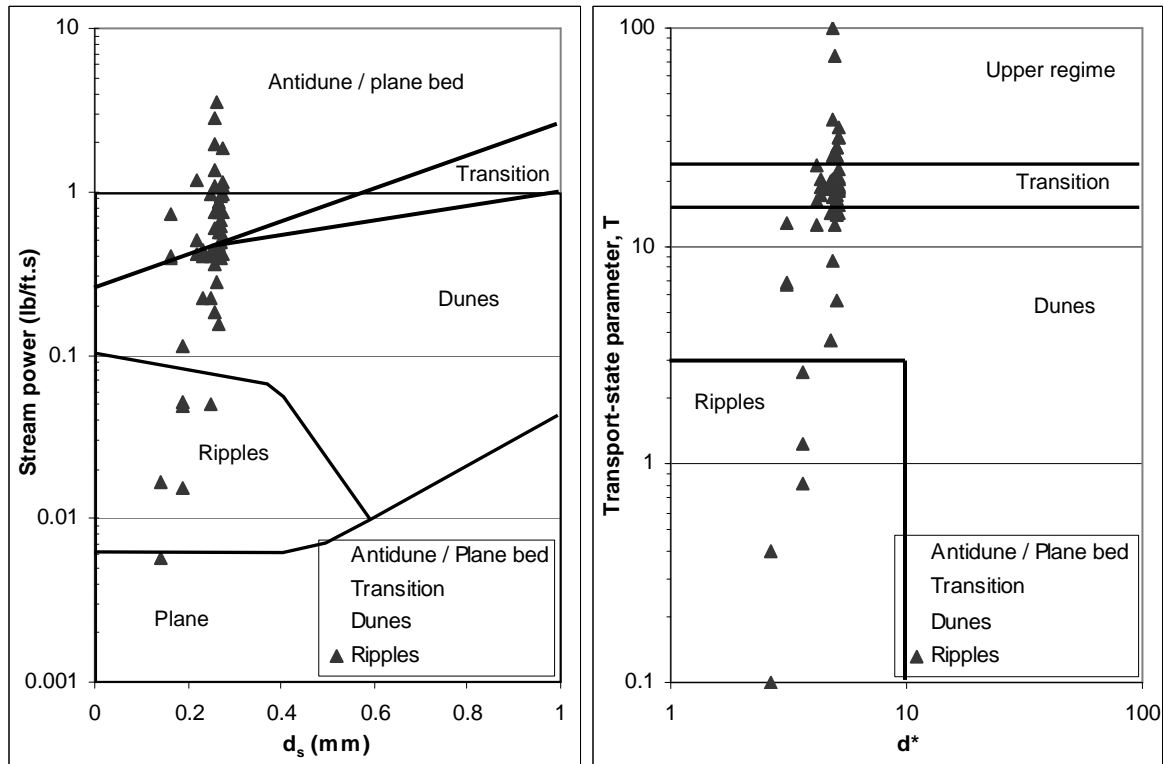


Figure 3.38 *Observed ripples plotted on graphs from Simons and Richardson (L) and van Rijn (R) (after Julien 1998)*

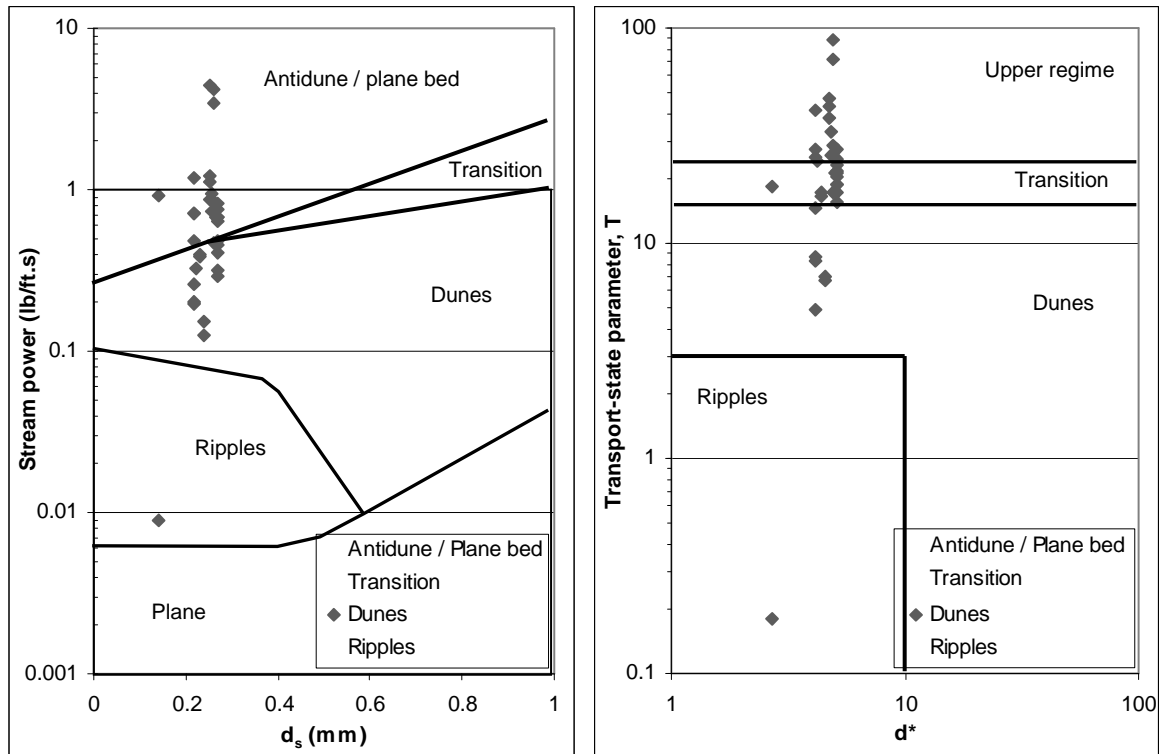


Figure 3.39 Observed dunes plotted on graph from Simons and Richardson (L) and van Rijn (R) (after Julien 1998)

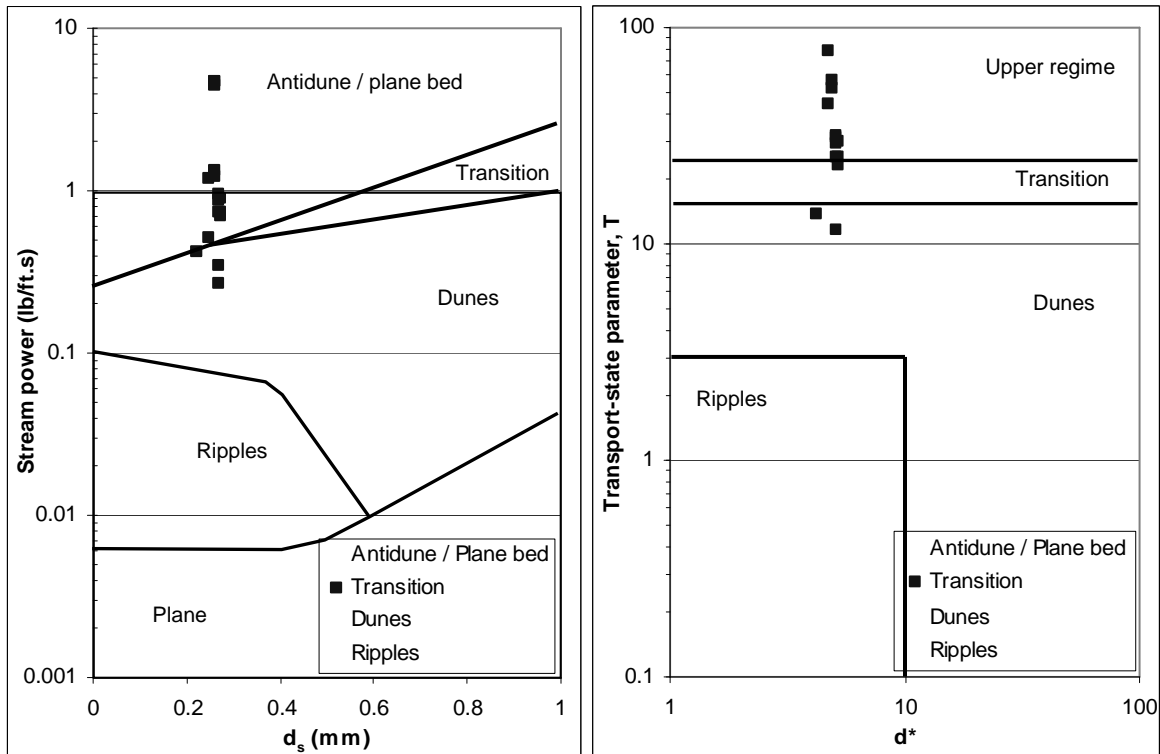


Figure 3.40 Observed transition bedforms plotted on graph from Simons and Richardson (L) and van Rijn (R) (after Julien 1998)

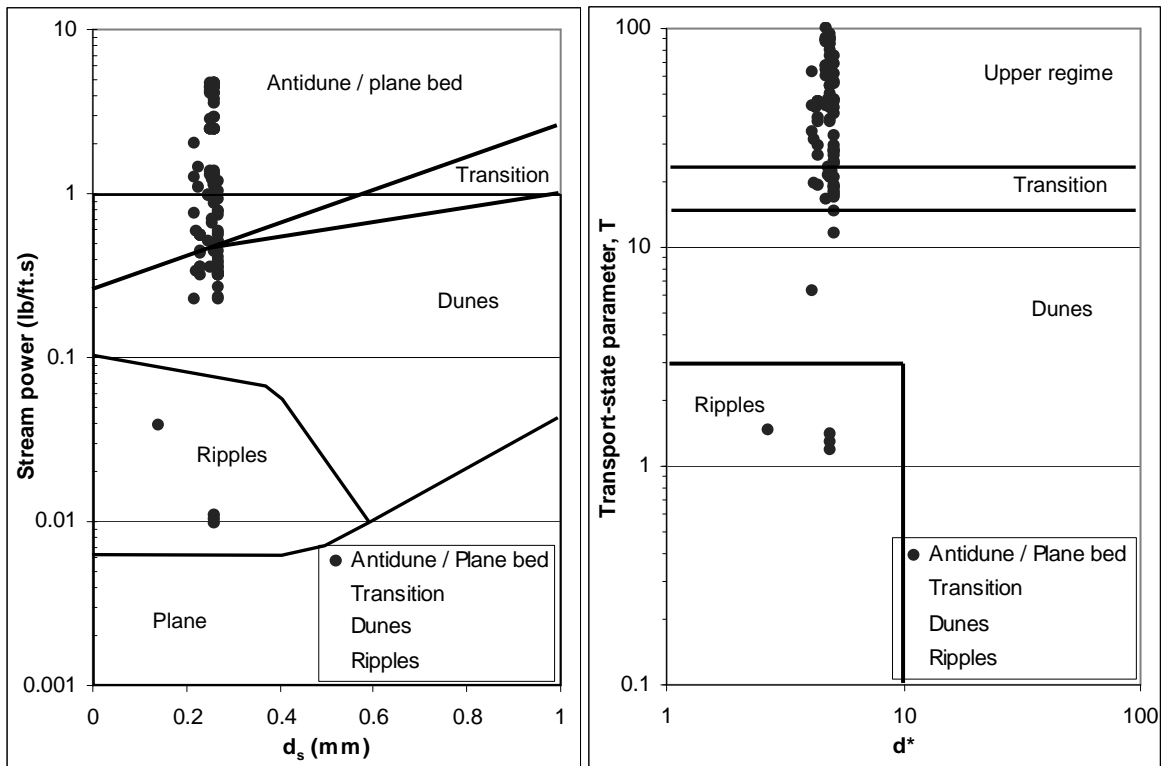


Figure 3.41 Observed antidunes/plane bed plotted on graph from Simons and Richardson (L) and van Rijn (R) (after Julien 1998)

Figures 3.38 – 3.41 show that the predicted bedforms match reasonably well with the predicted bedforms, but the plots show wide scatter. Antidunes were the most reliably predicted bedforms, while lower regime bedforms such as ripples and dunes were difficult to predict correctly.

A likely explanation for the discrepancy between the predicted and observed bedforms is the high variability in important parameters such as flow depth, slope and velocity across a cross-section. This variability results in the observation of several different bedforms in a single cross-section. The prediction methods are unable to account for the variability within the cross-section because they are based on cross-section average properties.

Figure 3.42 shows a typical cross-section with the bedform observations indicated on the cross-section. See Appendix E for the field notes for this cross-section. The width/depth ratio for this cross-section is about 400. This is typical of the Escondida reach and further explains the high variability in the cross-sections. The discharge at this cross-section was about 4400 cfs on the day of the survey. Simons and Richardson predicted antidunes and van Rijn predicted upper regime bedforms for this location. While upper regime bedforms were observed at the cross-section, lower regime bedforms were also observed. Both the upper and lower regime bedforms were present in the main flow area of the channel and both occupied similar portions of the cross-section.

Additional example cross-sections can be found in Appendix E.

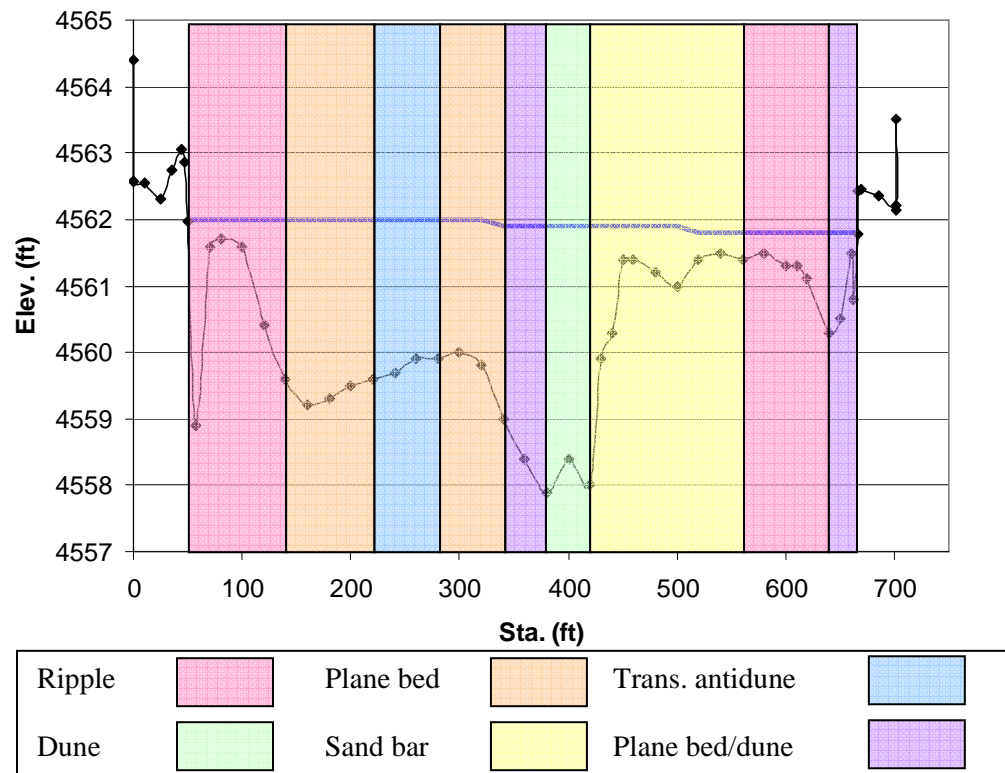


Figure 3.42 Typical cross-section with bedforms

3.6 Summary

Channel pattern

Based on visual observations of the GIS non-vegetated active channel planforms, the channel planform has become straighter since 1918. This observation is confirmed by a steady decrease in sinuosity (see Figures 3.12-3.14). The decrease in sinuosity is especially pronounced in subreach 3 between 1918 and 1935. The straightening was likely caused by flood control and irrigation efforts implemented during the 1920's and 1930's. At the same time, the upper portion of the channel transitioned from a braided, multi-thread channel to a much narrower, single thread channel.

The total channel has narrowed slightly between 1962 and 2002, with the greatest decrease in width occurring between 1985 and 1992 (see Figure 3.23). The decrease in top width is likely related to a corresponding increase in depth in the channel at the same time.

Channel classification

The results of the channel classification methods indicated that the channel was primarily a straight or braided channel. The methods that most closely estimated the actual channel planform were those that indicated a straight planform, as braiding is only seen in localized areas of the channel during low flows. Leopold and Wolman, Schumm and Kahn, and Nanson and Croke all indicated a straight channel planform. Rosgen's method also provides a good description of the channel planform. Rosgen describes the channel as slightly to moderately entrenched with well-developed floodplains.

Vertical movement

Both aggradation and degradation were observed through changes in the mean bed elevation over time (see Figure 3.19 and Figure 3.20). Between 1962 and 1985, subreach 1 and subreach 2 showed 2 to 4 feet of aggradation, while subreach 3 showed about 4 feet of degradation. This trend was reversed between 1985 and 2002. The cyclical nature of the aggradation and degradation may be caused by complex response. Complex response results in several periods of aggradation and degradation in a reach due to a single change in the system (Schumm 1979). The Escondida reach has been subjected to many changes, such as levee and dam construction and channelization. Any combination of these changes could have led to the complex response seen in the mean bed elevation.

The difference mass curve developed from suspended sediment gauge data also shows a cycle of aggradation and degradation. Aggradation was seen between 1960 and 1985. This was followed by about 5 years of degradation, then 5 years of aggradation. Finally, another cycle of degradation occurred from about 1992 until the end of the data in 1995. Continuing to analyze the difference mass curve as more data become available may give an indication as to whether the channel is approaching equilibrium. As the channel approaches equilibrium, the oscillations between aggradation and degradation should become smaller.

Channel geometry

Table 3.15 shows the changes in each channel geometry parameter. A plus (+) indicates an increase, a minus (-) a decrease, and an equals (=) no change in the parameter value.

Table 3.15 Channel geometry changes

Subreach	Area	Top Width	Wetted Perimeter	Hydraulic Depth	Max Depth	W/D	Velocity	Froude Number
1962-1972								
1	+	=	=	+	+	-	+	=
2	+	+	+	+	+	+	+	+
3	-	-	-	+	+	=	+	+
Total	+	+	+	+	+	+	+	+
1972-1985								
1	=	=	-	+	-	-	+	+
2	-	-	=	-	-	-	-	-
3	-	+	-	-	=	+	-	-
Total	-	-	-	-	-	-	-	-
1985-1992								
1	-	-	-	+	-	-	+	+
2	-	+	-	+	+	+	+	+
3	-	-	-	+	-	-	+	+
Total	-	-	-	+	+	-	+	+
1992-2002								
1	=	=	=	-	-	+	+	+
2	+	+	+	-	-	+	-	-
3	+	+	+	-	-	+	-	+
Total	+	+	+	-	-	+	-	-

Lateral movement

Significant bed migration occurred at numerous locations throughout the reach (see Table 3.10). Shifts in channel banks of more than 100 feet were not uncommon. The largest channel movements where seen between 1962 and 1972. The channel migration may be due to the placement of improvements such as levees that both straighten the channel and restrict the locations were migration is possible. The migration may also be a response to earlier channelization efforts.

Bed material

Sand-sized particles are the primary bed material throughout the reach.

Historically, the bed material has ranged from very fine sand to medium sand. A slight coarsening of the bed material has been seen between 1972 and 2002 (See Figure 3.28). This may be due to the effects of dam installation. The coarsening may also be due to new inputs of coarse material from tributaries and arroyos, a decreased supply of fine sediments, or increased transport capacity due to higher discharges.

Discharge

The daily discharge at both the San Acacia and San Marcial gauges shows a dry period from 1950 to 1979, a wet period between 1979 and 2000, and another dry period from 2000 to 2005 (see Figure 3.30). A similar increase in discharge around 1979 was observed in upstream reaches, although the increase was less dramatic upstream. Examining the magnitude of the discharges indicates that the Escondida reach had historically lower flows than the upstream reaches before 1979, but had flows of a magnitude similar to those seen in the upstream reaches after 1979. This suggests that less water is being lost as the river moves downstream than had been lost historically.

Suspended sediment

The daily suspended sediment discharge recorded at both gauges has changed little since the early 1960's (see Figure 3.31). As a result, the suspended sediment concentration has varied inversely with discharge over time. The concentration decreased by about 5 times following the increase in discharge in 1979. The effects of

the recent decrease in discharge are not known because suspended sediment data are unavailable after 1996.

Floodplain Inundation

Two locations in the lower portion of the reach have large, active floodplains. These floodplains typically become active at about 3000 cfs. The recurrence interval of a 3000 cfs flow indicates that the floodplain is inundated on about an annual basis. The floodplain became active between 1000 cfs and 2000 cfs before 1985 in the lowest section of the reach, indicating that the channel has entrenched since 1972.

Bedforms

Neither of the bedform predictors was able to adequately predict the bedforms observed in the Escondida reach. Upper regime bedforms were predicted correctly most often. The difficulty in calculating the expected bedforms stems from the high variability of the cross-sections in the reach. Two or more different types of bedforms were typically observed at a typical cross-section. Upper regime bedforms were easier to predict because the cross-section variability had less of an effect at the high flows necessary to produce upper regime bedforms.

Chapter 4: Equilibrium State Predictors

4.1 Hydraulic Geometry

4.1.1 Methods

Several hydraulic geometry equations were used to determine the equilibrium channel width. These methods use channel characteristics such as channel width and slope, sediment concentration, and discharge. All of the equilibrium width equations were developed in simplified conditions such as man-made channels.

Julien and Wargadalam (1995) used the concepts of resistance, sediment transport, continuity, and secondary flow to develop semi-theoretical hydraulic geometry equations.

$$\begin{aligned} h &= 0.2Q^{2/(5+6m)} d_s^{6m/(5+6m)} S^{-1/(5+6m)} \\ W &= 1.33Q^{(2+4m)/(5+6m)} d_s^{-4m/(5+6m)} S^{-(1+2m)/(5+6m)} \\ V &= 3.76Q^{(1+2m)/(5+6m)} d_s^{-2m(5+6m)} S^{(2+2m)/(5+6m)} \\ \tau^* &= 0.121Q^{2/(5+6m)} d_s^{-5/(5+6m)} S^{(4+6m)/(5+6m)} \\ m &= \frac{1}{\ln(\frac{12.2h}{d_{50}})} \end{aligned}$$

Where h is the average depth, W (m) is the average width, V (m/s) is the average one-dimensional velocity, and τ^* is the Shields parameter, and d_{50} (m) is the median grain size diameter.

Simons and Alberston (1963) used five sets of data from canals in India and America to develop equations to determine equilibrium channel width. Simons and Bender collected data from irrigation canals in Wyoming, Colorado and Nebraska. These canals had both cohesive and non cohesive bank material. Data were collected on the Punjab and Sind canals in India. The average bed material diameter found in the Indian canals varied from 0.43 mm in the Punjab canals to between 0.0346 mm and 0.1642 mm in the Sind canals. The USBR data were collected in the San Luis Valley in Colorado and consisted of coarse non-cohesive material. The final data set was collected in the Imperial Valley canal system, which has conditions similar to those seen in the Indian canals and the Simons and Bender canals (Simons and Albertson 1963).

Two figures were developed by Simons and Albertson to obtain the equilibrium width. Figures 4.1 and 4.2 show the relationships between wetted perimeter and discharge and average width and wetted perimeter, respectively.

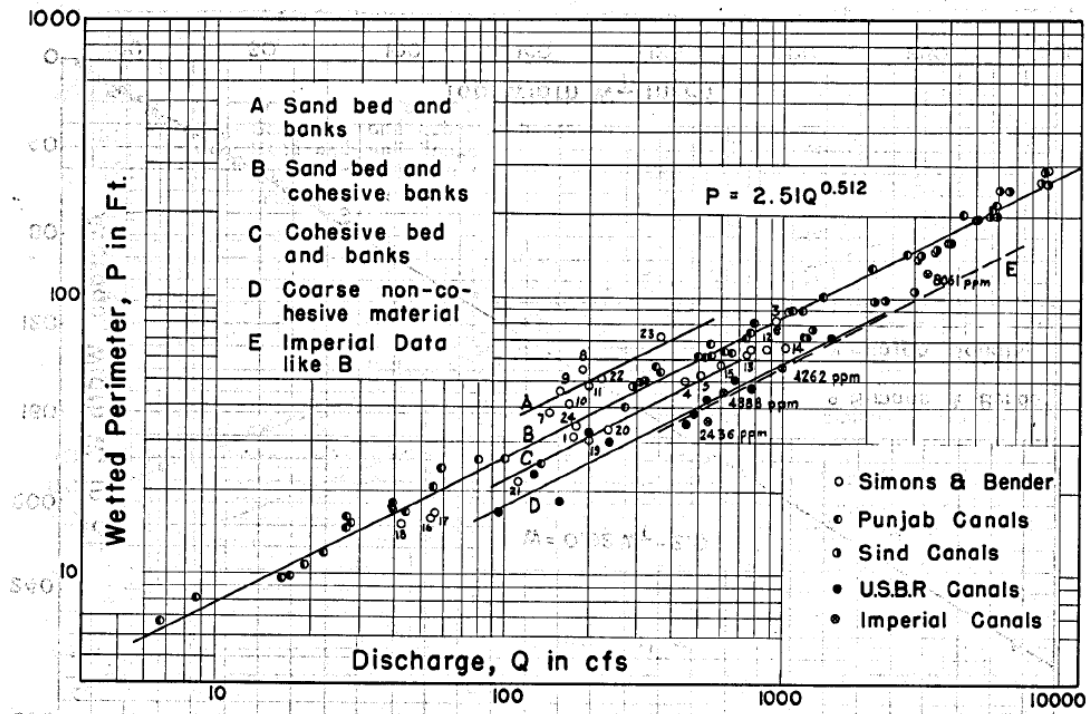


Figure 4.1 Variation of wetted perimeter P with discharge Q and type of channel (after Simons and Albertson 1963)

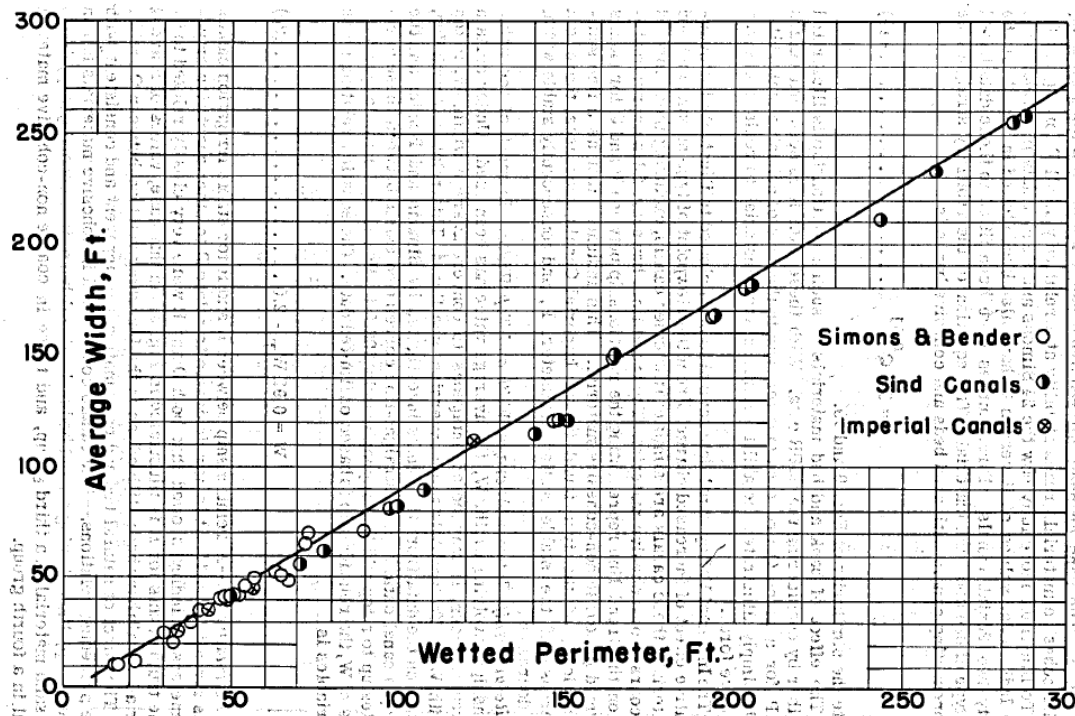


Figure 4.2 Variation of average width W with wetted perimeter P (after Simons and Albertson 1963)

Blench (1957) used flume data to develop regime equations. A bed and a side factor (F_s) were developed to account for differences in bed and bank material.

$$W = \left(\frac{9.6(1 + 0.012c)}{F_s} \right)^{1/2} d_{50}^{1/4} Q^{1/2}$$

Where W (ft) is channel width, c (ppm) is the sediment load concentration, d_{50} (mm) is the median grain diameter, and Q (cfs) is the discharge. The side factor, $F_s = 0.1$ for slight bank cohesiveness.

Lacey [(1930-1958), from Wargadalam (1993)] developed a power relationship for determining wetted perimeter based on discharge.

$$P_w = 2.667Q^{0.5}$$

Where P_w (ft) is wetted perimeter and Q (cfs) is discharge. For wide, shallow channels, the wetted perimeter is approximately equal to the width.

Klaassen and Vermeer (1988) used data from the Jamuna River in Bangladesh to develop a width relationship for braided rivers.

$$W = 16.1Q^{0.53}$$

Where W (m) is width, and Q (m^3/s) is discharge.

Nouh (1988) developed regime equations based on data collected in extremely arid regions of south and southwest Saudi Arabia.

$$W = 2.83 \left(\frac{Q_{50}}{Q} \right)^{0.83} + 0.018(1+d_{50})^{0.93} c^{1.25}$$

Where W (m) is channel width, Q_{50} (m^3/s) is the peak discharge for a 50 year return period, Q (m^3/s) is annual mean discharge, d_{50} (mm) is mean grain diameter, and c (kg/m^3) is mean suspended sediment concentration.

Table 4.1 shows the input values used to estimate channel width from the hydraulic geometry equations. The peak discharges for a 50-year return period were taken from Bullard and Lane (1993). The average sediment concentrations were obtained from the double mass curves (see Figure 4.3) developed for the San Acacia and San Marcial gauges. Suspended sediment data were only available until 1995, so all suspended sediment concentrations after 1995 were extrapolated from the double mass curves.

Table 4.1 Hydraulic geometry calculation inputs

	Q (cfs)	Q ₅₀ (cfs)	d ₅₀ (mm)	Channel Slope (ft/ft)	Sediment Concentration Avg C (ppm)
1962					
1	5000	28050	0.15	0.0009	13058
2	5000	28050	0.15	0.0008	12808
3	5000	28050	0.15	0.0005	12558
Total	5000	28050	0.15	0.0008	12808
1972					
1	5000	19800	0.11	0.0009	13058
2	5000	19800	0.11	0.0008	12808
3	5000	19800	0.11	0.0007	12558
Total	5000	19800	0.11	0.0008	12808
1985					
1	5000	19800	0.15	0.0008	2629
2	5000	19800	0.13	0.0009	2841
3	5000	19800	0.10	0.0005	3054
Total	5000	19800	0.13	0.0008	2841
1992					
1	5000	19800	0.22	0.0008	2629
2	5000	19800	0.27	0.0008	3588
3	5000	19800	0.25	0.0007	4547
Total	5000	19800	0.23	0.0008	3588
2002					
1	5000	19800	0.37	0.0008	2629
2	5000	19800	0.30	0.0008	3588
3	5000	19800	0.24	0.0008	4547
Total	5000	19800	0.31	0.0008	3588

An empirical width relationship was developed for the Escondida reach based on active channel widths determined from GIS channel planforms and peak flows for the 5 years prior to the survey date. Peak flows for the relationship were obtained from the San Acacia and San Marcial gauges. The resulting power relationship takes the form:

$$W = aQ^b$$

Where W (ft) is channel width and Q (cfs) is peak discharge. Table 4.2 shows the input values used to develop the empirical width relationship for the Escondida reach.

Table 4.2 Escondida empirical width-discharge inputs

Year	Average 5-year peak discharge (cfs)	GIS widths (ft)			
		Subreach 1	Subreach 2	Subreach 3	Overall
1962	3676	919	415	209	548
1972	2644	619	274	178	376
1985	6321	671	645	302	609
1992	4638	353	529	298	442
2001	2937	362	569	299	468
2002	2344	334	436	265	381
2005	3312	366	498	305	431

4.1.2 Results

The equilibrium channel widths predicted by the hydraulic geometry equations are shown in Table 4.3. All methods except Blench tend to under predict the channel width determined from HEC-RAS runs at 5000 cfs. Blench tends to over predict the channel widths determined from HEC-RAS, but shows the best overall agreement of the methods used to estimate the equilibrium channel width. This does not necessarily mean that Blench is the best predictor of equilibrium width because the channel was likely not in equilibrium between 1962 and 2002. Four methods, Simons and Albertson, Nouh, Lacey, and Julien-Wargadalam, predict similar equilibrium channel widths ranging from about 200 feet to about 300 feet. These methods may be a better indication of the expected equilibrium channel width because of their similar results. The channel is tending toward the narrower width predicted by the four methods discussed, but it is still much wider than the predicted equilibrium.

Table 4.3 Predicted equilibrium widths from hydraulic geometry equations with $Q = 5000 \text{ cfs}$

	Reach-Averaged HEC-RAS Main Channel Width (feet)	Predicted Width (ft)					
		Simons and Albertson	Klassen & Vermeer	Nouh	Blench	Lacey	Julien - Wargadalam
1962							
1	1417	274	729	390	2425	189	268
2	774	274	729	390	2402	189	277
3	3234	274	729	390	2378	189	298
Total	1291	274	729	390	2402	189	276
1972							
1	1416	274	729	293	2228	189	271
2	1296	274	729	293	2207	189	277
3	3158	274	729	293	2185	189	284
Total	1572	274	729	293	2207	189	275
1985							
1	1417	274	729	291	1102	189	273
2	774	274	729	291	1091	189	272
3	3239	274	729	291	1064	189	303
Total	1295	274	729	291	1102	189	275
1992							
1	468	274	729	291	1205	189	279
2	881	274	729	291	1474	189	275
3	1287	274	729	291	1629	189	281
Total	796	274	729	291	1427	189	277
2002							
1	505	274	729	291	1377	189	277
2	1024	274	729	291	1519	189	278
3	2000	274	729	291	1607	189	278
Total	982	274	729	291	1537	189	277

Julien-Wargadalam was also used to predict the equilibrium slope of the channel.

Table 4.4 shows the predicted equilibrium slope and the observed channel slope for each subreach and the total reach between 1962 and 2002.

Table 4.4 Equilibrium slope predictions with $Q = 5000 \text{ cfs}$

		1962	1972	1985	1992	2002
Observed Slope	1	0.00094	0.00089	0.00084	0.00076	0.00078
	2	0.00078	0.00080	0.00087	0.00081	0.00077
	3	0.00055	0.00070	0.00051	0.00072	0.00076
	Total	0.00080	0.00082	0.00081	0.00078	0.00077
Equilibrium Slope	1	0.00055	0.00036	0.00052	0.00075	0.00139
	2	0.00051	0.00035	0.00042	0.00098	0.00113
	3	0.00048	0.00033	0.00031	0.00089	0.00083
	Total	0.00051	0.00034	0.00044	0.00083	0.00117

The results of the equilibrium slope calculations indicate that the channel had a steeper slope than the predicted slope in 1962, 1972 and 1985. In 1992, however, the observed channel slope closely matches the predicted equilibrium slope. In 2002, the early trend is reversed with the predicted channel slope being steeper than the observed channel slope.

Figure 4.3 shows the plot and regressions used to find the empirical equations for the reach. The non-vegetated active channel width obtained from GIS planforms was plotted versus the 5-year average peak flow. Regressions were then developed for each subreach and the total reach. 1962 was the first year used in the regression because including data prior to 1962 would have resulted in regressions that predicted decreasing width with increasing discharge.

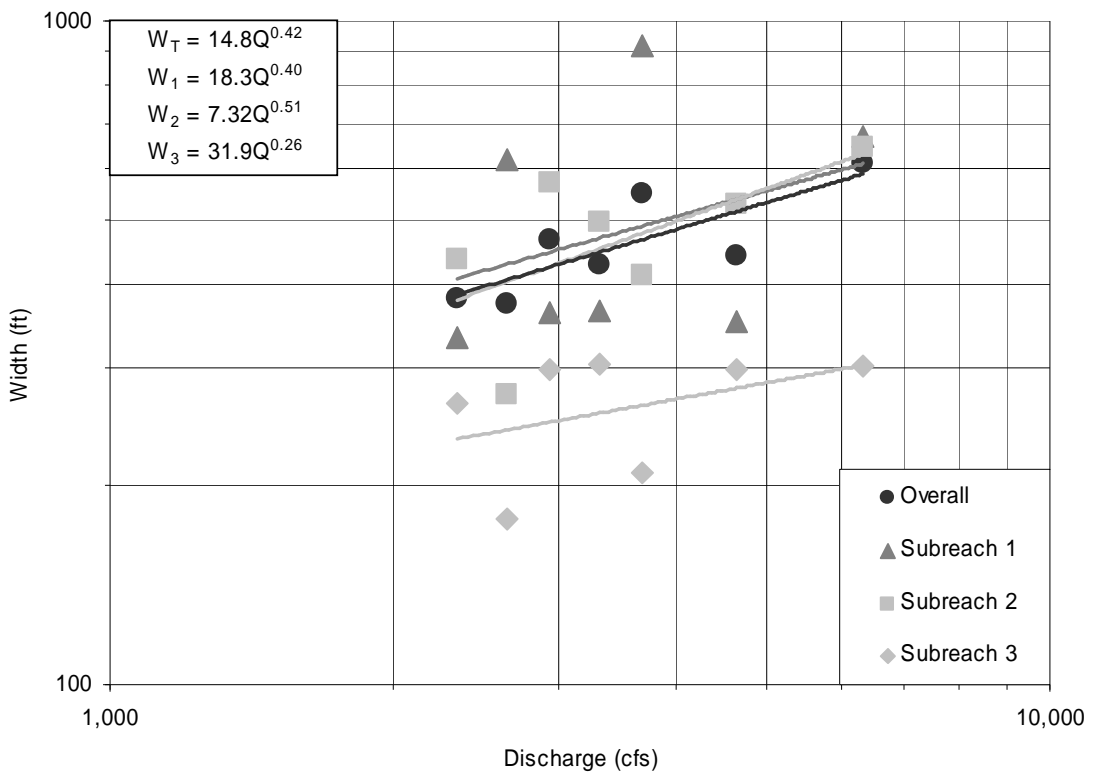


Figure 4.3 Escondida empirical width-discharge relationships

The results of the equilibrium width calculations performed using the empirical equation developed for the Escondida reach are shown in Table 4.5 along with the non-vegetated active channel widths.

Table 4.5 Escondida empirical width-discharge results

		1962	1972	1985	1992	2001	2002	2005
	Average 5-year peak discharge (cfs)	3676	2644	6321	4638	2937	2344	3312
Predicted Width (ft)	1	919	619	671	353	362	334	366
	2	415	274	645	529	569	436	498
	3	209	178	302	298	299	265	305
	Total	548	376	609	442	468	381	431
Width (ft)	1	490	430	609	538	448	409	470
	2	478	404	630	538	426	380	453
	3	263	242	303	279	248	234	256
	Total	468	407	587	516	426	387	448

The predicted widths closely match the measured widths in all subreaches and in all years. The empirical equations may be good indicators of the actual expected width at a given discharge because they are based on the historical conditions rather than an ideal, equilibrium state. These equations, however, may not be reliable in predicting the equilibrium width of the channel.

4.2 Width Regression Models

4.2.1 Methods

Hyperbolic Model

The downstream effects of dams on alluvial rivers were studied by Williams and Wolman (1984). They found a hyperbolic equation to describe the changes in channel width with time.

$$\frac{1}{Y} = C_1 + C_2 \frac{1}{t}$$

Where C_1 and C_2 are empirical coefficients, t is the time in years after the initial change in the channel, and Y is the relative change in channel width and is equal to the ratio of the initial width (W_i) to the wide at time t (W_t). The coefficients may be a function of channel characteristics such as discharge and boundary material.

A hyperbolic equation was fit to the data from each subreach. The initial time ($t=0$) was assumed to be the first year a narrowing trend was observed in the channel. The initial year was different in each subreach and in the total reach. To adjust the equations to an origin of 0, 1.0 was subtracted from the relative width ratio (W_t/W_i) before the regression was fit to the data. The constants $C1$ and $C2$ were determined by setting the R^2 of the regression as close to one as possible.

Exponential Model

Richard et al. (2005) developed prediction equations for active channel width, total channel width, migration rate and lateral mobility based on data collected in the Cochiti reach of the Middle Rio Grande and verified by data from four rivers including the Jemez river, the Arkansas river, Wolf creek and the North Canadian river. An exponential regression equation was developed to describe channel width as a function of time.

$$W(t) = W_e + (W_i - W_e)e^{-kt}$$

Where W_e is the equilibrium width, W_i is the channel width at the initial time, k is the rate of decay, and t is time after the initial time.

The exponential equation was fit to the GIS active channel width beginning in the first year showing a trend toward decreasing width. The decay constant k , and the equilibrium width, W_e , were determined by setting the R^2 of the exponential regression equation as close to one as possible. Table 4.6 shows the input information for the hyperbolic and exponential regression equations.

Table 4.6 Hyperbolic and exponential regression input

Subreach 1		
Year	t (year)	W(t) (ft)
1949	0	1591
1962	13	919
1972	23	619
1985	36	671
1992	43	353
2001	52	362
2002	53	334
2005	56	366

Subreach 2		
Year	t (year)	W(t) (ft)
1985	0	645
1992	7	529
2001	16	569
2002	17	436
2005	20	498

Subreach 3		
Year	t (year)	W(t) (ft)
1985	0	302
1992	7	298
2001	16	299
2002	17	265
2005	20	305

Total		
Year	t (year)	W(t) (ft)
1949	0	1081
1962	13	548
1972	23	376
1985	36	609
1992	43	442
2001	52	468
2002	53	381
2005	56	431

4.2.2 Results

Four hyperbolic and four exponential equations were developed for the Escondida reach. Figures 4.4 – 4.7 show the regression curves for each subreach and the total reach. All of the graphs start in the initial year and continue through 2020.

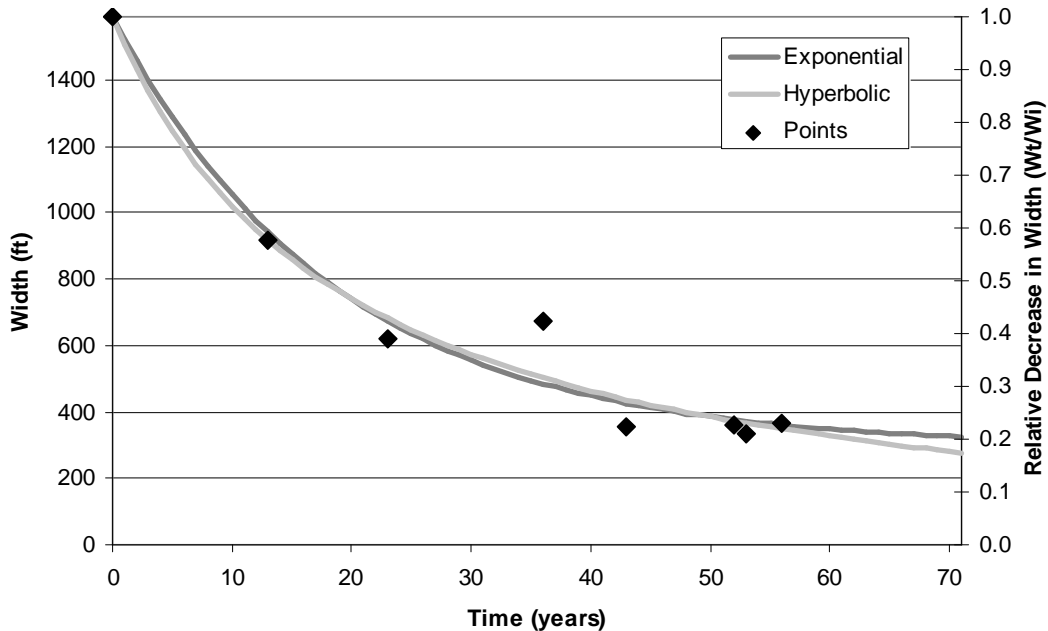


Figure 4.4 Hyperbolic and exponential regressions – subreach 1

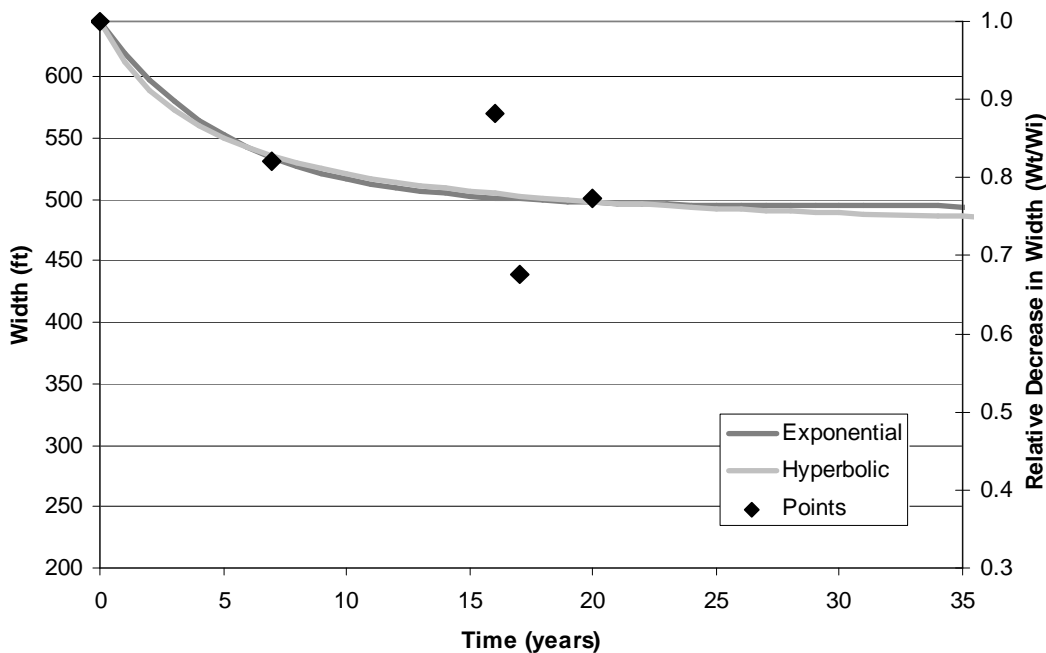


Figure 4.5 Hyperbolic and exponential regressions – subreach 2

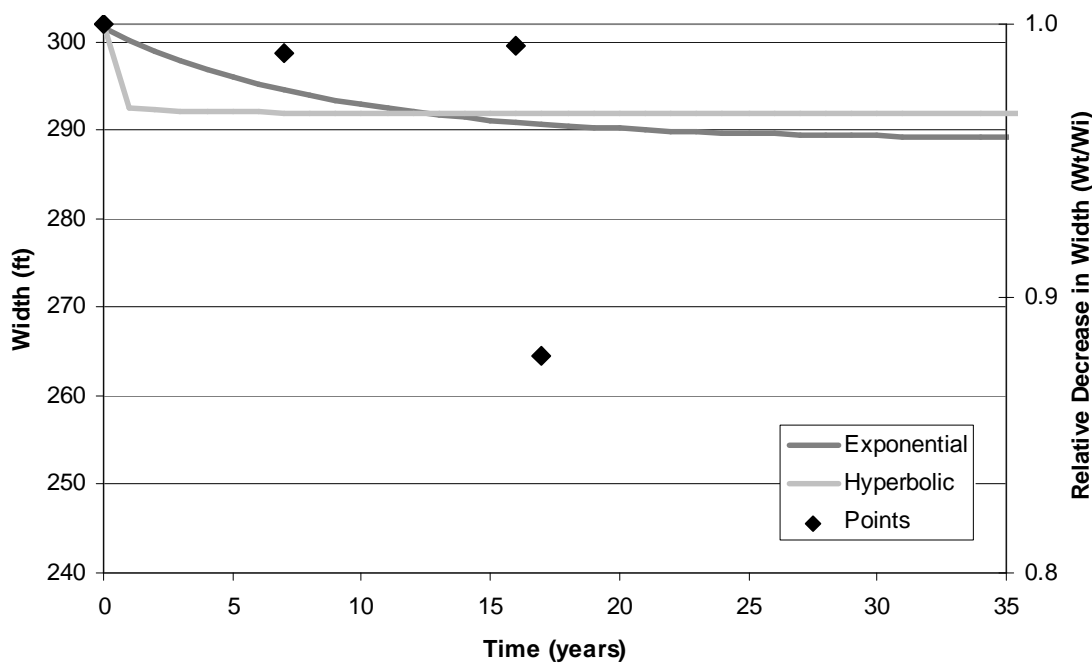


Figure 4.6 Hyperbolic and exponential regressions – subreach 3

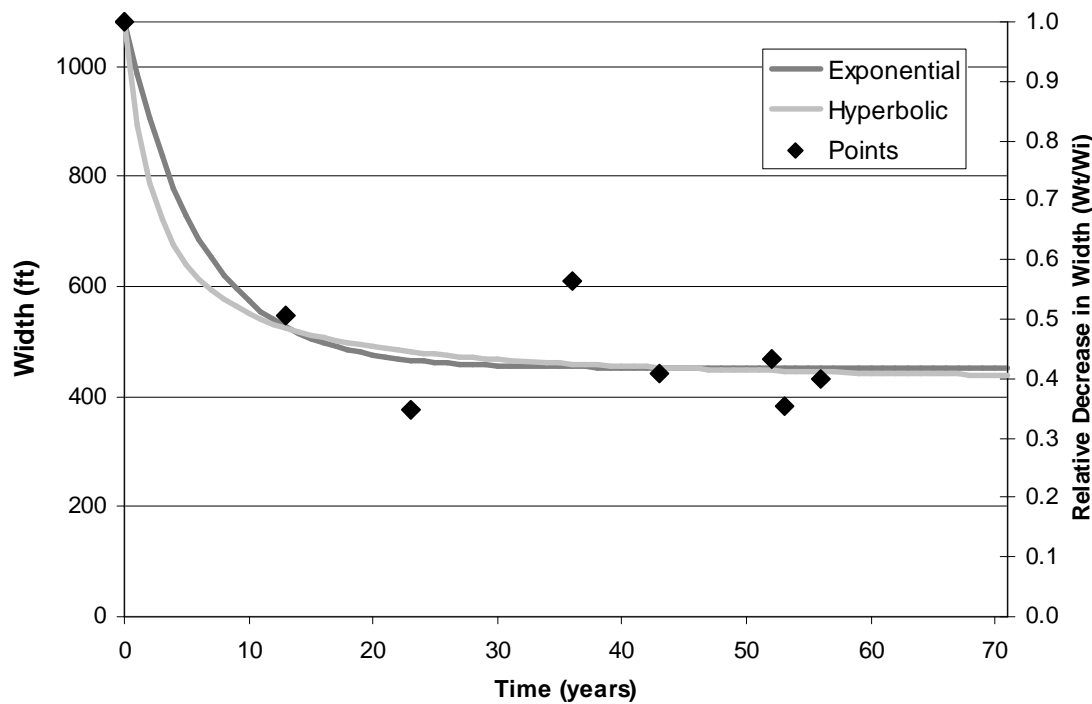


Figure 4.7 Hyperbolic and exponential regressions – total reach

As shown in Figures 4.4 – 4.7, the hyperbolic and exponential regression equations produce very similar results. Overall, the exponential regression seems to produce smoother regression curves.

Table 4.7 shows the hyperbolic regressions for each subreach, along with the predicted width in 2020 and the predicted equilibrium width. The widths predicted in 2020 are reasonable for all reaches and, in most cases, are near the predicted equilibrium width. In subreach 1, the equilibrium width is negative. This indicates that this equation is not a reliable predictor of the ultimate equilibrium width of the channel, but it seems to be a reasonable predictor of the 2020 width. Additional data should be added to the regression equation for subreach 1 as they become available to better refine the equation for long-term predictions.

Table 4.7 Hyperbolic regression equations and predicted widths

Subreach	R ²	Regression Equation	W ₂₀₂₀ (ft)	W _e (ft)
1	1.00	$\frac{W_t}{W_i} = \frac{t}{-0.95t - 18.34} + 1$	277	-79
2	1.00	$\frac{W_t}{W_i} = \frac{t}{-3.55t - 15.81} + 1$	484	463
3	1.00	$\frac{W_t}{W_i} = \frac{t}{-30.64t - 2.33} + 1$	292	292
Total	1.00	$\frac{W_t}{W_i} = \frac{t}{-1.62t - 4.13} + 1$	439	416

Table 4.8 shows the exponential regression equations and predicted equilibrium widths. All of the equations are able to produce reasonable equilibrium widths. The equilibrium widths predicted by the exponential regression are nearly identical to the equilibrium widths predicted by the hyperbolic regression, indicating that these methods may produce good predictions of the equilibrium channel width.

Table 4.8 Exponential regression equations and predicted widths

Subreach	R ²	Regression Equations	W _e (ft)
1	0.97	$W(t) = 296 + 1295e^{-0.045t}$	296
2	0.64	$W(t) = 494 + 151e^{-0.189t}$	494
3	0.10	$W(t) = 289 + 13e^{-0.117t}$	289
Total	0.90	$W(t) = 452 + 629e^{-0.164t}$	452

4.3 Sediment Transport

4.3.1 Methods

The equilibrium slope of the channel was estimated using sediment transport equations. Equilibrium is achieved when the incoming suspended sediment matches the sediment capacity of the reach. When supply and capacity are equal, the channel should not aggrade or degrade, and a constant slope should be maintained. The incoming sediment supply for each subreach was estimated using the BORAMEP and Psands programs. The channel slope was then varied in HEC-RAS until the calculated sediment transport capacity was within 20% of the incoming sediment supply.

The incoming sediment supply for subreach 1 was estimated using the Bureau of Reclamation Automated Modified Einstein Procedure (BORAMEP). Suspended sediment and bed material gradations were obtained from the San Acacia gauge between 1990 and 2004. In addition, channel geometry, flow conditions, and suspended sediment concentration were also obtained at the San Acacia gauge for the dates of the suspended sediment and bed material samples. The input and output from BORAMEP can be found in the Appendix F. The total sand-sized sediment load calculated by BORAMEP was

plotted vs. discharge. A power-law formula was fit to the data to obtain a regression used for estimating the incoming sediment load in subreach 1.

Psands was used to estimate the incoming sand-size sediment load for subreaches 2 and 3. The sediment load was calculated by Reclamation using Psands for data collected at SO-lines between 1987 and 1996. A power-law formula was fit to a plot of sediment load vs. discharge to obtain an estimate of the incoming sand-sized sediment load.

HEC-RAS calculates sediment transport capacity using several different methods including those developed by Ackers & White, Engelund & Hansen, Laursen, Meyer-Peter & Muller, Toffaleti, and Yang (sand). All methods except Meyer-Peter & Muller provide estimates of total load. Meyer-Peter & Muller estimates bed load only. For a complete listing of the limits of application for these methods as provided by HEC-RAS, see Appendix G.

The total load estimates from BORAMEP and Psands were compared directly with the HEC-RAS total load calculations for the five applicable methods. 1992 geometry data were used for the HEC-RAS runs because the sediment data used in both BORAMEP and Psands were obtained around 1992. Estimating the incoming bed load for each reach was necessary before making comparisons with the Meyer-Peter & Muller bed load. The suspended load was estimated as the portion of the total load that was larger than the d_{10} of the bed material samples collected at the San Acacia gauge for subreach 1 and at SO-lines for subreaches 2 and 3.

The total load for a discharge of 5000 cfs was determined from the rating curves developed from the BORAMEP and Psands results. The bed load was then determined

by multiplying the total load by the percent of material not considered to be suspended load. The slope of the channel was varied until a slope was reached that matched incoming sediment supply and transport capacity. The equilibrium slope was determined for each method in each subreach.

4.3.2 Results

The total load rating curve for the incoming sand-sized sediment is shown in Figure 4.8. Table 4.9 shows the total load obtained from the regression curves at a discharge of 500 cfs, the average d_{10} of the bed material for each subreach, the percent of the suspended sediment that is smaller than the d_{10} of the bed material, and the bed load for each subreach.

Table 4.9 Total load and bed load calculations

	Total Load (tons/day)	Bed material d_{10} (mm)	% smaller than d_{10} of bed	Bed Load (tons/day)
Subreach 1	33298	0.0625	71.9	9344
Subreach 2	35460	0.125	82.3	6263
Subreach 3	38790	0.125	81.8	7068

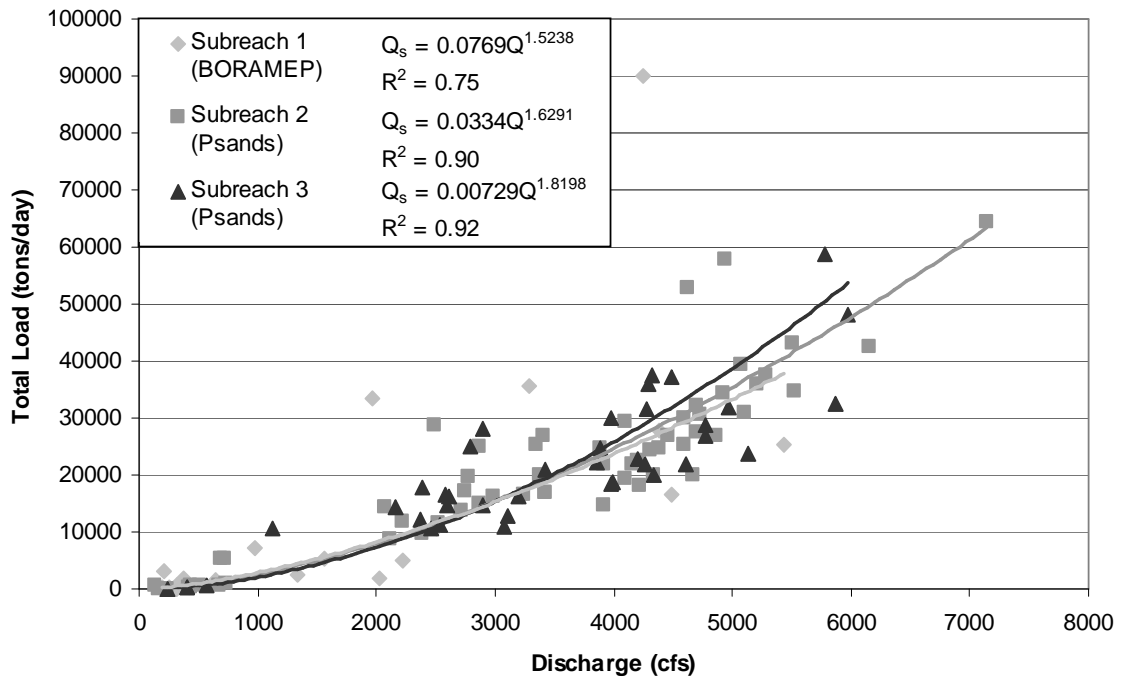


Figure 4.8 Total load rating curves from BORAMEP and Psands

The equilibrium sediment transport capacity and slope are shown for each reach and each method in Table 4.10. Some of the methods did not approach the target transport capacity within a reasonable range of slopes. These reaches do not show a specific equilibrium slope or transport capacity.

Table 4.10 Equilibrium slope determined from transport capacity equations

	Subreach 1	Subreach 2		Subreach 3		
Sediment Transport Equations	Transport Capacity (tons/day)	Slope	Transport Capacity (tons/day)	Slope	Transport Capacity (tons/day)	Slope
Estimated Total Load (tons/day)	33298		35460		38790	
Estimated Bed Material Load (tons/day)	9344		6263		7068	
Existing Channel Slope (from 1992)	0.000759		0.000809		0.000723	
Ackers & White	-	<0.00009	31255	0.00015	-	<0.00009
Engelund & Hansen	33234	0.00052	35020	0.00062	38141	0.00009
Laursen	-	<0.00009	40306	0.00041	-	<0.00009
Meyer-Peter & Muller	-	>0.01	6913	0.01	5668	0.01
Toffaleti	32519	0.00047	29191	0.00052	39097	0.00021
Yang - Sand	31348	0.00041	36112	0.00072	-	<0.00009
Average Slope		0.00193		0.00207		0.0018
Median Slope		0.00044		0.00057		0.00009

Methods by Engelund & Hansen and Toffaleti were the only methods able to determine an equilibrium slope for all subreaches, while Laursen and Ackers & White were only able to determine an equilibrium slope for subreach 2. The methods that predicted equilibrium slopes closest to the current slope were Engelund & Hansend in subreach 1, Yang in subreach 2, and Toffaleti in subreach 3. Meyer-Peter & Muller estimated very high slopes for all reaches. This may be due to the large amount of sediment typically transported as suspended load in this section of the river, leaving very little material to be transported as bed load. Based on their ability to predict reasonable slopes in all subreaches, Engelen & Hansend and Toffaleti seem to be the best methods for determining transport capacity in the Escondida reach.

The average equilibrium slopes predicted by the sediment transport methods are much higher than expected for all reaches due to the influence of the Meyer-Peter & Muller method. The median slopes, however, present a reasonable estimate of the equilibrium slopes for subreaches 1 and 2. The median slope estimated for subreach 3 is

very low compared to the other subreaches and the other methods used to predict the equilibrium slope. Based on the median slope estimates, the channel slope will decrease by 42% in subreach 1, 30% in subreach 2 and 88% in subreach 3. The decrease in slope correlates well with the aggradational trend seen recently in subreach 3, but does not correlate well with the degradational trend seen in subreaches 1 and 2.

4.4 SAM

4.4.1 Methods

The HEC-RAS stable channel design program, known as SAM, was used to determine the equilibrium slope and width for a series of suspended sediment inputs. SAM was developed for use as a preliminary design tool for flood control channels. The program assumes a trapezoidal channel and steady uniform flow in calculations. Given suspended sediment and water discharges, as well as a bed material gradation, SAM computes combinations of stable depth, width, and slope for the channel using Copeland's flow resistance and sediment transport equations. The series of slope and width combinations can then be plotted. The minimum point on the resulting slope vs. width graph is the point of minimum stream power for the input conditions.

The 2002 channel properties were used for the SAM analysis. The inputs included a bank slope of 2H:1V, a bank roughness of $n=0.4$, a discharge of 5000 cfs, and bed material gradation of $d_{84} = 0.45$ mm, $d_{50}=0.3$ mm, $d_{16}=0.18$ mm. A series of suspended sediment concentrations between 800 mg/L and 4500 mg/L were input into SAM as well.

4.4.2 Results

Figure 4.9 shows the slope vs. width curves for each suspended sediment concentration. The width and slope of the channel for 2002 conditions are plotted for comparison. The width was determined from GIS planform measurements and the channel slope was determined from HEC-RAS. The point of minimum stream power on the graph predicts a width of about 150 ft regardless of the suspended sediment concentration. The predicted width is much less than the equilibrium width predicted by any other method.

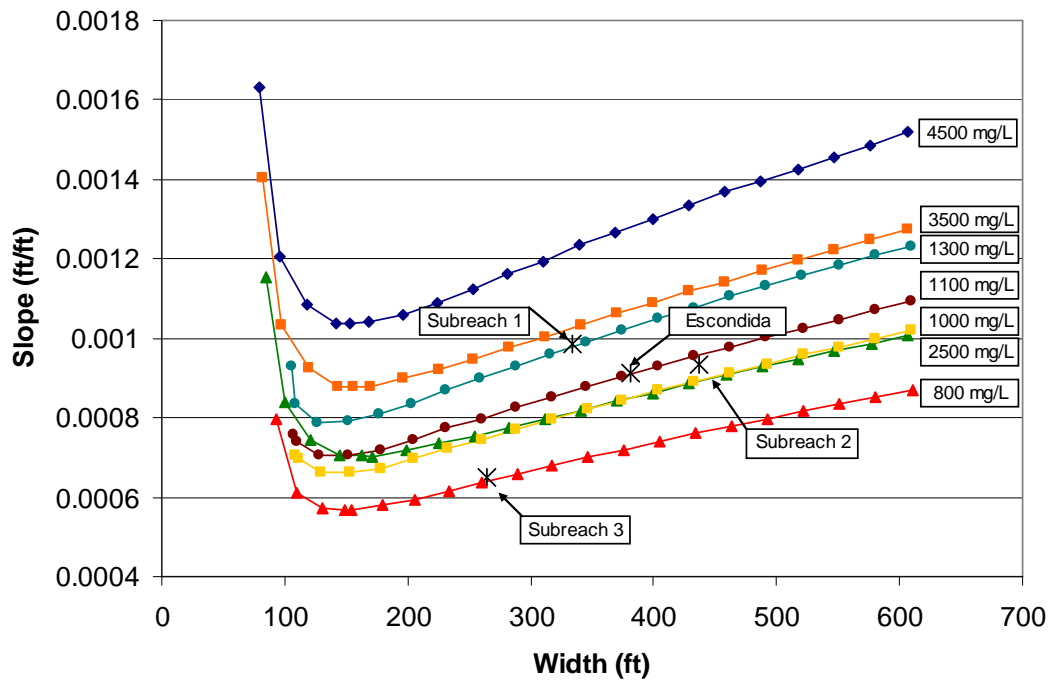


Figure 4.9 Results from SAM for 2002 conditions at $Q = 5000 \text{ cfs}$

Table 4.10 shows the width and slope for each subreach and the entire reach for the 2002 conditions. This width and slope are also plotted in Figure 4.9. Table 4.11 also shows the suspended sediment concentration at each location and the width and slope calculated by SAM for those suspended sediment concentrations. While the equilibrium

width is much lower than other methods predict, the equilibrium slope is reasonable when compared with other methods.

Table 4.11 Current conditions and equilibrium slope and width from SAM

		Subreach 1	Subreach 2	Subreach 3	Total
2002	SS C (mg/L)	2629	3588	4547	3588
	Slope	0.00099	0.00093	0.00065	0.00091
	Width (ft)	334	436	265	381
SAM	Slope	0.000704	0.000878	0.001037	0.000878
	Width (ft)	163.5	155.9	153.3	155.9

4.5 Schumm's (1969) river metamorphosis model

Schumm (1969) developed a model to describe a channel's response to changes in water and sediment discharge. Schumm hypothesized that changes in water and sediment discharge would affect channel width, depth, width/depth ratio, channel slope, sinuosity and meander wavelength. The response of these parameters can be described by the following equations, where a plus (+) exponent indicates an increase and a minus (-) exponent indicates a decrease.

Decreased bed material load:

$$Q_s^- \sim W^- D^+ P^+ L^- S^-$$

Increased bed material load:

$$Q_s^+ \sim W^+ D^- P^- L^+ S^+$$

Decreased water discharge:

$$Q^- \sim W^- D^- L^- S^+$$

Increased water discharge:

$$Q^+ \sim W^+ D^+ L^+ S^-$$

Decreased water discharge and bed material load:

$$Q^- Q_t^- \sim W^- D^\pm F^- L^- S^\pm P^+$$

Increased water discharge and bed material load:

$$Q^+ Q_t^+ \sim W^+ D^\pm F^+ L^+ S^\pm P^-$$

Where Q is water discharge, Q_s is bed material load, Q_t is the percent of the total load that is sand or bed material load, W is channel width, D is flow depth, F is width/depth ratio, L is meander wavelength, P is sinuosity, and S is channel slope.

Table 4.12 shows Schumm's equations in tabular form. In addition, Table 4.13 shows the observed changes in the Escondida reach for each year and subreach.

Table 4.12 Schumm's (1969) channel metamorphosis model

	W	D	S	F = W/D	P	L
Qs⁻	-	+	-		+	-
Qs⁺	+	-	+		-	+
Q⁻	-	-	+			-
Q⁺	+	+	-			+
Q⁻Qt⁻	-	+ -	+ -	-	+	-
Q⁺Qt⁺	+	+ -	+ -	+	-	+

Table 4.13 Observed channel changes at Q = 5000 cfs

Subreach	W	D	S	F = W/D	P
1962-1972					
1	=	+	-	-	+
2	+	+	+	+	-
3	-	+	+	=	=
Total	+	+	+	+	+
1972-1985					-
1	=	+	-	-	-
2	-	-	+	-	-
3	+	-	-	+	+
Total	-	-	=	-	-
1985-1992					
1	-	+	-	-	-
2	+	+	-	+	+
3	-	+	+	-	-
Total	-	+	-	-	+
1992-2002					
1	=	-	+	+	-
2	+	-	-	+	-
3	+	-	+	+	+
Total	+	-	-	+	-

Comparing the observed changes in channel properties to Schumm's equations gives an indication of what the channel may be responding to. Schumm's model seems to work best in the Escondida reach between 1985 and 2002. Few of the changes in the earlier years match the model. The model indicates that between 1985 and 1992, the channel was likely responding to a decrease in discharge and sediment load. This

observation is opposite to the changes in discharge and sediment load observed at the San Acacia and San Marcial gauges at the same time. In addition, the model indicates that between 1992 and 2002, the channel was responding to an increase in both discharge and sediment load. An increase in sediment load was observed during this time, but an increase in discharge was not. This may indicate that the channel is responding more to the changes in sediment supply than to changes in discharge.

4.6 Lane's (1955) balance

Lane's (1955) balance model is illustrated in Figure 4.10. The channel parameters examined by Lane were channel slope, discharge, median grain size, and sediment discharge. The model states that a change in any of the four driving variables will result in a change of the other three variables such that the channel will tend toward a new equilibrium state.

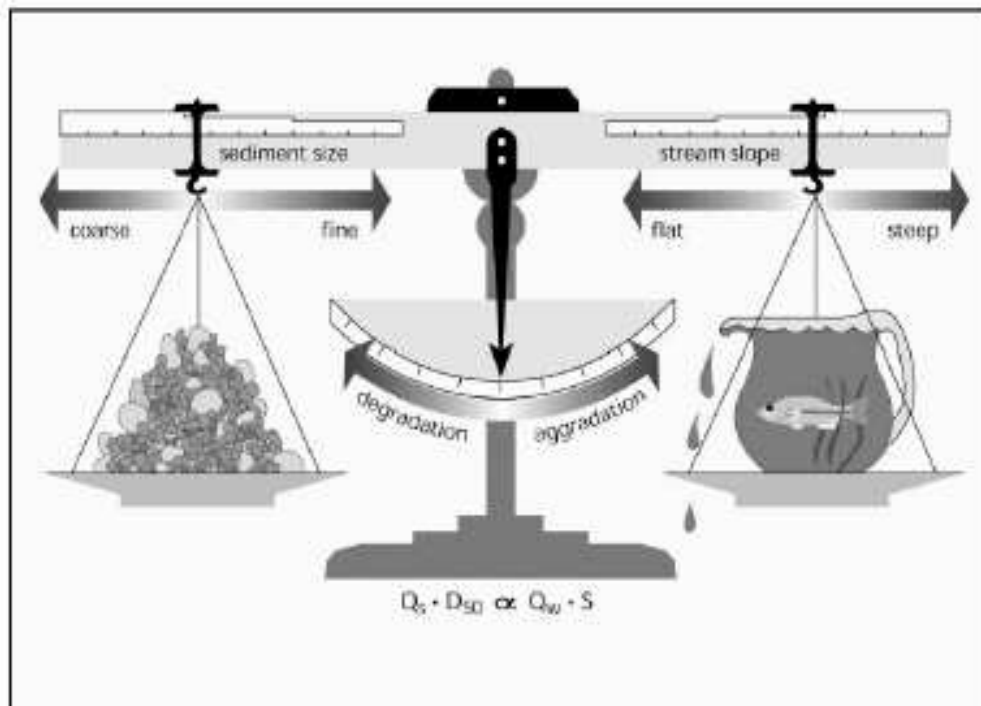


Figure 4.10 Lane's balance(1955)

Table 4.14 shows the observed channel changes from 1962 to 2002 as well as the variable to which the channel may be reacting. The variable initiating change was determined by selecting a variable as the initial point of change, and evaluating the changes in the other variables to determine if they followed the pattern outlined by Lane. If the changes balanced according to Lane, the variable could have been the trigger of channel change. Discharge and suspended sediment discharge were always considered first because the channel cannot change the amount of water or sediment entering the reach from upstream. Suspended sediment data were not available after 1996, so the change from 1992 to 2002 is unknown. The suspended sediment discharge for the unknown time was assumed to be constant for the purpose of this analysis.

Table 4.14 Change in channel characteristics for Lane's balance

Subreach	Q	S	Q _s	d ₅₀	Trigger variable
1962-1972					
1	=	-	+	-	d ₅₀
2	=	+	+	-	Q _s
3	=	+	+	-	Q _s
Total	=	+	+	-	Q _s
1972-1985					
1	+	-	+	+	Q
2	+	+	+	+	None
3	+	-	+	-	None
Total	+	=	+	+	None
1985-1992					
1	=	-	=	+	None
2	=	-	=	+	None
3	=	+	=	+	S or d ₅₀
Total	=	-	=	+	None
1992-2002					
1	-	+		+	None
2	-	-		+	d ₅₀
3	-	+		-	Q
Total	-	-		+	d ₅₀

According to Lane's balance, between 1962 and 1972 the channel was primarily reacting to a change in the incoming suspended sediment discharge. Between 1972 and 1992, the channel did not change in a way that was predicted by Lane. Assuming a constant suspended sediment discharge, the channel seemed to be reacting to an increase in median grain diameter, with some influence from a decrease in water discharge. It is likely that the channel is actually under the influence of multiple channel changes at any given time. However, this simplified approach gives some idea of what changes may be having the greatest influence on the channel morphology.

4.7 Summary

4.7.1 Equilibrium Width

Hydraulic Geometry

The hydraulic geometry equation developed by Blench (1957) gave equilibrium widths that most closely matched the current channel conditions. However, Blench may not be the best method for predicting equilibrium width because the channel was likely not in equilibrium between 1962 and 2002. Simons and Albertson (1963), Nouh (1988), Lacey [1930-1958, from Wargadalam (1993)], and Julien and Waradalam (1995) all predicted similar equilibrium widths between 200 ft and 300 ft. The consistent prediction by these four methods indicates that they may be the most effective in predicting equilibrium width.

Hyperbolic and Exponential Models

The hyperbolic model developed by Williams and Wolman (1984) fit well with historic width data from the Escondida reach. The widths predicted by the hyperbolic model ranged from about 300 ft to about 450 ft. The method predicted a negative equilibrium width for subreach 1, but predicted a reasonable width for 2020. More data should be added to the model to improve the equilibrium prediction for subreach 1.

The exponential model developed by Richard et al. (2005) produced results very similar to those calculated by the hyperbolic model. However, this model was able to predict reasonable equilibrium widths for all subreaches and the total reach.

SAM

The final equilibrium width prediction method used was the HEC-RAS stable channel design program (SAM). Based on the incoming suspended sediment concentration estimated for each subreach and the total reach, the equilibrium widths for the channel were all about 160 ft. This width is less than the widths predicted by the other methods, but it still provides a reasonable estimate of equilibrium channel width.

4.7.2 Equilibrium Slope

Hydraulic Geometry

Julien and Wargadalam (1995) predicted equilibrium slopes for the 2002 channel geometry between 0.00083 and 0.00139. These slopes are much steeper than the slopes observed in the channel during that time, indicating that the channel may not be in

equilibrium. The predicted slopes are, however, reasonable when compared to historic channel slopes.

SAM

The equilibrium slope was also estimated from the HEC-RAS stable channel design program. The program estimated the equilibrium slope to between 0.00065 and 0.00099 depending upon the incoming suspended sediment concentration. These results are very similar to the predictions made by Julien and Wargadalam.

Sediment Transport

The HEC-RAS sediment transport analysis was used to determine an equilibrium slope for the channel based on sediment transport. The equilibrium slope was estimated as the slope at which sediment supply equals sediment transport capacity. Engelund & Hansen and Toffaleti were the only methods able to provide reasonable slope predictions for all subreaches. These methods estimated the equilibrium slope to be between 0.00009 and 0.00062. This slope range is much less steep than the slopes estimated by Julien-Wargadalam and SAM. The slopes are also much less steep than the historic slopes in the reach. This method may not be the best for predicting equilibrium slope for this reach. A better accounting of incoming sediment from all sources, such as arroyos and other ungauged tributaries, may improve the predictions provided by the sediment transport analysis.

Chapter 5: Summary and Conclusion

The Escondida reach was analyzed for this study. The reach covers 17.7 miles of the Middle Rio Grande in central New Mexico. Important changes occurring in the Escondida reach between 1918 and 2005 were analyzed using a number of techniques. Changes in channel geometry and morphology and water and sediment discharge were observed. In addition, historic bedform data were analyzed. Finally, the equilibrium conditions of the reach were estimated.

Spatial and temporal trends in channel geometry and morphology were identified using visual observations of aerial photographs and GIS active channel planforms, cross-section surveys, hydraulic modeling using HEC-RAS, and channel classification methods. Observations of the GIS active channel planforms and aerial photographs show that the channel has narrowed between 1918 and 2005. The most significant narrowing has occurred in the upper portion of the reach. Analysis of channel geometry trends using HEC-RAS hydraulic modeling output shows a series of increases and decreases in most channel properties. The fluctuations in channel geometry may be the result of a complex response to past channel changes. Bed material samples obtained from cross-section surveys and at the San Acacia and San Marcial gauges between 1962 and 2002 show a slight coarsening of the bed from a mean diameter of 0.15 mm to 0.31 mm.

Historic bedform observations were compiled and compared to predicted bedforms at the survey locations. Simons and Richardson and van Rijn were used to calculate the expected bedforms at each survey locations. These predictions were compared with field observations of bedforms. The bedform predictor methods produced adequate results. Large scatter was observed in the data, especially in the prediction of lower regime bedforms. This scatter is likely due to the wide variability across individual cross-sections in the reach.

Trends in water and sediment discharge were analyzed using mass curves developed from USGS gauge data. The mass curves show a wet period between 1979 and 2000. This increase in discharge was also observed in upstream reaches. The increase in discharge caused the Escondida reach to carry a similar magnitude of discharge as the upstream reaches, where, historically, the reach carried much lower discharges. The daily mean suspended sediment discharge remained nearly constant for the entire period of record. The difference mass curve shows periods of aggradation and degradation that approximately correlate with changes in mean bed elevation.

Estimates of potential equilibrium slope and width conditions were made using hydraulic geometry equations, hyperbolic and exponential regressions, stable channel geometry, and sediment transport relationships. An equilibrium width of around 300 ft was estimated by several methods, indicating that this is a reasonable estimate of the future channel width. Julien-Wargadalam and SAM predicted equilibrium slopes between 0.00065 and 0.00139, depending on the subreach and the method used. These slopes are within a reasonable range of the current slope and provide a good estimate of the direction of potential slope change in each subreach.

The main conclusions of this study are

- The active channel has narrowed and the sinuosity decreased from 1.19 to 1.09 between 1918 and 2005. In addition, the mean bed material diameter increased from 0.15 mm to 0.31 mm between 1962 and 2002.
- Bedform prediction methods by van Rijn and Simons and Richardson produced a reasonable fit to the observed bedform data. The data showed wide scatter, likely caused by the high degree of variability across a cross-section.
- The water discharge indicated a period of increased water discharge between 1979 and 2000. The increase in discharge that occurred in 1979 was observed in upstream reaches, but was more dramatic in the Escondida reach.
- Equilibrium width and slope predictors forecast a channel width of about 300 ft and a slope between 0.00065 and 0.00139. These estimates were confirmed by multiple methods and seem to be reasonable estimates.

The collective observations of the reach indicate that this is a very dynamic reach that has not yet reached an equilibrium state. The channel will likely continue to narrow. Lateral movement and sinuosity changes are also likely as the channel attempts to reach an equilibrium slope.

References

- Ackers, P. (1982). Meandering Channels and the Influence of Bed Material. *Gravel Bed Rivers. Fluvial Processes, Engineering and Management.* Edited by R.D. Hey, J.C. Bathurst and C.R. Thorne. John Wiley & Sons Ltd. pp. 389-414.
- Albert, J., Sixta, M., Leon, C., and Julien, P.Y. (2003). Corrales Reach. Corrales Flood Channel to Montano Bridge. Hydraulic Modeling Analysis. 1962-2001. Middle Rio Grande, New Mexico. Prepared for U.S. Bureau of Reclamation. Albuquerque, New Mexico. Colorado State University, Fort Collins, CO. 130 p.
- Albert, J. (2004). Hydraulic Analysis and Double Mass Curves of the Middle Rio Grande from Cochiti to San Marcial, New Mexico. M.S. Thesis. Colorado State University, Fort Collins, CO. 207 p.
- Bauer, T.R. (2000). Morphology of the Middle Rio Grande from Bernalillo Bridge to the San Acacia Diversion Dam, New Mexico. M.S. Thesis. Colorado State University, Fort Collins, CO. 308 p.
- Blench, T. (1957). *Regime Behavior of Canals and Rivers.* London: Butterworths Scientific Publications. 138p.
- Bogan, M., Alllen, C., Muldavin, E., Platania, S., Stuart, J., Farley, G., Mehlhop, P., Belnap, J. (2006). "Southwest." *United States Geological Survey.* <<http://biology.usgs.gov/s+t/SNT/noframe/sw152.htm>> (June 27, 2006).
- Brown, M. (2006). Personal Communication. Graduate Student. Colorado State University. Fort Collins, CO.
- Bullard, K.L. and Lane, W.L. (1993). Middle Rio Grande Peak Flow Frequency Study. U.S. Department of the Interior, Bureau of Reclamation, Albuquerque, NM. 36 p.
- Chang, H.H. (1979). Minimum Stream Power and River Channel Patterns. *Journal of Hydrology.* 41, pp. 303-327.
- Clark, I. G. (1987). *Water in New Mexico: A History of its Management and Use.* Albuquerque, NM: University of New Mexico Press. 839 p.
- Dewey, J.D., Roybal, F.E., Funderburg, D.E. (1979). Hydraulic Data of Channel Adjustments 1970 to 1975, on the Rio Grande Downstream from Cochiti Dam, New Mexico Before and After Closure. U.S. Geological Survey, Water Resources Investigations. pp. 70-79.

- Earick, D. (1999). The History and Development of the Rio Grande River in the Albuquerque Region. Available at <http://www.unm.edu/~abqteach/EnvirCUs/99-03-04.htm>. Accessed June 27, 2006).
- Graf, W.L. (1994). *Plutonium and the Rio Grande. Environmental Change and Contamination in the Nuclear Age.* New York: Oxford University Press. 348 p.
- Hawley, J.W. (1987). Guidebook to Rio Grande Rift in New Mexico and Colorado. *New Mexico Bureau Mines & Mineral Resources.* Circular 163. 241+ p.
- Henderson, F.M. (1966). *Open Channel Flow.* New York, NY: Macmillan Publishing Co., Inc. 544 p.
- Herford, R. (1984). Climate and ephemeral-stream processes: Twentieth-century geomorphology and alluvial stratigraphy of the Little Colorado River, Arizona. *Geological Society of America Bulletin.* v.95, pp.654-688.
- Julien, P.Y. (1998). *Erosion and Sedimentation.* New York, NY: Cambridge University Press. 280 p.
- Julien, P.Y. and Wargadalam, J. (1995). Alluvial Channel Geometry: Theory and Applications. *Journal of Hydraulic Engineering,* 121(4), pp. 312-325.
- Klaassen, G.J. and Vermeer, K. (1988). Channel Characteristics of the Braiding Jamuna River, Bangladesh. *International Conference on River Regime,* 18-20 May 1988. W.R. White (ed.), Hydraulics Research Ltd., Wallingford, UK. pp. 173-189.
- Lagasse, P.F. (1980). An Assessment of the Response of the Rio Grande to Dam Construction – Cochiti to Isleta Reach. U.S. Army Corps of Engineers. Albuquerque, NM. 133 p.
- Lane, E.W. (1955). The importance of fluvial morphology in hydraulic engineering. *Proc. ASCE,* 81(745):1-17.
- Larsen, S. and Reilinger, R. (1983). “Recent measurements of crustal deformation related to the Socorro Magma Body, New Mexico.” *New Mexico Geological Society Guidebook, 34th Field Conference.* pp. 119-121.
- Leon, C. and Julien, P.Y. (2001a). Hydraulic Modeling on the Middle Rio Grande, NM. Corrales Reach. Corrales Flood Channel to Montano Bridge. Prepared for U.S. Bureau of Reclamation. Albuquerque, New Mexico. Colorado State University, Fort Collins, CO. 83 p.

- Leon, C. and Julien, P.Y. (2001b). Bernalillo Bridge Reach. Highway 44 Bridge to Corrales Flood Channel Outfall. Hydraulic Modeling Analyssi. 1962-2002. Middle Rio Grande, New Mexico. Prepared for the U.S. Bureau of Reclamation. Albuquerque, New Mexico. Colorado State University, Fort Collins, CO. 85 p.
- Leopold, L.B. and Wolman, M.G. (1957). River Channel Patterns: Braided, Meandering, and Straight. *USGS Professional Paper 282-B*. 85 p.
- Middle Rio Grande Conservancy District. (2004). About the District. Available at <http://www.mrgcd.com/?cmd=pages&what=About%20the%20District>. Accessed on June 27, 2006.
- Middle Rio Grande Conservancy District v. Norton*, 2002 10CIR 685, 294 F.3d 1220, (2002).
- Middle Rio Grande Endangered Species Act Collaborative Program. (2006a). The Rio Grande Silvery Minnow. Available at <http://www.fws.gov/mrgesacp/MRGSM.cfm>. Accessed on June 6, 2006.
- Middle Rio Grande Endangered Species Act Collaborative Program. (2006b). The Southwestern Willow Flycatcher. Available at <http://www.fws.gov/mrgesacp/SWWFC.cfm>. Accessed on June 6 ,2006.
- Nanson, G.C. and Croke, J.C. (1992). A genetic classification of floodplains. *Geomorphology*. 4, pp. 459-486.
- Nouh, M. (1988). Regime Channels of an Extremely Arid Zone. *International Conference of River Regime*, 18-20 May 1988. W.R. White (ed.). Hydraulics Research Ltd., Wallingford, UK. pp 55-66.
- Novak, S.J. (2006). Hydraulic modeling anlysis of the Middle Rio Grande River from Cochiti Dam to Galisteo Creek, New Mexico. M.S thesis, Civil Engineering Department, Colorado State University, Fort Collins, CO. 168 p.
- Novak, S.J., Julien, P.Y. (2005). Cochiti Dam Reach. Cochiti Dam to Galisteo Creek. Hydraulic Modeling Analysis. 1962-2002. Middle Rio Grande, New Mexico. Prepared for U.S. Bureau of Reclamation. Albuquerque, New Mexico. Colorado State University, Fort Collins, CO. 144 p.
- Ouchi, S. (1983). Response of alluvial rivers to active tectonics. PhD. dissertation, Earth Resources Department, Colorado State University, Fort Collins, CO. 205 p.
- Parker, G. (1976). On the Cause and Characteristic Scales of Meandering and Braiding in Rivers." *Journal of Fluid Mechanics*. vl. 76, part 3, pp. 457-480.

- Porter, M. and Massong, T. (2004). *Habitat fragmentation and modifications affecting distribution of the Rio Grande silvery minnow*. United States Department of the Interior, Bureau of Reclamation, Fishery and Aquatic GIS Research Group, Albuquerque, NM. pp. 421-432.
- Reclamation. (2003). *Geomorphologic assessment of the Rio Grande, San Acacia reach*. United States Department of the Interior, Bureau of Reclamation, Albuquerque Area Office, Albuquerque, NM. 75 p.
- Richard, G., Julien, P.Y., Baird, D.C., (2005). Case Study: Modeling the Lateral Mobility of the Rio Grande below Cochiti Dam, New Mexico. *Journal of Hydraulic Engineering*. 131(11), pp. 931-941.
- Richard, G., Leon, C., and Julien, P.Y. (2001). Hydraulic Modeling on the Middle Rio Grande, New Mexico. Rio Puerco Reach. Prepared for U.S. Bureau of Reclamation. Albuquerque, New Mexico. Colorado State University, Fort Collins, CO. 102 p.
- Richardson, E.V., Simons, D.B., Lagasee, P.F. (2001). *River Engineering for Highway Encroachments, Highways in the River Environment*. United States Department of the Transportation, Federal Highway Administration. 644 p.
- Rosgen, D. (1996). *Applied River Morphology*. Pagosa Springs, CO: Wildland Hydrology. 360 p.
- Schumm, S.A. (1969). River Metamorphosis. *Journal of Hydraulics Division, ASCE*. Vol. 95, No.1. pp. 255-273.
- Schumm, S.A. (1979). Geomorphic Thresholds: The Concept and Its Applications. *Transactions of the Institute of British Geographers*. New Series, Vol. 4, No. 4. pp. 485-515.
- Schumm, S.A and Khan, H.R. (1972). Experimental Study of Channel Patterns. *Geological Society of America Bulletin*. 83, pp. 1755-1770.
- Scurlock, D. (1998). *From the Rio to the Sierra: An Environmental History of the Middle Rio Grande Basin*. General Technical Report RMRS-GTR5. United States Department of Agriculture, Forest Service, Rocky Mountain Research Station, Fort Collins, CO. 440 p.
- Simons, D.B. and Albertson, M.L. (1963). Uniform Water Conveyance Channels in Alluvial Material. *Transactions of the American Society of Civil Engineers*. Paper No. 3399. Vol. 128, Part I. pp. 65-107.

- Sixta, M., Albert, J., Leon, C., and Julien, P.Y. (2003a). Bernalillo Bridge Reach. Highway 44 Bridge to Corrales Flood Channel Outfall. Hydraulic Modeling Analysis. 1962-2001. Middle Rio Grande, New Mexico. Prepared for U.S Bureau of Reclamation. Albuquerque, New Mexico. Colorado State University, Fort Collins, CO. 87 p.
- Sixta, M., Albert, J., Leon, C., and Julien, P.Y. (2003b). San Felipe Reach. Arroyo Tonque to Angostura Diversion Dam. Hydraulic Modeling Analysis. 1962-1998. Middle Rio Grande, New Mexico. Prepared for U.S Bureau of Reclamation. Albuquerque, New Mexico. Colorado State University, Fort Collins, CO. 85 p.
- Tetra Tech, Inc. (2002). *Development of the Middle Rio Grande FLO-2D Flood Routing Model Cochiti Dam to Elephant Butte Reservoir*. Tetra Tech, Inc. 48 p.
- U.S. Army Corps of Engineers, USACE (2005). HEC-RAS River Analysis System. v.3.1.3. U.S Army Corps of Engineers Institute for Water Resources. Hydrologic Engineering Center, Davis, CA.
- van den Berg, J.H. (1995). Prediction of Alluvial Channel Pattern of Perennial Rivers. *Geomorphology*. 12, pp. 259-279.
- van Rijn, L.C. (1984). Sediment Transport, part III: Bedforms and Alluvial Roughness. *Journal of the Hydraulic Division, ASCE*. 110 (12), pp. 1733-1754.
- Vensel, C., Richard, G., Leon, C.L., and Julien, P.Y. (2005). Hydraulic Modeling on the Middle Rio Grande, New Mexico. Rio Puerco Reach. Prepared for U.S. Bureau of Reclamation. Albuquerque, New Mexico. Colorado State University, Fort Collins, CO. 100 p.
- Wargadalam, J. (1993). Hydraulic Geometry of Alluvial Channels. Ph.D. Dissertation. Colorado State University, Fort Collins, CO. 203 p.
- Williams, G. and Wolman, G. (1984). Downstream Effects of Dams on Alluvial Rivers. U.S. Geological Survey Professional Paper 1286, 83 p.
- Woodson, R.C. and Martin, J.T. (1962). The Rio Grande Comprehensive Plan in New Mexico and its Effects on the River Regime Through the Middle valley. Control of Alluvial Rivers by Steel Jetties. *Proceedings of the American Society of Civil Engineers. Journal of Waterways and Harbor Division*. Carlson, E.L. and Dodge, E.A. eds. American Society of Civil Engineers, New York, NY, pp. 53-81.

Appendix A –
Socorro Line Survey Plots

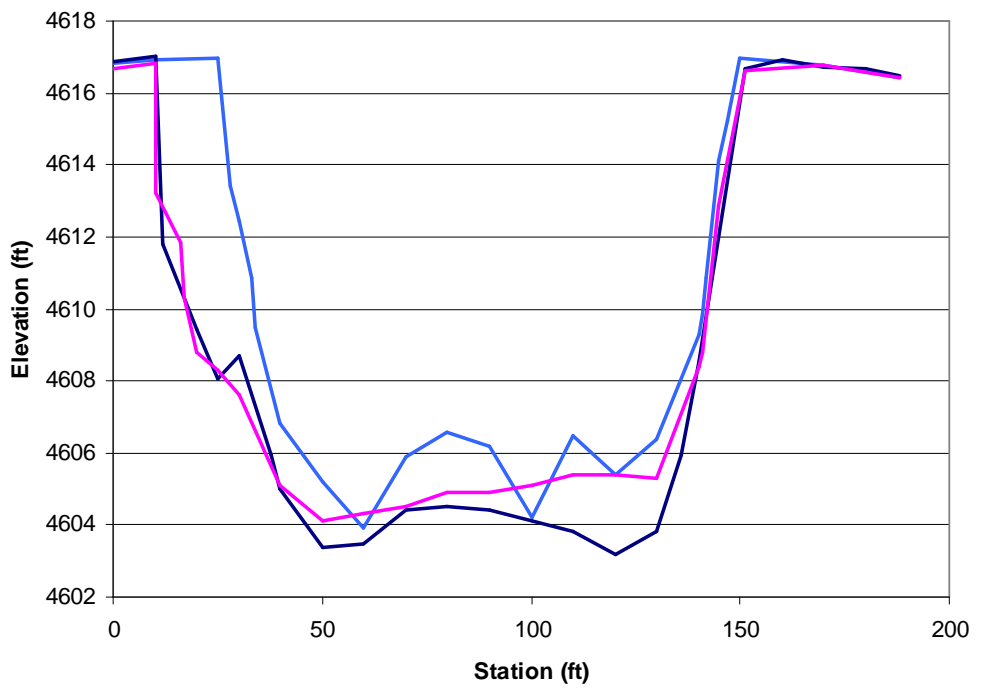


Figure A.1 Cross-section survey at SO-line 1313

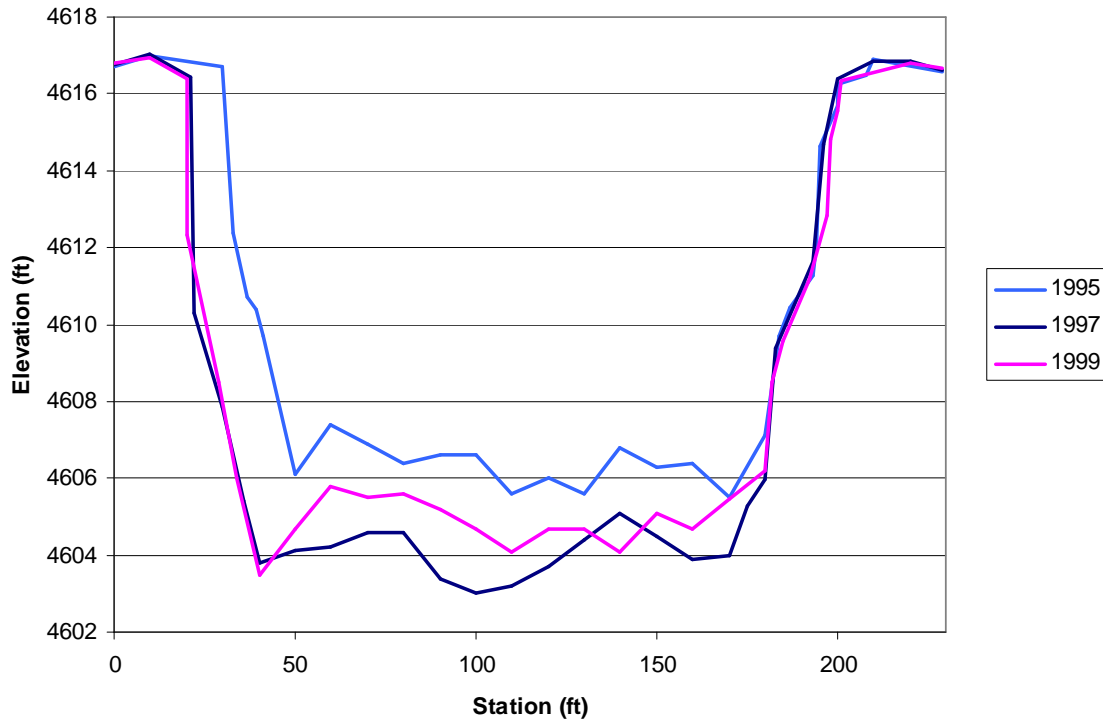


Figure A.2 Cross-section survey at SO-line 1314

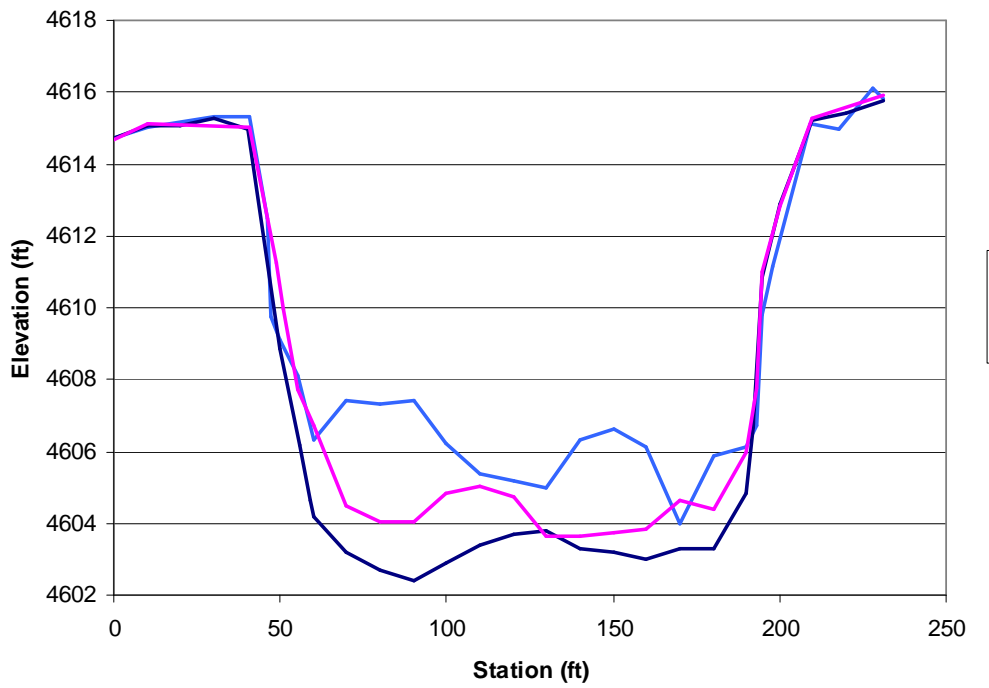


Figure A.3 Cross-section survey at SO-line 1316

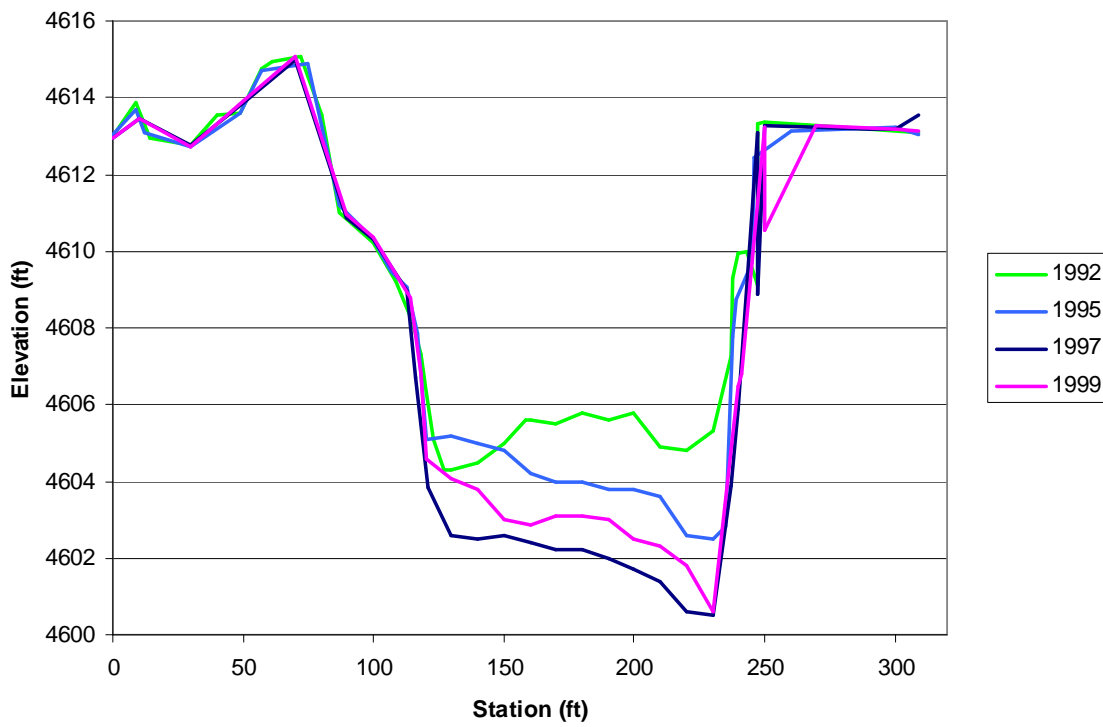


Figure A.4 Cross-section survey at SO-line 1320

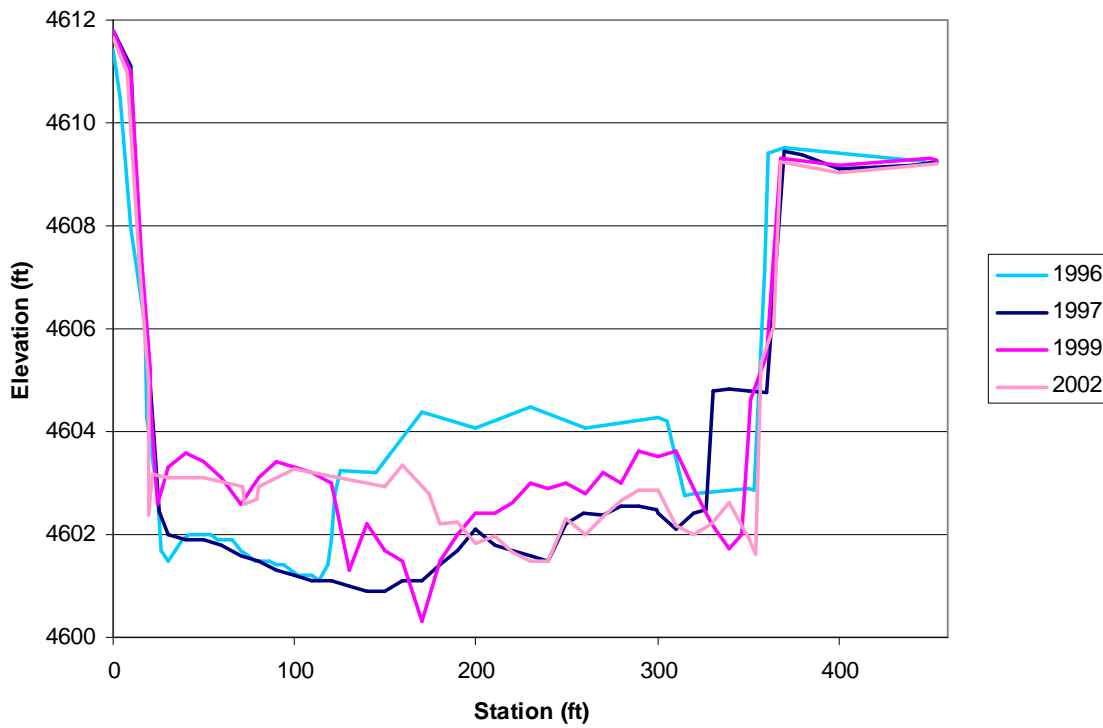


Figure A.5 Cross-section survey at SO-line 1327

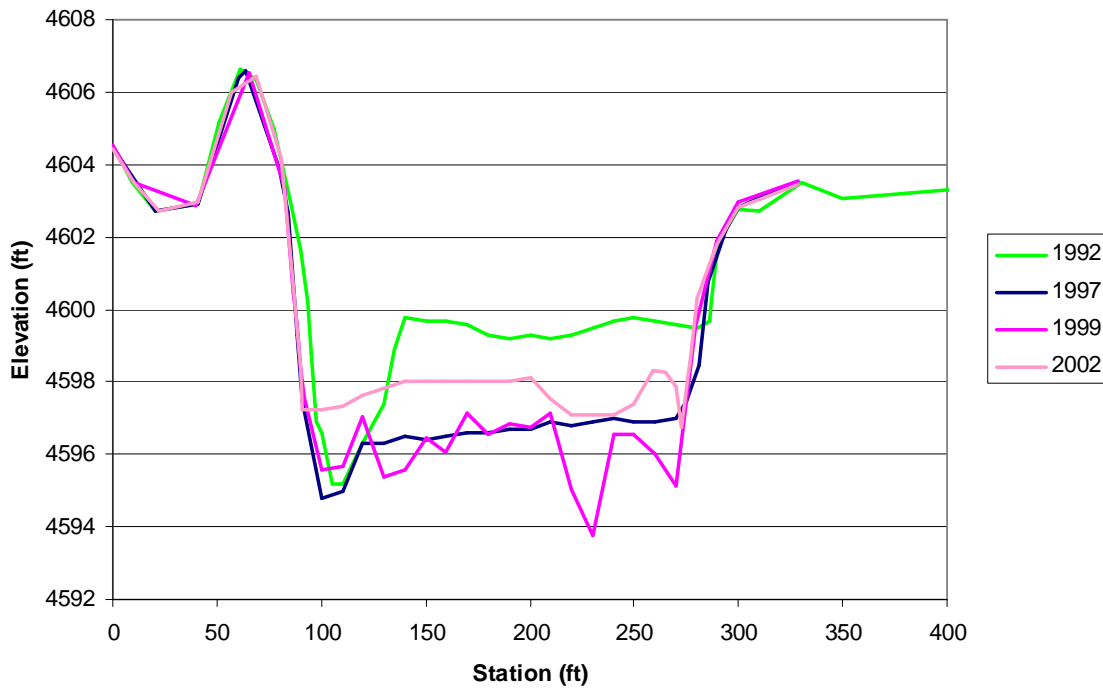


Figure A.6 Cross-section survey at SO-line 1339

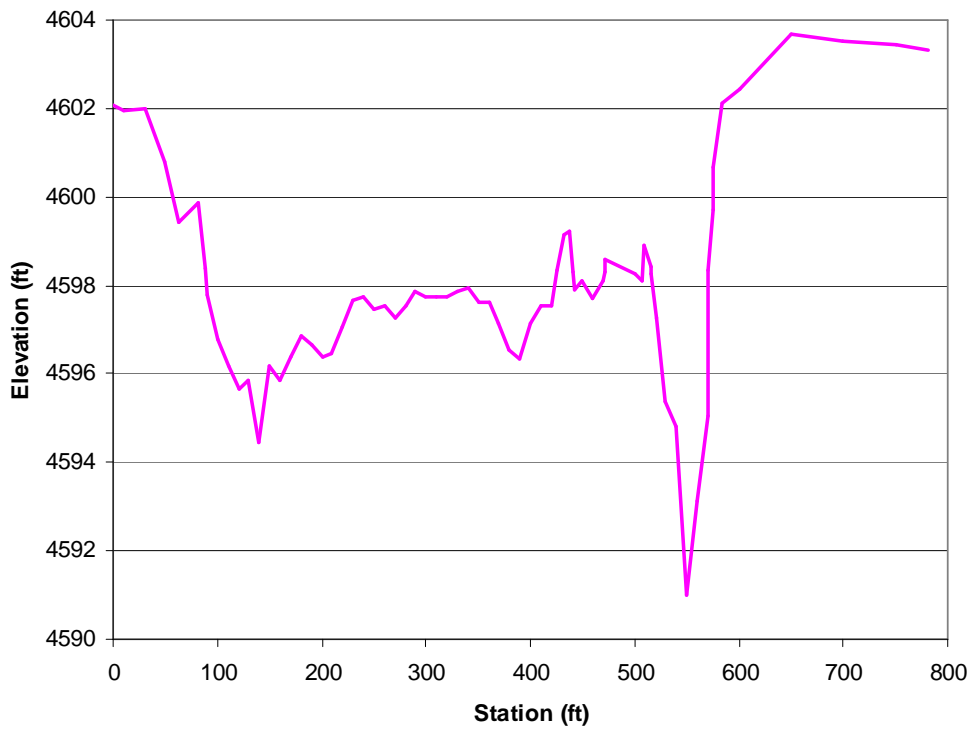


Figure A.7 Cross-section survey at SO-line 1342.5

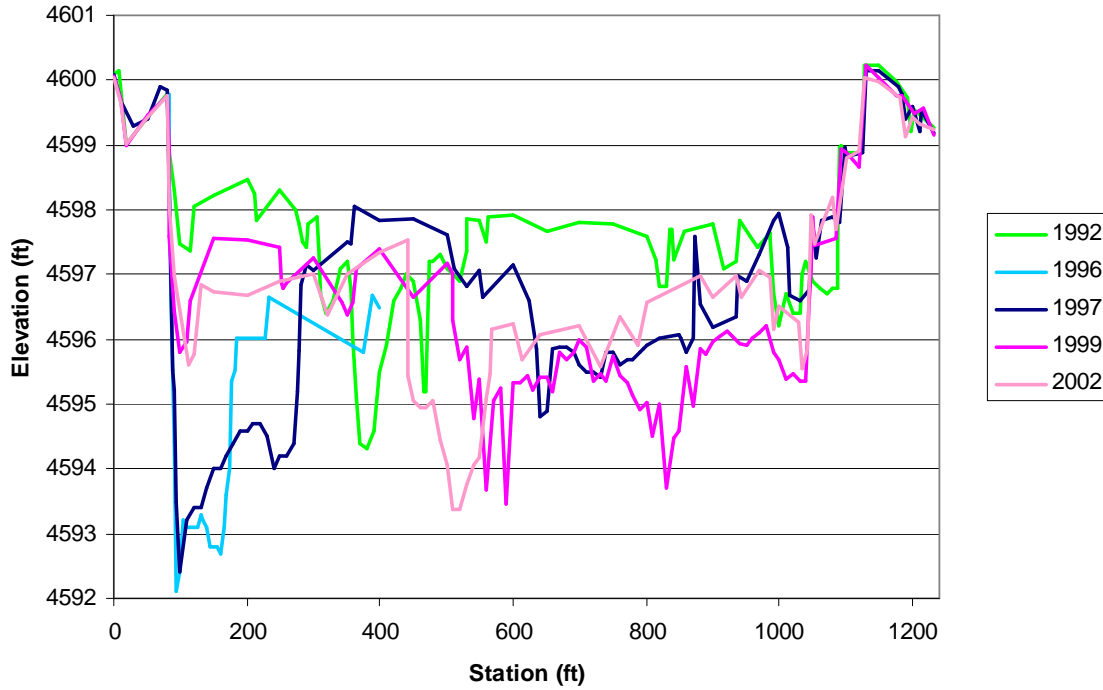


Figure A.8 Cross-section survey at SO-line 1346

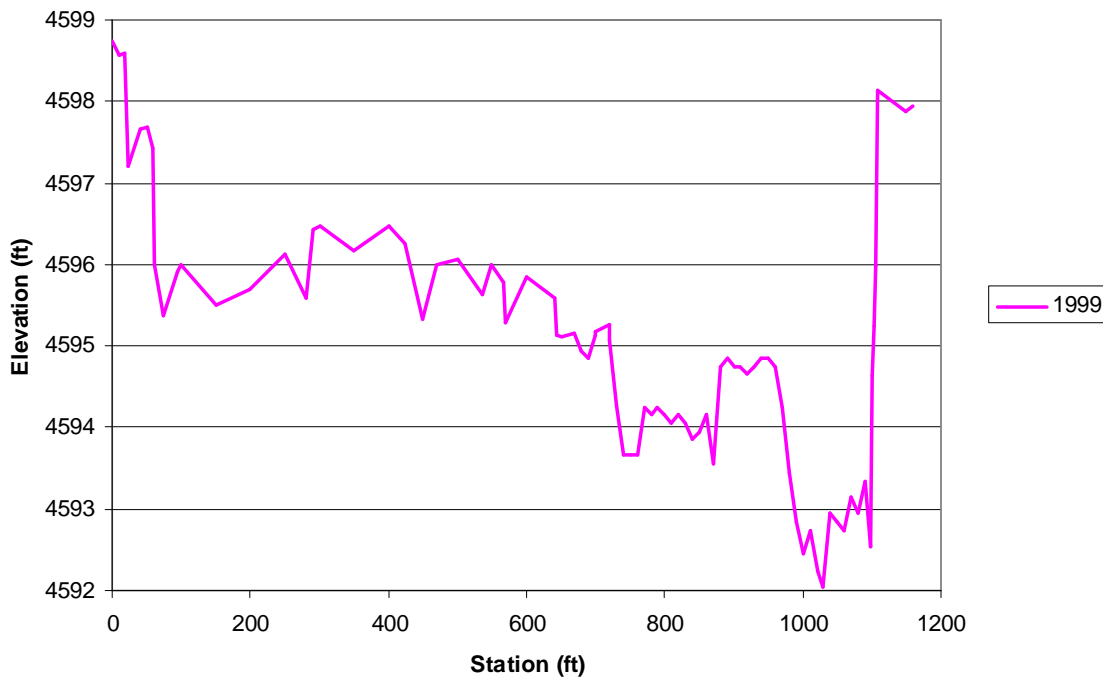


Figure A.9 Cross-section survey at SO-line 1349

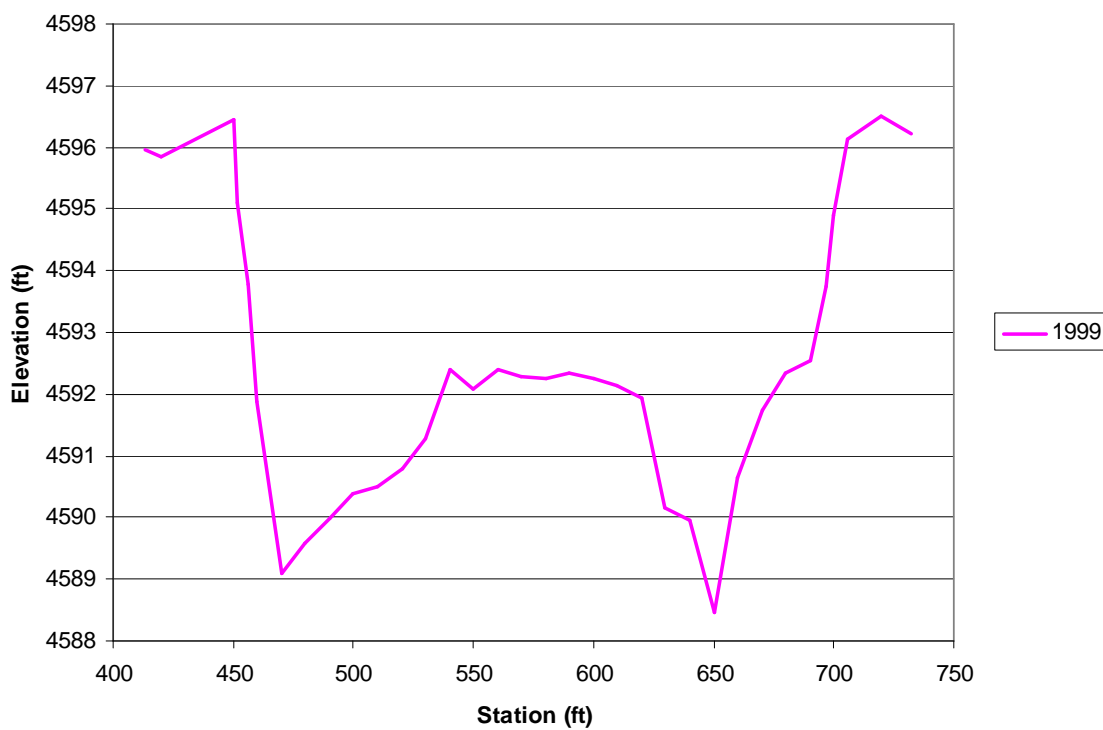


Figure A.10 Cross-section survey at SO-line 1352

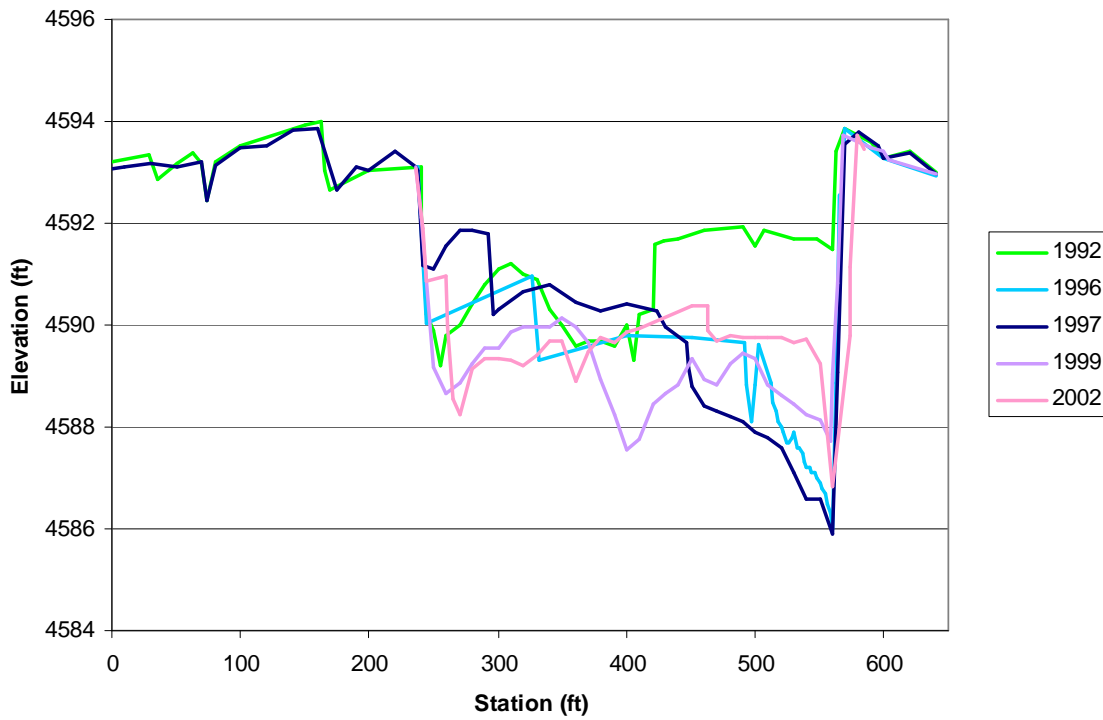


Figure A.11 Cross-section survey at SO-line 1360

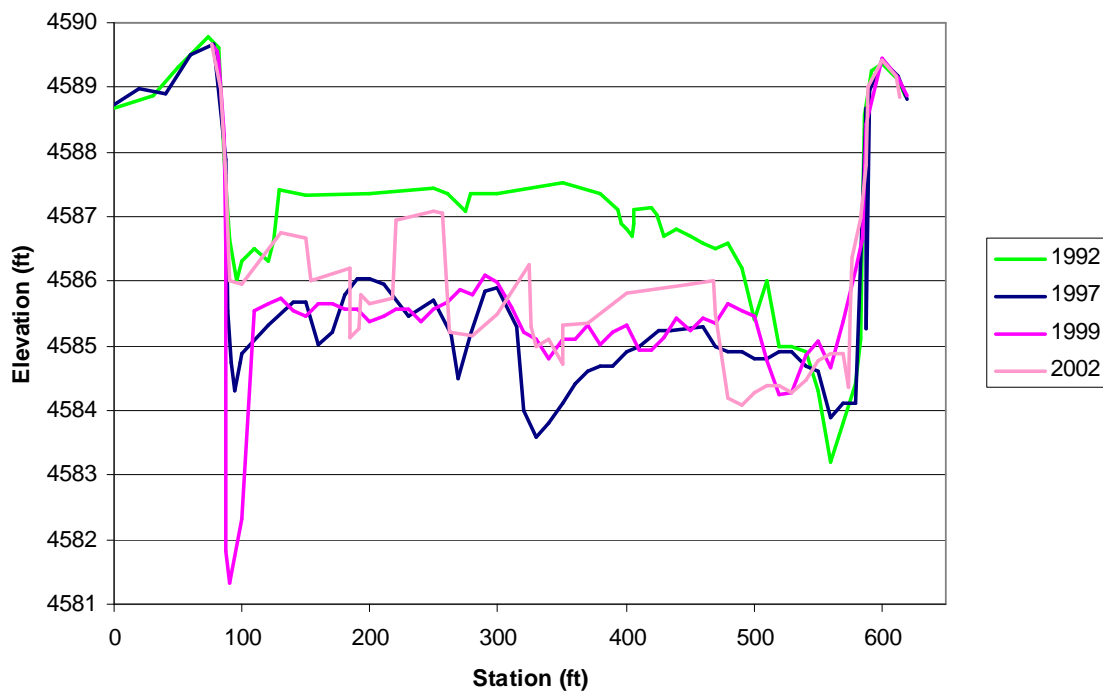


Figure A.12 Cross-section survey at SO-line 1371

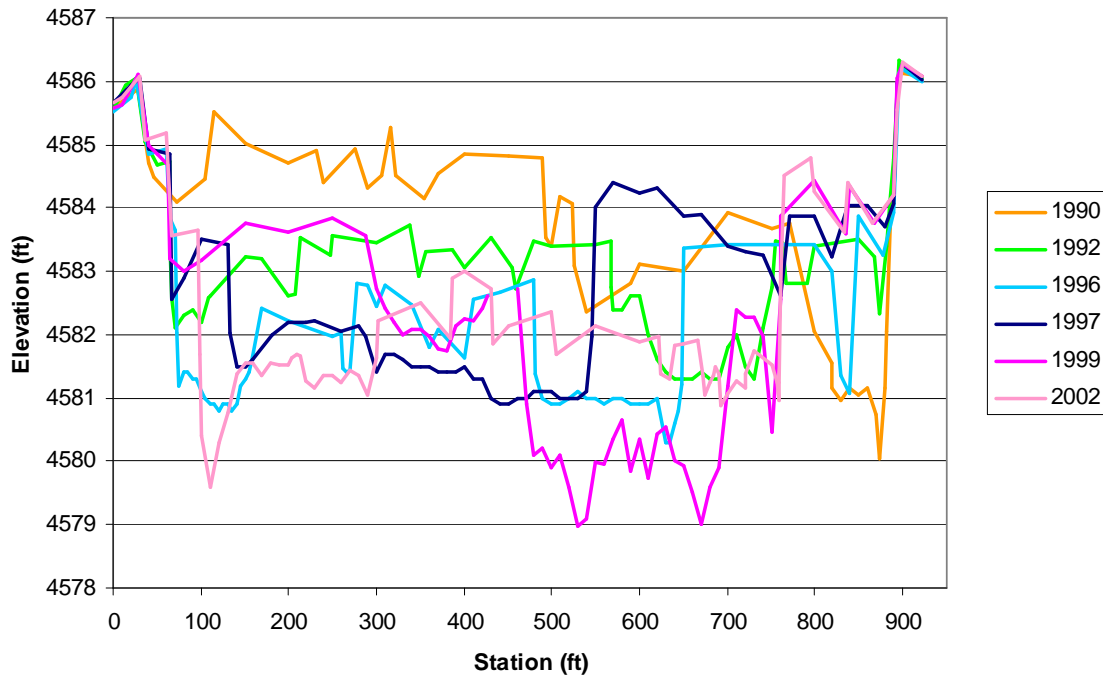


Figure A.13 Cross-section survey at SO-line 1380

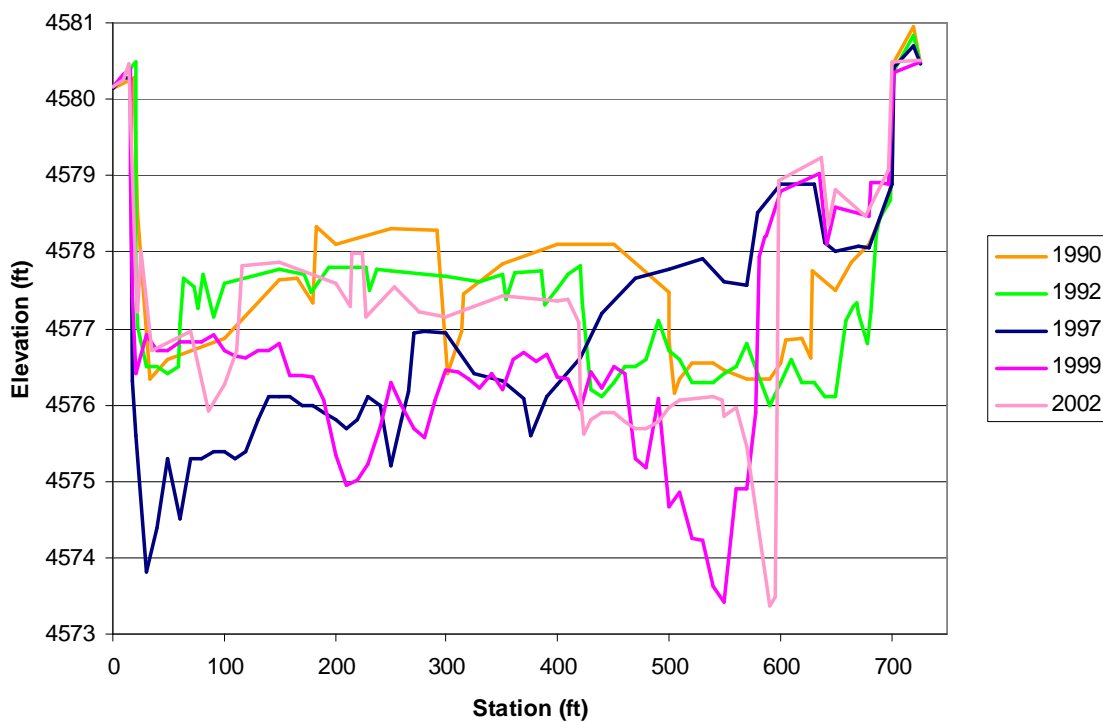


Figure A.14 Cross-section survey at SO-line 1394

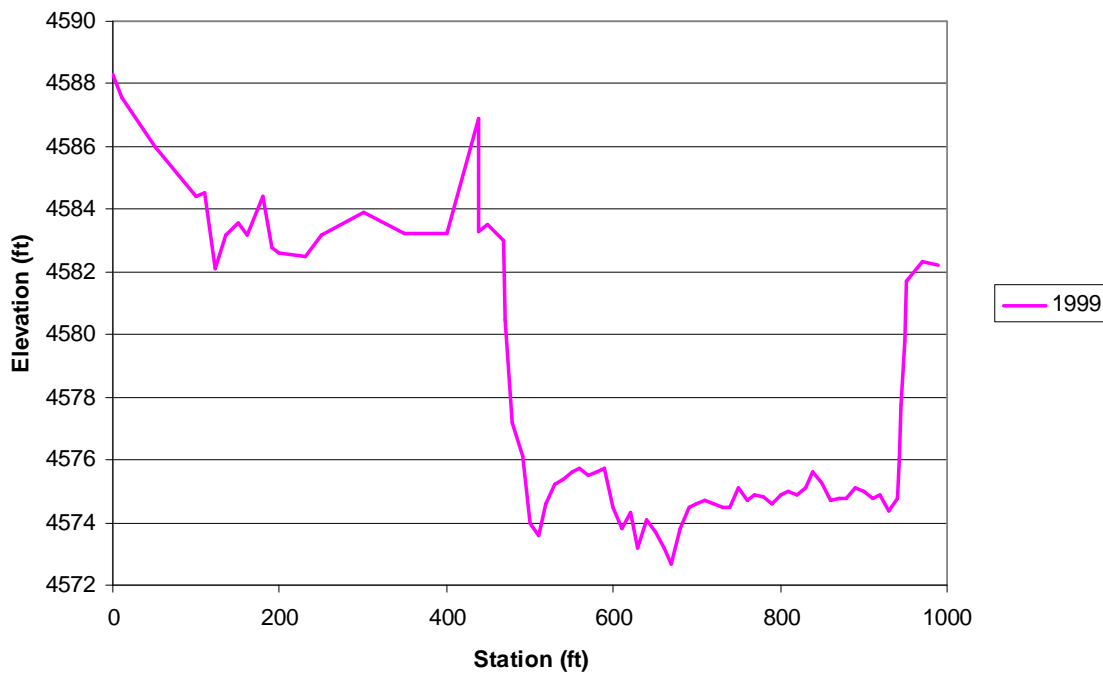


Figure A.15 Cross-section survey at SO-line 1396.5

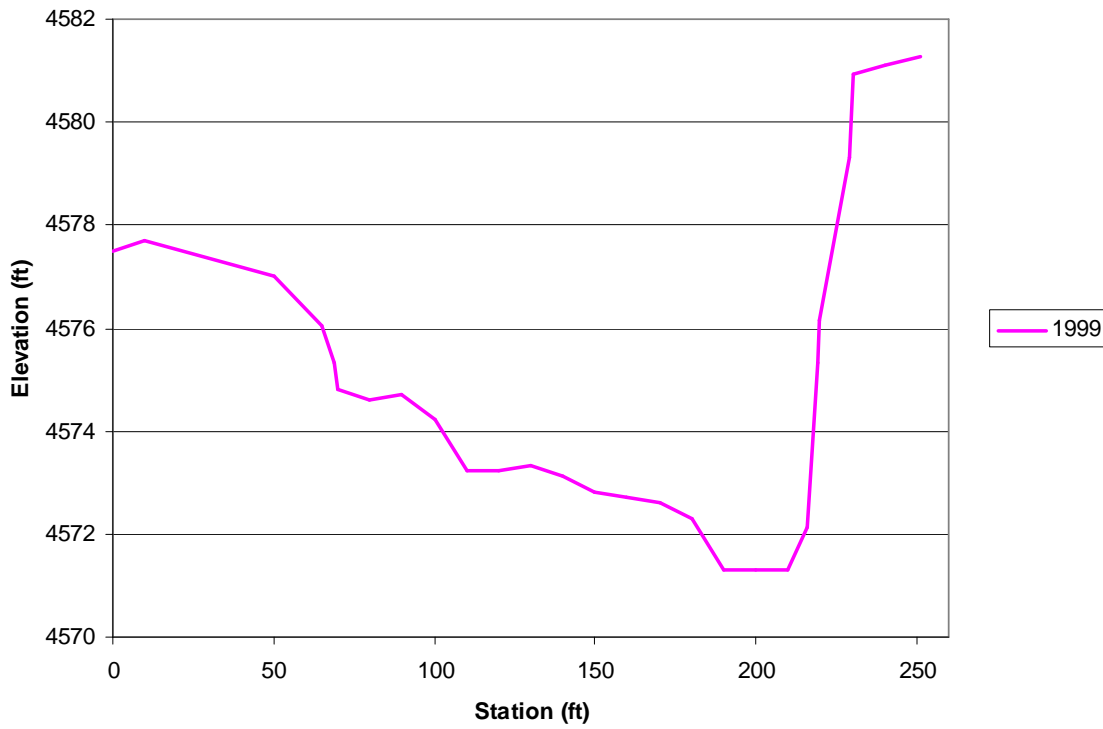


Figure A.16 Cross-section survey at SO-line 1398

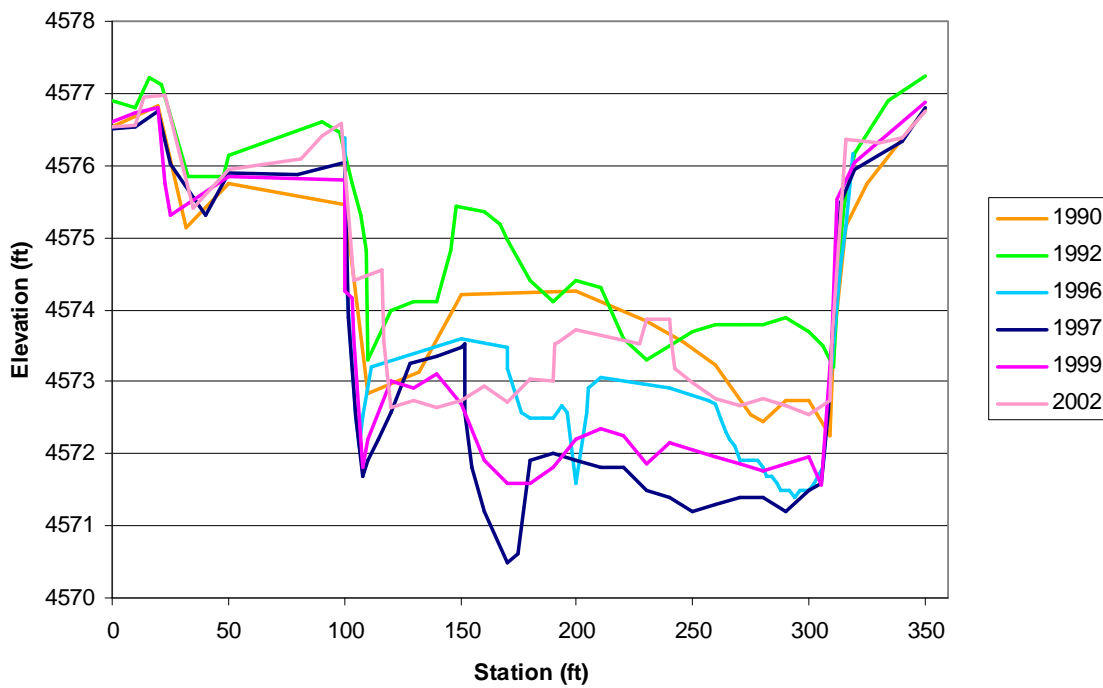


Figure A.17 Cross-section survey at SO-line 1401

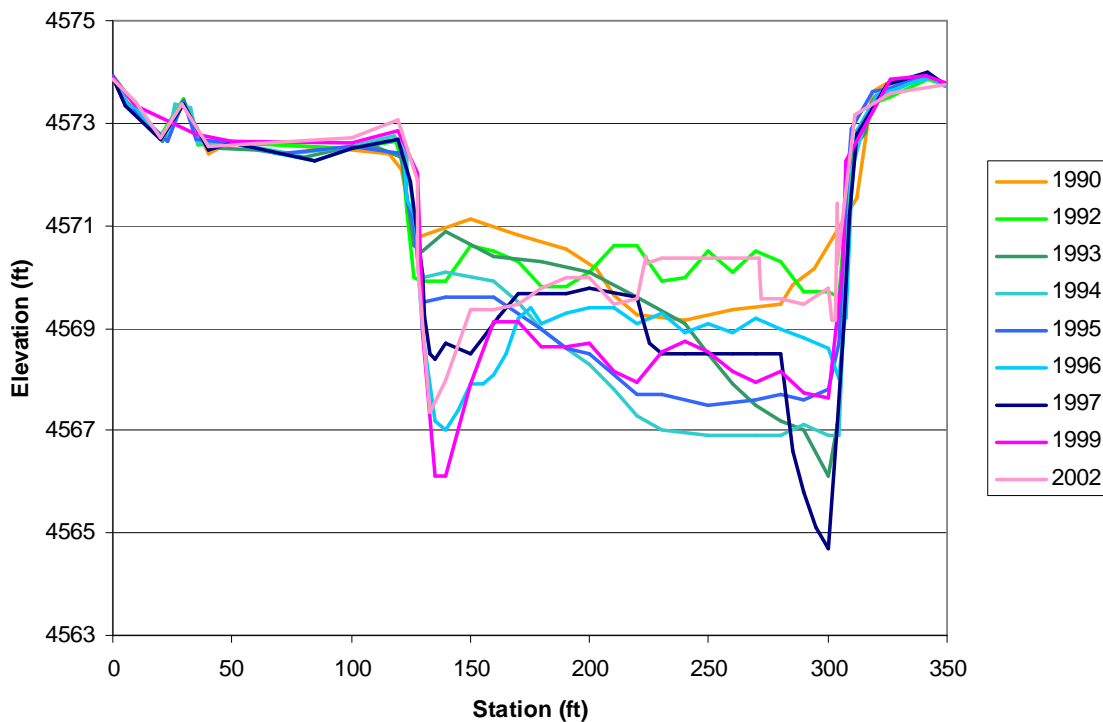


Figure A.18 Cross-section survey at SO-line 1410

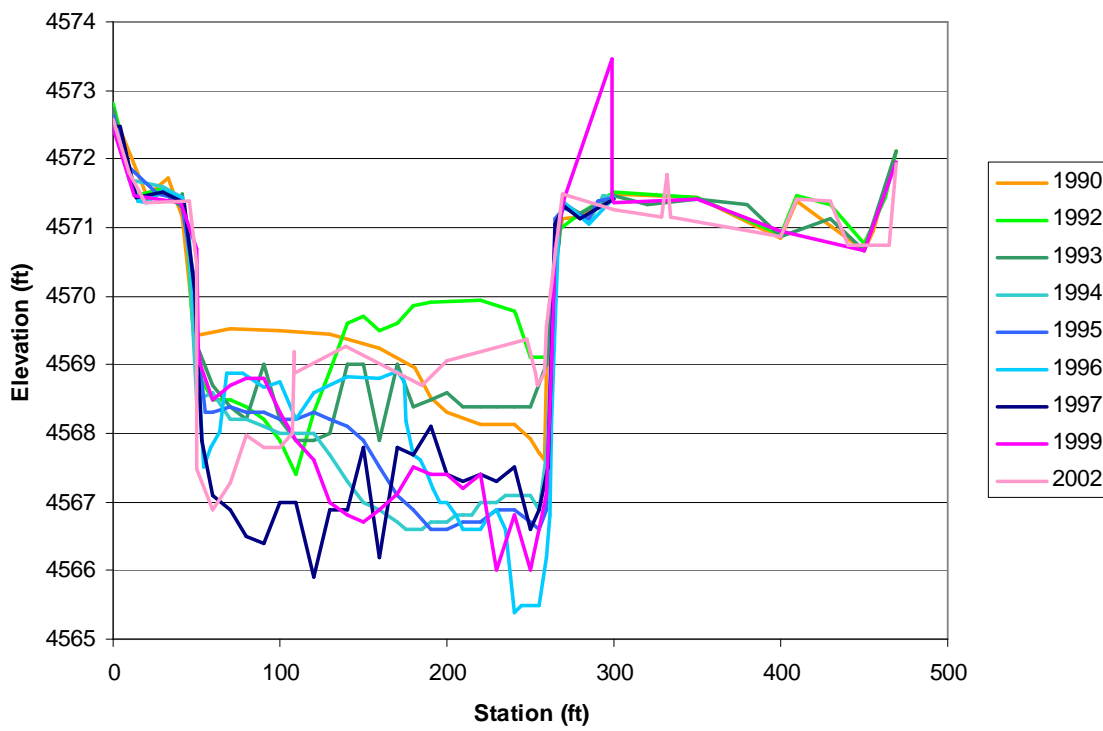


Figure A.19 Cross-section survey at SO-line 1414

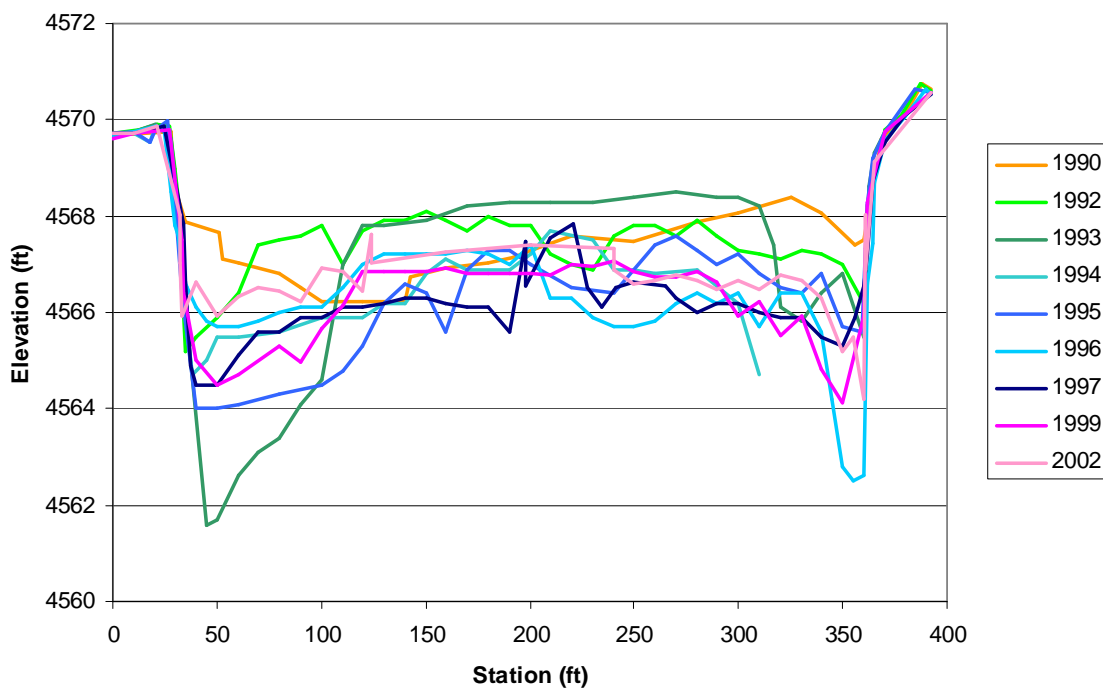


Figure A.20 Cross-section survey at SO-line 1420

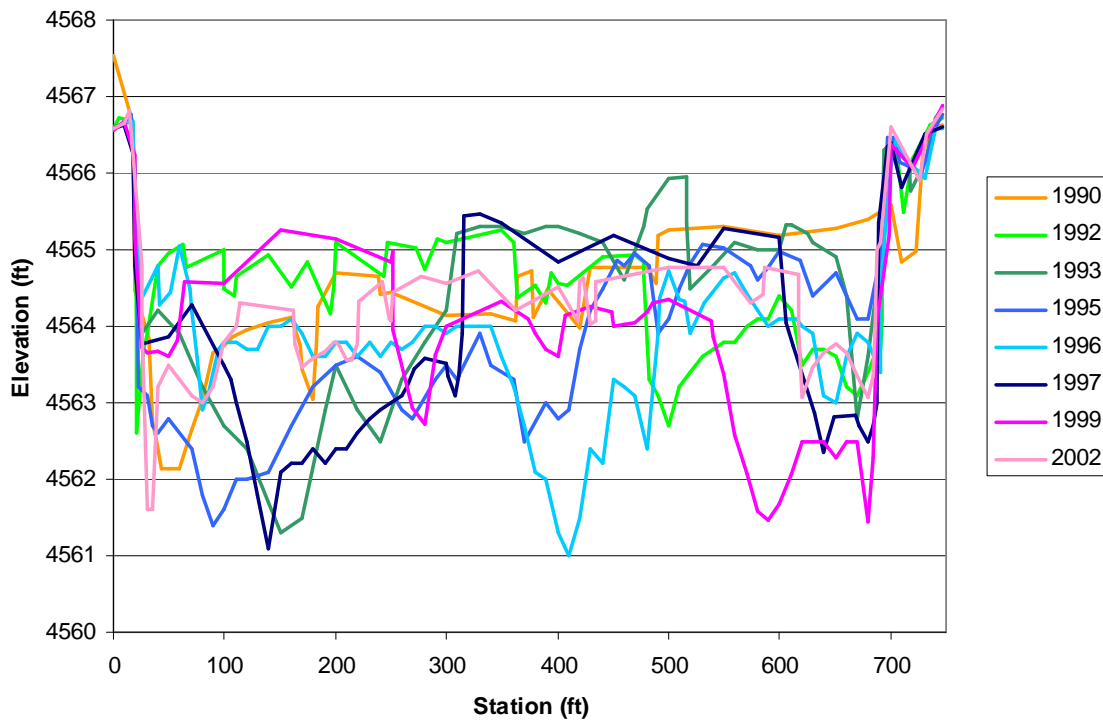


Figure A.21 Cross-section survey at SO-line 1428

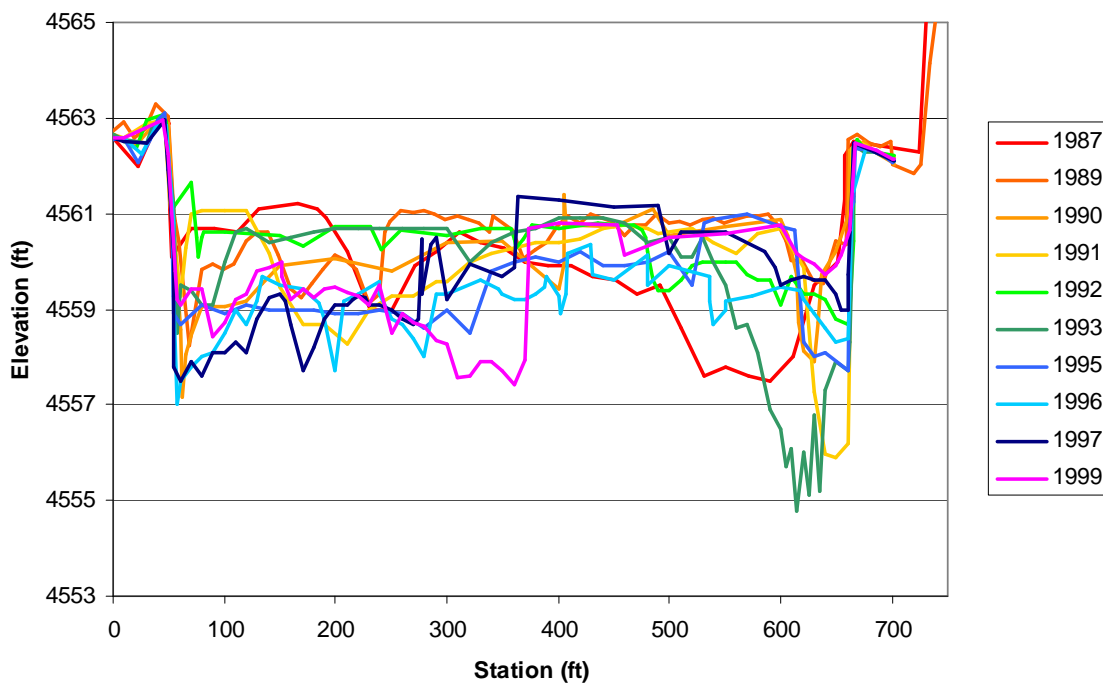


Figure A.22 Cross-section survey at SO-line 1437.9

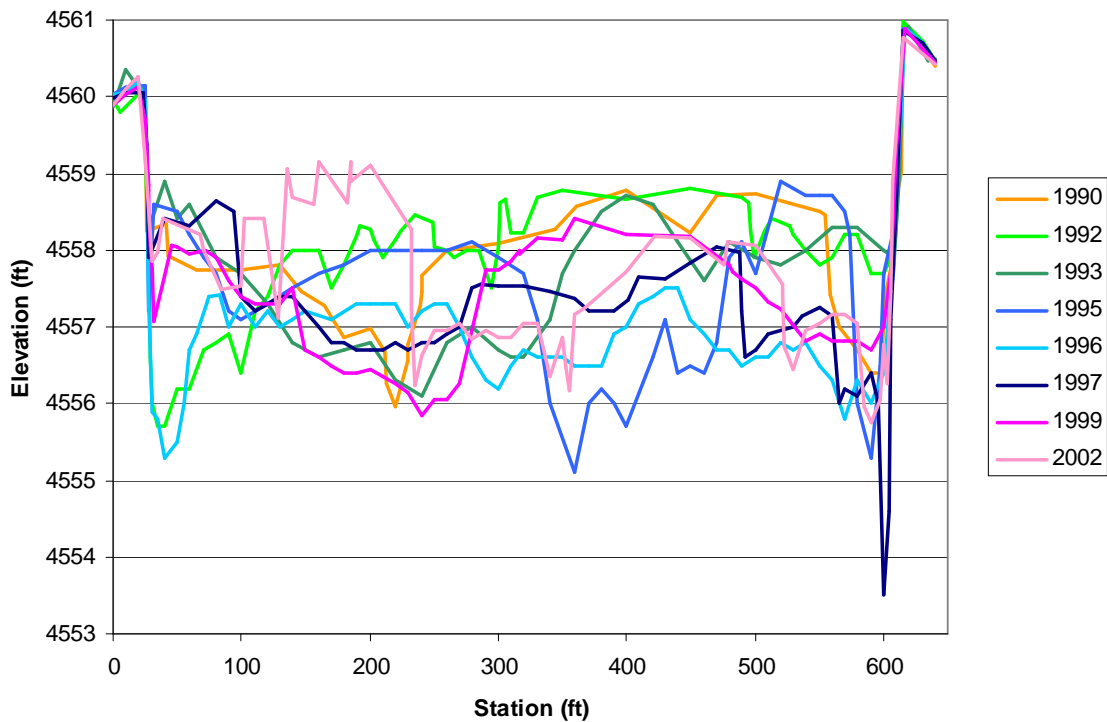


Figure A.23 Cross-section survey at SO-line 1443

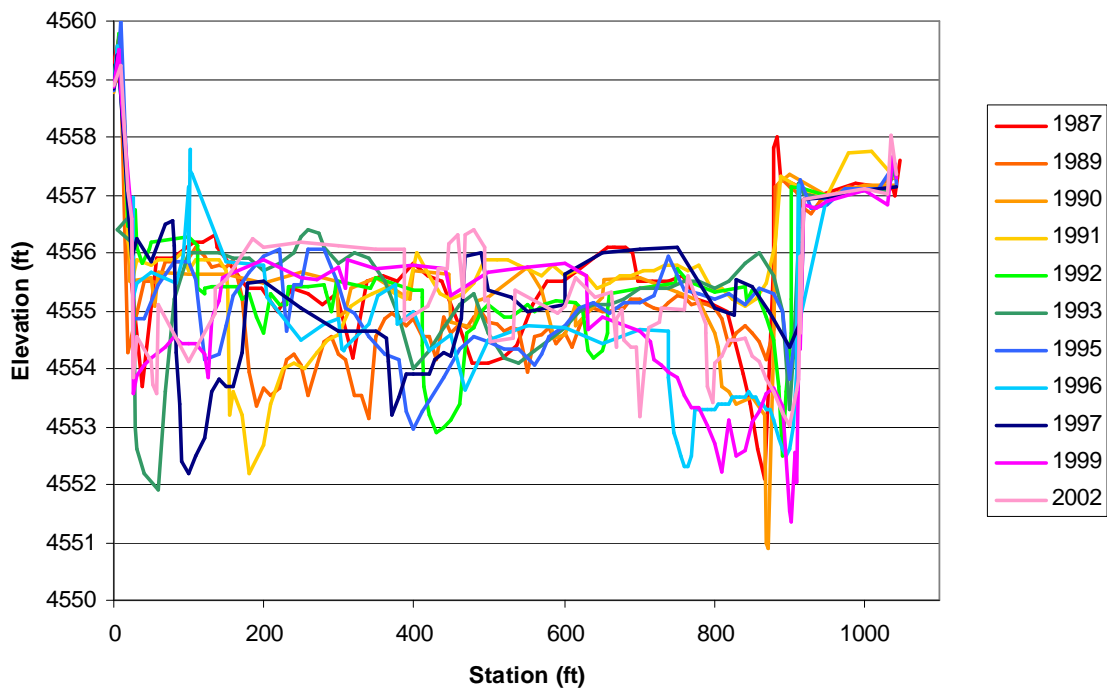


Figure A.24 Cross-section survey at SO-line 1450

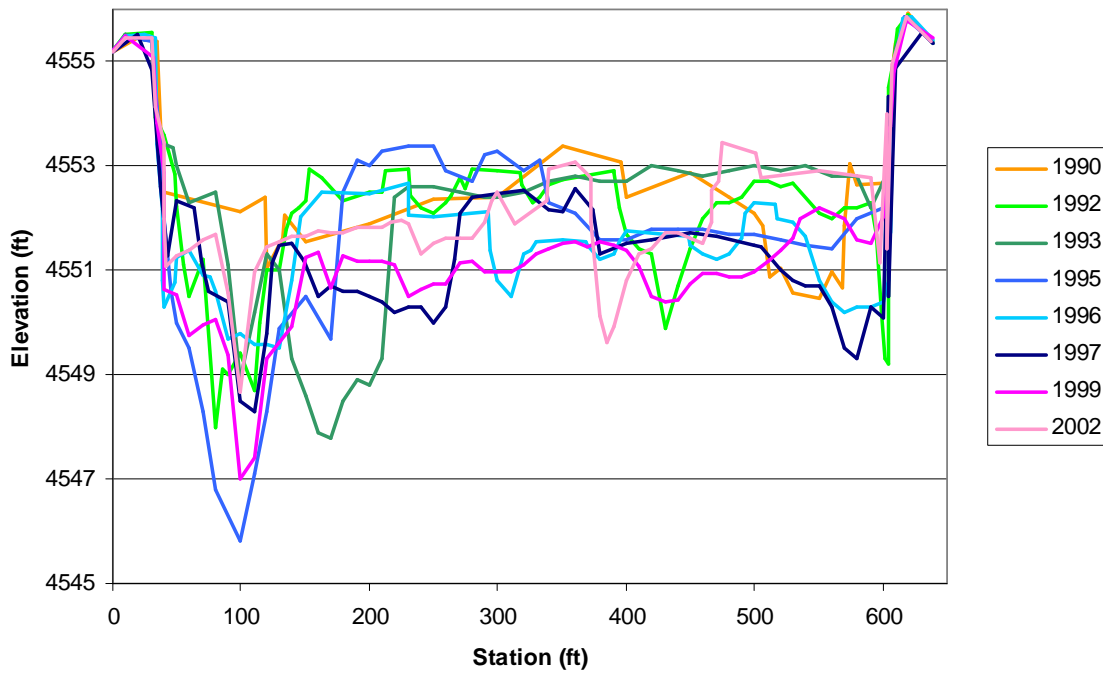


Figure A.25 Cross-section survey at SO-line 1456

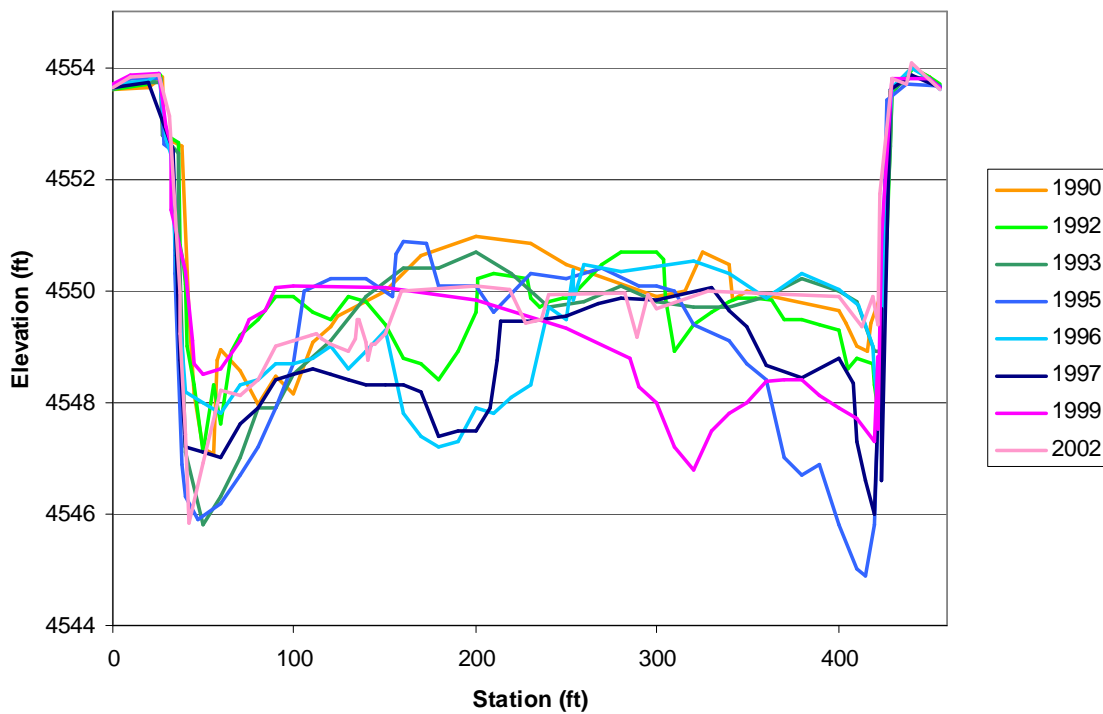


Figure A.26 Cross-section survey at SO-line 1462

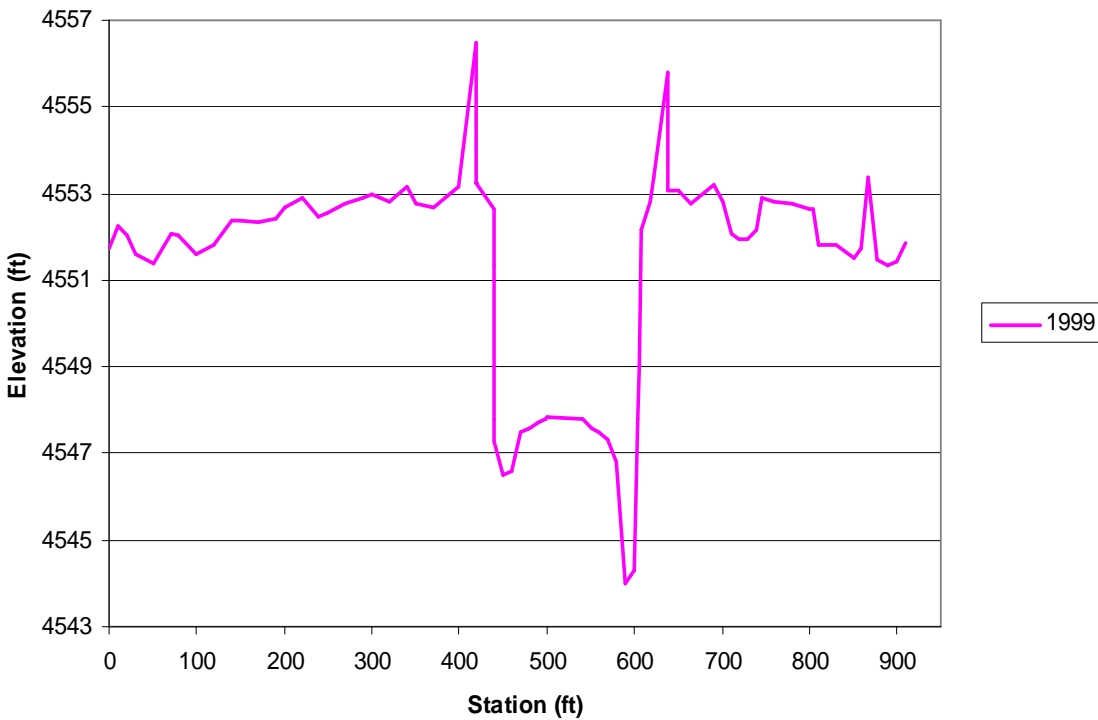


Figure A.27 Cross-section survey at SO-line 1464.5

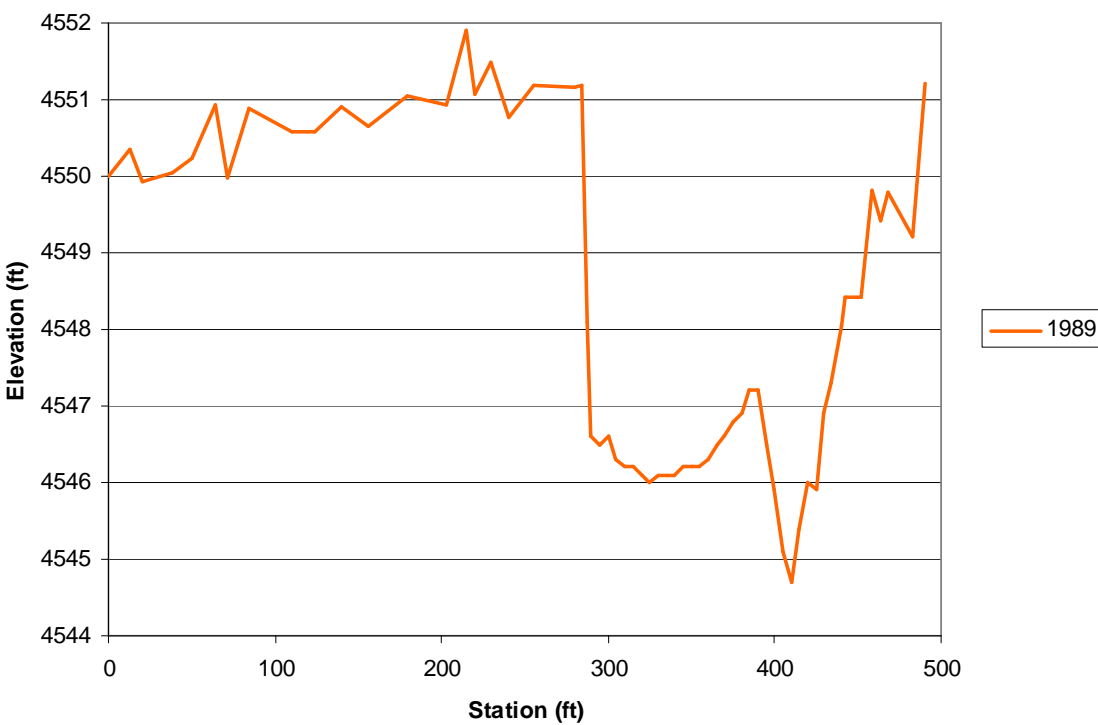


Figure A.28 Cross-section survey at SO-line 1469.5

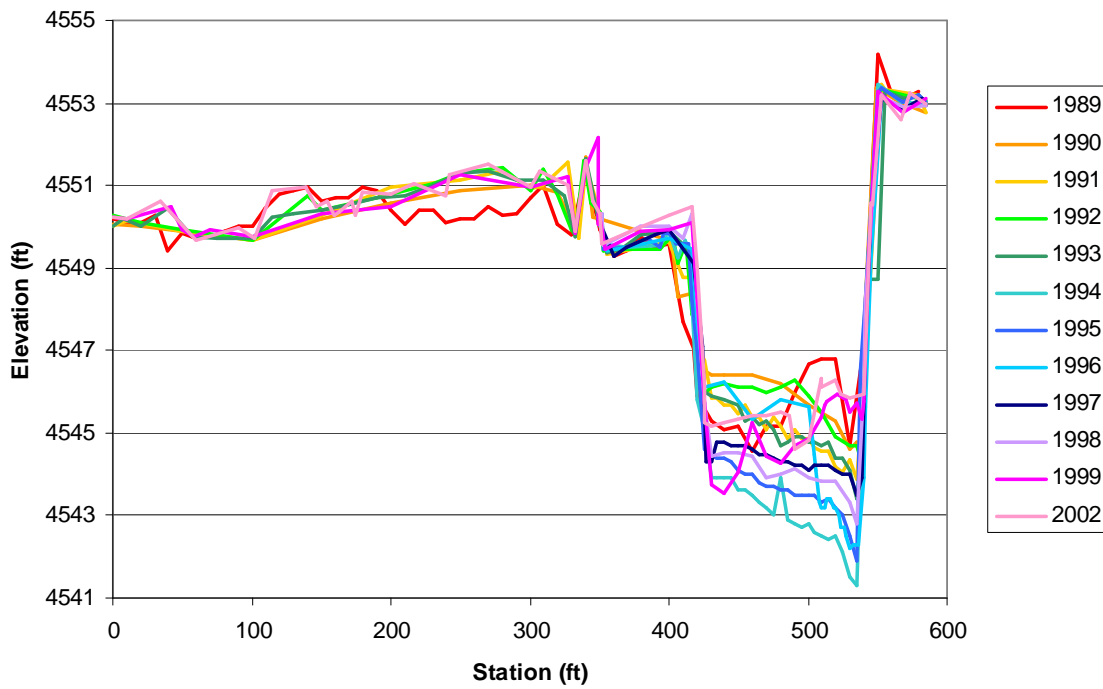


Figure A.29 Cross-section survey at SO-line 1470.5

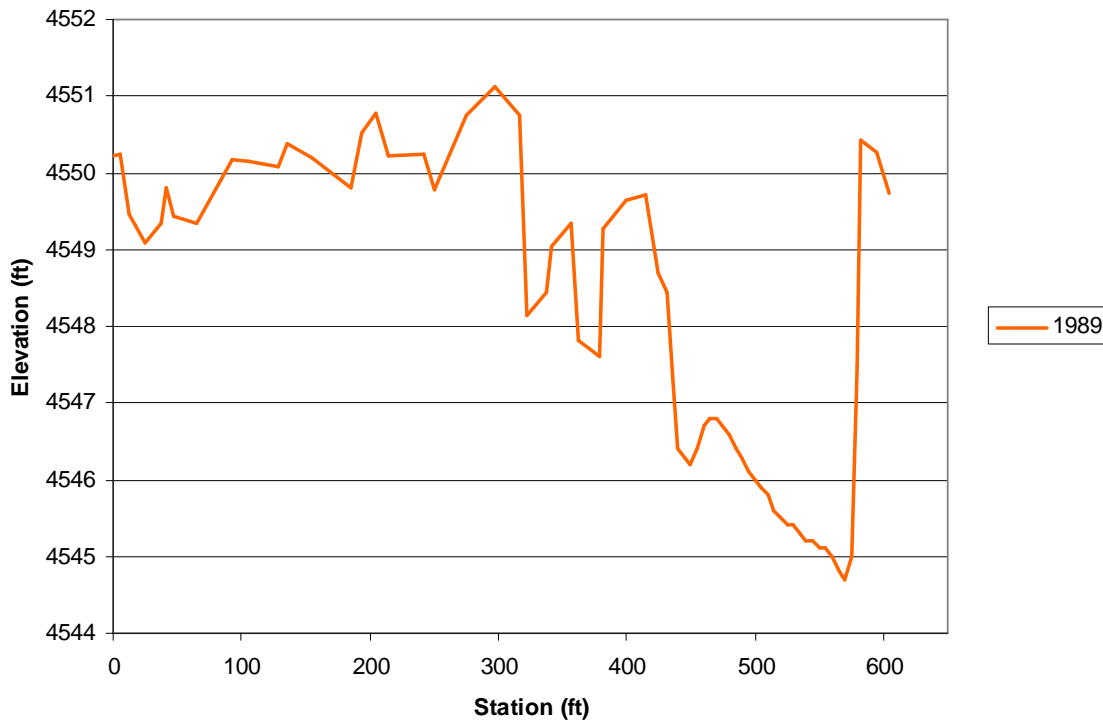


Figure A.30 Cross-section survey at SO-line 1471.2

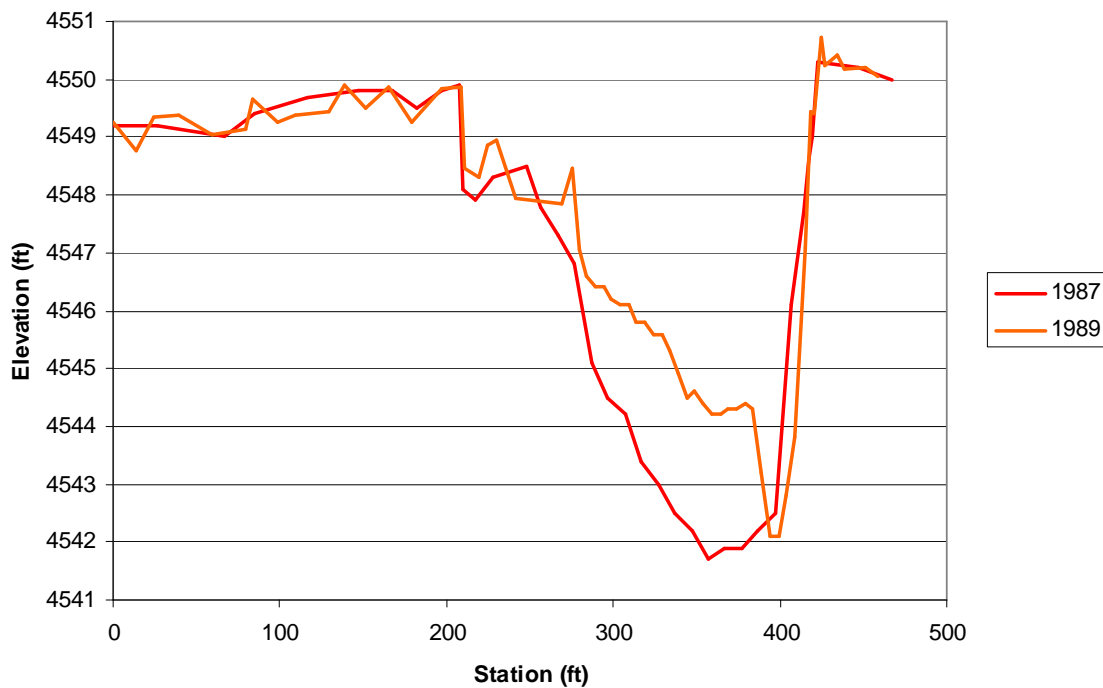


Figure A.31 Cross-section survey at SO-line 1472

Appendix B –

Aerial Photography Information

Table B.1 Aerial photography survey dates and information

Mean Daily Discharge				
Date	San Acacia	San Marcial	Scale	Notes (1918-2002:from Novak 2006 2005: from ArcGIS metadata)
1918	No Data	No Data	1:12,000	Hand-drafted linens (39 sheets). USBR Albuquerque Area Office. Surveyed in 1918. Published in 1922.
1935	No Data	No Data	1:8,00	Black and white photography. USBR Albuquerque Area Office. Flown in 1935. Published in 1936.
1949	No Data	No Data	1:5,000	Photo-mosaic. J-Ammann Photogrammetric Engineers, San Antonio, TX. USBR Albuquerque Area Office.
March 1962	25 cfs	0 cfs	1:4,800	Photo-mosaic. Abram Aerial Survey Corp, Lansing, MI. USBR Albuquerque Area Office.
April 1972	4 cfs	0 cfs	1:4,800	Photo-mosaic. Limbaugh Engineers, Inc., Albuquerque, NM. USBR Albuquerque Area Office.
March 1985	1900 cfs	1320 cfs	1:4,800	Orthophoto. M&I Consulting Engineers, Fort Collins, CO. Aero-Metric Engineering, Sheboygan, MN. USBR Albuquerque Area Office.
February 1992	1020 cfs	630 cfs	1:4,800	Ratio-rectified photo-mosaic. Koogle and Poules Engineering, Albuquerque, NM. USBR Albuquerque Area Office.
February 2001	770 cfs	560 cfs	1:4,800	Ratio-rectified photo-mosaic. Pacific Western Technologies, Ltd., Albuquerque, NM. USBR Albuquerque Area Office.
March 2002	310 cfs	150 cfs	1:4,800	Digital ortho-imagery. Pacific Western Technologies, Ltd., Albuquerque, NM. USBR Albuquerque Area Office.
April 2005	2270 cfs	1680 cfs	1:4,800	Digital ortho-rectified imagery. Aero-Metric, Inc., Fort Collins, Co. USBR Albuquerque Area Office.

Appendix C –

HEC-RAS Model Output

1962
1972
1985
1992
2002

Table C.1 HEC-RAS output for 1962 geometry

HEC-RAS Plan: 1962(8-7-06) River: Middle Rio Grande Reach: Socorro Profile: PF 1													
Agg/Deg #	Discharge	Min. Channel Elev.	W.S. Elev.	E.G. Elev.	E.G. Slope	Velocity	Flow Area	Top Width	Froude #	Frctn Slope	Hydr Radius	Wetted Perimeter	Hydr Depth
	(cfs)	(ft)	(ft)	(ft)	(ft/ft)	(ft/s)	(sq ft)	(ft)		(ft/ft)	(ft)	(ft)	(ft)
1313	5000	4610.8	4615.57	4616.04	0.001525	5.55	948.55	301.71	0.52	0.000873	3.13	303.47	3.14
1314	5000	4610.7	4615.29	4615.43	0.000565	3.26	2115.41	871.06	0.32	0.000462	2.43	872.05	2.43
1315	5000	4610.9	4615.12	4615.18	0.000385	2.74	3593.21	1396.01	0.26	0.000436	2.57	1399.44	2.57
1316	5000	4610.7	4614.92	4614.99	0.000498	2.81	3074.4	1169.95	0.29	0.000785	2.62	1172.92	2.63
1317	5000	4609.9	4614.31	4614.6	0.001418	4.7	1401.96	563.79	0.49	0.001703	2.48	565.21	2.49
1318	5000	4609.6	4613.37	4613.69	0.002085	4.69	1185.99	611.7	0.56	0.001869	1.93	613.84	1.94
1319	5000	4608.7	4612.52	4612.65	0.001686	3.35	2131.56	1489.74	0.48	0.001054	1.43	1492.73	1.43
1320	5000	4608.6	4612.01	4612.09	0.000721	2.65	2586.3	1474.03	0.33	0.000733	1.75	1475.92	1.75
1321	5000	4608.4	4611.64	4611.72	0.000744	2.49	2612.82	1471.74	0.33	0.001083	1.77	1474.01	1.78
1322	5000	4607.6	4611.01	4611.16	0.001717	3.42	1855.28	1449.29	0.49	0.001115	1.28	1450.18	1.28
1323	5000	4606.9	4610.49	4610.59	0.000782	2.63	2105.17	1293.4	0.34	0.000875	1.63	1294.4	1.63
1324	5000	4606.9	4610	4610.12	0.000986	3.03	2033.83	1211.97	0.38	0.001242	1.68	1213.53	1.68
1325	5000	4605.6	4609.29	4609.48	0.001611	3.51	1514.84	991.65	0.48	0.001081	1.53	992.55	1.53
1326	5000	4605.1	4608.79	4608.88	0.000776	2.46	2208.75	1413.86	0.33	0.001091	1.56	1414.56	1.56
1327	5000	4605.1	4608.16	4608.28	0.001646	2.81	1808.38	1607.33	0.46	0.001226	1.12	1607.98	1.13
1328	5000	4604.2	4607.58	4607.65	0.000948	2.24	2248.78	1779.35	0.35	0.001007	1.26	1780.2	1.26
1329	5000	4603.4	4607.06	4607.14	0.001072	2.26	2226.33	1915.85	0.37	0.000963	1.16	1917.28	1.16
1330	5000	4602.7	4606.55	4606.63	0.000869	2.23	2255.24	1680.59	0.34	0.001262	1.34	1682.74	1.34
1331	5000	4603.3	4605.84	4605.98	0.001997	3.02	1653.72	1447.28	0.5	0.001677	1.14	1447.76	1.14
1332	5000	4601.2	4605.06	4605.2	0.001428	2.99	1674.51	1161.07	0.44	0.001501	1.44	1162.48	1.44
1333	5000	4599.6	4604.37	4604.5	0.001581	2.9	1722.89	1345.04	0.45	0.001053	1.28	1345.87	1.28

1334	5000	4600.4	4603.89	4603.96	0.000752	2.06	2430.36	1820.33	0.31	0.000863	1.33	1821.22	1.34
1335	5000	4600.8	4603.47	4603.55	0.001001	2.14	2335.1	2041.55	0.35	0.000833	1.14	2042.45	1.14
1336	5000	4600	4603.08	4603.14	0.000704	1.89	2651.15	2153.26	0.3	0.000952	1.23	2154.78	1.23
1337	5000	4599.4	4602.6	4602.68	0.00136	2.37	2107.58	1988.85	0.41	0.00073	1.06	1989.5	1.06
1338	5000	4598.9	4602.28	4602.32	0.000454	1.68	2970.12	2060.53	0.25	0.000616	1.44	2061.53	1.44
1339	5000	4598.5	4601.95	4602.03	0.000883	2.24	2231.37	1658.15	0.34	0.000743	1.34	1659.35	1.35
1340	5000	4596.9	4601.61	4601.67	0.000634	2.12	2786.61	2018.11	0.3	0.000906	1.38	2020.23	1.38
1341	5000	4596.3	4601.07	4601.22	0.0014	3.15	1595.04	1023.58	0.44	0.001375	1.55	1026.96	1.56
1342	5000	4596.1	4600.45	4600.56	0.00135	2.68	1864.92	1461.06	0.42	0.001297	1.28	1462.59	1.28
1343	5000	4593.5	4599.79	4599.89	0.001247	2.58	1992.03	1794.2	0.4	0.001078	1.11	1800.45	1.11
1344	5000	4595.6	4599.23	4599.32	0.000941	2.32	2327.23	2176.72	0.35	0.000961	1.07	2178.71	1.07
1345	5000	4593.9	4598.74	4598.83	0.000982	2.4	2083.18	1511.62	0.36	0.000772	1.38	1513.9	1.38
1346	5000	4593.3	4598.37	4598.42	0.000623	1.89	2988.73	2746.23	0.29	0.000521	1.09	2749.54	1.09
1347	5000	4592.7	4598.09	4598.14	0.000443	1.75	2921.33	2023.98	0.25	0.00062	1.44	2026.83	1.44
1348	5000	4593.1	4597.64	4597.77	0.00093	2.92	1715.11	892.72	0.37	0.001136	1.92	893.91	1.92
1349	5000	4592.4	4596.99	4597.12	0.001418	3	1870.07	1642.06	0.44	0.001226	1.14	1643.96	1.14
1350	5000	4591.9	4596.35	4596.49	0.001071	2.99	1724.06	1313.12	0.45	0.001092	1.31	1315.43	1.31
1351	5000	4592.6	4595.89	4596.03	0.001113	3.07	1679.11	1387.34	0.46	0.00131	1.21	1388.08	1.21
1352	5000	4590.8	4595.27	4595.42	0.001564	3.12	1604.39	1464.84	0.52	0.001251	1.09	1468.71	1.1
1353	5000	4591.7	4594.68	4594.85	0.001023	3.27	1529.78	947.33	0.45	0.001604	1.61	948.2	1.61
1354	5000	4589.6	4593.71	4593.99	0.002868	4.26	1175	1061.24	0.71	0.001014	1.11	1062.24	1.11
1355	5000	4589.3	4593.32	4593.4	0.000514	2.24	2230.78	1465.45	0.32	0.000466	1.52	1466.16	1.52
1356	5000	4589.5	4593.1	4593.16	0.000425	2.04	2470.63	1636.76	0.29	0.00047	1.51	1637.96	1.51
1357	5000	4588.6	4592.83	4592.92	0.000523	2.36	2116.76	1291.54	0.33	0.000642	1.64	1292.18	1.64
1358	5000	4588.7	4592.43	4592.54	0.000807	2.75	1821.83	1234.65	0.4	0.000664	1.47	1235.42	1.48
1359	5000	4588.6	4592.14	4592.23	0.000556	2.48	2038.51	1238.18	0.34	0.000623	1.64	1239.53	1.65

1360	5000	4587.4	4591.79	4591.91	0.000704	2.78	1798.81	1078.3	0.38	0.001222	1.66	1080.65	1.67
1361	5000	4588.6	4590.99	4591.29	0.002628	4.39	1138.03	917.88	0.7	0.001193	1.24	918.55	1.24
1362	5000	4586.8	4590.48	4590.63	0.000678	3.08	1623.75	807.83	0.38	0.000525	2.01	808.72	2.01
1363	5000	4585.2	4590.22	4590.34	0.000418	2.73	1834.07	761.64	0.31	0.000547	2.4	762.93	2.41
1364	5000	4586.4	4589.89	4590.04	0.000746	3.15	1586.47	818.36	0.4	0.000356	1.94	819.53	1.94
1365	5000	4583.4	4589.76	4589.84	0.000208	2.27	2241.55	800.83	0.23	0.000289	2.79	803.12	2.8
1366	5000	4585.4	4589.54	4589.69	0.000429	3.08	1621.38	570.54	0.32	0.000441	2.84	571.66	2.84
1367	5000	4584.4	4589.29	4589.48	0.000453	3.43	1513.91	586.77	0.34	0.000322	2.57	588.3	2.58
1368	5000	4583.5	4589.18	4589.3	0.00024	2.82	1847.3	581.54	0.25	0.000347	3.17	582.9	3.18
1369	5000	4583.5	4588.89	4589.12	0.000545	3.9	1282.6	377.63	0.37	0.000486	3.37	380.86	3.4
1370	5000	4582.4	4588.69	4588.89	0.000435	3.56	1403.21	398.01	0.33	0.000561	3.49	402.4	3.53
1371	5000	4583.3	4588.28	4588.61	0.000751	4.63	1126.79	423.06	0.44	0.001053	2.65	425.02	2.66
1372	5000	4582.2	4587.59	4588.12	0.001585	5.8	861.7	310.81	0.61	0.001226	2.75	313.55	2.77
1373	5000	4582.2	4587.07	4587.44	0.000977	4.9	1037.09	405.84	0.49	0.000482	2.55	407.41	2.56
1374	5000	4581.6	4587.03	4587.15	0.000287	3.06	2880.83	1737.9	0.28	0.000562	1.66	1740.57	1.66
1375	5000	4580.5	4586.26	4586.85	0.001564	6.21	913.49	481.47	0.62	0.00095	1.88	486.31	1.9
1376	5000	4580.4	4586.01	4586.28	0.000638	4.34	1514.48	788.25	0.41	0.00071	1.92	789.8	1.92
1377	5000	4578.2	4585.62	4585.91	0.000796	4.54	1453.97	705.16	0.44	0.000855	2.05	710.88	2.06
1378	5000	4579.4	4585.15	4585.46	0.000921	4.56	1291.51	749.33	0.47	0.000632	1.72	751.69	1.72
1379	5000	4579.4	4584.99	4585.17	0.000461	3.5	1745.43	786.26	0.34	0.00064	2.21	788.64	2.22
1380	5000	4579.4	4584.57	4584.9	0.000947	4.63	1133.81	469.78	0.48	0.001075	2.41	470.79	2.41
1381	5000	4578.7	4584.08	4584.47	0.001229	5.01	1043.42	479	0.54	0.001292	2.17	481.05	2.18
1382	5000	4578.2	4583.48	4583.85	0.00136	4.85	1074.27	560.72	0.56	0.001012	1.91	562.16	1.92
1383	5000	4578.2	4583.18	4583.35	0.000782	3.26	1534.25	779.87	0.41	0.000658	1.96	780.86	1.97
1384	5000	4577.9	4582.91	4583.04	0.000562	2.88	1738.53	853.31	0.35	0.000772	2.03	855.77	2.04
1385	5000	4578.3	4582.41	4582.67	0.001128	4.1	1242.83	613.2	0.5	0.000679	2.02	614.53	2.03

1386	5000	4578	4582.19	4582.3	0.000454	2.72	1965.55	1025.71	0.32	0.000538	1.91	1026.68	1.92
1387	5000	4576.4	4581.9	4582.05	0.00065	3.15	1680.3	838.56	0.38	0.000556	2	840.86	2
1388	5000	4576.4	4581.64	4581.77	0.000482	2.87	1740.21	743.82	0.33	0.00057	2.34	744.75	2.34
1389	5000	4576.1	4581.25	4581.46	0.000684	3.68	1370.77	529.63	0.4	0.000557	2.58	531.72	2.59
1390	5000	4575.9	4580.98	4581.18	0.000462	3.73	1798.74	865.89	0.35	0.000796	2.07	868.37	2.08
1391	5000	4575.7	4580.22	4580.76	0.001686	6.16	1170.04	862.19	0.64	0.001	1.36	863.07	1.36
1392	5000	4574.9	4579.91	4580.16	0.000661	4.45	2028.4	1212.63	0.41	0.000612	1.67	1214.31	1.67
1393	5000	4574.3	4579.62	4579.85	0.000569	4.14	2018.38	1197.46	0.38	0.000586	1.68	1200.45	1.69
1394	5000	4573.8	4579.31	4579.55	0.000605	4.07	1562.24	857.86	0.39	0.00079	1.82	860.65	1.82
1395	5000	4573.9	4578.85	4579.17	0.001075	4.48	1116.62	443.47	0.5	0.000546	2.49	448.18	2.52
1396	5000	4572.9	4578.74	4578.86	0.00033	2.72	1946.29	880.17	0.28	0.0004	2.2	883.16	2.21
1397	5000	4572.2	4578.46	4578.65	0.000494	3.61	1698.13	746.24	0.35	0.00048	2.27	748.65	2.28
1398	5000	4572.6	4578.19	4578.4	0.000466	3.68	1461.94	590.55	0.35	0.000717	2.47	592.05	2.48
1399	5000	4572.2	4577.49	4578.01	0.00124	5.93	1021.75	470.23	0.56	0.001292	2.16	472.08	2.17
1400	5000	4572.5	4576.85	4577.32	0.001347	5.51	948.71	498.28	0.57	0.000997	1.9	499.76	1.9
1401	5000	4571.6	4576.48	4576.77	0.000767	4.36	1146.09	369.72	0.44	0.00035	3.09	371.31	3.1
1402	5000	4570.9	4576.45	4576.54	0.000199	2.51	2653.24	1133.78	0.23	0.000248	2.33	1137.98	2.34
1403	5000	4570.1	4576.32	4576.4	0.000316	2.71	3018.29	1168.63	0.28	0.000458	2.57	1172.42	2.58
1404	5000	4571.1	4575.84	4576.15	0.000724	4.47	1120.66	339.83	0.43	0.000933	3.28	341.25	3.3
1405	5000	4570.7	4575.25	4575.65	0.001248	5.13	980.68	388.03	0.55	0.001302	2.52	389.85	2.53
1406	5000	4570.2	4574.54	4574.98	0.001359	5.33	938.55	343.66	0.57	0.000229	2.71	345.93	2.73
1407	5000	4569.3	4574.73	4574.74	0.000091	1.64	7968.58	3562.84	0.15	0.000073	2.23	3566.02	2.24
1408	5000	4569.4	4574.7	4574.71	0.00006	1.28	9561.79	3562.69	0.12	0.000149	2.68	3565.62	2.68
1409	5000	4569.1	4574.22	4574.6	0.000826	4.99	1117.71	451.21	0.46	0.001586	2.47	453.11	2.48
1410	5000	4568.7	4572.56	4573.75	0.004205	8.74	573.57	254.59	0.98	0.000184	2.25	255.37	2.25
1411	5000	4567.7	4573.22	4573.23	0.000057	1.25	10146.49	4009.95	0.12	0.000135	2.53	4012.2	2.53

1412	5000	4567.7	4572.89	4573.14	0.000624	4.1	1352.77	501.17	0.4	0.000552	2.69	502.86	2.7
1413	5000	4567.2	4572.61	4572.85	0.000492	4.02	1392.79	477.54	0.36	0.000455	2.9	479.71	2.92
1414	5000	4566.9	4572.44	4572.59	0.000421	3.19	1719.82	669.8	0.32	0.000479	2.56	672.13	2.57
1416	5000	4566.8	4572.08	4572.34	0.000549	4.11	1274.67	406.78	0.38	0.000475	3.12	408.26	3.13
1417	5000	4565.5	4571.89	4572.09	0.000415	3.61	1427.21	454.67	0.33	0.000614	3.12	457.52	3.14
1418	5000	4566.3	4571.43	4571.77	0.000999	4.83	1297.01	776.41	0.49	0.001133	1.67	778.3	1.67
1419	5000	4566.6	4570.78	4571.16	0.001295	5.03	1122.98	558.39	0.55	0.001104	2.01	559.25	2.01
1420	5000	4565.6	4570.31	4570.57	0.000952	4.29	1437.41	715.58	0.47	0.001064	2.01	716.74	2.01
1421	5000	4565.3	4569.69	4570	0.001196	4.5	1116.85	489.54	0.52	0.001403	2.28	490.77	2.28
1422	5000	4564.7	4568.83	4569.21	0.001668	5.06	1199.36	741.13	0.61	0.001667	1.62	742.32	1.62
1423	5000	4562.2	4567.86	4568.22	0.001666	4.89	1090.23	586.59	0.6	0.001106	1.85	589.94	1.86
1424	5000	4563	4567.33	4567.47	0.000787	3.02	1718.76	1073.46	0.4	0.000693	1.6	1074.67	1.6
1425	5000	4563.1	4566.93	4567.03	0.000615	2.49	2008.71	1278.33	0.35	0.000681	1.57	1279.45	1.57
1426	5000	4562.8	4566.56	4566.69	0.000758	2.94	1805.98	1174.87	0.39	0.000375	1.53	1177.06	1.54
1427	5000	4562.2	4566.39	4566.46	0.000223	2.05	2433.81	966.15	0.23	0.0003	2.52	967.09	2.52
1428	5000	4561.2	4566.16	4566.3	0.000425	2.96	1747.67	684.65	0.32	0.000437	2.54	687.52	2.55
1429	5000	4560.3	4565.92	4566.07	0.000449	3.16	1644.9	618.57	0.33	0.000666	2.65	620.98	2.66
1430	5000	4559.8	4565.41	4565.71	0.001088	4.41	1171.7	513.2	0.5	0.00063	2.28	514.47	2.28
1431	5000	4559.6	4565.18	4565.34	0.000411	3.14	1591.88	527.26	0.32	0.000492	3.01	528.21	3.02
1432	5000	4559.2	4564.8	4565.06	0.000601	4.08	1225.88	364.95	0.39	0.000699	3.35	365.67	3.36
1433	5000	4558.7	4564.34	4564.68	0.000825	4.68	1069.32	329.42	0.46	0.000939	3.23	331.48	3.25
1434	5000	4558.5	4563.81	4564.2	0.001078	5.05	1004.24	435.86	0.51	0.000808	2.29	437.88	2.3
1435	5000	4558	4563.48	4563.73	0.000629	3.97	1263.68	439.66	0.4	0.000765	2.86	441.29	2.87
1436	5000	4557.7	4563.02	4563.31	0.000951	4.32	1159.88	447.56	0.47	0.000812	2.57	451.06	2.59
1437	5000	4557.4	4562.61	4562.86	0.000701	3.99	1254.49	436.5	0.41	0.000635	2.86	438.33	2.87
1438	5000	4556.4	4562.31	4562.51	0.000578	3.64	1391.58	538.63	0.38	0.000449	2.57	541.33	2.58

1439	5000	4556.3	4562.11	4562.26	0.000359	3.08	1675.54	549.25	0.3	0.000646	3.04	550.36	3.05
1440	5000	4556.2	4561.23	4561.87	0.001495	6.46	813.6	270.64	0.62	0.0006	2.98	272.64	3.01
1441	5000	4555.6	4561.3	4561.41	0.000322	3.33	3522.16	1944.45	0.29	0.000583	1.81	1946.37	1.81
1442	5000	4555.7	4560.61	4561.09	0.001369	5.55	905.73	330.19	0.58	0.001416	2.73	331.29	2.74
1443	5000	4555.5	4559.91	4560.35	0.001465	5.34	955.07	438.55	0.59	0.001307	2.17	439.51	2.18
1444	5000	4554.9	4559.37	4559.68	0.001172	4.46	1120.56	481.53	0.52	0.001376	2.32	482.39	2.33
1445	5000	4554.5	4558.66	4558.95	0.001637	4.29	1165.65	682.05	0.58	0.001273	1.7	683.73	1.71
1446	5000	4553.6	4558.04	4558.29	0.001018	4.03	1239.53	556.7	0.48	0.000929	2.22	558.3	2.23
1447	5000	4553	4557.59	4557.81	0.000851	3.77	1408.45	689.74	0.44	0.000803	2.04	690.95	2.04
1448	5000	4552	4557.18	4557.41	0.000758	3.81	1313.08	515.16	0.42	0.000584	2.54	517.01	2.55
1449	5000	4551.9	4556.95	4557.12	0.000464	3.24	1542.32	531.8	0.34	0.000561	2.88	534.89	2.9
1450	5000	4552	4556.69	4556.85	0.000693	3.18	1571.88	755.33	0.39	0.000547	2.07	757.67	2.08
1451	5000	4550.7	4556.45	4556.58	0.000443	2.83	1814.85	763.88	0.32	0.000306	2.37	766.35	2.38
1452	5000	4551.4	4556.34	4556.4	0.000224	2.15	2936.52	1204.6	0.23	0.000315	2.43	1206.47	2.44
1453	5000	4551.3	4556.1	4556.24	0.000476	3.08	1740.07	708.91	0.33	0.00052	2.44	711.92	2.45
1454	5000	4550.5	4555.82	4555.98	0.000571	3.33	1937.65	1433.5	0.37	0.000549	1.35	1435.65	1.35
1455	5000	4550.6	4555.52	4555.72	0.000528	3.61	1482.13	558.73	0.36	0.000476	2.65	560.16	2.65
1456	5000	4550.9	4555.31	4555.48	0.000432	3.25	1611.94	601.55	0.33	0.000725	2.67	602.62	2.68
1457	5000	4550.3	4554.6	4555.1	0.001462	5.69	919.57	458.21	0.59	0.000041	2	460.08	2.01
1458	5000	4550.1	4554.93	4554.93	0.000012	0.6	18959.91	5313.99	0.06	0.000012	3.57	5316.43	3.57
1459	5000	4550.1	4554.93	4554.93	0.000012	0.56	19043.94	5323.2	0.06	0.000044	3.58	5325.66	3.58
1460	5000	4549.9	4553.96	4554.82	0.003073	7.78	914.06	687.07	0.85	0.000028	1.33	688.27	1.33
1461	5000	4549.9	4554.36	4554.36	0.000008	0.48	23078.19	5768.61	0.04	0.000028	4	5770.98	4
1462	5000	4549.7	4552.51	4554.18	0.006689	10.45	515.83	304.76	1.22	0.000065	1.69	305.9	1.69
1463	5000	4549.2	4552.39	4552.39	0.000018	0.63	17484.53	5588.97	0.07	0.000013	3.13	5590.44	3.13
1464	5000	4548.3	4552.38	4552.38	0.00001	0.47	20802.79	5588.35	0.05	0.000009	3.72	5590.27	3.72

1465	5000	4548.2	4552.38	4552.38	0.000008	0.45	22550.46	5594.13	0.04	0.000008	4.03	5596.49	4.03
1466	5000	4547.7	4552.38	4552.38	0.000009	0.53	21818.23	5716.61	0.05	0.00001	3.82	5718.48	3.82
1467	5000	4547.8	4552.37	4552.37	0.000012	0.57	19538.56	5440.42	0.05	0.000042	3.59	5442.72	3.59
1468	5000	4547.7	4550.93	4552.22	0.004183	9.11	548.84	209.54	0.99	0.000108	2.61	210.25	2.62
1469	5000	4547.5	4551.4	4551.41	0.000032	0.86	13642.11	4732.27	0.09	0.000029	2.88	4734.18	2.88
1470	5000	4547.4	4551.39	4551.39	0.000026	0.82	13821.17	4216.51	0.08	0.000031	3.28	4218.26	3.28
1471	5000	4546.8	4551.37	4551.38	0.000038	1.1	11079.49	3372.58	0.1	0.000125	3.28	3373.93	3.29
1472	5000	4546.3	4549.85	4551.18	0.003857	9.26	557.44	225.77	0.97	0.000614	2.46	226.5	2.47
1473	5000	4546.2	4549.36	4549.38	0.000239	1.82	5510.32	2668.38	0.23	0.00026	2.06	2669.25	2.07
1474	5000	4546.1	4549.23	4549.26	0.000284	2.11	5039.72	2473	0.25	0.000286	2.04	2473.68	2.04
1475	5000	4545.9	4549.07	4549.09	0.000287	2.12	5513.46	3061.9	0.25	0.000555	1.8	3063.27	1.8
1476	5000	4545	4548.24	4548.72	0.001501	5.71	1132.87	767.55	0.6		1.47	768.3	1.48

Table C.2 HEC-RAS output for 1972 geometry

HEC-RAS Plan: 1972(8-7-06) River: Middle Rio Grande Reach: Socorro Profile: PF 1													
Agg/Deg #	Discharge	Min. Channel Elev.	W.S. Elev.	E.G. Elev.	E.G. Slope	Velocity	Flow Area	Top Width	Froude #	Frctn Slope	Hydr Radius	Wetted Perimeter	Hydr Depth
	(cfs)	(ft)	(ft)	(ft)	(ft/ft)	(ft/s)	(sq ft)	(ft)		(ft/ft)	(ft)	(ft)	(ft)
1313	5000	4611.3	4616.02	4617.37	0.004129	9.37	611.54	291.61	0.87	0.001404	2.09	292.78	2.1
1314	5000	4609.5	4616.02	4616.2	0.000699	4.14	3116.85	1302.48	0.36	0.000635	2.39	1305.61	2.39
1315	5000	4609.9	4615.74	4615.88	0.000579	3.87	3910.56	1404.76	0.33	0.000581	2.77	1409.75	2.78
1316	5000	4610.5	4615.49	4615.61	0.000583	3.79	4185.73	1455.91	0.33	0.00054	2.87	1460.58	2.87
1317	5000	4610	4615.26	4615.36	0.000501	3.55	4514.7	1498.46	0.31	0.000882	3.01	1502.07	3.01
1318	5000	4609.3	4614.33	4614.86	0.001951	6.16	1238.44	520.97	0.59	0.001028	2.36	523.98	2.38
1319	5000	4607.9	4614.09	4614.21	0.000633	3.49	3666.07	1491.06	0.33	0.000962	2.45	1496.89	2.46
1320	5000	4606.7	4613.24	4613.68	0.001632	5.5	1226.42	533.81	0.53	0.000909	2.29	536.47	2.3

1321	5000	4607.2	4613.01	4613.11	0.000578	2.99	3538.51	1491.69	0.31	0.000948	2.37	1495.42	2.37
1322	5000	4608.1	4612.17	4612.61	0.001835	5.32	945.19	344.63	0.56	0.001128	2.72	346.97	2.74
1323	5000	4607.7	4611.8	4611.96	0.000763	3.18	1572.69	622.9	0.35	0.000623	2.52	624.29	2.52
1324	5000	4607	4611.51	4611.61	0.000519	2.65	2232.15	937.98	0.29	0.00071	2.37	939.95	2.38
1325	5000	4606.7	4611.03	4611.24	0.00103	3.91	1807.3	757.29	0.41	0.001221	2.38	758.31	2.39
1326	5000	4606.3	4610.31	4610.59	0.001469	4.38	1566.38	783.08	0.49	0.001395	2	785.01	2
1327	5000	4605.4	4609.63	4609.78	0.001326	3.21	1636.46	1003.86	0.43	0.00124	1.63	1005.1	1.63
1328	5000	4605.1	4609.04	4609.15	0.001162	2.65	1932.91	1414.4	0.39	0.001119	1.36	1416.26	1.37
1329	Cross-section removed - incorrect geometry data												
1330	5000	4604	4607.92	4608.02	0.001078	2.46	2171.43	1703.87	0.38	0.001167	1.27	1707.88	1.27
1331	5000	4602.4	4607.3	4607.42	0.001269	2.81	1830.38	1323.62	0.41	0.001341	1.38	1325.09	1.38
1332	5000	4601.2	4606.63	4606.78	0.001419	3.15	1914.09	1373	0.44	0.001425	1.39	1375.03	1.39
1333	5000	4601.6	4605.96	4606.1	0.001431	2.99	1699.96	1215.68	0.44	0.00106	1.4	1218.48	1.4
1334	5000	4601.4	4605.41	4605.49	0.000816	2.23	2335.16	1651.03	0.33	0.000688	1.41	1653.29	1.41
1335	5000	4600.4	4605.09	4605.15	0.000588	2	2719.71	1949.25	0.28	0.000411	1.39	1952	1.4
1336	5000	4599.9	4604.89	4604.95	0.000304	1.84	2754.17	1253.82	0.22	0.000521	2.19	1256.38	2.2
1337	5000	4600.6	4604.56	4604.69	0.00109	2.92	1784.04	1090.12	0.39	0.001369	1.63	1091.85	1.64
1338	5000	4600.2	4603.8	4604.03	0.001769	3.83	1373.12	853.31	0.5	0.001649	1.6	856.37	1.61
1339	5000	4599.9	4603.05	4603.23	0.001541	3.7	2559.14	2103.33	0.48	0.001103	1.22	2106.17	1.22
1340	5000	4598.6	4602.55	4602.7	0.000828	3.36	2531.66	1594.25	0.37	0.000924	1.59	1596.52	1.59
1341	5000	4598	4601.9	4602.05	0.001038	3.11	1682.3	906.64	0.39	0.000881	1.85	907.23	1.86
1342	5000	4596.9	4601.41	4601.5	0.000757	2.49	2170.42	1302.09	0.33	0.000964	1.66	1303.69	1.67
1343	5000	4595.9	4600.86	4600.95	0.001269	2.66	3235.96	2733.42	0.41	0.000854	1.18	2735.33	1.18
1344	5000	4595	4600.42	4600.47	0.000614	2.17	4666.91	3396.84	0.29	0.001252	1.37	3399.7	1.37
1345	5000	4595	4599.33	4599.75	0.003834	5.26	951.41	591.99	0.73	0.001605	1.61	592.73	1.61
1346	5000	4594.5	4598.68	4598.78	0.000877	2.69	2638.62	1767.12	0.36	0.000791	1.49	1768.19	1.49
1347	5000	4593.1	4598.28	4598.36	0.000717	2.35	2683.65	1864.1	0.32	0.00088	1.44	1865.77	1.44

1348	5000	4593.2	4597.74	4597.87	0.001104	2.85	1755.15	1075.94	0.39	0.000885	1.63	1077	1.63
1349	5000	4592.9	4597.29	4597.39	0.000725	2.5	2002.34	1091.03	0.32	0.000379	1.83	1092.76	1.84
1350	5000	4592.4	4597.13	4597.18	0.000232	1.84	2712.99	1305.5	0.23	0.000238	2.08	1306.81	2.08
1351	5000	4591.8	4597.03	4597.08	0.000243	1.87	3538.29	2203.09	0.23	0.000204	1.6	2205.1	1.61
1352	5000	4590.8	4596.94	4596.98	0.000174	1.72	4119.34	2310.09	0.2	0.000118	1.78	2311.56	1.78
1353	5000	4590.4	4596.88	4596.92	0.000085	1.74	5316.21	2448.03	0.15	0.000108	2.17	2449.73	2.17
1354	5000	4591.1	4596.8	4596.85	0.000141	2.01	5405.14	2450.42	0.19	0.000194	2.2	2452.86	2.21
1355	5000	4591.4	4596.6	4596.72	0.000286	2.85	1921.66	663.67	0.27	0.000264	2.89	664.91	2.9
1356	5000	4590.4	4596.51	4596.6	0.000244	2.79	4397.85	2153.96	0.25	0.000392	2.04	2156.75	2.04
1357	5000	4591.2	4596.16	4596.44	0.000729	4.53	2241.12	1260.36	0.43	0.001198	1.78	1262.32	1.78
1358	5000	4590.2	4594.65	4595.64	0.002327	8.32	1169.25	982.78	0.78	0.001924	1.19	984.65	1.19
1359	5000	4588.3	4593.97	4594.62	0.001618	6.85	1668.16	1355.25	0.65	0.001247	1.23	1357.62	1.23
1360	5000	4588.6	4593.44	4593.82	0.000991	5.6	2597.26	1478.05	0.51	0.000831	1.75	1481.18	1.76
1361	5000	4587.1	4593.1	4593.35	0.000707	4.64	3260.76	1770.83	0.43	0.000663	1.84	1775.29	1.84
1362	5000	4586.7	4592.8	4592.97	0.000624	4.32	4460.67	2279.76	0.4	0.000457	1.95	2286.2	1.96
1363	5000	4587	4592.63	4592.71	0.000349	3.21	5819.4	2479.88	0.3	0.000844	2.34	2484.61	2.35
1364	5000	4586.8	4590.98	4592.17	0.004266	8.75	571.25	234.44	0.99	0.001235	2.42	235.82	2.44
1365	5000	4583	4590.36	4590.54	0.000578	3.77	3316.84	2277.36	0.38	0.000489	1.45	2285.59	1.46
1366	5000	4584.3	4590.18	4590.3	0.000419	2.98	3393.56	1886.24	0.32	0.000314	1.8	1889.14	1.8
1367	5000	4585.3	4590.07	4590.14	0.000244	2.27	3936.17	1991.32	0.24	0.000261	1.98	1992.32	1.98
1368	5000	4585.2	4589.93	4590.01	0.000279	2.47	3530.14	1770.29	0.26	0.000263	1.99	1771.98	1.99
1369	5000	4584.6	4589.79	4589.89	0.000249	2.68	3098.48	1424.73	0.25	0.000253	2.17	1426.72	2.17
1370	5000	4583.5	4589.65	4589.77	0.000258	2.88	3159.28	1405.76	0.26	0.000399	2.24	1408.2	2.25
1371	5000	4583.9	4589.25	4589.56	0.000696	4.5	1219.93	479.54	0.42	0.000685	2.53	481.57	2.54
1372	5000	4583.8	4588.95	4589.25	0.000675	4.67	2307.1	1262.51	0.42	0.000542	1.82	1266.47	1.83
1373	5000	4582.3	4588.73	4588.94	0.000445	4.01	3204.4	1721.78	0.35	0.000426	1.86	1723.76	1.86
1374	5000	4582.5	4588.56	4588.74	0.000409	3.7	3205.69	1857.39	0.33	0.000459	1.72	1860.49	1.73

1375	5000	4582.4	4588.26	4588.52	0.000519	4.41	2961.01	2224.88	0.38	0.000789	1.33	2227.55	1.33
1376	5000	4581.7	4587.53	4588.07	0.001344	6.78	2161.41	1190.12	0.6	0.001317	1.81	1192.76	1.82
1377	5000	4581.2	4586.87	4587.39	0.001291	6.53	2034.48	1116.97	0.59	0.00112	1.82	1118.91	1.82
1378	5000	4580.4	4586.35	4586.78	0.00098	5.78	2156.55	1410.44	0.51	0.000977	1.53	1413.39	1.53
1379	5000	4580.4	4586	4586.38	0.000974	5.52	2080.8	878.81	0.51	0.000876	2.36	882.41	2.37
1380	5000	4580.3	4585.68	4586.02	0.000792	5.01	1893.21	813.73	0.46	0.000483	2.32	816.4	2.33
1381	5000	4579.6	4585.63	4585.76	0.000325	3.31	3735.14	1868.77	0.3	0.000452	1.99	1873.3	2
1382	5000	4579	4585.25	4585.54	0.000671	4.38	1576.17	670.55	0.42	0.000595	2.34	673.01	2.35
1383	5000	4579	4585	4585.24	0.000532	4	1456.28	543.31	0.37	0.000873	2.67	545.42	2.68
1384	5000	4578.4	4584.32	4584.82	0.001689	5.74	1060.34	495.81	0.63	0.001376	2.12	499.19	2.14
1385	5000	4578.1	4583.7	4584.13	0.001143	5.27	1005.83	454.76	0.53	0.00072	2.21	455.8	2.21
1386	5000	4577.3	4583.5	4583.68	0.000495	3.66	2762.7	1793.26	0.35	0.000545	1.54	1798.32	1.54
1387	5000	4577.5	4583.18	4583.42	0.000603	4.16	2557.48	1791.19	0.39	0.000916	1.42	1797.51	1.43
1388	5000	4577.3	4582.44	4582.93	0.001554	5.6	904.95	368.26	0.61	0.001373	2.45	369.58	2.46
1389	5000	4576.4	4581.81	4582.14	0.001221	4.64	1077.47	450.37	0.53	0.000541	2.39	450.96	2.39
1390	5000	4575.5	4581.69	4581.8	0.000304	2.69	1857.98	618.45	0.27	0.000527	2.99	620.63	3
1391	5000	4575.3	4581.17	4581.51	0.001125	4.66	1141.84	597.01	0.51	0.000821	1.9	599.54	1.91
1392	5000	4574.8	4580.86	4581.04	0.000625	3.44	1490.26	645.69	0.38	0.000797	2.3	648.7	2.31
1393	5000	4574.6	4580.09	4580.61	0.001051	5.83	858.11	227.34	0.53	0.000892	3.76	228.11	3.77
1394	5000	4573.8	4579.67	4580.15	0.000767	5.56	898.59	200.44	0.46	0.00049	4.45	201.97	4.48
1395	5000	4574.6	4579.67	4579.81	0.00034	2.95	1692.8	532.1	0.29	0.000161	3.17	534.14	3.18
1396	5000	4573.4	4579.65	4579.7	0.000094	1.8	2891.68	756.07	0.16	0.000167	3.78	764.17	3.82
1397	5000	4573	4579.36	4579.59	0.000374	3.85	1322.79	344.76	0.32	0.000463	3.83	345.35	3.84
1398	5000	4572.4	4579.03	4579.35	0.000587	4.58	1444.19	783.9	0.4	0.000465	1.84	786.26	1.84
1399	5000	4571.2	4578.82	4579.1	0.000378	4.58	2397.17	834.33	0.34	0.000449	2.86	837.31	2.87
1400	5000	4572	4578.53	4578.86	0.000544	4.75	1910.71	901.8	0.39	0.000556	2.11	905.02	2.12
1401	5000	4571.8	4578.22	4578.56	0.000569	4.93	1911.71	835.61	0.4	0.001065	2.28	838.16	2.29

1402	5000	4571.6	4576.59	4577.94	0.002668	9.31	537.89	144.74	0.84	0.001557	3.68	146.27	3.72
1403	5000	4570	4576.4	4576.92	0.001019	6.62	2392.88	1282.47	0.54	0.00064	1.86	1285.81	1.87
1404	5000	4570.7	4576.36	4576.46	0.000439	3.53	4880.45	1833.09	0.34	0.000307	2.66	1835.52	2.66
1405	5000	4569.9	4576.26	4576.31	0.000227	2.65	6956.9	2298.81	0.24	0.000425	3.02	2300.71	3.03
1406	5000	4569.5	4575.44	4576.05	0.001069	6.3	808.62	236.36	0.54	0.000377	3.39	238.19	3.42
1407	5000	4569.1	4575.65	4575.7	0.000191	2.58	8564	3532.81	0.23	0.000466	2.42	3535.9	2.42
1408	5000	4568.6	4574.18	4575.35	0.002425	8.72	683.95	423.08	0.8	0.000125	1.61	424.44	1.62
1409	5000	4568.1	4574.93	4574.94	0.00004	1.4	18110.83	5118.67	0.11	0.000031	3.54	5122.4	3.54
1410	5000	4567.6	4574.92	4574.93	0.000025	1.16	20866.35	5089.76	0.09	0.000031	4.1	5093.59	4.1
1411	5000	4567.7	4574.91	4574.91	0.000039	1.4	17738.37	4877.65	0.11	0.000112	3.63	4881.75	3.64
1412	5000	4567.5	4573.93	4574.78	0.001254	7.72	1172.25	465	0.6	0.00188	2.5	469	2.52
1413	5000	4567.3	4572.17	4573.73	0.003128	10.13	640.78	403.24	0.91	0.000298	1.58	405.22	1.59
1414	5000	4566.5	4573.01	4573.03	0.000104	2.18	12860	4925.82	0.17	0.000272	2.61	4929.33	2.61
1416	5000	4565.9	4571.84	4572.81	0.001827	7.92	700.31	273.1	0.7	0.000302	2.55	274.2	2.56
1417	5000	4565.5	4572.34	4572.37	0.000119	2.48	11799.05	4601.34	0.19	0.000295	2.56	4605.38	2.56
1418	5000	4564.6	4571.07	4572.13	0.001637	8.26	669.75	219.93	0.68	0.001408	3.03	221.4	3.05
1419	5000	4565.6	4570.58	4571.25	0.001224	6.59	759	186.88	0.58	0.001188	4.03	188.14	4.06
1420	5000	4564.1	4570.02	4570.64	0.001153	6.31	792.55	198.86	0.56	0.001268	3.95	200.47	3.99
1421	5000	4564.1	4569.24	4569.99	0.001401	6.95	734.49	232.22	0.61	0.000951	3.15	233.35	3.16
1422	5000	4562.8	4569.08	4569.4	0.000688	4.59	1089.78	308.56	0.42	0.00057	3.51	310.08	3.53
1423	5000	4563.2	4568.85	4569.12	0.00048	4.19	1436.94	524.75	0.36	0.000525	2.7	532.99	2.74
1424	5000	4562.7	4568.63	4568.88	0.000576	4.02	1242.85	365.9	0.38	0.000516	3.39	366.75	3.4
1425	5000	4562.5	4568.31	4568.64	0.000465	4.71	1569.8	522.88	0.37	0.000399	2.99	524.51	3
1426	5000	4562	4568.17	4568.41	0.000346	4.17	2064.45	543.52	0.32	0.00056	3.75	549.88	3.8
1427	5000	4562.4	4567.49	4568.09	0.001059	6.23	802.81	193.35	0.54	0.000972	4.14	194.13	4.15
1428	5000	4561.6	4567.13	4567.53	0.000895	5.97	2604.39	1584.15	0.5	0.000714	1.64	1590.73	1.64
1429	5000	4561	4566.86	4567.11	0.000582	4.02	1323.85	436.72	0.39	0.000536	3.01	439.22	3.03

1430	5000	4560.2	4566.63	4566.81	0.000494	3.48	1519.56	534.36	0.35	0.000369	2.83	536.09	2.84
1431	5000	4560.5	4566.48	4566.6	0.000286	2.79	1870.25	599.13	0.27	0.00061	3.11	600.65	3.12
1432	5000	4559.4	4565.33	4566.2	0.002105	7.56	819.66	397.36	0.73	0.001664	2.05	399.25	2.06
1433	5000	4559.8	4564.65	4565.23	0.001349	6.21	991.52	492.27	0.59	0.001258	2.01	493.62	2.01
1434	5000	4558.4	4564.06	4564.56	0.001176	5.69	985.8	470.54	0.55	0.000435	2.08	473.21	2.1
1435	5000	4558.4	4564.13	4564.23	0.000224	3.16	6046.04	2530.55	0.25	0.00018	2.39	2533.22	2.39
1436	5000	4556.8	4564.07	4564.14	0.000148	2.71	7052.48	2645.39	0.21	0.000302	2.66	2648.64	2.67
1437	5000	4558	4563.46	4563.94	0.000924	5.72	1340.1	560.32	0.5	0.000989	2.38	562.14	2.39
1438	5000	4558	4562.92	4563.43	0.001062	5.98	1481.74	662.81	0.53	0.000815	2.23	664.15	2.24
1439	5000	4557.4	4562.66	4562.91	0.000645	4.77	3430.79	1642.28	0.42	0.000747	2.08	1645.68	2.09
1440	5000	4557	4562.27	4562.55	0.000876	5.2	3277.04	1697.19	0.48	0.001162	1.93	1700.32	1.93
1441	5000	4557.5	4561.56	4561.96	0.001614	6.1	2759.54	1855.2	0.63	0.001506	1.49	1856.94	1.49
1442	5000	4556.7	4560.86	4561.21	0.001408	6	3441.16	2493.19	0.59	0.000831	1.38	2496.36	1.38
1443	5000	4554.9	4560.58	4560.77	0.000548	4.39	4455.8	2578.94	0.38	0.00052	1.73	2582.64	1.73
1444	5000	4554.2	4560.36	4560.52	0.000494	3.95	4555.66	2414.57	0.36	0.000494	1.88	2417.9	1.89
1445	5000	4555.2	4560.11	4560.26	0.000494	3.89	4407.57	2394.59	0.36	0.000497	1.84	2398.48	1.84
1446	5000	4555.1	4559.9	4560.02	0.0005	3.57	4499.06	2203.75	0.35	0.00039	2.04	2208.41	2.04
1447	5000	4554.2	4559.74	4559.82	0.000313	2.89	5224.67	2366.07	0.28	0.000706	2.21	2369.34	2.21
1448	5000	4553.8	4558.41	4559.39	0.002855	7.93	630.83	226.97	0.83	0.002642	2.75	229.28	2.78
1449	5000	4552.9	4557.29	4558.21	0.002452	7.67	663.04	240.67	0.78	0.00136	2.73	242.6	2.75
1450	5000	4552.1	4557.09	4557.38	0.000863	4.33	1154.51	410.41	0.46	0.000464	2.8	413.04	2.81
1451	5000	4551.7	4557.02	4557.11	0.000289	2.5	1996.59	713.35	0.26	0.000505	2.79	714.82	2.8
1452	5000	4550.9	4556.53	4556.84	0.001098	4.44	1125.18	462.51	0.5	0.000466	2.43	463.97	2.43
1453	5000	4550.9	4556.46	4556.55	0.000256	2.35	2130.08	772.46	0.25	0.000136	2.74	776.4	2.76
1454	5000	4550.4	4556.43	4556.46	0.000084	1.62	8142.39	4207.88	0.15	0.000136	1.93	4212.24	1.94
1455	5000	4550.8	4556.26	4556.39	0.000255	2.92	2786.65	1783.55	0.26	0.000464	1.56	1786.24	1.56
1456	5000	4550.1	4555.67	4556.13	0.001097	5.43	942.06	356.75	0.53	0.001266	2.63	358.37	2.64

1457	5000	4549.9	4554.98	4555.5	0.001476	5.77	907.33	447.09	0.6	0.00011	2.03	447.8	2.03
1458	5000	4549.6	4555.3	4555.3	0.000037	1.11	18941.09	5310.22	0.1	0.000034	3.56	5318.02	3.57
1459	5000	4549.3	4555.29	4555.29	0.000031	1.08	20506.08	5373.71	0.09	0.000104	3.81	5376.38	3.82
1460	5000	4548.2	4553.5	4555.08	0.004281	10.12	523.61	244.76	1.03	0.000181	2.13	246.2	2.14
1461	5000	4548.6	4553.58	4553.58	0.000056	1.27	18063.49	5465.18	0.12	0.000059	3.3	5467.38	3.31
1462	5000	4549.2	4553.55	4553.55	0.000062	1.06	17869.78	5745.51	0.12	0.000049	3.11	5748.26	3.11
1463	5000	4547	4553.52	4553.53	0.000039	1.1	20046.26	5703.18	0.1	0.000037	3.51	5706.48	3.51
1464	5000	4547.8	4553.51	4553.51	0.000035	0.95	20799.56	5612.03	0.09	0.000102	3.7	5616.55	3.71
1465	5000	4546.4	4552.76	4553.4	0.00124	6.55	1128.58	487.04	0.58	0.001603	2.3	490.8	2.32
1466	5000	4546.7	4551.79	4552.58	0.002152	7.11	703.54	236.54	0.73	0.0002	2.96	237.61	2.97
1467	5000	4545.8	4552.23	4552.24	0.00007	1.46	15837.7	5423.06	0.14	0.000071	2.92	5426.89	2.92
1468	5000	4546.1	4552.2	4552.21	0.000072	1.57	15320.33	5288.22	0.14	0.00007	2.9	5291.13	2.9
1469	5000	4545.6	4552.16	4552.17	0.000069	1.71	15278.64	5088.98	0.14	0.000069	3	5093.35	3
1470	5000	4546	4552.12	4552.14	0.000069	1.66	14102.42	4254.76	0.14	0.000079	3.31	4256.76	3.31
1471	5000	4545.2	4552.07	4552.09	0.000092	1.93	11338.88	3427.11	0.16	0.000275	3.31	3429.13	3.31
1472	5000	4545.7	4550.13	4551.79	0.003814	10.35	483.04	141.5	0.99	0.001074	3.39	142.56	3.41
1473	5000	4544.3	4550.41	4550.57	0.000497	4.25	4880.54	2294.02	0.37	0.000475	2.12	2297.5	2.13
1474	5000	4544.2	4550.2	4550.35	0.000454	4.03	4780.13	2267.22	0.35	0.00046	2.11	2268.99	2.11
1475	5000	4543.5	4549.93	4550.08	0.000467	3.98	4841.74	2463.12	0.35	0.001047	1.96	2466.65	1.97
1476	5000	4543.6	4548.01	4549.33	0.004146	9.23	541.99	201.67	0.99		2.68	202.41	2.69

Table C.3 HEC-RAS output for 1985 geometry

HEC-RAS Plan: 1985(8-7-06) River: Middle Rio Grande Reach: Socorro Profile: PF 1													
Agg/Deg #	Discharge	Min. Channel Elev.	W.S. Elev.	E.G. Elev.	E.G. Slope	Velocity	Flow Area	Top Width	Froude #	Frctn Slope	Hydr Radius	Wetted Perimeter	Hydr Depth
	(cfs)	(ft)	(ft)	(ft)	(ft/ft)	(ft/s)	(sq ft)	(ft)		(ft/ft)	(ft)	(ft)	(ft)
1313	5000	4610.3	4616.31	4617.3	0.001846	7.96	627.93	117.7	0.61	0.000871	5.18	121.25	5.34
1314	5000	4608.6	4616.29	4616.57	0.000505	4.28	1167.49	213.64	0.32	0.000556	5.4	216.2	5.46
1315	5000	4609.7	4616.05	4616.28	0.000614	4.14	2688.47	1393.78	0.35	0.000699	1.93	1396.37	1.93
1316	5000	4609.7	4615.76	4615.95	0.000802	3.89	2880.79	1458.2	0.38	0.000309	1.97	1461.5	1.98
1317	5000	4606.2	4615.66	4615.78	0.000163	2.96	4036.11	1493.67	0.19	0.000271	2.69	1499.22	2.7
1318	5000	4609.6	4615.48	4615.63	0.000539	3.64	3331.48	1489.41	0.32	0.000429	2.23	1492.33	2.24
1319	5000	4606.9	4615.28	4615.39	0.00035	3.13	3783.05	1493.73	0.26	0.000526	2.52	1501.01	2.53
1320	5000	4608.6	4614.79	4615.1	0.000877	4.5	1232.36	404.47	0.4	0.001813	3.03	406.05	3.05
1321	5000	4609.4	4612.58	4614.07	0.00574	9.8	510.2	167.56	0.99	0.001721	3.02	168.95	3.04
1322	5000	4607.5	4612.28	4612.6	0.000816	4.71	1809.44	1373.97	0.4	0.000433	1.32	1375.41	1.32
1323	5000	4605.6	4612.19	4612.32	0.000268	3.06	2745.58	1288.7	0.23	0.00038	2.13	1291.78	2.13
1324	5000	4605.4	4611.96	4612.12	0.000579	3.29	1789.62	669.43	0.32	0.00053	2.66	672.74	2.67
1325	5000	4607	4611.68	4611.83	0.000487	3.17	1578.37	440.57	0.29	0.00068	3.53	447.32	3.58
1326	5000	4607	4611.21	4611.45	0.001015	3.86	1293.95	469.88	0.41	0.000554	2.74	471.93	2.75
1327	5000	4605.8	4611.01	4611.11	0.000348	2.55	2695.05	1171.61	0.25	0.000209	2.29	1177.29	2.3
1328	5000	4605	4610.93	4610.99	0.00014	1.91	3354.93	1116.2	0.16	0.00012	2.99	1123.87	3.01
1329	5000	4605.4	4610.88	4610.92	0.000104	1.66	3882	1136.52	0.14	0.000225	3.41	1139.34	3.42
1330	5000	4605.6	4610.41	4610.77	0.000799	4.83	1035.04	222.58	0.39	0.001155	4.59	225.68	4.65
1331	5000	4605.1	4609.47	4610.18	0.001816	6.77	738.02	177.15	0.58	0.000535	4.11	179.39	4.17
1332	5000	4604.8	4609.65	4609.75	0.000252	2.72	3694.82	1451.79	0.22	0.000122	2.54	1456.15	2.55
1333	5000	4603.5	4609.64	4609.67	0.000072	1.44	5387.37	1423.84	0.12	0.000077	3.77	1427.89	3.78
1334	5000	4602.8	4609.6	4609.63	0.000083	1.66	5766.42	1509.33	0.13	0.000142	3.81	1514.99	3.82

1335	5000	4603.4	4609.42	4609.56	0.000299	3.4	3493.79	1017.22	0.25	0.000194	3.42	1022.06	3.43
1336	5000	4602.8	4609.4	4609.43	0.000136	2.1	8529.88	2461.54	0.16	0.00031	3.46	2467.2	3.47
1337	5000	4603.1	4608.61	4609.21	0.001282	6.19	807.53	169.1	0.5	0.00235	4.67	172.95	4.78
1338	5000	4602.8	4606.3	4607.98	0.005634	10.4	480.92	140.9	0.99	0.004052	3.35	143.72	3.41
1339	5000	4602.2	4605	4605.4	0.003053	5.48	1575.32	1151.21	0.68	0.001089	1.37	1152.3	1.37
1340	5000	4601.2	4604.74	4604.85	0.000554	2.67	2249.59	1088.58	0.3	0.000638	2.06	1090.14	2.07
1341	5000	4600.9	4604.41	4604.52	0.000744	3.4	4418.1	2439.03	0.35	0.000961	1.81	2440.87	1.81
1342	5000	4601.1	4603.96	4604.06	0.001288	3.23	3172.49	1542.88	0.43	0.002655	2.06	1543.53	2.06
1343	5000	4600.3	4602.02	4602.47	0.008339	5.41	1020.24	1168.47	0.98	0.000585	0.87	1169.8	0.87
1344	5000	4597.6	4601.52	4601.55	0.000194	1.66	6577.56	3341.77	0.18	0.000274	1.97	3344.37	1.97
1345	5000	4597.8	4601.33	4601.39	0.000414	2.42	5407.58	3186.9	0.26	0.000451	1.7	3189.31	1.7
1346	5000	4597.5	4601.05	4601.13	0.000492	3.03	5332.23	2832.13	0.29	0.000801	1.88	2833.52	1.88
1347	5000	4598.3	4600.6	4600.71	0.001529	3.68	3753.32	2223.09	0.47	0.000907	1.69	2224.93	1.69
1348	5000	4597	4600.14	4600.2	0.000599	2.33	4051.28	2006.74	0.3	0.000242	2.02	2008.73	2.02
1349	5000	4594.9	4600.03	4600.05	0.00013	1.32	5786.96	2569.21	0.15	0.000262	2.25	2572.02	2.25
1350	5000	4595.5	4599.75	4599.91	0.000776	3.14	1593.56	852.11	0.4	0.000639	1.87	854.11	1.87
1351	5000	4596	4599.52	4599.63	0.000535	2.6	1921.61	1029.55	0.34	0.000644	1.86	1031.82	1.87
1352	5000	4596.3	4599.24	4599.37	0.00079	3.04	2302.66	1409.55	0.4	0.001165	1.63	1411.06	1.63
1353	5000	4595.8	4598.35	4598.58	0.001884	3.88	1509.86	1360.19	0.6	0.00164	1.11	1360.71	1.11
1354	5000	4594.7	4597.18	4597.42	0.00144	3.98	1257.25	749.94	0.54	0.000698	1.68	750.27	1.68
1355	5000	4592.9	4596.9	4597.02	0.00041	2.79	1789.64	706.38	0.31	0.000856	2.53	707.71	2.53
1356	5000	4592.4	4595.97	4596.59	0.00277	6.33	789.69	382.77	0.78	0.001545	2.06	383.24	2.06
1357	5000	4591.5	4595.56	4595.94	0.000984	4.95	1010.16	325.41	0.5	0.000935	3.09	326.39	3.1
1358	5000	4591.2	4595.06	4595.36	0.00089	4.36	1147.79	415.13	0.46	0.001153	2.75	416.71	2.76
1359	5000	4590.7	4594.45	4594.8	0.00155	4.73	1165.6	859.9	0.58	0.001454	1.35	861.01	1.36
1360	5000	4590.5	4593.62	4593.91	0.001366	4.36	1496.11	1358.49	0.54	0.000824	1.1	1359.56	1.1

1361	5000	4590	4593.31	4593.43	0.00055	3.17	3502.65	1814	0.36	0.0007	1.93	1815.2	1.93
1362	5000	4589.2	4592.81	4593.05	0.000921	3.95	1265.15	543.71	0.46	0.001185	2.32	544.98	2.33
1363	5000	4588.6	4592.14	4592.54	0.001581	5.02	995.87	448.24	0.59	0.00042	2.22	449.44	2.22
1364	5000	4588.3	4592.16	4592.19	0.00019	1.58	6108.45	2559.76	0.2	0.000333	2.38	2562.95	2.39
1365	5000	4588.7	4591.93	4592.01	0.000726	2.84	4408.66	2366.85	0.38	0.000697	1.86	2368.62	1.86
1366	5000	4588.1	4591.57	4591.67	0.000669	3.05	4061.79	2259.89	0.38	0.000613	1.8	2261.65	1.8
1367	5000	4587.5	4591.25	4591.37	0.000563	3.25	3851.43	1973.61	0.36	0.000561	1.95	1974.77	1.95
1368	5000	4587.2	4590.98	4591.09	0.000559	3.16	3740.22	1777.9	0.36	0.000517	2.1	1779.67	2.1
1369	5000	4587.2	4590.73	4590.84	0.00048	2.87	3153.49	1449.27	0.33	0.000684	2.17	1451.33	2.18
1370	5000	4587	4590.26	4590.49	0.001053	3.87	1291.38	633.34	0.48	0.000926	2.03	634.66	2.04
1371	5000	4587	4589.86	4590.01	0.00082	3.29	2527.8	1506.38	0.42	0.001245	1.68	1507.88	1.68
1372	5000	4585.9	4589.03	4589.42	0.00211	5.01	998.44	559.4	0.66	0.000874	1.78	561.69	1.78
1373	5000	4585.5	4588.76	4588.88	0.000475	2.81	2403.2	1653.44	0.33	0.000657	1.45	1655.68	1.45
1374	5000	4585.9	4588.44	4588.59	0.000966	3.16	1580.28	984.31	0.44	0.000621	1.6	985.39	1.61
1375	5000	4585.3	4588.16	4588.24	0.000433	2.29	2207.92	1365.83	0.3	0.001059	1.62	1366.88	1.62
1376	5000	4585	4587.1	4587.59	0.005586	5.75	1048.61	1064.43	0.99	0.001294	0.98	1065.25	0.99
1377	5000	4583.7	4586.24	4586.35	0.000561	2.6	1922.18	1068.54	0.34	0.000572	1.8	1069.61	1.8
1378	5000	4582.9	4585.92	4586.04	0.000584	2.87	2290.82	1249.68	0.36	0.000528	1.83	1250.83	1.83
1379	5000	4582	4585.72	4585.83	0.00048	2.73	2528.45	1424.31	0.33	0.000405	1.77	1426.38	1.78
1380	5000	4582.2	4585.57	4585.65	0.000347	2.39	2379.7	1251.79	0.28	0.000519	1.9	1253.62	1.9
1381	5000	4582.9	4585.31	4585.44	0.000859	2.97	2013.6	1339.07	0.41	0.000741	1.5	1341.73	1.5
1382	5000	4581.7	4584.99	4585.09	0.000646	2.58	2161.92	1381.44	0.36	0.001214	1.56	1384.08	1.56
1383	5000	4581.2	4584.21	4584.49	0.003069	4.26	1173.56	1111.32	0.73	0.000823	1.05	1114.38	1.06
1384	5000	4580.5	4583.91	4583.98	0.000375	2.16	2393.59	1665.55	0.28	0.000364	1.43	1668.72	1.44
1385	5000	4580.6	4583.72	4583.79	0.000353	2.19	2593.93	1674.36	0.28	0.00045	1.55	1676.11	1.55
1386	5000	4580.5	4583.44	4583.56	0.000593	2.75	1961.34	1315.26	0.35	0.0008	1.49	1316.6	1.49

1387	5000	4580	4583.02	4583.19	0.001139	3.27	1530.43	1027.95	0.47	0.001126	1.49	1028.99	1.49
1388	5000	4579.8	4582.43	4582.62	0.001113	3.45	1450.26	882.95	0.47	0.000679	1.64	884.13	1.64
1389	5000	4578.7	4582.14	4582.25	0.000457	2.64	1890.83	878.27	0.32	0.000385	2.15	880.72	2.15
1390	5000	4579.1	4581.96	4582.04	0.000329	2.35	2130.21	924.53	0.27	0.000463	2.3	926.83	2.3
1391	5000	4577.5	4581.63	4581.8	0.0007	3.32	1508.43	700.24	0.39	0.000864	2.14	703.28	2.15
1392	5000	4577.4	4581.13	4581.35	0.001094	3.77	1328.68	729.6	0.48	0.002091	1.82	731.36	1.82
1393	5000	4577.9	4579.68	4580.29	0.005488	6.27	797.69	655.32	1	0.000576	1.22	656.32	1.22
1394	5000	4575.3	4579.48	4579.56	0.000205	2.31	2247.59	833.05	0.23	0.00024	2.69	834.45	2.7
1395	5000	4575.6	4579.36	4579.45	0.000284	2.32	2154.17	852.33	0.26	0.000171	2.52	853.72	2.53
1396	5000	4574.2	4579.3	4579.35	0.000114	1.88	3414.89	1097.18	0.17	0.000227	3.11	1098.99	3.11
1397	5000	4575	4578.98	4579.22	0.00066	3.9	1281.78	436.68	0.4	0.000985	2.92	438.58	2.94
1398	5000	4574.4	4578.28	4578.68	0.001626	5.07	985.43	446.1	0.6	0.000879	2.2	447.19	2.21
1399	5000	4573.6	4577.96	4578.2	0.00055	3.99	1476.54	569.97	0.38	0.000584	2.58	573.21	2.59
1400	5000	4573.6	4577.67	4577.92	0.000622	4.01	1283.04	498.38	0.39	0.000394	2.56	501.51	2.57
1401	5000	4571.4	4577.54	4577.69	0.000272	3.23	2005.73	763.55	0.27	0.000361	2.62	765.26	2.63
1402	5000	4572.7	4577.25	4577.49	0.000503	3.99	1621.09	681.88	0.36	0.000537	2.37	683.23	2.38
1403	5000	4573	4577	4577.2	0.000575	3.97	2837.25	1404.06	0.38	0.000732	2.02	1405	2.02
1404	5000	4572.7	4576.58	4576.82	0.000964	3.95	1343.43	696.41	0.46	0.000436	1.93	697.82	1.93
1405	5000	4572	4576.48	4576.58	0.000247	2.49	2056.65	752.67	0.25	0.000278	2.73	753.94	2.73
1406	5000	4572	4576.31	4576.44	0.000314	2.86	1747.13	544.06	0.28	0.000124	3.2	545.17	3.21
1407	5000	4572.2	4576.33	4576.34	0.000066	1.32	12716.66	4095.31	0.13	0.000087	3.1	4097.12	3.11
1408	5000	4570.9	4576.26	4576.3	0.000121	2.19	8808.12	3885.51	0.18	0.000289	2.27	3888.15	2.27
1409	5000	4571.6	4575.7	4576.11	0.0014	5.17	967.04	379.81	0.57	0.002293	2.54	381.14	2.55
1410	5000	4570.9	4573.84	4574.9	0.004422	8.25	605.81	279.02	0.99	0.000178	2.16	280.58	2.17
1411	5000	4570.1	4574.3	4574.31	0.000055	1.14	15669.67	4916.94	0.12	0.000135	3.19	4918.91	3.19
1412	5000	4569.5	4574.01	4574.23	0.000713	3.72	1405.77	615.97	0.41	0.000879	2.27	619.26	2.28

1413	5000	4569.8	4573.51	4573.76	0.001112	4.03	1276.45	662.34	0.49	0.0013	1.92	663.54	1.93
1414	5000	4569.5	4572.77	4573.1	0.001539	4.64	1078.21	536.55	0.58	0.00162	2.01	537.31	2.01
1416	5000	4568.7	4571.93	4572.31	0.001706	4.94	1030.74	538.57	0.61	0.001533	1.91	539.67	1.91
1417	5000	4568.2	4571.24	4571.51	0.001384	4.2	1189.18	632.42	0.54	0.000814	1.88	633.85	1.88
1418	5000	4567.1	4570.94	4571.07	0.000535	2.99	1692.37	857.59	0.35	0.000504	1.97	858.61	1.97
1419	5000	4566.1	4570.68	4570.81	0.000476	2.83	1808.78	851.13	0.33	0.000664	2.12	853.01	2.13
1420	5000	4566.8	4570.27	4570.51	0.00103	3.87	1290.55	621.83	0.47	0.001159	2.07	622.92	2.08
1421	5000	4566.6	4569.7	4569.92	0.001314	3.71	1398.72	897.53	0.51	0.001526	1.56	899.48	1.56
1422	5000	4566	4568.78	4569.19	0.001794	5.11	1040.18	620.99	0.63	0.000707	1.67	622.01	1.68
1423	5000	4565.5	4568.68	4568.77	0.000375	2.44	2140.41	1011.87	0.29	0.000346	2.11	1013.57	2.12
1424	5000	4564.7	4568.51	4568.6	0.000319	2.47	2513.74	1269.61	0.27	0.000413	1.98	1272.03	1.98
1425	5000	4565	4568.23	4568.4	0.000554	3.66	3095.37	1903.76	0.37	0.000514	1.62	1905.07	1.63
1426	5000	4563.9	4567.99	4568.13	0.000478	2.96	2354.17	1469.03	0.33	0.00095	1.6	1470.62	1.6
1427	5000	4564.5	4567.27	4567.6	0.002728	4.71	1203.17	881.48	0.72	0.00205	1.36	882.59	1.36
1428	5000	4564.1	4566.28	4566.53	0.001596	4.06	1232.21	769.96	0.57	0.000481	1.6	770.98	1.6
1429	5000	4561.4	4566.15	4566.23	0.000228	2.35	3201.01	1673.99	0.24	0.000268	1.91	1675.65	1.91
1430	5000	4562.4	4565.99	4566.09	0.00032	2.65	2865.56	1804.51	0.28	0.000398	1.59	1806.25	1.59
1431	5000	4562.4	4565.76	4565.88	0.000509	2.95	2911	1968.88	0.34	0.000816	1.48	1970.57	1.48
1432	5000	4562.7	4565.12	4565.43	0.001516	4.42	1194.36	752.88	0.57	0.000705	1.58	753.92	1.59
1433	5000	4562.2	4564.9	4564.98	0.000406	2.69	4433.72	1996.53	0.3	0.000254	2.22	1998.2	2.22
1434	5000	4561.2	4564.81	4564.83	0.000174	1.76	7300.98	2282.8	0.2	0.000382	3.2	2283.79	3.2
1435	5000	4560.7	4564.33	4564.64	0.001422	4.44	1160.11	639.06	0.55	0.001	1.81	640.2	1.82
1436	5000	4560.7	4563.87	4564.08	0.000742	3.72	1345.37	539.44	0.41	0.001057	2.49	540.69	2.49
1437	5000	4560.1	4563.16	4563.51	0.001625	4.75	1052.56	525.74	0.59	0.001449	2	526.88	2
1438	5000	4559.3	4562.43	4562.71	0.001301	4.24	1180.14	591.29	0.53	0.001255	1.99	593.56	2
1439	5000	4558.4	4561.82	4561.99	0.001212	3.62	2262.3	1485.44	0.5	0.000593	1.52	1487.19	1.52

1440	5000	4557.5	4561.58	4561.67	0.00035	2.6	3161.94	1610.18	0.29	0.000359	1.96	1611.34	1.96
1441	5000	4557.5	4561.41	4561.5	0.000367	2.56	3415.48	1821.37	0.29	0.000297	1.87	1822.24	1.88
1442	5000	4557.2	4561.27	4561.35	0.000245	2.43	4080.6	2381.18	0.25	0.00038	1.71	2383.21	1.71
1443	5000	4557.5	4561.01	4561.16	0.00067	3.34	2942.36	2374.23	0.39	0.00112	1.24	2376.59	1.24
1444	5000	4557.8	4560.25	4560.6	0.002237	4.74	1054.69	672.22	0.67	0.000937	1.57	673.02	1.57
1445	5000	4557.4	4559.92	4560.05	0.000512	2.81	1781.06	823.92	0.34	0.001097	2.16	824.92	2.16
1446	5000	4556.6	4559.12	4559.49	0.003816	4.9	1021.1	925.46	0.82	0.00217	1.1	926.59	1.1
1447	5000	4554.9	4558.15	4558.36	0.001398	3.61	1384.44	930.75	0.52	0.001168	1.48	934.04	1.49
1448	5000	4554.4	4557.59	4557.78	0.000991	3.5	1428.45	779.05	0.46	0.001027	1.83	780.22	1.83
1449	5000	4554.5	4557.08	4557.29	0.001065	3.71	1346.26	709.34	0.48	0.000804	1.9	710.19	1.9
1450	5000	4553.9	4556.74	4556.88	0.000628	2.94	1698.72	853.39	0.37	0.00079	1.99	855.06	1.99
1451	5000	4553.9	4556.36	4556.52	0.001024	3.26	1532.96	953.1	0.45	0.000934	1.61	954.09	1.61
1452	5000	4553.4	4555.92	4556.08	0.000855	3.23	1547.85	853.02	0.42	0.001313	1.81	853.68	1.81
1453	5000	4553.1	4555.11	4555.42	0.002268	4.81	1828.18	1474.2	0.67	0.000753	1.24	1475.25	1.24
1454	5000	4551.4	4554.86	4554.96	0.000371	2.67	3397.59	1884.54	0.29	0.000338	1.8	1886.95	1.8
1455	5000	4550	4554.7	4554.8	0.000308	2.49	2008.72	759.97	0.27	0.000342	2.64	762.08	2.64
1456	5000	4549.8	4554.49	4554.63	0.000382	3.04	1643.64	540.46	0.31	0.000449	3.03	541.79	3.04
1457	5000	4550.5	4554.26	4554.42	0.000536	3.23	1703.08	998.79	0.35	0.000415	1.7	999.58	1.71
1458	5000	4549.7	4554.08	4554.21	0.00033	2.92	1711.12	536	0.29	0.000425	3.18	537.39	3.19
1459	5000	4549.8	4553.85	4554.02	0.000566	3.36	1486.7	565.03	0.37	0.000336	2.62	566.53	2.63
1460	5000	4549.2	4553.73	4553.83	0.000222	2.55	1961.41	560.17	0.24	0.000088	3.49	561.45	3.5
1461	5000	4548	4553.74	4553.76	0.000047	1.32	14595.67	5685.52	0.11	0.00005	2.57	5688.32	2.57
1462	5000	4548	4553.72	4553.73	0.000053	1.4	15118.16	5631	0.12	0.0001	2.68	5632.42	2.68
1463	5000	4548.5	4553.52	4553.67	0.000253	3.11	1610.04	376.22	0.26	0.000527	4.26	377.53	4.28
1464	5000	4548.6	4552.53	4553.34	0.001712	7.21	693.13	191.59	0.67	0.001608	3.59	192.84	3.62
1465	5000	4547.5	4551.78	4552.52	0.001512	6.91	723.76	195.04	0.63	0.001219	3.7	195.76	3.71

1466	5000	4546.1	4551.22	4551.88	0.001004	6.6	1049.49	507.67	0.53	0.000239	2.06	509.66	2.07
1467	5000	4545.2	4551.53	4551.57	0.000105	2.39	11377.17	4754.64	0.18	0.00009	2.39	4758.53	2.39
1468	5000	4544.4	4551.5	4551.52	0.000078	1.57	13397.1	5109.48	0.14	0.000072	2.62	5115.46	2.62
1469	5000	4543.3	4551.46	4551.48	0.000067	1.67	12523.34	4691.2	0.14	0.000087	2.67	4696.23	2.67
1470	5000	4545	4551.41	4551.44	0.000119	2.22	11006.55	4190.94	0.18	0.000089	2.63	4192.49	2.63
1471	5000	4543.1	4551.35	4551.39	0.000069	2.07	10811.87	3406.36	0.15	0.000084	3.17	3409.76	3.17
1472	5000	4543.2	4551.27	4551.34	0.000106	2.49	6885.17	2552.45	0.18	0.000125	2.69	2555.87	2.7
1473	5000	4543.4	4551.17	4551.28	0.00015	3	5575.7	2425.83	0.21	0.000183	2.29	2429.53	2.3
1474	5000	4543.4	4551	4551.19	0.000229	3.94	4310.79	2220.94	0.27	0.000328	1.94	2225.55	1.94
1475	5000	4544.7	4550.71	4550.98	0.000508	4.68	3352.09	2001.92	0.38	0.000192	1.67	2004.37	1.67
1476	5000	4544.7	4550.75	4550.79	0.0001	2.29	9130.32	2865.36	0.17		3.18	2867.26	3.19

Table C.4 HEC-RAS output for 1992 geometry

HEC-RAS Plan: 1992(8-7-06) River: Middle Rio Grande Reach: Socorro Profile: PF 1													
Agg/Deg #	Discharge	Min. Channel Elev.	W.S. Elev.	E.G. Elev.	E.G. Slope	Velocity	Flow Area	Top Width	Froude #	Frctn Slope	Hydr Radius	Wetted Perimeter	Hydr Depth
	(cfs)	(ft)	(ft)	(ft)	(ft/ft)	(ft/s)	(sq ft)	(ft)		(ft/ft)	(ft)	(ft)	(ft)
1313	5000	4608.1	4614.9	4615.55	0.000996	6.44	776.11	124.1	0.45	0.000989	5.99	129.61	6.25
1314	5000	4608.2	4614.46	4614.92	0.000983	5.44	919.47	192	0.44	0.000999	4.69	196.06	4.79
1315	5000	4607.8	4613.85	4614.42	0.001017	6.09	854.08	175.96	0.46	0.000969	4.75	179.83	4.85
1316	5000	4607.5	4613.45	4613.96	0.000924	5.75	869.97	158.84	0.43	0.001012	5.34	163.07	5.48
1317	5000	4607.4	4612.95	4613.48	0.001112	5.87	851.71	173.77	0.47	0.000879	4.79	177.66	4.9
1318	5000	4606.1	4612.56	4612.99	0.000712	5.31	942.25	158.79	0.38	0.000683	5.76	163.6	5.93
1319	5000	4605.5	4612.23	4612.63	0.000657	5.04	991.14	169.98	0.37	0.000976	5.67	174.85	5.83
1320	5000	4604.65	4611.39	4612.1	0.001601	6.74	741.77	161.56	0.55	0.001452	4.49	165.23	4.59
1321	5000	4605.7	4610.75	4611.34	0.001324	6.17	810.15	174.71	0.51	0.001151	4.53	178.67	4.64

1322	5000	4605.5	4610.29	4610.72	0.001009	5.29	945.78	211.1	0.44	0.00091	4.41	214.64	4.48
1323	5000	4605	4609.88	4610.24	0.000824	4.8	1041.4	231.4	0.4	0.000827	4.44	234.64	4.5
1324	5000	4605	4609.46	4609.8	0.00083	4.7	1064.59	244.66	0.4	0.000853	4.27	249.09	4.35
1325	5000	4604.8	4609.05	4609.35	0.000878	4.45	1122.92	291.87	0.4	0.001042	3.78	297.07	3.85
1326	5000	4604.6	4608.45	4608.8	0.001255	4.72	1059.33	330.34	0.46	0.001102	3.16	335.58	3.21
1327	5000	4603.7	4607.9	4608.18	0.000975	4.29	1166.79	346.49	0.41	0.001308	3.3	353.51	3.37
1328	5000	4604	4607.27	4607.56	0.001848	4.31	1196.88	611.76	0.53	0.001137	1.94	615.5	1.96
1329	5000	4603.4	4606.8	4606.95	0.000769	3.11	1644.11	790.14	0.35	0.000558	2.07	793.19	2.08
1330	5000	4602.5	4606.53	4606.65	0.000423	2.76	1813.47	560.32	0.27	0.000523	3.18	569.58	3.24
1331	5000	4602.2	4606.2	4606.38	0.000661	3.39	1476.95	471.82	0.34	0.000443	3.1	476.36	3.13
1332	5000	4601.5	4606.05	4606.15	0.000318	2.51	1989.9	569.51	0.24	0.000321	3.44	579.26	3.49
1333	5000	4601.6	4605.89	4606	0.000324	2.69	1861.7	489.26	0.24	0.000229	3.74	497.55	3.81
1334	5000	4600.7	4605.81	4605.88	0.00017	2.07	2416.96	581.75	0.18	0.000242	4.1	590.06	4.15
1335	5000	4600.5	4605.59	4605.75	0.00037	3.16	1581.12	355.78	0.26	0.000608	4.33	365.51	4.44
1336	5000	4600.4	4604.94	4605.42	0.001176	5.55	900.92	209.84	0.47	0.000861	4.23	213.15	4.29
1337	5000	4599.7	4604.66	4604.96	0.000658	4.42	1131.75	240.76	0.36	0.000624	4.64	243.95	4.7
1338	5000	4599	4604.36	4604.66	0.000593	4.38	1140.8	225.76	0.34	0.000915	4.96	230.11	5.05
1339	5000	4595.73	4603.69	4604.21	0.001595	5.81	861.22	236.69	0.54	0.000791	3.6	239.37	3.64
1340	5000	4598.3	4603.57	4603.79	0.000471	3.78	1420.45	556.94	0.3	0.001007	2.53	560.58	2.55
1341	5000	4598.2	4602.12	4603.23	0.003485	8.46	590.79	165.21	0.79	0.002026	3.52	167.65	3.58
1342	5000	4597.9	4601.54	4601.93	0.001323	4.96	1007.95	313.72	0.48	0.001046	3.17	317.73	3.21
1343	5000	4597.6	4601.13	4601.28	0.000847	3.04	1645.83	746.34	0.36	0.001319	2.19	751.83	2.21
1344	5000	4597.5	4600.26	4600.56	0.002333	4.4	1136.83	632.35	0.58	0.001291	1.78	637.42	1.8
1345	5000	4596.9	4599.7	4599.84	0.000818	3.07	1627.46	708.56	0.36	0.000867	2.29	712.07	2.3
1346	5000	4594.39	4599.26	4599.38	0.000921	2.73	1830.94	1042.3	0.36	0.000626	1.75	1044.82	1.76
1347	5000	4596	4598.97	4599.04	0.000453	2.11	2365.36	1159.56	0.26	0.000443	2.03	1163.38	2.04

1348	5000	4595.4	4598.73	4598.8	0.000433	2.08	2403.38	1169.36	0.26	0.000366	2.05	1171.9	2.06
1349	5000	4594.5	4598.53	4598.59	0.000313	2.1	2681.93	1380.87	0.23	0.000405	1.94	1383.67	1.94
1350	5000	4593.5	4598.08	4598.37	0.000543	4.28	1167.69	294.02	0.38	0.000658	3.89	300.04	3.97
1351	5000	4593.8	4597.71	4598.09	0.000814	4.94	1156.05	682.29	0.46	0.000896	1.69	684.58	1.69
1352	5000	4593.6	4597.24	4597.66	0.000991	5.2	1009.48	498.3	0.5	0.000743	2.02	500.27	2.03
1353	5000	4593.2	4597	4597.26	0.000578	4.17	1596.87	669.23	0.39	0.000399	2.38	671.48	2.39
1354	5000	4592.6	4596.84	4596.96	0.000292	2.8	1782.57	536.19	0.27	0.000349	3.29	542.21	3.32
1355	5000	4592.2	4596.59	4596.73	0.000425	3.06	1635.12	575.62	0.32	0.000487	2.82	579.71	2.84
1356	5000	4592.1	4596.35	4596.53	0.000563	3.43	1457.02	533.68	0.37	0.000975	2.72	536.6	2.73
1357	5000	4591.3	4595.22	4596.12	0.002079	7.61	656.8	191.99	0.73	0.001022	3.37	195	3.42
1358	5000	4591.2	4595.05	4595.34	0.000606	4.38	1188.33	433.84	0.4	0.000866	2.72	437.07	2.74
1359	5000	4590.9	4594.49	4594.92	0.001339	5.32	1235.51	840.54	0.56	0.001244	1.46	845.45	1.47
1360	5000	4589.2	4593.88	4594.3	0.001158	5.19	1025.5	399.49	0.53	0.000878	2.55	402.15	2.57
1361	5000	4589.5	4593.54	4593.81	0.000688	4.21	1187.72	370.78	0.41	0.000461	3.18	374.05	3.2
1362	5000	4589	4593.36	4593.54	0.00033	3.37	1483.33	372.62	0.3	0.000544	3.95	375.65	3.98
1363	5000	4588.9	4592.88	4593.23	0.001062	4.76	1051.05	386.84	0.5	0.000723	2.68	392.24	2.72
1364	5000	4588.4	4592.6	4592.82	0.000524	3.85	1401.34	512.15	0.37	0.000448	2.71	516.71	2.74
1365	5000	4588.4	4592.41	4592.58	0.000387	3.3	1513.84	443.61	0.31	0.000478	3.37	449.61	3.41
1366	5000	4588	4592.1	4592.35	0.000605	4.03	1239.44	371.43	0.39	0.000837	3.28	377.98	3.34
1367	5000	4587.6	4591.42	4591.93	0.001234	5.74	871.62	263.93	0.56	0.001213	3.26	267.4	3.3
1368	5000	4587.1	4590.86	4591.34	0.001193	5.57	898.14	276	0.54	0.000817	3.2	281.01	3.25
1369	5000	4587.1	4590.65	4590.89	0.000595	3.89	1284.49	402.8	0.38	0.000581	3.15	407.83	3.19
1370	5000	4586.5	4590.41	4590.61	0.000567	3.54	1410.59	491.92	0.37	0.00087	2.83	497.63	2.87
1371	5000	4584.22	4589.83	4590.17	0.001501	4.72	1060.04	502.64	0.57	0.001069	2.1	505.4	2.11
1372	5000	4585.6	4589.43	4589.67	0.0008	3.91	1290.26	560.02	0.43	0.00086	2.28	565.19	2.3
1373	5000	4585.5	4589.01	4589.23	0.000928	3.77	1325.45	608.94	0.45	0.000647	2.15	616.08	2.18

1374	5000	4585.2	4588.78	4588.91	0.000476	2.88	1743.11	759.66	0.33	0.000425	2.27	767.38	2.29
1375	5000	4585.1	4588.61	4588.71	0.000381	2.59	1969.95	882.63	0.29	0.000727	2.22	888	2.23
1376	5000	4584.9	4587.97	4588.26	0.001902	4.32	1158.12	751.11	0.61	0.001035	1.54	752.94	1.54
1377	5000	4583.4	4587.57	4587.71	0.00065	3.09	1649.8	823.75	0.38	0.001429	1.99	828.1	2
1378	5000	4582.8	4586.18	4586.82	0.005345	6.43	777.15	599.15	1	0.001036	1.29	602.86	1.3
1379	5000	4581.9	4585.99	4586.11	0.000426	2.8	1815.04	765.01	0.31	0.000465	2.35	771.3	2.37
1380	5000	4582.03	4585.81	4585.93	0.000511	2.78	1815.12	884.72	0.34	0.000361	2.05	886.66	2.05
1381	5000	4581.3	4585.7	4585.77	0.000268	2.2	2275.21	930.66	0.25	0.00015	2.43	937.93	2.44
1382	5000	4580.6	4585.65	4585.69	0.000096	1.64	3869.05	1596.59	0.16	0.000161	2.41	1605.23	2.42
1383	5000	4580.3	4585.46	4585.61	0.000321	3.19	2613.39	1539.4	0.29	0.000441	1.69	1544.27	1.7
1384	5000	4580.2	4585.19	4585.41	0.000644	3.91	2271.88	1637.41	0.4	0.000783	1.38	1642.9	1.39
1385	5000	4580.2	4584.75	4585.06	0.000974	4.95	2526.58	1673.97	0.49	0.001203	1.51	1677.93	1.51
1386	5000	4580.1	4584.09	4584.48	0.001524	5.57	2177.77	1603.17	0.6	0.001783	1.36	1606.5	1.36
1387	5000	4579.3	4582.86	4583.58	0.002114	7.04	1258.11	1171.03	0.72	0.001575	1.07	1174.1	1.07
1388	5000	4578.9	4582.47	4582.67	0.001219	3.67	1503.33	985.06	0.5	0.00174	1.52	988.54	1.53
1389	5000	4578.7	4581.36	4581.71	0.002684	4.72	1060.09	777.37	0.71	0.000845	1.36	781.42	1.36
1390	5000	4577.3	4581.1	4581.2	0.000408	2.5	2044.87	988.99	0.3	0.000531	2.06	994.66	2.07
1391	5000	4577.2	4580.8	4580.93	0.00072	2.91	1719.48	972.28	0.39	0.000766	1.76	975.78	1.77
1392	5000	4576.8	4580.36	4580.53	0.000817	3.26	1532.24	800.9	0.42	0.000567	1.9	804.49	1.91
1393	5000	4576.1	4580.11	4580.24	0.000417	2.89	1731.62	651.6	0.31	0.000372	2.63	659.43	2.66
1394	5000	4576	4579.94	4580.05	0.000334	2.67	1985.88	930.92	0.28	0.000285	2.12	937.36	2.13
1395	5000	4575.7	4579.82	4579.9	0.000246	2.23	2246.28	843.19	0.24	0.000186	2.64	849.58	2.66
1396	5000	4575	4579.75	4579.81	0.000146	1.97	2892.93	1084.36	0.19	0.000148	2.65	1090.18	2.67
1397	5000	4574.2	4579.63	4579.73	0.00015	2.56	2004.76	436.26	0.21	0.000283	4.53	442.66	4.6
1398	5000	4573.7	4579.15	4579.56	0.000719	5.21	1122.82	305.21	0.44	0.000938	3.64	308.75	3.68
1399	5000	4573.9	4578.49	4579.07	0.001276	6.24	1149.15	593.78	0.58	0.000733	1.93	596.87	1.94

1400	5000	4573.2	4578.33	4578.61	0.000475	4.33	1556.31	527.76	0.36	0.000738	2.92	533.42	2.95
1401	5000	4573.2	4577.7	4578.22	0.001301	5.97	1284.91	734.82	0.57	0.000816	1.74	737.91	1.75
1402	5000	4572.5	4577.42	4577.76	0.000559	4.76	1420.54	640.21	0.39	0.000529	2.21	643.53	2.22
1403	5000	4572	4577.17	4577.48	0.000501	4.53	1495.67	637.34	0.37	0.000498	2.33	641.4	2.35
1404	5000	4571.7	4576.95	4577.22	0.000495	4.2	1579.04	672.01	0.36	0.000688	2.31	682.61	2.35
1405	5000	4571.8	4576.53	4576.87	0.001021	4.72	1209.98	606.91	0.49	0.00064	1.98	611.23	1.99
1406	5000	4571.7	4576.32	4576.5	0.000438	3.38	1631.77	623.69	0.33	0.000117	2.61	626.3	2.62
1407	5000	4570.9	4576.38	4576.4	0.000053	1.49	11859.53	3908.71	0.12	0.000121	3.03	3915.6	3.03
1408	5000	4570.9	4576.05	4576.31	0.000508	4.1	1218.96	311.15	0.37	0.001117	3.84	317.82	3.92
1409	5000	4571.1	4574.38	4575.68	0.00418	9.18	544.84	203.29	0.99	0.000128	2.64	206.31	2.68
1410	5000	4570.36	4574.98	4574.99	0.000038	1.08	19125.62	4973.22	0.1	0.000112	3.84	4976.54	3.85
1411	5000	4570.6	4574.3	4574.88	0.00133	6.18	915.9	344.22	0.58	0.000806	2.64	346.59	2.66
1412	5000	4569.6	4574.11	4574.37	0.00054	4.1	1313.15	516.68	0.38	0.000733	2.52	520.2	2.54
1413	5000	4568.9	4573.53	4573.98	0.001053	5.43	1143.54	622.27	0.51	0.001718	1.82	628.92	1.84
1414	5000	4567.59	4572.09	4573.07	0.003287	8.01	777.02	524.86	0.88	0.001465	1.47	527.32	1.48
1416	5000	4567.7	4571.8	4572.17	0.000825	4.89	1119.4	519.13	0.46	0.000499	2.14	522.7	2.16
1417	5000	4567.4	4571.69	4571.85	0.000334	3.27	1711.73	677.57	0.3	0.000447	2.5	684	2.53
1418	5000	4566.8	4571.44	4571.64	0.000628	3.54	1413.58	532.72	0.38	0.000475	2.62	539.89	2.65
1419	5000	4566.8	4571.22	4571.38	0.000372	3.3	2054.51	822.88	0.31	0.000724	2.48	827.5	2.5
1420	5000	4565.85	4570.46	4570.98	0.001974	5.87	1095.3	607.63	0.67	0.001303	1.79	610.48	1.8
1421	5000	4566.3	4569.92	4570.28	0.000924	4.79	1043.16	331.91	0.48	0.00164	3.09	337.39	3.14
1422	5000	4566	4568.81	4569.43	0.00368	6.32	790.84	471.35	0.86	0.001868	1.66	476.03	1.68
1423	5000	4565.1	4568.12	4568.31	0.001127	3.53	1416.7	832.43	0.48	0.000351	1.68	841.74	1.7
1424	5000	4563	4568.02	4568.08	0.000169	1.96	2800.99	1416.18	0.2	0.000165	1.96	1427.46	1.98
1425	5000	4563.4	4567.93	4568	0.000162	2.03	3062.87	1725.15	0.2	0.000298	1.76	1736.28	1.78
1426	5000	4563.4	4567.71	4567.84	0.000722	2.95	1692.23	933.36	0.39	0.00067	1.8	940.19	1.81

1427	5000	4563.4	4567.36	4567.49	0.000623	2.93	1904.58	1366.67	0.37	0.000732	1.39	1370.8	1.39
1428	5000	4563	4566.91	4567.1	0.000873	3.56	1406.01	676.92	0.43	0.000888	2.06	681.75	2.08
1429	5000	4562.5	4566.42	4566.65	0.000903	3.88	1287.79	556.85	0.45	0.000785	2.29	561.41	2.31
1430	5000	4562.3	4566.05	4566.23	0.000689	3.44	2252.76	1688.84	0.39	0.00099	1.33	1696.71	1.33
1431	5000	4562.3	4565.39	4565.7	0.001541	4.46	1121.24	586.76	0.57	0.000774	1.89	593.05	1.91
1432	5000	4561.2	4565.11	4565.24	0.000464	2.98	2870.88	1808.5	0.33	0.000876	1.58	1815.72	1.59
1433	5000	4560.6	4564.33	4564.74	0.002231	5.15	970.23	537.11	0.68	0.000459	1.78	545.22	1.81
1434	5000	4560	4564.32	4564.41	0.000192	2.51	1991.13	518.53	0.23	0.000427	3.81	522.55	3.84
1435	5000	4560.4	4563.79	4564.16	0.001654	4.91	1019	487.18	0.6	0.001176	2.07	492.46	2.09
1436	5000	4560.5	4563.26	4563.51	0.000879	4.02	1245.11	502.23	0.45	0.000861	2.46	505.95	2.48
1437	5000	4559.6	4562.81	4563.04	0.000844	3.86	1296.51	539.19	0.44	0.001175	2.39	542.77	2.4
1438	5000	4558.7	4562.12	4562.44	0.001748	4.53	1103.75	623.49	0.6	0.000974	1.76	626.69	1.77
1439	5000	4558.2	4561.72	4561.87	0.00062	3.15	2136.28	1350.06	0.37	0.000977	1.58	1353.21	1.58
1440	5000	4558.1	4561.06	4561.37	0.001762	4.5	1112.13	637.73	0.6	0.001382	1.73	642.41	1.74
1441	5000	4557.3	4560.43	4560.66	0.001113	3.91	1304.52	708	0.49	0.000401	1.82	715.01	1.84
1442	5000	4556.7	4560.33	4560.42	0.000205	2.42	2089.86	668.52	0.23	0.000459	3.11	672.51	3.13
1443	5000	4555.7	4559.83	4560.17	0.001809	4.69	1067.05	587.92	0.61	0.001094	1.81	591.03	1.81
1444	5000	4556.4	4559.43	4559.6	0.000732	3.35	1494.42	692.05	0.4	0.000716	2.15	695.62	2.16
1445	5000	4555.7	4559.09	4559.23	0.0007	3.02	1653.82	863.34	0.38	0.001016	1.91	867.07	1.92
1446	5000	4555.2	4558.54	4558.75	0.001606	3.64	1374.85	1013.86	0.55	0.000738	1.35	1018.54	1.36
1447	5000	4554.5	4558.25	4558.35	0.000422	2.49	2004.8	955.42	0.3	0.000328	2.09	960.43	2.1
1448	5000	4554.5	4558.11	4558.19	0.000262	2.31	2160.28	801.46	0.25	0.00033	2.67	808.27	2.7
1449	5000	4554.6	4557.9	4558.03	0.000428	2.86	1750.91	686.09	0.32	0.000719	2.53	691.34	2.55
1450	5000	4553.26	4557.45	4557.67	0.001453	3.74	1337.05	876.97	0.53	0.001332	1.52	881.29	1.52
1451	5000	4554	4556.83	4557.03	0.001226	3.58	1396.27	860.14	0.5	0.002324	1.62	864.56	1.62
1452	5000	4553.5	4555.58	4556.04	0.005984	5.47	914.61	981.99	1	0.000596	0.93	985.92	0.93

1453	5000	4552.1	4555.46	4555.51	0.00021	1.7	3029.65	1572.47	0.21	0.0002	1.92	1581.35	1.93
1454	5000	4551.8	4555.37	4555.41	0.000191	1.64	3164.33	1678.91	0.2	0.000219	1.88	1685.53	1.88
1455	5000	4551.5	4555.25	4555.3	0.000255	1.92	2793.27	1598.14	0.24	0.000425	1.74	1604.35	1.75
1456	5000	4548.54	4554.86	4555.08	0.000844	3.72	1344.78	588.85	0.43	0.000392	2.26	595.07	2.28
1457	5000	4550.4	4554.75	4554.85	0.000225	2.56	2217.03	1020.45	0.24	0.000304	2.16	1028.31	2.17
1458	5000	4550.2	4554.54	4554.7	0.000431	3.18	1570.04	523.48	0.32	0.00062	2.97	529.49	3
1459	5000	4550.4	4554.2	4554.43	0.000965	3.87	1290.76	588.09	0.46	0.00063	2.17	593.53	2.19
1460	5000	4549.7	4553.93	4554.08	0.000443	3.13	1597.34	555.96	0.33	0.000099	2.83	564.04	2.87
1461	5000	4549	4553.98	4553.99	0.000043	1.09	16622.59	5561.51	0.1	0.000105	2.99	5566.94	2.99
1462	5000	4547.92	4553.7	4553.92	0.000552	3.75	1413.16	628.37	0.37	0.000408	2.23	632.95	2.25
1463	5000	4548.3	4553.52	4553.7	0.000313	3.34	1496.58	363.59	0.29	0.000389	4.05	369.6	4.12
1464	5000	4547.5	4553.11	4553.49	0.000496	4.92	1015.74	192.55	0.38	0.000103	5.13	198.02	5.28
1465	5000	4546.6	4553.32	4553.33	0.000043	1.35	17991.64	5702.45	0.11	0.000112	3.15	5707.83	3.16
1466	5000	4546.7	4552.65	4553.21	0.000744	6.04	828.07	156.91	0.46	0.000769	5.14	161	5.28
1467	5000	4546.5	4552.25	4552.82	0.000796	6.08	821.81	162.3	0.48	0.001024	4.94	166.2	5.06
1468	5000	4546.1	4551.41	4552.3	0.001367	7.56	661.19	140.46	0.61	0.000344	4.57	144.78	4.71
1469	5000	4545	4551.8	4551.88	0.000153	2.87	8825.27	4577.03	0.21	0.000294	1.93	4584.52	1.93
1470	5000	4544.6	4551.12	4551.68	0.000777	6.02	830.55	161.58	0.47	0.000765	4.95	167.63	5.14
1471	5000	4544.5	4550.69	4551.28	0.000752	6.22	889.63	239.68	0.47	0.000776	3.63	245.22	3.71
1472	5000	4544.4	4550.4	4550.86	0.000801	5.94	2478.62	1837.33	0.47	0.000438	1.35	1842.75	1.35
1473	5000	4544.3	4550.38	4550.59	0.000275	3.86	2642.01	1595	0.29	0.0003	1.65	1599.42	1.66
1474	5000	4544.3	4550.25	4550.43	0.000329	3.53	2624.16	1601.93	0.3	0.000616	1.63	1609.87	1.64
1475	5000	4544	4549.32	4550.01	0.001548	6.64	753.1	216.16	0.63	0.002357	3.42	220.02	3.48
1476	5000	4544	4547.07	4548.51	0.004016	9.61	520.15	175.88	0.99		2.92	178.3	2.96

Table C.5 HEC-RAS output for 2002 geometry

HEC-RAS Plan: 2002(8-7-06) River: Middle Rio Grande Reach: Socorro Profile: PF 1													
Agg/Deg #	Discharge	Min. Channel Elev.	W.S. Elev.	E.G. Elev.	E.G. Slope	Velocity	Flow Area	Top Width	Froude #	Frctn Slope	Hydr Radius	Wetted Perimeter	Hydr Depth
	(cfs)	(ft)	(ft)	(ft)	(ft/ft)	(ft/s)	(sq ft)	(ft)		(ft/ft)	(ft)	(ft)	(ft)
1313	5000	4607.93	4614.14	4614.69	0.000631	5.95	840.13	140.97	0.43	0.000842	5.7	147.44	5.96
1314	5000	4608.96	4613.51	4614.19	0.001181	6.65	752.18	177.05	0.57	0.000818	4.2	179.02	4.25
1315	5000	4607.18	4613.24	4613.74	0.0006	5.7	877.49	153.7	0.42	0.000771	5.54	158.34	5.71
1316	5000	4607.64	4612.69	4613.37	0.001028	6.6	757.63	162.09	0.54	0.000719	4.61	164.3	4.67
1317	5000	4606.5	4612.51	4612.96	0.00053	5.38	929.62	161.67	0.4	0.000826	5.57	166.83	5.75
1318	5000	4607.08	4611.65	4612.49	0.001458	7.38	677.47	158.66	0.63	0.0009	4.2	161.45	4.27
1319	5000	4605.94	4611.47	4611.9	0.000611	5.28	947.47	191.46	0.42	0.000715	4.87	194.44	4.95
1320	5000	4602.69	4610.87	4611.52	0.000848	6.47	773.37	142.82	0.49	0.000873	5.17	149.68	5.41
1321	5000	4605.53	4610.49	4611.06	0.000899	6.06	824.77	180.61	0.5	0.001097	4.49	183.73	4.57
1322	5000	4605.98	4609.84	4610.5	0.001368	6.55	763.22	205.52	0.6	0.000944	3.68	207.34	3.71
1323	5000	4604.5	4609.56	4609.95	0.00069	5.01	998.68	240.23	0.43	0.00141	4.11	243.11	4.16
1324	5000	4605.38	4607.93	4609.12	0.004334	8.75	571.47	237.62	0.99	0.002006	2.39	238.85	2.4
1325	5000	4603.91	4607.27	4607.72	0.001152	5.35	934.42	300.48	0.53	0.001358	3.09	302.35	3.11
1326	5000	4603.37	4606.5	4606.99	0.001625	5.65	885.46	337.28	0.61	0.000932	2.59	342.06	2.63
1327	5000	4601.48	4606.15	4606.42	0.000603	4.15	1205.84	346.85	0.39	0.000794	3.43	351.98	3.48
1328	5000	4602.42	4605.76	4606.04	0.001093	4.22	1200.38	575.36	0.49	0.001075	2.07	579.24	2.09
1329	5000	4602.08	4605.26	4605.49	0.001057	3.83	1306.8	669.18	0.48	0.001054	1.94	672.49	1.95
1330	5000	4601.19	4604.72	4604.95	0.00105	3.86	1296.26	632.07	0.47	0.000709	2.03	639.37	2.05
1331	5000	4601.69	4604.42	4604.56	0.00051	2.93	1705.5	735.83	0.34	0.000231	2.31	738.82	2.32
1332	5000	4600.85	4604.37	4604.42	0.000131	1.86	2699.99	851.01	0.18	0.000227	3.15	857.87	3.17
1333	5000	4600.83	4604.15	4604.31	0.000489	3.21	1558.14	567.74	0.34	0.000486	2.73	570.51	2.74
1334	5000	4601.11	4603.92	4604.07	0.000484	3.12	1603.96	607.37	0.34	0.000355	2.64	608.64	2.64

1335	5000	4599.75	4603.78	4603.89	0.000271	2.72	1843.93	563.9	0.26	0.000358	3.23	570.36	3.27
1336	5000	4600.29	4603.51	4603.71	0.000494	3.55	1407.69	444.44	0.35	0.000314	3.16	446.15	3.17
1337	5000	4598.3	4603.4	4603.55	0.000217	3.11	1605.68	329.38	0.25	0.000329	4.81	334.11	4.87
1338	5000	4598.3	4603.01	4603.37	0.000559	4.79	1043.95	238.4	0.39	0.000602	4.31	242.19	4.38
1339	5000	4596.76	4602.67	4603.08	0.000651	5.14	973.3	215.1	0.43	0.000673	4.46	218.23	4.52
1340	5000	4598.05	4602.46	4602.78	0.000695	4.53	1103.42	310.62	0.42	0.001273	3.52	313.62	3.55
1341	5000	4598.08	4601.08	4602.11	0.003046	8.17	612.02	216.34	0.86	0.001542	2.81	217.63	2.83
1342	5000	4596.9	4600.79	4601.18	0.000928	5.02	996.6	297.53	0.48	0.00111	3.3	302.07	3.35
1343	5000	4597.6	4600.3	4600.54	0.001352	3.95	1266.27	741.2	0.53	0.001297	1.7	743.53	1.71
1344	5000	4596.76	4599.63	4599.85	0.001246	3.8	1317.27	753.94	0.51	0.001455	1.74	756.33	1.75
1345	5000	4596.76	4598.84	4599.09	0.001722	4.01	1247.23	840.29	0.58	0.000583	1.48	841.17	1.48
1346	5000	4593.37	4598.66	4598.73	0.00029	2.18	2298.32	1016.17	0.25	0.000255	2.26	1018.22	2.26
1347	5000	4594.91	4598.53	4598.59	0.000226	2.01	2674.05	1189.86	0.23	0.000348	2.24	1195.97	2.25
1348	5000	4594.78	4598.26	4598.4	0.000603	3.06	2076.08	1223.56	0.36	0.000524	1.69	1231.26	1.7
1349	5000	4594.8	4597.97	4598.11	0.00046	3.11	2545.01	1353.19	0.33	0.000587	1.88	1354.78	1.88
1350	5000	4594.65	4597.59	4597.8	0.000775	3.72	1346.34	578.97	0.42	0.000782	2.32	579.97	2.33
1351	5000	4594.02	4597.23	4597.48	0.00079	4.02	1252.42	563.02	0.43	0.000725	2.22	564.03	2.22
1352	5000	4593.38	4596.88	4597.14	0.000668	4.09	1409.12	655.69	0.41	0.0011	2.14	657.12	2.15
1353	5000	4593.33	4596.18	4596.61	0.002142	5.29	962.08	599.24	0.67	0.001214	1.6	600.07	1.61
1354	5000	4592.65	4595.73	4595.94	0.000781	3.69	1374.2	611.7	0.42	0.000569	2.24	613.99	2.25
1355	5000	4592.25	4595.49	4595.63	0.000433	3.06	1679.41	738.27	0.32	0.000385	2.27	739.6	2.27
1356	5000	4591.79	4595.33	4595.47	0.000344	2.96	1688.95	533.26	0.29	0.000705	3.15	536.46	3.17
1357	5000	4591.28	4594.55	4595.14	0.00218	6.41	1068.05	479	0.71	0.001339	2.22	480.92	2.23
1358	5000	4590.46	4593.98	4594.28	0.000905	4.34	1151.26	422.97	0.46	0.000772	2.71	424.95	2.72
1359	5000	4590.08	4593.74	4593.91	0.000666	3.34	1494.77	647.34	0.39	0.000707	2.3	648.59	2.31
1360	5000	4587.09	4593.23	4593.54	0.000753	4.47	1118.45	340.98	0.43	0.000971	3.25	344.32	3.28

1361	5000	4589.69	4592.66	4593.05	0.001302	5	1000.9	392.15	0.55	0.001269	2.54	393.38	2.55
1362	5000	4589.04	4592.03	4592.4	0.001238	4.89	1022.53	398.18	0.54	0.001243	2.56	399.65	2.57
1363	5000	4588.62	4591.38	4591.73	0.001248	4.73	1127.57	594.6	0.54	0.001119	1.89	595.64	1.9
1364	5000	4587.69	4590.85	4591.15	0.001009	4.44	1566.1	987.94	0.49	0.000954	1.58	989.19	1.59
1365	5000	4587.04	4590.39	4590.65	0.000903	4.09	1221.07	490.56	0.46	0.00065	2.48	491.52	2.49
1366	5000	4586.17	4590.12	4590.34	0.00049	3.72	1351.31	484.2	0.35	0.000597	2.77	487.68	2.79
1367	5000	4585.94	4589.69	4590.04	0.000742	4.75	1051.72	290.06	0.44	0.000508	3.6	292.05	3.63
1368	5000	4584.96	4589.54	4589.76	0.00037	3.83	1305.42	293.24	0.32	0.000562	4.39	297.3	4.45
1369	5000	4586.34	4589.18	4589.49	0.000954	4.49	1114.44	406.43	0.48	0.001057	2.73	407.79	2.74
1370	5000	4585.93	4588.7	4589	0.001176	4.4	1137.17	499.15	0.51	0.000872	2.27	501.59	2.28
1371	5000	4584.09	4588.35	4588.56	0.000672	3.7	1350.23	503.04	0.4	0.000922	2.67	506.55	2.68
1372	5000	4585.3	4587.83	4588.14	0.001342	4.49	1132.56	639.26	0.54	0.001267	1.76	642.46	1.77
1373	5000	4585.1	4587.23	4587.48	0.001198	4.05	1237.42	659.99	0.51	0.001317	1.87	661.32	1.87
1374	5000	4584.67	4586.67	4586.93	0.001455	4.06	1231.36	715.58	0.55	0.001275	1.72	717.79	1.72
1375	5000	4583.45	4586.14	4586.34	0.001127	3.61	1383.8	791.66	0.48	0.001094	1.74	793.72	1.75
1376	5000	4582.87	4585.57	4585.77	0.001063	3.59	1391.35	768.87	0.47	0.000605	1.81	769.99	1.81
1377	5000	4582.01	4585.35	4585.46	0.00039	2.67	1874.77	781.91	0.3	0.000599	2.39	785.93	2.4
1378	5000	4582.76	4584.94	4585.15	0.001038	3.64	1372.27	730.2	0.47	0.000851	1.88	730.87	1.88
1379	5000	4581.82	4584.62	4584.81	0.00071	3.5	1427.75	604.56	0.4	0.000543	2.35	606.88	2.36
1380	5000	4579.59	4584.46	4584.57	0.000429	2.69	1860.54	802.13	0.31	0.000346	2.31	806.09	2.32
1381	5000	4581.22	4584.35	4584.43	0.000285	2.36	3129.01	1509.71	0.26	0.00022	2.07	1513.64	2.07
1382	5000	4580.83	4584.27	4584.31	0.000175	1.86	3815.22	1636.27	0.2	0.000159	2.32	1643.68	2.33
1383	5000	4579.96	4584.19	4584.24	0.000145	1.89	3524.73	1548.7	0.19	0.000214	2.27	1555.13	2.28
1384	5000	4579.42	4584.03	4584.14	0.000346	2.73	1910.63	725.11	0.29	0.000488	2.62	729.34	2.63
1385	5000	4578.83	4583.76	4583.92	0.000739	3.43	2429.97	1681.41	0.4	0.001033	1.44	1686.57	1.45
1386	5000	4579.17	4583.14	4583.41	0.001547	4.62	2269.33	1626.36	0.58	0.001423	1.39	1628.87	1.4

1387	5000	4578.46	4582.5	4582.81	0.001314	4.62	1593.34	1005.32	0.54	0.001288	1.58	1007.64	1.58
1388	5000	4578.18	4581.9	4582.19	0.001263	4.34	1415.21	807.51	0.53	0.001396	1.75	809.29	1.75
1389	5000	4578.14	4581.15	4581.49	0.001551	4.72	1411.19	1014.55	0.58	0.001922	1.39	1016.71	1.39
1390	5000	4577.83	4580.1	4580.54	0.002445	5.31	957.89	584.04	0.71	0.001136	1.64	585.81	1.64
1391	5000	4576.86	4579.74	4579.89	0.000654	3.15	1653.2	811.78	0.38	0.000663	2.03	813.62	2.04
1392	5000	4576.1	4579.45	4579.54	0.000673	2.83	2862.25	1141.48	0.37	0.000506	2.5	1144.78	2.51
1393	5000	4575.35	4579.19	4579.29	0.000395	2.65	2861.83	1135.81	0.3	0.000361	2.5	1144.05	2.52
1394	5000	4572.55	4578.99	4579.11	0.000331	2.79	2005.8	770.12	0.28	0.000188	2.59	774.56	2.6
1395	5000	4574.71	4578.94	4579	0.000121	1.98	3297.59	1004.58	0.18	0.0001	3.27	1009.12	3.28
1396	5000	4574.24	4578.91	4578.95	0.000084	1.8	4454.27	1087.77	0.15	0.000124	4.08	1092.78	4.09
1397	5000	4573.64	4578.76	4578.88	0.0002	2.79	1863.77	462.46	0.24	0.0003	4.02	464.2	4.03
1398	5000	4572.41	4578.43	4578.71	0.000498	4.23	1185.13	304.55	0.37	0.000744	3.85	307.88	3.89
1399	5000	4573.19	4577.76	4578.31	0.001232	6.18	1320.44	620.34	0.57	0.000689	2.11	624.36	2.13
1400	5000	4572.78	4577.61	4577.88	0.000439	4.25	1543.07	532.8	0.35	0.000681	2.87	537.15	2.9
1401	5000	4572.55	4577.06	4577.52	0.001196	5.6	1252.78	755.23	0.55	0.00099	1.65	757.96	1.66
1402	5000	4572.18	4576.59	4577.02	0.000833	5.49	1702.77	1151.21	0.48	0.000698	1.48	1154.37	1.48
1403	5000	4572.04	4576.38	4576.6	0.000594	4.35	3090.34	1331.12	0.4	0.00029	2.32	1334.23	2.32
1404	5000	4570.5	4576.36	4576.41	0.000171	2.37	5932.6	1857.68	0.21	0.000261	3.18	1865.59	3.19
1405	5000	4571.7	4576.02	4576.27	0.000444	4.07	1497.35	657.22	0.35	0.000574	2.27	660.63	2.28
1406	5000	4572.01	4575.73	4575.98	0.000771	4.07	1403.18	635.89	0.43	0.000489	2.19	640.58	2.21
1407	5000	4571.24	4575.56	4575.71	0.000337	3.14	1591.14	453.03	0.3	0.000639	3.49	455.45	3.51
1408	5000	4571.96	4574.82	4575.35	0.001645	5.87	853.62	323.23	0.63	0.001958	2.63	324.83	2.64
1409	5000	4570.12	4573.81	4574.43	0.002369	6.3	793.77	342.46	0.73	0.00025	2.3	345.3	2.32
1410	5000	4567.37	4574.11	4574.12	0.000089	1.47	13846.12	4985.72	0.15	0.000274	2.77	4994.17	2.78
1411	5000	4570.04	4572.95	4573.91	0.004589	7.86	635.85	323.72	0.99	0.000293	1.95	325.58	1.96
1412	5000	4569.6	4573.1	4573.1	0.000096	1.34	13539.34	5076.82	0.15	0.000184	2.67	5080.1	2.67

1413	5000	4567.52	4572.79	4573.01	0.000488	3.7	1364.52	433.51	0.35	0.000725	3.12	437.4	3.15
1414	5000	4566.88	4572.39	4572.64	0.001186	4.03	1240.68	630.77	0.5	0.001803	1.95	635.73	1.97
1416	5000	4568.17	4571.2	4571.73	0.003066	5.87	935.73	639.96	0.79	0.000554	1.46	641.34	1.46
1417	5000	4566.05	4571.23	4571.31	0.000223	2.39	2092.63	656.03	0.24	0.000334	3.16	662.79	3.19
1418	5000	4567.86	4570.98	4571.15	0.000552	3.24	1585.9	724.17	0.36	0.000402	2.19	725.75	2.19
1419	5000	4566.42	4570.82	4570.92	0.000306	2.48	2013.19	759.23	0.27	0.000434	2.64	761.7	2.65
1420	5000	4564.18	4570.53	4570.69	0.000662	3.23	1547.72	719.36	0.38	0.000544	2.13	727.35	2.15
1421	5000	4566.49	4570.29	4570.41	0.000455	2.72	1928.82	912.62	0.32	0.001089	2.11	915.75	2.11
1422	5000	4566.88	4569.17	4569.81	0.005325	6.42	779.26	603.38	0.99	0.002038	1.29	605.25	1.29
1423	5000	4565.86	4568	4568.18	0.001068	3.4	1537.96	986.56	0.47	0.000498	1.56	987.64	1.56
1424	5000	4564.22	4567.79	4567.88	0.000287	2.45	2480.79	1141.19	0.26	0.000452	2.17	1145.25	2.17
1425	5000	4564.74	4567.46	4567.63	0.000812	3.28	1531.04	800.77	0.42	0.000659	1.91	803.45	1.91
1426	5000	4564.46	4567.16	4567.29	0.000545	2.9	1793.71	996.44	0.35	0.000486	1.8	998.11	1.8
1427	5000	4564.17	4566.95	4567.05	0.000435	2.59	1933.71	896.05	0.31	0.000453	2.15	897.56	2.16
1428	5000	4561.6	4566.68	4566.82	0.000472	2.94	1778.57	801.8	0.33	0.000748	2.21	806.32	2.22
1429	5000	4563.71	4566.16	4566.42	0.001362	4.22	1808.11	1478.67	0.54	0.000859	1.22	1480.98	1.22
1430	5000	4563.28	4565.81	4565.94	0.00059	3.19	2775.66	1719.41	0.37	0.000799	1.61	1720.18	1.61
1431	5000	4562.94	4565.29	4565.52	0.001143	3.85	1593.01	1700.26	0.49	0.000986	0.94	1702.27	0.94
1432	5000	4562.68	4564.83	4564.98	0.00086	3.48	3050.47	1982.71	0.43	0.000807	1.54	1985.39	1.54
1433	5000	4561.88	4564.37	4564.55	0.000759	3.45	2305.25	2147.16	0.41	0.000519	1.07	2148.06	1.07
1434	5000	4561.19	4564.15	4564.26	0.000378	2.91	3721.7	1988.14	0.3	0.000495	1.87	1989.54	1.87
1435	5000	4560.91	4563.79	4564	0.000678	3.69	1400.49	639.27	0.4	0.001192	2.19	640.41	2.19
1436	5000	4560.62	4562.88	4563.35	0.002627	5.54	903.31	514.58	0.74	0.001529	1.75	515.5	1.76
1437	5000	4558.97	4562.2	4562.46	0.000999	4.07	1227.28	535.2	0.47	0.001221	2.28	537.11	2.29
1438	5000	4559.53	4561.6	4561.83	0.001527	4	1827.67	1362.43	0.55	0.000867	1.34	1363.2	1.34
1439	5000	4558.63	4561.21	4561.34	0.000558	3	2403.07	1433.1	0.35	0.000915	1.67	1434.83	1.68

1440	5000	4558.1	4560.56	4560.87	0.00177	4.44	1126.87	663.85	0.6	0.001681	1.69	666.28	1.7
1441	5000	4557.05	4559.74	4560.04	0.001598	4.4	1140.25	696.04	0.58	0.000456	1.63	697.62	1.64
1442	5000	4554.83	4559.66	4559.75	0.000212	2.38	2109.06	691.54	0.23	0.000466	3	702.13	3.05
1443	5000	4555.4	4559.17	4559.5	0.001724	4.62	1082.27	586.58	0.6	0.00079	1.83	590.57	1.85
1444	5000	4555.95	4558.96	4559.06	0.000451	2.69	3586.72	2249.19	0.32	0.00056	1.59	2256.3	1.59
1445	5000	4556.29	4558.63	4558.77	0.000714	3.02	1658.36	883.66	0.39	0.00073	1.87	885.81	1.88
1446	5000	4555.96	4558.3	4558.42	0.000747	2.82	1770.27	1076.84	0.39	0.000697	1.64	1079.54	1.64
1447	5000	4555.61	4557.95	4558.08	0.000651	2.84	1763	961.77	0.37	0.00064	1.83	963.88	1.83
1448	5000	4554.85	4557.63	4557.77	0.00063	2.96	1711.05	977.44	0.37	0.00075	1.75	979.12	1.75
1449	5000	4554.9	4557.22	4557.41	0.000909	3.55	1497.13	994.83	0.44	0.001225	1.5	997.67	1.5
1450	5000	4553.02	4556.57	4556.81	0.001741	3.91	1301.31	997.18	0.58	0.001466	1.3	1004.71	1.3
1451	5000	4553.64	4555.92	4556.1	0.001251	3.41	1467.79	992.25	0.49	0.000767	1.48	994.21	1.48
1452	5000	4552.91	4555.52	4555.6	0.000518	2.32	2158.87	1344.46	0.32	0.000404	1.6	1347.16	1.61
1453	5000	4552.47	4555.39	4555.45	0.000323	1.9	2636.37	1553.51	0.26	0.000376	1.69	1558.55	1.7
1454	5000	4552.04	4555.2	4555.26	0.000444	2.08	2424.15	1651.59	0.3	0.000394	1.46	1661.55	1.47
1455	5000	4552.65	4555	4555.08	0.000353	2.13	2363.5	1332.44	0.27	0.000402	1.77	1333.98	1.77
1456	5000	4548.67	4554.72	4554.87	0.000463	3.13	1598.83	575.06	0.33	0.000768	2.74	583.98	2.78
1457	5000	4551.97	4554.13	4554.48	0.001518	4.72	1059.66	512.63	0.58	0.000549	2.07	513.12	2.07
1458	5000	4550.38	4554.04	4554.16	0.000281	2.78	1817.04	605.48	0.27	0.000342	2.99	608.72	3
1459	5000	4550.64	4553.86	4554.01	0.000427	3.09	1667.36	657.73	0.32	0.000406	2.52	660.8	2.54
1460	5000	4550.03	4553.67	4553.8	0.000387	2.92	1746.2	669.19	0.31	0.000072	2.6	672.04	2.61
1461	5000	4548.8	4553.72	4553.73	0.000029	1.11	17201	5689.29	0.09	0.000032	3.02	5693.03	3.02
1462	5000	4545.56	4553.71	4553.71	0.000036	1.12	17719.79	5785.57	0.1	0.000032	3.06	5791.14	3.06
1463	5000	4548.44	4553.69	4553.7	0.000028	1.07	18575.22	5025.32	0.09	0.000075	3.69	5029.68	3.7
1464	5000	4547.91	4553.47	4553.64	0.000521	3.33	1502.27	543.21	0.35	0.000719	2.75	546.42	2.77
1465	5000	4547.95	4552.86	4553.25	0.001056	5.13	1273.98	512.08	0.51	0.001173	2.48	514.43	2.49

1466	5000	4546.82	4552.14	4552.67	0.001312	6	1146.06	510.95	0.58	0.000176	2.23	513.8	2.24
1467	5000	4545.99	4552.41	4552.43	0.000066	1.7	15322.64	5309.26	0.14	0.00018	2.88	5313.92	2.89
1468	5000	4546.31	4551.52	4552.27	0.001484	7.05	955.74	487.23	0.63	0.00174	1.95	489.99	1.96
1469	5000	4546.43	4550.65	4551.38	0.002068	6.93	835.01	425.1	0.71	0.000492	1.96	426.72	1.96
1470	5000	4545.53	4550.87	4550.93	0.000215	3.04	8648.08	4086.25	0.25	0.00023	2.11	4089.7	2.12
1471	5000	4545.15	4550.75	4550.8	0.000247	2.65	7087.71	3110.51	0.25	0.000298	2.28	3114.27	2.28
1472	5000	4544.23	4550.53	4550.64	0.000368	3.42	5047.54	2382.58	0.31	0.000336	2.11	2387.91	2.12
1473	5000	4544.82	4550.32	4550.48	0.000308	3.49	3282.61	2043.24	0.29	0.000336	1.6	2047.7	1.61
1474	5000	4544.69	4550.14	4550.33	0.000367	3.59	2656.29	1761.86	0.31	0.000562	1.5	1765.24	1.51
1475	5000	4544.73	4549.55	4549.97	0.000964	5.27	1235.28	764.11	0.5	0.001371	1.61	767.02	1.62
1476	5000	4544.6	4548.33	4549.1	0.002104	7.16	962.1	645.72	0.72		1.49	647.08	1.49

Appendix D –

Bed Material Grain Size Distributions

Table D.1 Grain size distribution (subreach 1)

(mm)	Bed Material Percent Finer				
	1962	1972	1985	1992	2002
0.0625	5	25	15	14	0
0.125	30	62	38	27	3
0.25	94	96	81	66	21
0.5	100	100	96	90	73
1	100	100	98	95	86
2	100	100	98	96	91
4	100	100	99	97	94
8	100	100	100	97	95
16	100	100	100	98	96
32	100	100	100	98	96
64	100	100	100	100	100

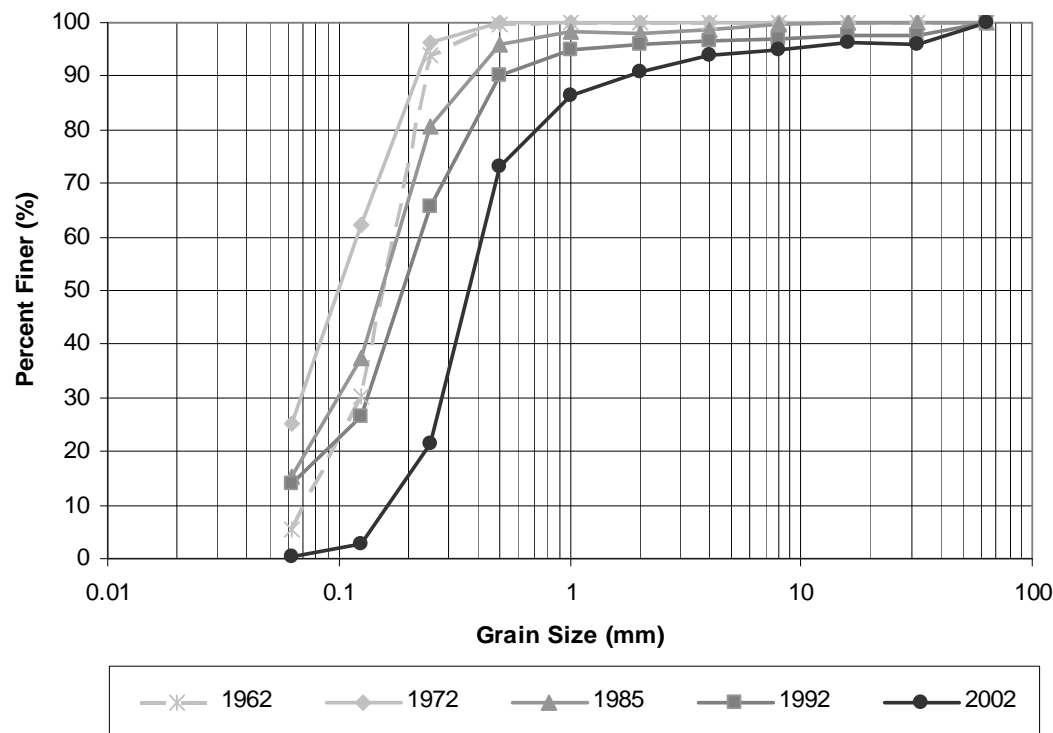


Figure D.1 Bed material grain size distribution (subreach 1)

Table D.2 Grain size distribution (subreach 2)

(mm)	Bed Material Percent Finer				
	1962	1972	1985	1992	2002
0.0625	5	25	25	5	0
0.125	30	62	50	12	1
0.25	94	96	88	49	33
0.5	100	100	98	99	90
1	100	100	99	100	99
2	100	100	99	100	100
4	100	100	99	100	100
8	100	100	100	100	100
16	100	100	100	100	100
32	100	100	100	100	100
64	100	100	100	100	100

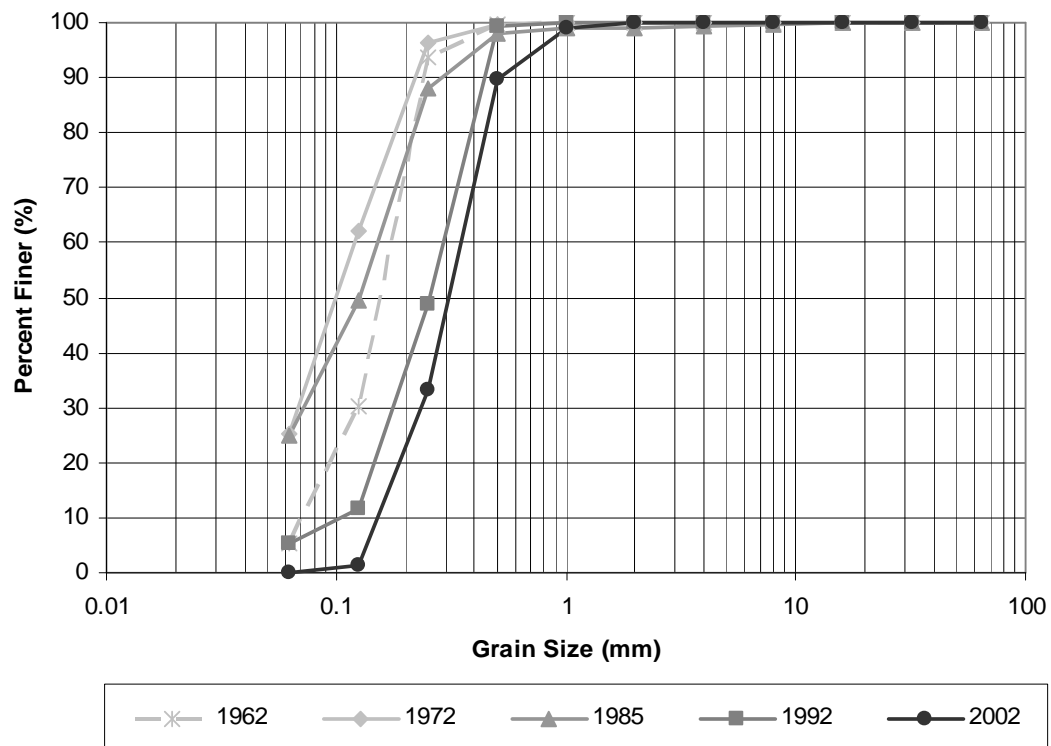


Figure D.2 Bed material grain size distribution (subreach 2)

Table D.3 Grain size distribution (subreach 3)

(mm)	Bed Material Percent Finer				
	1962	1972	1985	1992	2002
0.0625	5	25	35	1	0
0.125	30	62	62	10	5
0.25	94	96	95	54	54
0.5	100	100	100	99	98
1	100	100	100	100	100
2	100	100	100	100	100
4	100	100	100	100	100
8	100	100	100	100	100
16	100	100	100	100	100
32	100	100	100	100	100
64	100	100	100	100	100

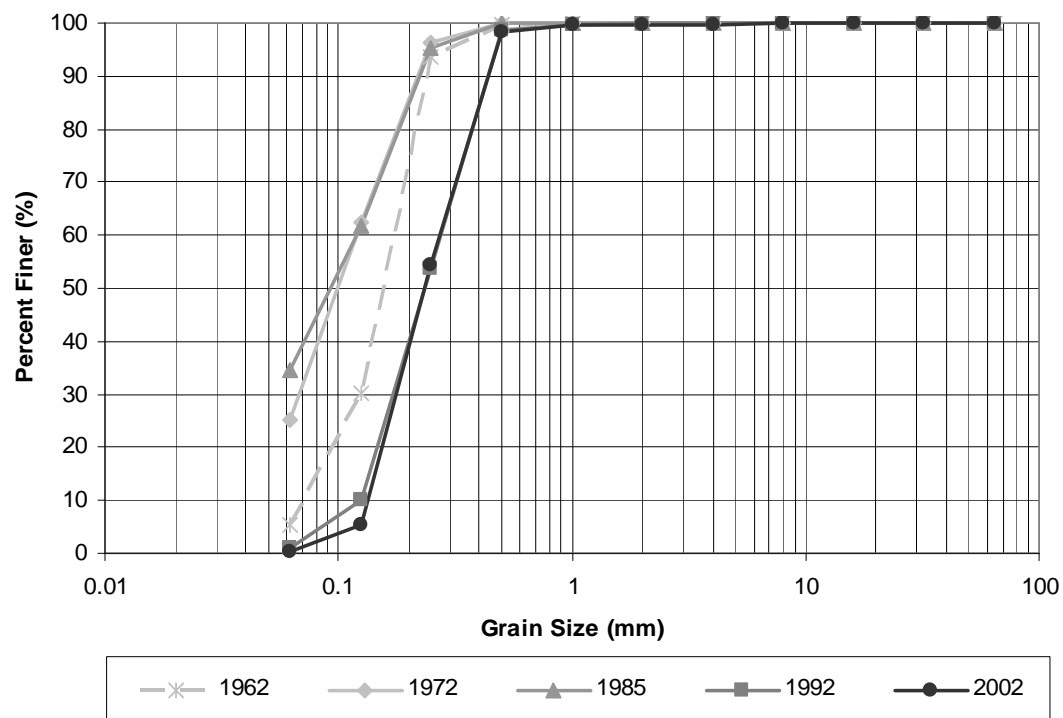


Figure D.3 Bed material grain size distribution (subreach 3)

Table D.4 Grain size distribution (Escondida reach)

(mm)	Bed Material Percent Finer				
	1962	1972	1985	1992	2002
0.0625	5	25	23	4	0
0.125	30	62	47	13	4
0.25	94	96	86	54	45
0.5	100	100	97	98	93
1	100	100	99	99	98
2	100	100	99	99	99
4	100	100	99	100	99
8	100	100	100	100	99
16	100	100	100	100	100
32	100	100	100	100	100
64	100	100	100	100	100

Appendix E –

Example Bedform Field Notes
Example Cross-sections with Bedform Information
Summary of Bedform Observations

U.S.B.R. ALBUQUERQUE PROJECT OFFICE CROSS SECTION FIELD NOTES

Cross Section SD-1437.9 Party WTT, GRS, BAT, RET Page 1 of 3
 Date 6-5-94 Weather Sunny, 80°F Length 702

LEP B&C 4562.57 TLP 4564.94 REP B&C 4562.14 TLP 4563.51
 TOTAL LOAD & PHONES FLO 4-30-94 HI#1 4568.00 HI#2 HI#3

Station	Rod	Depth	Elevation	Notes
0	5.43		4562.57	LEP B&C
0	3.59		4564.41	LEP + TLP
0	5.43		4562.57	GEND TRMS
10	5.45		4562.55	
25	5.69		4562.31	
35	5.26		4562.74	
44	4.95		4563.05	
47	5.13		4562.87	TOP OF BANK
50	6.02	0	4561.98	LEW
57		3.1	4558.9	Trans Ripples / Dunes (USE W.S. 4562.0)
70		0.4	4561.6	Ripples
80		0.3	4561.7	
100		0.4	4561.6	
120		1.6	4560.4	PLANE BED
140		2.4	4559.6	
160		2.8	4559.2	
180		2.7	4559.3	
200		2.5	4559.5	
220		2.4	4559.6	
240		2.8	4559.7	TRANS PLANE BD / ANTI DUNES
260		2.1	4559.9	
280		2.1	4559.9	
300		2.0	4560.0	PLANE BD
320		2.2	4559.8	
				RECD CHKD ENTER FN=

Figure E.1 Field notes for example cross-section (pg.1)

U.S.B.R. ALBUQUERQUE PROJECT OFFICE CROSS SECTION FIELD NOTES

Cross Section SO-1437.9 Party W+F GRS BAP RET Page 2 of 3
 Date 6-5-94 Weather Partly cloudy Length 702

LEP B&C 4562.57 TLP 4564.94
 AVG. WS. F1# 4-30-94 HI#1 4568.00 HI#2 F1# 4-30-94 HI#3 4563.51
E/C +/- =

Station	Rod	Depth	Elevation	Notes
340		92.9	4559.0	TRANS PLANE Bd / DUNES (USE W.S. 4561.9)
360		3.5	4558.4	↓
380		4.0	4557.9	DUNES
400		3.5	4558.4	"
420		3.9	4558.0	SAND DEP BELOW LARGE BAR
430		2.0	4559.9	↓
440		1.6	4560.3	↓
450		0.5	4561.4	↓
460		0.5	4561.4	↓
480		0.7	4561.2	LARGE TRANSIENT BAR
500		0.9	4561.0	" " "
520		0.4	4561.4	" " "
540		0.3	4561.5	" " "
560		0.4	4561.4	USE W.S. 4561.8
580		0.3	4561.5	" " "
600		0.5	4561.3	ripples
610		0.5	4561.3	↓
620		0.7	4561.1	TRANS RIPP/DUNE
640		1.5	4560.3	TRANS DUNES/ PLANE Bd
650		1.3	4560.5	↓
660		1.3	4560.5	↓
662		1.0	4560.8	REW
666	6.21	0	4561.79	TAB
666	5.58		4562.42	RECD CHKD ENTER FN=

Figure E.2 Field notes for example cross-section (pg.2)

Figure E.3 Field notes for example cross-section (pg.3)

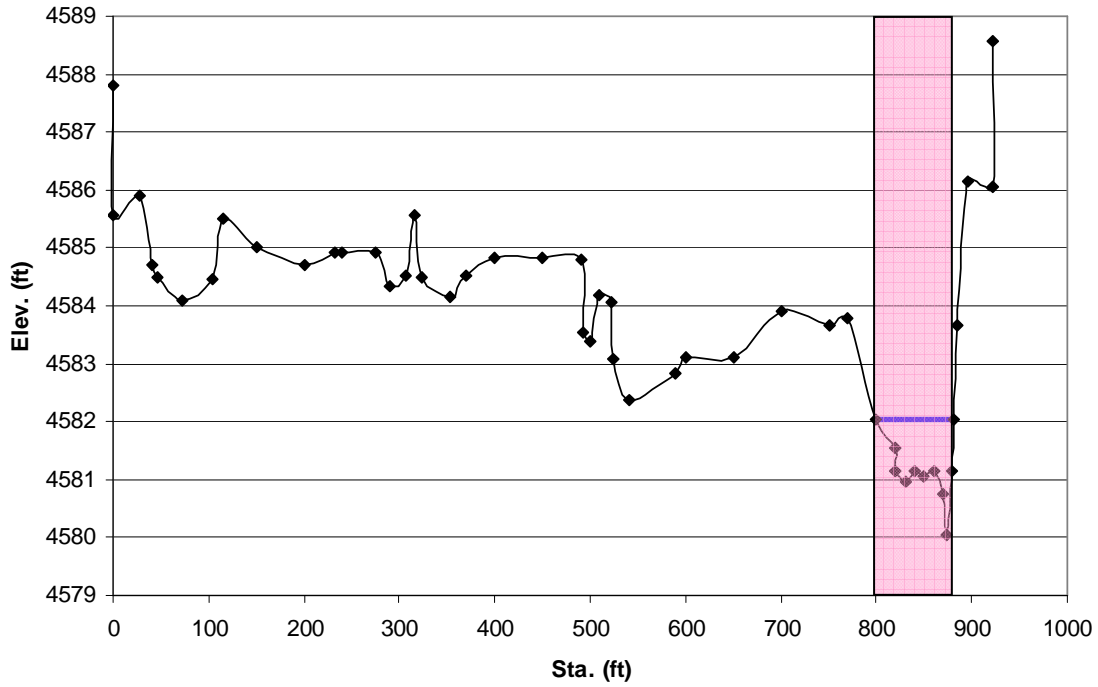
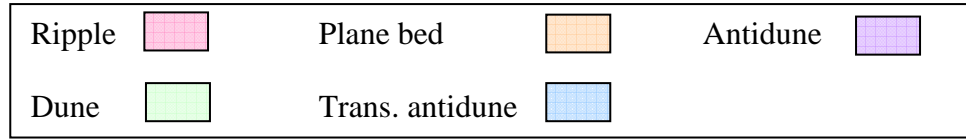


Figure E.4 Cross-section 1380 (surveyed 9/12/1990, $Q = 70 \text{ cfs}$)

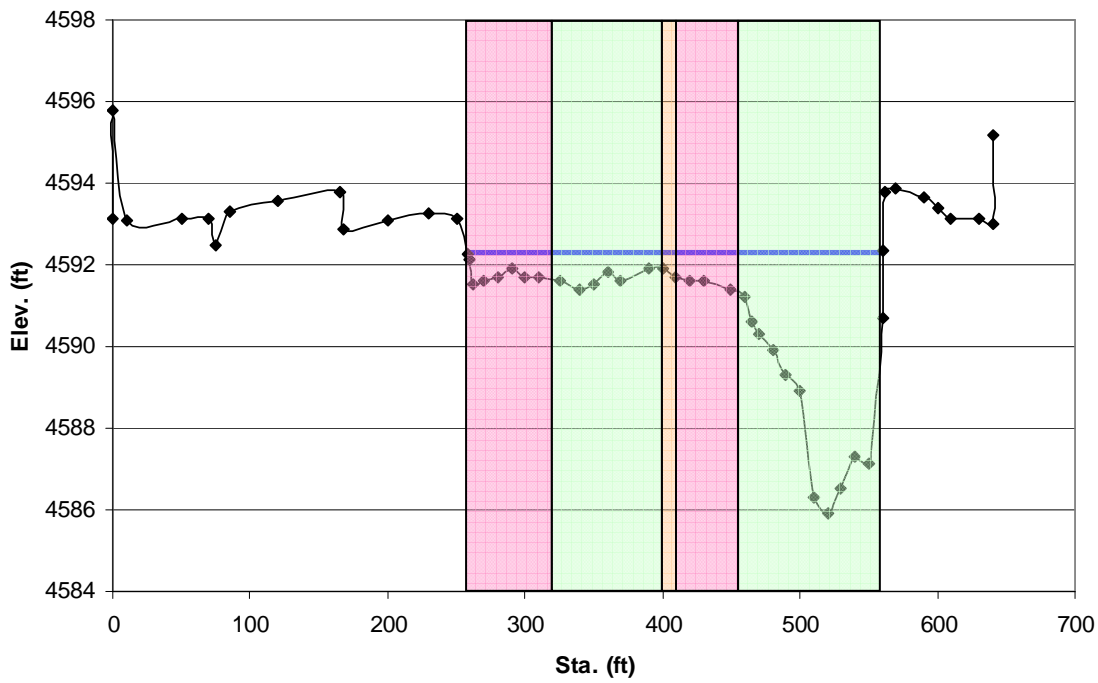


Figure E.5 Cross-section 1360 (surveyed 4/23/1991, $Q = 2300 \text{ cfs}$)

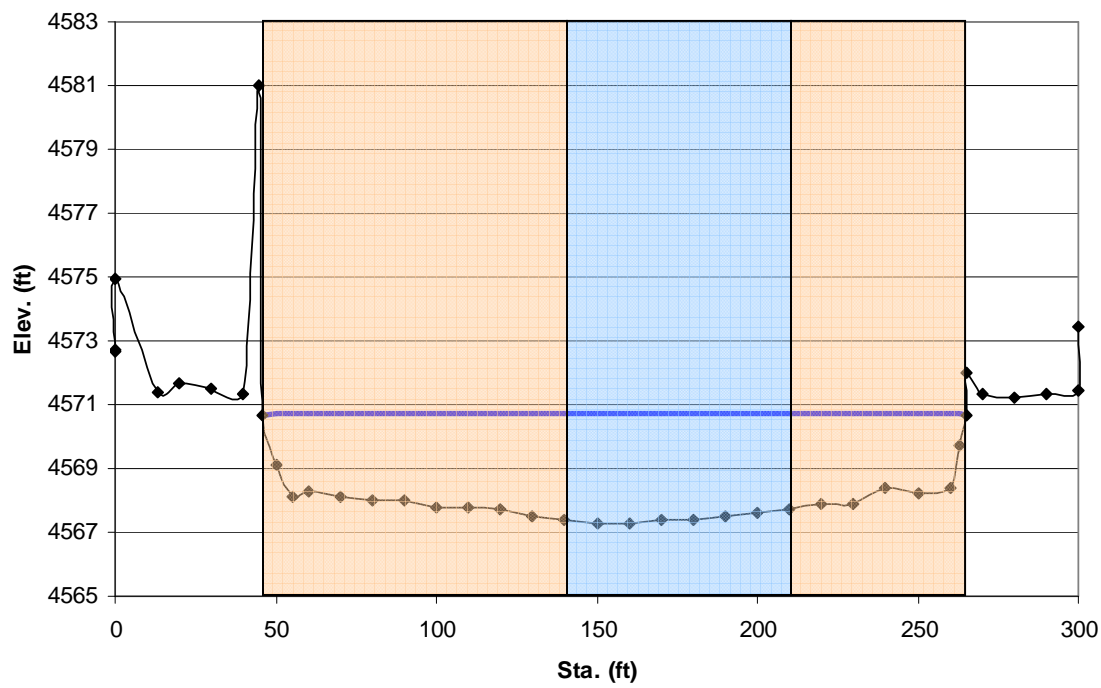


Figure E.6 Cross-section 1414 (surveyed 5/23/1992, $Q = 3800 \text{ cfs}$)

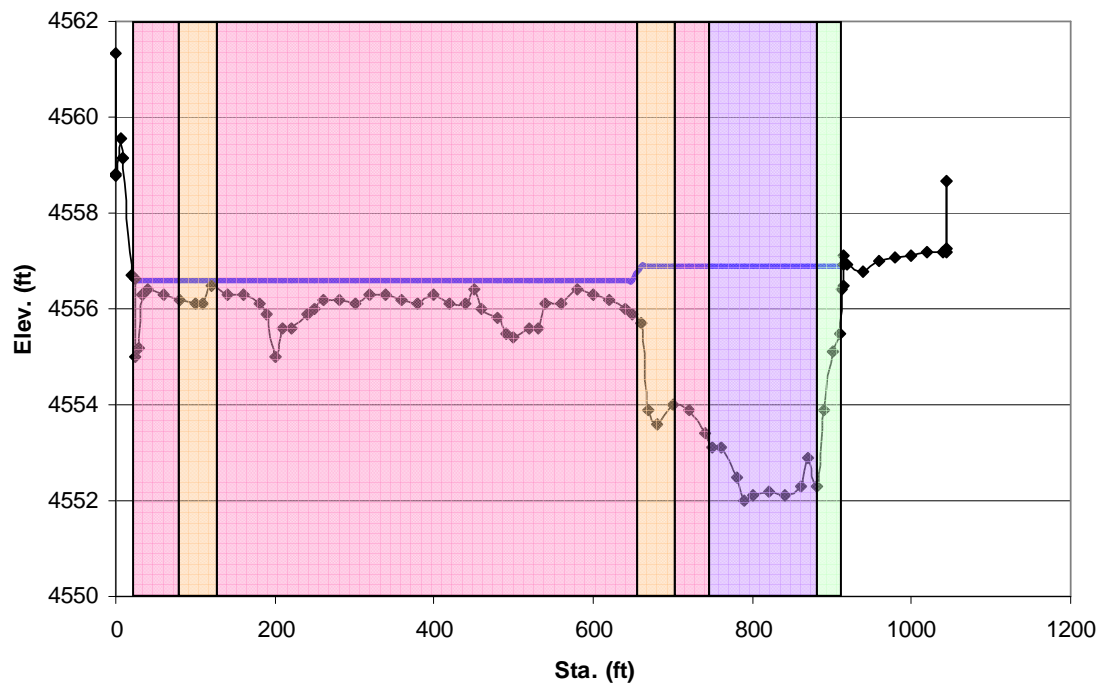


Figure E.7 Cross-section 1450 (surveyed 5/27/1993, $Q = 5000 \text{ cfs}$)

Table E.1 Summary of bedform observations

Date	SO-line	Dominant Bedform	Description	Discharge (cfs)		
				Calculated at cross-section	San Acacia	San Marcial
9/12/1990	1380	R	ripples		92	58
9/12/1990	1394	R	ripples		92	58
9/12/1990	1401	R	ripples		92	58
9/12/1990	1410	R	ripples		92	58
9/13/1990	1414	R	ripples		186	31
9/13/1990	1428	R	ripples		186	31
9/13/1990	1437.9	R	ripples		186	31
9/13/1990	1443	PB-R	flat bed w/ no motion, ripples		186	31
9/13/1990	1450	PB	flat bed w/ motion		186	31
9/14/1990	1456	R-D	dunes, ripples		114	52
9/14/1990	1462	R-D	dunes, ripples, flat bed		114	52
9/14/1990	1470.5	R	ripples		114	52
4/23/1991	1320	D	dunes		2300	1660
4/23/1991	1346	UPB	upper regime plane bed, dunes, ripples		2300	1660
4/23/1991	1360	R-D	ripples, small dunes, flat bed		2300	1660
4/24/1991	1380	D-UPB	flat bed, dunes, ripples, anti-dunes		2430	1820
4/24/1991	1401	UPB	dunes, flat bed		2430	1820
4/25/1991	1437.9	PB-R	dunes, ripples, plane bed w/ motion		2760	1880
4/25/1991	1450	R	dunes, plane bed, ripples		2760	1880
4/26/1991	1470.5	D-UPB	plane bed w/ motion, dunes		2740	2020
6/4/1991	1437.9	PB	ripples, small dunes, flat bed		3460	3030
6/5/1991	1450	UPB-AD	ripples, flat bed, anti-dunes, dunes		3470	3130
6/5/1991	1470.5	PB	flat bed		3470	3130
6/11/1991	1306	PB	plane bed w/ motion, dunes		3560	3100
6/11/1991	1320	PB	plane bed		3560	3100
6/11/1991	1346	R-D	plane bed, ripples, dunes		3560	3100
6/11/1991	1360	PB	plane bed, dunes		3560	3100
6/12/1991	1380	D	plane bed, ripples, dunes		3280	2920
6/12/1991	1401	PB	plane bed w/ motion		3280	2920
2/20/1992	1306	R-D	ripples, dunes		615	375
2/21/1992	1320	R-D	ripples, small dunes		609	357
2/21/1992	1339	R	ripples		609	357

2/21/1992	1346	R-D	ripples, dunes		609	357
2/21/1992	1360	R-D	ripples, dunes		609	357
2/21/1992	1371	R-D	ripples, small dunes		609	357
2/21/1992	1380	PB	ripples, plane bed		609	357
2/21/1992	1394	PB-R	ripples, flat bed		609	357
2/21/1992	1401	PB-R	ripples, flat bed		609	357
2/22/1992	1410	PB-R	ripples, flat bed		668	380
2/22/1992	1414	PB-R	flat bed, ripples, dunes		668	380
2/22/1992	1420	R	ripples		668	380
2/22/1992	1428	R	ripples, flat bed		668	380
2/22/1992	1437.9	R	ripples, flat bed		668	380
2/22/1992	1443	R	small dunes, ripples		668	380
2/22/1992	1450	R	ripples, flat bed		668	380
2/22/1992	1456	PB-R	ripples, flat bed w/o motion, flat bed w/ motion		668	380
2/22/1992	1462	R	small dunes, ripples, flat bed		668	380
2/22/1992	1470.5	PB-R	ripples, flat bed		668	380
4/25/1992	1414	UPB	flat bed		4010	3950
4/26/1992	1437.9	UPB-AD	flat bed, small anti-dunes, ripples		4330	3890
4/27/1992	1414	UPB-AD	flat bed, slight anti-dunes		4340	3960
4/27/1992	1470.5	UPB	flat bed		4340	3960
5/8/1992	1410	UPB	flat bed w/ movement, ripples		5460	5230
5/8/1992	1414	R	ripples		5460	5230
5/8/1992	1420	UPB-AD	dunes, flat bed w/ movement, anti-dunes		5460	5230
5/9/1992	1428	PB-R	ripples, flat bed, dunes		5400	4930
5/9/1992	1437.9	UPB-AD	ripples, flat bed, trans. anti-dunes,dunes		5400	4930
5/10/1992	1443	PB-R	ripples, dunes, flat bed		5380	4760
5/10/1992	1450	R	ripples, flat bed, small anti-dunes, dunes		5380	4760
5/10/1992	1456	R	anti-dunes, flat bed, dunes, ripples		5380	4760
5/10/1992	1462	PB-R	flat bed, ripples		5380	4760
5/10/1992	1470.5	PB	flat bed		5380	4760
5/11/1992	1414	UPB	flat bed w/ movement		5500	4700
5/11/1992	1470.5	UPB	flat bed w/ movement, dunes		5500	4700
5/23/1992	1414	UPB-AD	flat bed, slight anti-dunes		3790	3920
5/23/1992	1470.5	UPB-AD	flat bed, slight anti-dunes		3790	3920
5/24/1992	1414	UPB-AD	flat bed, slight anti-dunes		4190	4620
5/24/1992	1437.9	UPB-AD	flat bed, slight anti-dunes, anti-dunes, ripples		4190	4620
5/25/1992	1470.5	UPB-AD	flat bed, slight anti-dunes		3690	5570

3/29/1993	1470.5	PB	plane bed		2750	2600
3/30/1993	1410	PB	plane bed		3200	2880
3/30/1993	1414	PB	plane bed		3200	2880
3/30/1993	1420	PB	plane bed, ripples		3200	2880
3/30/1993	1428	PB	plane bed, ripples, dunes		3200	2880
3/31/1993	1437.9	R	dunes, plane bed, ripples		3090	3880
3/31/1993	1443	PB-D	ripples, trans. dunes, plane bed		3090	3880
3/31/1993	1450	PB-R	ripples, dunes, plane bed		3090	3880
3/31/1993	1456	PB	ripples, plane bed		3090	3880
3/31/1993	1462	PB	plane bed, ripples		3090	3880
4/2/1993	1414	PB	plane bed		2400	2790
4/2/1993	1470.5	PB	plane bed		2400	2790
4/20/1993	1414	PB	ripples, plane bed		3250	3570
4/22/1993	1437.9	PB-R	plane bed, ripples		3030	2950
4/23/1993	1470.5	PB	plane bed		3060	2520
4/24/1993	1470.5	PB	plane bed, small anti- dunes		3060	2230
4/25/1993	1414	PB-R	ripples, plane bed		3290	2020
5/26/1993	1410	PB	plane bed		5200	4820
5/26/1993	1414	PB	plane bed		5200	4820
5/26/1993	1420	PB	plane bed		5200	4820
5/26/1993	1428	PB-R	ripples, plane bed		5200	4820
5/26/1993	1443	UPB-AD	plane bed, small anti- dunes		5200	4820
5/27/1993	1437.9	D-AD	small dunes, ripples, plane bed, anti-dunes		5340	4980
5/27/1993	1450	AD	ripples, plane bed, small anti-dunes, dunes		5340	4980
5/27/1993	1456	PB	ripples, dunes, plane bed		5340	4980
5/27/1993	1462	D	dunes, plane bed, ripples		5340	4980
5/28/1993	1414	PB	plane bed		5240	4900
5/28/1993	1470.5	PB	plane bed		5240	4900
6/11/1993	1414	PB	plane bed		5790	5290
6/11/1993	1470.5	PB	plane bed		5790	5290
6/12/1993	1437.9	PB-R	plane bed, ripples, small dunes		5510	5440
6/16/1993	1414	PB	ripples, plane bed		3590	2030
6/16/1993	1470.5	PB	plane bed		3590	2030
6/18/1993	1414	PB	plane bed		4030	2080
6/18/1993	1470.5	PB	plane bed		4030	2080
6/21/1993	1410	UPB-AD	ripples, plane bed, small anti-dunes		4350	4040
6/21/1993	1420	PB	plane bed, small anti- dunes		4350	4040

6/22/1993	1462	PB	plane bed		4590	4730
6/24/1993	1428	PB	ripples, plane bed, dunes		3350	4560
6/24/1993	1437.9	PB-R	ripples, plane bed, dunes		3350	4560
6/24/1993	1443	PB-D	ripples, plane bed, dunes		3350	4560
6/24/1993	1450	PB-D	ripples, plane bed, dunes		3350	4560
6/24/1993	1456	PB	ripples, plane bed, dunes		3350	4560
6/25/1993	1414	PB-D	plane bed, dunes		3110	3080
6/25/1993	1470.5	UPB-AD	plane bed, trans. anti-dunes		3110	3080
4/29/1994	1410	PB	plane bed		4240	3680
4/29/1994	1414	PB	plane bed		4240	3680
4/30/1994	1420	PB	plane bed, dunes		3080	3350
4/30/1994	1428	R	ripples, plane bed, small dunes		3080	3350
4/30/1994	1437.9	PB-R	ripples, plane bed, small dunes		3080	3350
4/30/1994	1443	PB	ripples, plane bed, small dunes		3080	3350
4/30/1994	1450	PB-R	ripples, plane bed, small dunes		3080	3350
4/30/1994	1456	D	ripples, dunes		3080	3350
4/30/1994	1462	PB-R	plane bed, ripples		3080	3350
5/1/1994	1470.5	PB	plane bed		2960	2920
5/4/1994	1414	D	ripples, plane bed, small dunes		2710	2250
5/4/1994	1470.5	PB	ripples, plane bed		2710	2250
5/19/1994	1414	PB	ripples, plane bed		5120	4150
5/19/1994	1437.9	PB-R	small dunes, plane bed, ripples		5120	4150
5/20/1994	1414	PB	plane bed, ripples		5150	4190
5/20/1994	1470.5	PB	plane bed		5150	4190
5/20/1994	1470.5	PB	plane bed		5150	4190
5/21/1994	1410	PB	plane bed, dunes		5010	4230
5/21/1994	1414	PB	plane bed		5010	4230
5/21/1994	1420	PB	plane bed		5010	4230
5/21/1994	1428	PB	plane bed, dunes, ripples		5010	4230
5/21/1994	1437.9	R-D	plane bed, dunes, ripples		5010	4230
5/21/1994	1462	R	plane bed, ripples, anti-dunes		5010	4230
5/22/1994	1414	PB	plane bed		4740	4120
5/22/1994	1443	R-D	ripples, plane bed, dunes		4740	4120
5/22/1994	1450	R-D	plane bed, dunes, ripples		4740	4120
5/22/1994	1456	R	plane bed, ripples, dunes		4740	4120
5/22/1994	1470.5	PB	plane bed		4740	4120
5/22/1994	1470.5	PB	plane bed		4740	4120

6/5/1994	1410	PB	plane bed		4810	3990
6/5/1994	1414	PB	plane bed		4810	3990
6/5/1994	1420	PB	plane bed, dunes, ripples		4810	3990
6/5/1994	1428	PB-R	ripples, plane bed		4810	3990
6/5/1994	1437.9	R-D	ripples, plane bed, trans. anti-dunes, dunes		4810	3990
6/6/1994	1443	PB	plane bed, ripples, dunes		3200	3760
6/6/1994	1450	R	ripples, dunes, plane bed		3200	3760
6/6/1994	1456	R-D	ripples, dunes, plane bed		3200	3760
6/6/1994	1462	PB	ripples, plane bed		3200	3760
6/6/1994	1470.5	PB	plane bed		3200	3760
6/10/1994	1414	PB	plane bed		4270	3590
6/10/1994	1470.5	PB	plane bed		4270	3590
4/14/1995	1312	D	ripples, dunes		1930	1370
4/14/1995	1314	D	ripples, plane bed, dunes		1930	1370
4/14/1995	1316	D	ripples, plane bed, dunes		1930	1370
4/19/1995	1306	PB	ripples, plane bed, dunes		2450	2040
4/19/1995	1308	PB-D	ripples, plane bed, dunes		2450	2040
4/19/1995	1310	PB-R	ripples, plane bed, trans. dunes		2450	2040
4/19/1995	1311	PB	ripples, plane bed, dunes		2450	2040
4/19/1995	1312	PB	plane bed		2450	2040
4/19/1995	1320	PB	plane bed		2450	2040
5/12/1995	1410	PB-D	plane bed, trans. dunes		3100	2940
5/12/1995	1414	PB	plane bed, trans. dunes		3100	2940
5/12/1995	1420	R-D	plane bed, dunes, ripples		3100	2940
5/12/1995	1428	D-AD	plane bed, trans. anti-dunes, ripples, trans. dunes		3100	2940
5/12/1995	1437.9	PB-R	plane bed, dunes, ripples		3100	2940
5/13/1995	1443	R-D	ripples, plane bed, dunes		3340	2830
5/13/1995	1450	PB-R	ripples, plane bed, dunes, trans. anti-dunes		3340	2830
5/13/1995	1456	PB-R	plane bed, ripples, trans. anti-dunes		3340	2830
5/13/1995	1462	PB-R	plane bed, ripples		3340	2830
5/13/1995	1470.5	PB	plane bed		3340	2830
5/13/1995	1470.5	R-D	ripples, small dunes		3340	2830
5/15/1995	1414	PB	plane bed		3580	3140
5/15/1995	1470.5	PB	plane bed	3240 cfs	3580	3140
5/22/1995	1414	PB	plane bed		4790	4050
5/22/1995	1437.9	UPB-AD	plane bed, trans. anti-dunes, ripples		4790	4050
5/23/1995	1470.5	PB	plane bed		5280	4220

5/27/1995	1414	PB	plane bed		5900	4590
5/27/1995	1470.5	PB	plane bed		5900	4590
5/30/1995	1410	PB	plane bed, dunes		4410	4580
5/30/1995	1414	PB	plane bed, dunes		4410	4580
5/30/1995	1437.9	PB-R	plane bed, dunes, ripples		4410	4580
5/30/1995	1443	R	dunes, ripples		4410	4580
5/30/1995	1450	R-D	ripples, dunes, plane bed		4410	4580
5/30/1995	1456	PB-D	ripples, dunes, plane bed		4410	4580
5/30/1995	1462	PB	plane bed, ripples		4410	4580
5/30/1995	1470.5	PB	plane bed		4410	4580
6/1/1995	1414	PB	plane bed, dunes		4920	4190
6/1/1995	1437.9	PB-R	plane bed, dunes, ripples	4588 cfs	4920	4190
6/1/1995	1443	R	plane bed, ripples		4920	4190
6/1/1995	1450	PB-R	ripples, dunes, plane bed		4920	4190
6/1/1995	1470.5	PB	plane bed	4279 cfs	4920	4190
6/15/1995	1414	PB	plane bed	4100 cfs	4530	3880
6/15/1995	1437.9	D	plane bed, dunes, ripples	3920 cfs	4530	3880
6/15/1995	1470.5	PB	plane bed	3861 cfs	4530	3880
6/20/1995	1414	PB-D	plane bed, trans. dunes	4342 cfs	4760	4030
6/20/1995	1470.5	PB	plane bed	4200 cfs	4760	4030
6/28/1995	1410	PB	plane bed		4590	4090
6/28/1995	1414	PB	plane bed		4590	4090
6/28/1995	1420	PB-D	plane bed, dunes, ripples		4590	4090
6/28/1995	1428	PB	ripples, plane bed		4590	4090
6/28/1995	1437.9	PB	plane bed, trans. anti-dunes, ripples		4590	4090
6/29/1995	1443	PB-D	ripples, plane bed, dune, trans. anti-dunes		4580	4010
6/29/1995	1450	PB-R	plane bed, ripples, dunes		4580	4010
6/29/1995	1456	PB	plane bed, dunes		4580	4010
6/29/1995	1462	R-D	dunes, ripples, plane bed, anti-dunes		4580	4010
6/29/1995	1470.5	PB	plane bed	3999.09 cfs	4580	4010
7/1/1995	1414	PB	plane bed, dunes, ripples	4490 cfs	5350	4290
7/1/1995	1470.5	PB	plane bed	4469.56 cfs	5350	4290
9/12/1990	1380	R	ripples		92	58

Appendix F –

**BORAMEP Input
BORAMEP Output**

Table F.1 BORAMEP Input – general information

Input Variables	Title	Date	Time	S_energy	g (ft/s2)	γw (lb/ft3)	γs (lb/ft3)	Q (cfs)	Vavg (ft/s)	h (ft)	W (ft)	T (F)	dn (ft)	Cs (ppm)	d65 (mm)	d35 (mm)	ds (ft)
###	5/2/1990	5/2/1990	1430	0.00011	32.17	62.4	165	648	2.08	1.8	197	49.1	0.3	636	0.21	0.15	4.8
###	6/9/1990	6/9/1990	1430	0.00011	32.17	62.4	165	18	1.1	0.46	60	78.8	0.3	1678	0.48	0.33	4.8
###	5/22/1991	5/22/1991	1430	0.00011	32.17	62.4	165	4530	4.97	5.4	160	62.6	0.3	2107	0.21	0.09	4.8
###	6/17/1991	6/17/1991	1430	0.00011	32.17	62.4	165	4070	5.1	5.1	160	73.4	0.3	3701	0.16	0.08	4.8
###	5/7/1992	5/7/1992	1430	0.00011	32.17	62.4	165	5560	4.39	6.3	203	64.4	0.3	2486	2.83	0.13	4.8
###	5/21/1992	5/21/1992	1430	0.00011	32.17	62.4	165	3230	4.07	5.1	155	68	0.3	1209	0.06	0.01	4.8
###	6/4/1992	6/4/1992	1430	0.00011	32.17	62.4	165	3940	4.78	5.2	161	64.4	0.3	603	0.10	0.04	4.8
###	6/18/1992	6/18/1992	1430	0.00011	32.17	62.4	165	2030	2.69	4.9	155	71.6	0.3	219	0.34	0.21	4.8
###	5/17/1994	5/17/1994	1430	0.00011	32.17	62.4	165	5440	5.12	6.3	170	60.8	0.3	1298	0.37	0.24	4.8
###	6/22/1994	6/22/1994	1430	0.00011	32.17	62.4	165	4490	5.07	5.3	167	77	0.3	866	0.35	0.21	4.8
###	5/16/1995	5/16/1995	1430	0.00011	32.17	62.4	165	3370	3.86	5.3	165	65.84	0.3	950	0.23	0.17	4.8
###	6/8/1995	6/8/1995	1430	0.00011	32.17	62.4	165	4390	4.63	5.7	165	63.5	0.3	1848	0.47	0.24	4.8
###	6/19/1996	6/19/1996	1430	0.00011	32.17	62.4	165	5010	2.23	1.4	74	73.94	0.3	213	0.43	0.28	4.8
###	5/20/1997	5/20/1997	1430	0.00011	32.17	62.4	165	4250	4.59	5.7	162	62.6	0.3	7376	16.00	0.63	4.8
###	6/24/1997	6/24/1997	1430	0.00011	32.17	62.4	165	978	2.85	3	114	71.06	0.3	1788	0.35	0.22	4.8
###	5/18/1998	5/18/1998	1430	0.00011	32.17	62.4	165	2510	4.49	4.8	160	60.8	0.3	1259	2.00	0.17	4.8
###	4/7/1999	4/7/1999	1430	0.00011	32.17	62.4	165	418	2.1	2	106	51.8	0.3	100	0.64	0.39	4.8
###	5/21/1999	5/21/1999	1430	0.00011	32.17	62.4	165	2220	2.65	5.2	162	69.8	0.3	787	1.57	0.55	4.8
###	4/7/2000	4/7/2000	1430	0.00011	32.17	62.4	165	375	2.14	2	104	65	0.3	1638	0.84	0.49	4.8
###	5/3/2000	5/3/2000	1430	0.00011	32.17	62.4	165	321	1.92	1.7	109	77	0.3	83	0.85	0.41	4.8
###	4/21/2001	4/21/2001	1430	0.00011	32.17	62.4	165	664	2.27	1.9	162	59.9	0.3	217	0.71	0.40	4.8
###	5/22/2001	5/22/2001	1430	0.00011	32.17	62.4	165	1340	2.41	3.6	164	72.5	0.3	673	1.17	0.41	4.8
###	6/20/2001	6/20/2001	1430	0.00011	32.17	62.4	165	274	1.78	1.8	92	51.44	0.3	98	0.76	0.38	4.8
###	5/7/2002	5/7/2002	1430	0.00011	32.17	62.4	165	210	1.64	1.1	122	68	0.3	84.3	0.27	0.03	4.8
###	4/3/2003	4/3/2003	1430	0.00011	32.17	62.4	165	199	1.6	1	142	59.9	0.3	289	0.02	0.01	4.8
###	5/12/2003	5/12/2003	1430	0.00011	32.17	62.4	165	193	1.58	0.99	137	73.4	0.3	260	0.39	0.27	4.8
###	6/6/2003	6/6/2003	1430	0.00011	32.17	62.4	165	254	1.7	1.3	107	64.4	0.3	573	0.47	0.33	4.8
###	4/15/2004	4/15/2004	1430	0.00011	32.17	62.4	165	1960	4.72	2.5	162	62.6	0.3	4756	0.40	0.28	4.8
###	5/24/2004	5/24/2004	1430	0.00011	32.17	62.4	165	1560	2.56	4	158	68	0.3	1139	0.78	0.43	4.8

Table F.2 BORAMEP Input – suspended sediment percent in range

Title	0.001 0.002 mm	0.002 0.004 mm	0.004 0.016 mm	0.016 0.0625 mm	0.0625 0.125 mm	0.125 0.25 mm	0.25 0.5 mm	0.5 1 mm	1 2 mm	2 4 mm	4 8 mm	8 16 mm	16 32 mm	32 64 mm	64 128 mm	128 256 mm
5/2/1990	0	0	0	40	22	34	4	0	0	0	0	0	0	0	0	0
6/9/1990	0	0	0	36	3	30	31	0	0	0	0	0	0	0	0	0
5/22/1991	0	27	7	25	29	12	0	0	0	0	0	0	0	0	0	0
6/17/1991	0	76	12	11	1	0	0	0	0	0	0	0	0	0	0	0
5/7/1992	26	2	7	27	25	13	0	0	0	0	0	0	0	0	0	0
5/21/1992	40	6	18	18	11	7	0	0	0	0	0	0	0	0	0	0
6/4/1992	47	10	12	27	2	2	0	0	0	0	0	0	0	0	0	0
6/18/1992	0	0	0	66	17	16	1	0	0	0	0	0	0	0	0	0
5/17/1994	0	0	0	46	27	25	2	0	0	0	0	0	0	0	0	0
6/22/1994	0	0	0	23	24	48	5	0	0	0	0	0	0	0	0	0
5/16/1995	0	0	0	69	14	17	0	0	0	0	0	0	0	0	0	0
6/8/1995	37	6	9	18	9	19	2	0	0	0	0	0	0	0	0	0
6/19/1996	0	0	0	86	1	10	3	0	0	0	0	0	0	0	0	0
5/20/1997	33	7	16	14	18	11	1	0	0	0	0	0	0	0	0	0
6/24/1997	0	0	0	13	1	23	58	5	0	0	0	0	0	0	0	0
5/18/1998	41	6	8	16	18	10	1	0	0	0	0	0	0	0	0	0
4/7/1999	0	0	0	44	1	30	25	0	0	0	0	0	0	0	0	0
5/21/1999	23	4	10	44	16	2	1	0	0	0	0	0	0	0	0	0
4/7/2000	73	15	6	1	0	1	2	2	0	0	0	0	0	0	0	0
5/3/2000	0	0	0	55	13	18	14	0	0	0	0	0	0	0	0	0
4/21/2001	0	0	0	37	3	27	33	0	0	0	0	0	0	0	0	0
5/22/2001	58	8	9	15	6	3	1	0	0	0	0	0	0	0	0	0
6/20/2001	0	0	0	65	4	24	7	0	0	0	0	0	0	0	0	0
5/7/2002	0	0	0	0	1	18	70	8	1	1	1	0	0	0	0	0
4/3/2003	0	0	0	0	1	8	52	23	8	4	3	1	0	0	0	0
5/12/2003	0	0	0	95	1	3	1	0	0	0	0	0	0	0	0	0
6/6/2003	76	13	6	0	1	2	2	0	0	0	0	0	0	0	0	0
4/15/2004	53	8	7	8	2	16	6	0	0	0	0	0	0	0	0	0
5/24/2004	0	0	0	51	2	9	33	4	1	0	0	0	0	0	0	0

Table F.3 BORAMEP Input – bed material percent in range

Title	0.001 mm	0.002 mm	0.004 mm	0.016 mm	0.0625 mm	0.125 mm	0.25 mm	0.5 mm	1 mm	2 mm	4 mm	8 mm	16 mm	32 mm	64 mm	128 mm	256 mm
5/2/1990	0	0	0	1	13	68	18	0	0	0	0	0	0	0	0	0	0
6/9/1990	0	0	0	0	11	57	18	7	3	3	1	0	0	0	0	0	0
5/22/1991	0	3	0	18	32	35	10	2	0	0	0	0	0	0	0	0	0
6/17/1991	0	3	0	18	32	35	10	2	0	0	0	0	0	0	0	0	0
5/7/1992	0	0	0	35	0	7	10	9	3	2	2	4	1	27	0	0	0
5/21/1992	0	0	0	64	19	16	1	0	0	0	0	0	0	0	0	0	0
6/4/1992	0	0	0	40	40	19	1	0	0	0	0	0	0	0	0	0	0
6/18/1992	0	0	0	0	6	40	42	9	1	0	0	2	0	0	0	0	0
5/17/1994	0	0	0	0	2	36	48	14	0	0	0	0	0	0	0	0	0
6/22/1994	0	0	0	0	2	46	35	5	3	2	3	4	0	0	0	0	0
5/16/1995	0	0	0	4	0	68	26	0	0	0	1	1	0	0	0	0	0
6/8/1995	0	0	0	0	4	32	32	9	6	6	4	7	0	0	0	0	0
6/19/1996	0	0	0	1	1	25	49	5	1	1	3	9	5	0	0	0	0
5/20/1997	0	0	0	0	4	24	6	3	2	4	6	16	35	0	0	0	0
6/24/1997	0	0	0	1	4	37	46	7	0	1	1	3	0	0	0	0	0
5/18/1998	0	0	0	2	13	47	2	0	1	1	3	8	3	20	0	0	0
4/7/1999	0	0	0	0	0	2	51	33	8	4	0	2	0	0	0	0	0
5/21/1999	0	0	0	0	1	5	26	22	17	17	15	11	3	0	0	0	0
4/7/2000	0	0	0	0	0	3	33	39	15	6	3	1	0	0	0	0	0
5/3/2000	0	0	0	0	1	5	40	25	11	7	6	5	0	0	0	0	0
4/21/2001	0	0	0	0	0	6	42	21	6	5	6	8	6	0	0	0	0
5/22/2001	0	0	0	1	3	8	32	19	0	0	0	0	0	0	0	0	0
6/20/2001	0	0	0	0	1	8	42	23	11	6	5	4	0	0	0	0	0
5/7/2002	0	0	0	43	0	17	40	0	0	0	0	0	0	0	0	0	0
4/3/2003	0	0	0	88	1	6	5	0	0	0	0	0	0	0	0	0	0
5/12/2003	0	0	0	0	1	27	59	12	1	0	0	0	0	0	0	0	0
6/6/2003	0	0	0	0	2	7	62	22	5	2	0	0	0	0	0	0	0
4/15/2004	0	0	0	0	2	24	58	13	1	1	0	1	0	0	0	0	0
5/24/2004	0	0	0	0	0	4	40	33	10	6	4	3	0	0	0	0	0

Table F.4 BORAMEP Output

OUTPUT 5/21/1992									
METHOD OF COMPUTATION		MODIFIED EINSTEIN		DATE OF COMPUTATION		1430		TEMPERATURE	
D65 = 0.06 mm	D35 = 0.01 mm	velocity (ft/s) = 4.07 ft/s	width (ft) = 155 ft	Depth (ft) = 5.1 ft				68	SLOPE OF ENERGY GRADIENT 0.00011
dn (ft) = 0.3	Ds (ft) = 4.8								
SIZE FRACTION IN MILLIMETERS	PERCENT OF MATERIAL SUSPENDED BED	IBQB T/D	QPRIME SUBS(T/D)	Z-VALUES COMPUTED FITTED	COMPUTATIONAL FACTORS F(J) F(I)+1	COMPUTED TOTAL LOAD			
0.001 0.002	40 0	-9999 0	4025.749 -9999	0.486 1.308	-9999 1.365	5264.013 824.481			
0.002 0.004	60 0	-9999 0	603.861 -9999	0.534 1.489	-9999 1.499	2697.952 322.201			
0.004 0.016	18 0	-9999 0	1811.387 -9999	0.614 1.743	-9999 2.434	322.325 1786.223			
0.016 0.0625	18 64	147.272 72.337	1811.387 -9999	0.739 0.847	0.77 1.131	84.692 15.799			
0.0625 0.125	11 19	1107.081 704.306	0.847 0.916	0.77 0.916	2.415 2.434	32.566 107.634			
0.125 0.25	7 16	84.345 6.814	704.306 6.814	0.916 0.965	21.178 15.799	21.178 107.634			
0.25 0.5	0 1	-9999 0	-9999 0	-9999 0.965	-9999 15.799	-9999 107.634			
0.5 1	0 0	-9999 0	-9999 0	-9999 1.000	-9999 0	-9999 0			
1 2	0 0	-9999 0	-9999 0	-9999 1.028	-9999 0	-9999 0			
2 4	0 0	-9999 0	-9999 0	-9999 1.054	-9999 0	-9999 0			
4 8	0 0	-9999 0	-9999 0	-9999 1.079	-9999 0	-9999 0			
8 16	0 0	-9999 0	-9999 0	-9999 1.105	-9999 0	-9999 0			
16 32	0 0	-9999 0	-9999 0	-9999 1.131	-9999 0	-9999 0			
32 64	0 0	-9999 0	-9999 0	-9999 1.158	-9999 0	-9999 0			
64 128	0 0	-9999 0	-9999 0	-9999 1.185	-9999 0	-9999 0			
128 256	0 0	-9999 0	-9999 0	-9999 1.213	-9999 0	-9999 0			
TOTAL						16254.848			
6/4/1992, 6/4/1992, -9999, FITTED Z-VALUES GENERATED NEGATIVE EXPONENT, NOT CONTINUING...									
OUTPUT 6/18/1992									
METHOD OF COMPUTATION		MODIFIED EINSTEIN		DATE OF COMPUTATION		1430		TEMPERATURE	
DATE OF SAMPLE	6/18/1992	TIME OF SAMPLE		1430				71.6	SLOPE OF ENERGY GRADIENT 0.00011
D65 = 0.34 mm	D35 = 0.21 mm	velocity (ft/s) = 2.69 ft/s	width (ft) = 155 ft	Depth (ft) = 4.9 ft					
dn (ft) = 0.3	Ds (ft) = 4.8								
SIZE FRACTION IN MILLIMETERS	PERCENT OF MATERIAL SUSPENDED BED	IBQB T/D	QPRIME SUBS(T/D)	Z-VALUES COMPUTED FITTED	COMPUTATIONAL FACTORS F(J) F(I)+1	COMPUTED TOTAL LOAD			
0.001 0.002	0 0	-9999 0	0 -9999	0.007 -9999	-9999 -9999	0 0			
0.002 0.004	0 0	-9999 0	0 -9999	0.014 -9999	-9999 -9999	0 0			
0.004 0.016	0 0	-9999 0	0 -9999	0.043 -9999	-9999 -9999	0 0			
0.016 0.0625	66 0	-9999 0	758.600 -9999	0.183 1.099	-9999 1.099	834.067 248.782			
0.0625 0.125	17 6	1.193 195.397	0.543 0.529	1.343 2.647	248.782 14.909	262.424 486.852			
0.125 0.25	16 40	22.494 183.903	0.906 0.968	1.455 2.647	2.647 14.909	251.258 50.419			
0.25 0.5	1 42	66.805 11.494	1.514 1.455	10.802 2.434	10.802 2.434	3.761 50.419			
0.5 1	0 9	20.718 0	1.907 0	-9999 2.019	-9999 2.019	1.576 1.576			
1 2	0 1	0.780 0	2.364 0	-9999 0	-9999 0	0 0			
2 4	0 0	-9999 0	-9999 0	-9999 2.872	-9999 2.872	0 0			
4 8	0 0	-9999 0	-9999 0	-9999 3.465	-9999 3.465	0 0			
8 16	0 2	0 0	0 0	-9999 4.169	-9999 4.169	0 0			
16 32	0 0	-9999 0	-9999 0	-9999 5.011	-9999 5.011	0 0			
32 64	0 0	-9999 0	-9999 0	-9999 6.022	-9999 6.022	0 0			
64 128	0 0	-9999 0	-9999 0	-9999 7.236	-9999 7.236	0 0			
128 256	0 0	-9999 0	-9999 0	-9999 8.695	-9999 8.695	0 0			
TOTAL						1886.596			
OUTPUT 5/17/1994									
METHOD OF COMPUTATION		MODIFIED EINSTEIN		DATE OF COMPUTATION		7/18/2006		60.8	
DATE OF SAMPLE	5/17/1994	TIME OF SAMPLE		1430				60.8	SLOPE OF ENERGY GRADIENT 0.00011
D65 = 0.37 mm	D35 = 0.24 mm	velocity (ft/s) = 5.12 ft/s	width (ft) = 170 ft	Depth (ft) = 6.3 ft					
dn (ft) = 0.3	Ds (ft) = 4.8								
SIZE FRACTION IN MILLIMETERS	PERCENT OF MATERIAL SUSPENDED BED	IBQB T/D	QPRIME SUBS(T/D)	Z-VALUES COMPUTED FITTED	COMPUTATIONAL FACTORS F(J) F(I)+1	COMPUTED TOTAL LOAD			
0.001 0.002	0 0	-9999 0	0 -9999	0.001 -9999	-9999 -9999	0 0			
0.002 0.004	0 0	-9999 0	-9999 0	0.002 -9999	-9999 -9999	0 0			
0.004 0.016	0 0	-9999 0	-9999 0	0.011 -9999	-9999 -9999	0 0			
0.016 0.0625	46 0	-9999 0	8397.694 -9999	0.074 1.066	-9999 1.066	8953.738 5700.272			
0.0625 0.125	27 2	2.347 4929.082	0.9999 0.306	1.156 1.156	1707.124 1.156	1707.124 5700.272			
0.125 0.25	25 36	118.514 4963.964	0.716 0.706	1.540 1.540	63.631 63.631	63.631 7484.328			
0.25 0.5	25 46	470.716 305.117	0.576 0.576	1.756 1.756	51.516 51.516	51.516 2340.435			
0.5 1	0 14	305.812 0	-9999 1.820	-9999 3.540	-9999 3.540	776.638 776.638			
1 2	0 0	-9999 0	-9999 0	-9999 2.451	-9999 2.451	0 0			
2 4	0 0	-9999 0	-9999 0	-9999 3.182	-9999 3.182	0 0			
4 8	0 0	-9999 0	-9999 0	-9999 4.087	-9999 4.087	0 0			
8 16	0 0	-9999 0	-9999 0	-9999 5.228	-9999 5.228	0 0			
16 32	0 0	-9999 0	-9999 0	-9999 6.680	-9999 6.680	0 0			
32 64	0 0	-9999 0	-9999 0	-9999 8.530	-9999 8.530	0 0			
64 128	0 0	-9999 0	-9999 0	-9999 10.890	-9999 10.890	0 0			
128 256	0 0	-9999 0	-9999 0	-9999 13.903	-9999 13.903	0 0			
TOTAL						25455.410			
OUTPUT 6/22/1994									
METHOD OF COMPUTATION		MODIFIED EINSTEIN		DATE OF COMPUTATION		7/18/2006		77	
DATE OF SAMPLE	6/22/1994	TIME OF SAMPLE		1430				77	SLOPE OF ENERGY GRADIENT 0.00011
D65 = 0.35 mm	D35 = 0.21 mm	velocity (ft/s) = 3.07 ft/s	width (ft) = 167 ft	Depth (ft) = 5.3 ft					
dn (ft) = 0.3	Ds (ft) = 4.8								
SIZE FRACTION IN MILLIMETERS	PERCENT OF MATERIAL SUSPENDED BED	IBQB T/D	QPRIME SUBS(T/D)	Z-VALUES COMPUTED FITTED	COMPUTATIONAL FACTORS F(J) F(I)+1	COMPUTED TOTAL LOAD			
0.001 0.002	0 0	-9999 0	0 -9999	0.002 -9999	-9999 -9999	0 0			
0.002 0.004	0 0	-9999 0	-9999 0	0.004 -9999	-9999 -9999	0 0			
0.004 0.016	0 0	-9999 0	-9999 0	0.036 -9999	-9999 -9999	0 0			
0.016 0.0625	23 0	-9999 0	2312.175 -9999	0.095 1.071	-9999 1.071	2476.947 1042.177			
0.0625 0.125	24 2	2.689 2412.704	0.348 0.350	1.182 1.182	1042.177 2850.951	2850.951 2850.951			
0.125 0.25	48 46	174.923 4825.409	0.740 0.729	1.688 1.688	51.516 51.516	51.516 8143.417			
0.25 0.5	5 35	376.445 502.647	1.179 1.179	4.510 4.510	6.638 6.638	6.638 2498.696			
0.5 1	0 5	107.396 0	-9999 0	1.652 2.149	-9999 2.149	3.028 149.548			
1 2	0 3	67.833 0	-9999 0	2.731 3.442	-9999 3.442	1.856 53.044			
2 4	0 2	28.582 0	-9999 0	3.442 4.046	-9999 4.046	1.856 20.317			
4 8	0 3	12.190 0	-9999 0	4.76 5.420	-9999 5.420	1.514 0.576			
8 16	0 4	3.930 0	-9999 0	5.420 6.814	-9999 6.814	0 0			
16 32	0 0	-9999 0	-9999 0	-9999 8.550	-9999 8.550	-9999 0			
32 64	0 0	-9999 0	-9999 0	-9999 10.728	-9999 10.728	-9999 0			
64 128	0 0	-9999 0	-9999 0	-9999 0	-9999 0	-9999 0			
128 256	0 0	-9999 0	-9999 0	-9999 0	-9999 0	-9999 0			
TOTAL						16518.671			
5/16/1995, 5/16/1995, -9999, NOT ENOUGH OVERLAPPING BINS FOR MEP									

OUTPUT 6/8/1995											
METHOD OF COMPUTATION		MODIFIED EINSTEIN		DATE OF COMPUTATION		1430		TEMPERATURE		63.5 SLOPE OF ENERGY GRADIENT 0.00011	
DATE OF SAMPLE	6/8/1995	TIME OF SAMPLE		D65 =	0.47 mm	D35 =	0.24 mm				
velocity (ft/s) =	4.63	width (ft) =	165	Depth (ft) =							
dn (ft) =	0.3	ds (ft) =	4.8								
SIZE FRACTION IN MILLIMETERS	PERCENT OF MATERIAL SUSPENDED BED	IBQB T/D	QPRIME SUBS(T/D)	Z-VALUES COMPUTED FITTED	COMPUTATIONAL FACTORS F(J) F(I)+1	COMPUTED TOTAL LOAD					
0.001	0.002	37	0	-9999 7760.628 -9999 0.007	1.050 -9999	8150.707					
0.002	0.004	6	0	-9999 1258.48 -9999 0.014	1.052 -9999	1323.482					
0.004	0.016	9	0	-9999 1887.72 -9999 0.038	1.057 -9999	198.149					
0.016	0.0625	18	0	-9999 3702.11 -9999 0.107	1.107 -9999	4104.149					
0.0625	0.125	9	4	3.853 1887.72 0.420 0.407	1.220 671.140	2303.938					
0.125	0.25	19	32	87.181 3985.187 0.673 0.728	1.677 51.747	6684.619					
0.25	0.5	2	32	246.586 419.493 1.135 1.084	3.352 8.931	2202.312					
0.5	1	0	9	159.856 0 -9999 1.408	-9999 4.121	658.744					
1	2	0	6	103.898 0 -9999 1.727	-9999 2.894	300.654					
2	4	0	6	56.915 0 -9999 2.075	-9999 2.367	134.741					
4	8	0	4	8.725 0 -9999 2.793	-9999 2.066	18.024					
8	16	0	7	0.168 0 -9999 2.61	-9999 1.860	0.127					
16	32	0	0	-9999 0 -9999 3.494	-9999 0	0					
32	64	0	0	-9999 0 -9999 4.150	-9999 0	0					
64	128	0	0	-9999 0 -9999 4.927	-9999 0	0					
128	256	0	0	-9999 0 -9999 5.851	-9999 0	0					
TOTAL						27876.904					
OUTPUT 6/19/1996											
METHOD OF COMPUTATION		MODIFIED EINSTEIN		DATE OF COMPUTATION		1430		TEMPERATURE		73.94 SLOPE OF ENERGY GRADIENT 0.00011	
DATE OF SAMPLE	6/19/1996	TIME OF SAMPLE		D65 =	0.43 mm	D35 =	0.28 mm				
velocity (ft/s) =	2.23	width (ft) =	74	Depth (ft) =							
dn (ft) =	0.3	ds (ft) =	4.8								
SIZE FRACTION IN MILLIMETERS	PERCENT OF MATERIAL SUSPENDED BED	IBQB T/D	QPRIME SUBS(T/D)	Z-VALUES COMPUTED FITTED	COMPUTATIONAL FACTORS F(J) F(I)+1	COMPUTED TOTAL LOAD					
0.001	0.002	0	0	-9999 0 -9999 0.001	-9999 -9999	0					
0.002	0.004	0	0	-9999 0 -9999 0.002	-9999 -9999	0					
0.004	0.016	0	0	-9999 0 -9999 0.009	-9999 -9999	0					
0.016	0.0625	86	1	0.008 2372.709 -9999 0.060	1.059 8388.584	2513.052					
0.0625	0.125	1	1	0.039 27.590 0.246 0.236	1.113 850.733	30.717					
0.125	0.25	10	25	27.770 275.896 0.500 0.513	1.183 92.222	336.661					
0.25	0.5	49	151.57	82.769 0.922 0.944	1.860 14.665	244.763					
0.5	1	5	4.317	0 -9999 1.223	-9999 5.277	22.781					
1	2	0	1	0.259 0 -9999 1.614	-9999 3.132	0.811					
2	4	0	1	0.008 0 -9999 2.077	-9999 2.329	0.019					
4	8	0	3	0.000 0 -9999 2.648	-9999 1.919	0.000					
8	16	0	9	0 0 -9999 3.365	-9999 1.662	0					
16	32	0	5	0 0 -9999 4.271	-9999 1.477	0					
32	64	0	0	-9999 0 -9999 5.420	-9999 0	0					
64	128	0	0	-9999 0 -9999 6.877	-9999 0	0					
128	256	0	0	-9999 0 -9999 8.724	-9999 0	0					
TOTAL						3148.503					
OUTPUT 5/20/1997											
METHOD OF COMPUTATION		MODIFIED EINSTEIN		DATE OF COMPUTATION		1430		TEMPERATURE		62.6 SLOPE OF ENERGY GRADIENT 0.00011	
DATE OF SAMPLE	5/20/1997	TIME OF SAMPLE		D65 =	16 mm	D35 =	0.63 mm				
velocity (ft/s) =	4.59	width (ft) =	162	Depth (ft) =							
dn (ft) =	0.3	ds (ft) =	4.8								
SIZE FRACTION IN MILLIMETERS	PERCENT OF MATERIAL SUSPENDED BED	IBQB T/D	QPRIME SUBS(T/D)	Z-VALUES COMPUTED FITTED	COMPUTATIONAL FACTORS F(J) F(I)+1	COMPUTED TOTAL LOAD					
0.001	0.002	33	0	-9999 26998.76 -9999 0.003	1.040 -9999	28078.61					
0.002	0.004	7	0	-9999 5727.011 -9999 0.006	1.041 -9999	5959.037					
0.004	0.016	16	0	-9999 13090.31 -9999 0.019	1.043 -9999	13647.43					
0.016	0.0625	14	0	-9999 11454.02 -9999 0.080	1.054 -9999	12070.86					
0.0625	0.125	18	4	2.846 14726.6 -9999 0.233	1.094 1809.552	16110.14					
0.125	0.25	11	24	48.298 8999.588 0.435 0.435	1.188 222.309	10688.7					
0.25	0.5	1	6	34.532 818.144 0.668 0.668	1.181 34.500	11.803					
0.5	1	0	3	48.298 0 -9999 0.884	-9999 10.020	465.953					
1	2	0	2	0.072 0 -9999 1.001	-9999 4.702	428.260					
2	4	0	4	209.478 0 -9999 1.339	-9999 3.006	629.743					
4	8	0	6	180.511 0 -9999 1.616	-9999 2.304	415.953					
8	16	0	16	119.546 0 -9999 1.945	-9999 1.947	232.788					
16	32	0	35	2.171 0 -9999 2.339	-9999 1.730	3.755					
32	64	0	0	-9999 0 -9999 2.811	-9999 0	0					
64	128	0	0	-9999 0 -9999 3.378	-9999 0	0					
128	256	0	0	-9999 0 -9999 4.059	-9999 0	0					
TOTAL						89929.530					
OUTPUT 6/24/1997											
METHOD OF COMPUTATION		MODIFIED EINSTEIN		DATE OF COMPUTATION		1430		TEMPERATURE		71.06 SLOPE OF ENERGY GRADIENT 0.00011	
DATE OF SAMPLE	6/24/1997	TIME OF SAMPLE		D65 =	0.35 mm	D35 =	0.22 mm				
velocity (ft/s) =	2.85	width (ft) =	114	Depth (ft) =							
dn (ft) =	0.3	ds (ft) =	4.8								
SIZE FRACTION IN MILLIMETERS	PERCENT OF MATERIAL SUSPENDED BED	IBQB T/D	QPRIME SUBS(T/D)	Z-VALUES COMPUTED FITTED	COMPUTATIONAL FACTORS F(J) F(I)+1	COMPUTED TOTAL LOAD					
0.001	0.002	0	0	-9999 0 -9999 0.355	-9999 -9999	0					
0.002	0.004	0	0	-9999 0 -9999 0.447	-9999 -9999	0					
0.004	0.016	0	0	-9999 0 -9999 0.447	-9999 -9999	0					
0.016	0.0625	13	1	0.043 587.731 -9999 0.538	1.348 283.081	792.346					
0.0625	0.125	1	4	0.801 45.210 0.645 0.615	1.452 104.390	65.638					
0.125	0.25	23	37	20.946 1039.831 0.628 0.664	1.525 60.011	1586.113					
0.25	0.5	58	46	73.656 2622.183 0.640 0.699	1.571 39.638	4118.983					
0.5	1	5	7	19.231 226.050 0.796 0.724	1.582 28.616	550.298					
1	2	0	0	-9999 0 -9999 0.744	-9999 -9999	0					
2	4	0	1	0.170 0 -9999 0.762	-9999 16.399	2.779					
4	8	0	1	0.000 0 -9999 0.811	-9999 12.570	0.000					
8	16	0	3	0 0 -9999 0.799	-9999 9.607	0					
16	32	0	0	-9999 0 -9999 0.818	-9999 0	0					
32	64	0	0	-9999 0 -9999 0.837	-9999 0	0					
64	128	0	0	-9999 0 -9999 0.857	-9999 0	0					
128	256	0	0	-9999 0 -9999 0.877	-9999 0	0					
TOTAL						7116.158					

OUTPUT 5/18/1998											
METHOD OF COMPUTATION			MODIFIED EINSTEIN		DATE OF COMPUTATION		7/18/2006				
DATE OF SAMPLE		5/18/1998	TIME OF SAMPLE		1430	TEMPERATURE		60.8	SLOPE OF ENERGY GRADIENT		0.00011
D65 =	2 mm	D35 = 0.17 mm	velocity (ft/s) =	4.49 ft/s	width (ft) = 160	Depth (ft) = 4.8					
dn (ft) =	0.3	Ds (ft) = 4.8									
SIZE FRACTION IN MILLIMETERS	PERCENT OF MATERIAL SUSPENDED BED	IBQB T/D	QPRIME SUBS(T/D)	Z-VALUES COMPUTED FITTED	COMPUTATIONAL FACTORS F(j) F(i)+1	COMPUTED TOTAL LOAD					
0.001	0.002	41	0	-9999 3349.747 -9999 0.083	1.062 -9999	3558.289					
0.002	0.004	6	0	-9999 490.207 -9999 0.117	1.071 -9999	524.995					
0.004	0.016	5	0	-9999 651.609 -9999 0.138	1.076 -9999	716.218					
0.016	0.0625	16	2	-9999 1301.018 -9999 0.307	1.194 -978.833	1560.158					
0.0625	0.125	18	13	-9999 1470.62 -9999 0.661	1.483 -73.019	2381.099					
0.125	0.25	10	47	-9999 243.093 817.011 0.994	0.892 2.065	15.698	1687.505				
0.25	0.5	1	2	-9999 29.258 81.701 1.026	1.097 3.091	6.544	191.453				
0.5	1	0	0	-9999 0 -9999 1.255	-9999 -9999	0					
1	2	0	1	-9999 25.936 0 -9999 1.394	3.533 -9999	91.618					
2	4	0	1	-9999 18.152 0 -9999 1.531	-9999 3.071	55.746					
4	8	0	3	-9999 18.036 0 -9999 1.675	-9999 2.769	49.783					
8	16	0	8	-9999 2.543 0 -9999 1.829	-9999 2.510	6.406					
16	32	0	3	-9999 0 -9999 1.977	-9999 2.307	0.000					
32	64	0	20	-9999 0 -9999 2.181	-9999 2.102	0					
64	128	0	0	-9999 0 -9999 2.380	-9999 0						
128	256	0	0	-9999 0 -9999 2.598	-9999 0						
TOTAL						10624.470					
OUTPUT 4/7/1999											
METHOD OF COMPUTATION			MODIFIED EINSTEIN		DATE OF COMPUTATION		7/18/2006				
DATE OF SAMPLE		4/7/1999	TIME OF SAMPLE		1430	TEMPERATURE		51.8	SLOPE OF ENERGY GRADIENT		0.00011
D65 =	0.64 mm	D35 = 0.39 mm	velocity (ft/s) =	2.1 ft/s	width (ft) = 106	Depth (ft) = 2					
dn (ft) =	0.3	Ds (ft) = 4.8									
SIZE FRACTION IN MILLIMETERS	PERCENT OF MATERIAL SUSPENDED BED	IBQB T/D	QPRIME SUBS(T/D)	Z-VALUES COMPUTED FITTED	COMPUTATIONAL FACTORS F(j) F(i)+1	COMPUTED TOTAL LOAD					
0.001	0.002	0	0	-9999 0 -9999 0.000	-9999 -9999	0					
0.002	0.004	0	0	-9999 0 -9999 0.000	-9999 -9999	0					
0.004	0.016	0	0	-9999 0 -9999 0.000	-9999 -9999	0					
0.016	0.0625	44	0	-9999 47.551 -9999 0.004	1.047 -9999	49.804					
0.0625	0.125	1	0	-9999 1.081 -9999 0.056	1.058 -9999	1.144					
0.125	0.25	30	2	-9999 0.085 32.421 0.295	0.295 1.138	436.860	36.938				
0.25	0.5	25	51	-9999 27.017 0.403 0.963	0.963 2.037	10.819	66.496				
0.5	1	0	33	-9999 1.187 0 -9999 2.077	2.077 0.999	2.030	23.72				
1	2	0	8	-9999 1.863 0 -9999 3.685	3.685 -9999	1.444	2.690				
2	4	0	4	-9999 0.010 0 -9999 6.135	6.135 -9999	1.252	0.012				
4	8	0	0	-9999 0 -9999 9.969	-9999 -9999	0					
8	16	0	2	-9999 0 -9999 16.060	-9999 1.101	0					
16	32	0	0	-9999 0 -9999 25.793	-9999 0						
32	64	0	0	-9999 0 -9999 41.382	-9999 0						
64	128	0	0	-9999 0 -9999 66.366	-9999 0						
128	256	0	0	-9999 0 -9999 106.421	-9999 0						
TOTAL						180.355					
OUTPUT 5/21/1999											
METHOD OF COMPUTATION			MODIFIED EINSTEIN		DATE OF COMPUTATION		7/18/2006				
DATE OF SAMPLE		5/21/1999	TIME OF SAMPLE		1430	TEMPERATURE		69.8	SLOPE OF ENERGY GRADIENT		0.00011
D65 =	1.57 mm	D35 = 0.55 mm	velocity (ft/s) =	2.65 ft/s	width (ft) = 162	Depth (ft) = 5.2					
dn (ft) =	0.3	Ds (ft) = 4.8									
SIZE FRACTION IN MILLIMETERS	PERCENT OF MATERIAL SUSPENDED BED	IBQB T/D	QPRIME SUBS(T/D)	Z-VALUES COMPUTED FITTED	COMPUTATIONAL FACTORS F(j) F(i)+1	COMPUTED TOTAL LOAD					
0.001	0.002	23	0	-9999 1038.925 -9999 0.000	1.046 -9999	1086.742					
0.002	0.004	4	0	-9999 180.683 -9999 0.000	1.046 -9999	189.010					
0.004	0.016	10	0	-9999 451.006 -9999 0.003	1.047 -9999	472.201					
0.016	0.0625	44	0	-9999 197.739 -9999 0.030	1.052 -9999	2090.468					
0.0625	0.125	16	1	-9999 0.033 722.730 -9999	0.170 1.088	3931.462	786.258				
0.125	0.25	2	5	-9999 0.463 90.341 0.459	0.459 1.245	243.733	112.496				
0.25	0.5	1	26	-9999 6.816 45.171 0.899	0.899 2.088	14.840	101.153				
0.5	1	0	22	-9999 16.313 0 -9999 1.405	1.405 -9999	3.446	56.222				
1	2	0	17	-9999 32.592 0 -9999 1.998	1.998 -9999	2.038	66.435				
2	4	0	17	-9999 5.151 0 -9999 2.748	2.748 -9999	1.634	8.414				
4	8	0	15	-9999 0.001 0 -9999 3.735	3.735 -9999	1.443	0.001				
8	16	0	11	-9999 0 -9999 5.055	5.055 -9999	0.326	0				
16	32	0	3	-9999 0 -9999 6.832	6.832 -9999	1.246	0				
32	64	0	0	-9999 0 -9999 9.227	9.227 -9999	-9999	0				
64	128	0	0	-9999 0 -9999 12.460	12.460 -9999	-9999	0				
128	256	0	0	-9999 0 -9999 16.825	16.825 -9999	-9999	0				
TOTAL						4969.917					
OUTPUT 4/7/2000											
METHOD OF COMPUTATION			MODIFIED EINSTEIN		DATE OF COMPUTATION		7/18/2006				
DATE OF SAMPLE		4/7/2000	TIME OF SAMPLE		1430	TEMPERATURE		65	SLOPE OF ENERGY GRADIENT		0.00011
D65 =	0.84 mm	D35 = 0.49 mm	velocity (ft/s) =	2.14 ft/s	width (ft) = 104	Depth (ft) = 2					
dn (ft) =	0.3	Ds (ft) = 4.8									
SIZE FRACTION IN MILLIMETERS	PERCENT OF MATERIAL SUSPENDED BED	IBQB T/D	QPRIME SUBS(T/D)	Z-VALUES COMPUTED FITTED	COMPUTATIONAL FACTORS F(j) F(i)+1	COMPUTED TOTAL LOAD					
0.001	0.002	73	0	-9999 1159.302 -9999 0.000	1.046 -9999	1212.579					
0.002	0.004	15	0	-9999 238.213 -9999 0.001	1.046 -9999	249.193					
0.004	0.016	6	0	-9999 95.285 -9999 0.005	1.047 -9999	99.751					
0.016	0.0625	1	0	-9999 15.881 -9999 0.038	1.053 -9999	16.729					
0.0625	0.125	0	0	-9999 0 -9999 0.167	-9999 -9999	0					
0.125	0.25	1	3	-9999 0.078 15.881 0.377	0.377 1.191	222.688	18.907				
0.25	0.5	2	33	-9999 2.421 31.762 0.761	0.698 1.317	29.391	48.170				
0.5	1	2	39	-9999 8.093 31.762 0.761	0.761 1.024	2.036	64.12				
1	2	0	15	-9999 5.077 0 -9999 1.132	1.132 -9999	3.871	19.65				
2	4	0	6	-9999 0.054 0 -9999 1.809	1.809 -9999	2.590	0.139				
4	8	0	3	-9999 0 -9999 2.343	2.343 -9999	2.031	0				
8	16	0	1	-9999 0 -9999 3.023	3.023 -9999	1.720	0				
16	32	0	0	-9999 0 -9999 3.895	3.895 -9999	-9999	0				
32	64	0	0	-9999 0 -9999 5.017	5.017 -9999	-9999	0				
64	128	0	0	-9999 0 -9999 6.461	6.461 -9999	-9999	0				
128	256	0	0	-9999 0 -9999 8.319	8.319 -9999	-9999	0				
TOTAL						1729.834					

OUTPUT 5/3/2000											
METHOD OF COMPUTATION			MODIFIED EINSTEIN		DATE OF COMPUTATION		7/18/2006				
DATE OF SAMPLE		5/3/2000	TIME OF SAMPLE		1430	TEMPERATURE		77	SLOPE OF ENERGY GRADIENT		
D ₆₅ =	0.85	mm	D ₃₅ =	0.41	mm	velocity (ft/s) =	1.92	width (ft) =	109	Depth (ft) =	1.7
D _n (ft) =	0.3	ds (ft) =	4.8							0.00011	
SIZE FRACTION IN MILLIMETERS	PERCENT OF MATERIAL SUSPENDED BED	IBQB T/D	QPRIME SUBS(T/D)	Z-VALUES COMPUTED FITTED	COMPUTATIONAL FACTORS F(J) F(I)+1	COMPUTED TOTAL LOAD					
0.001	0.002	0	-9999	0	-9999 0.000	-9999 -9999	0				
0.002	0.004	0	-9999	0	-9999 0.001	-9999 -9999	0				
0.004	0.016	0	-9999	0	-9999 0.005	-9999 -9999	0				
0.016	0.0625	55	0	-9999 37,886	-9999 0.122	1.054 -9999	39.917				
0.0625	0.125	13	1	0.010 8,955	0.219 0.211	1.101 1100.593	9.857				
0.125	0.25	18	5	0.135 12,399	0.477 0.523	1.295 88.391	16.053				
0.25	0.5	14	40	3.054 9,644	1.012 0.957	2.143 10.041	30.666				
0.5	1	0	25	5.399 0	-9999 1.435	-9999 3.451	18.629				
1	2	0	11	1.776 0	-9999 1.985	-9999 2.206	3.918				
2	4	0	7	0.004 0	-9999 2.668	-9999 1.763	0.006				
4	8	0	6	0	-9999 4.550	-9999 1.175	0				
8	16	0	5	0	-9999 4.155	-9999 1.300	0				
16	32	0	0	-9999 0	-9999 6.230	-9999 -9999	0				
32	64	0	0	-9999 0	-9999 8.244	-9999 -9999	0				
64	128	0	0	-9999 0	-9999 10.908	-9999 -9999	0				
128	256	0	0	-9999 0	-9999 14.433	-9999 -9999	0				
TOTAL						119.047					
OUTPUT 4/21/2001											
METHOD OF COMPUTATION			MODIFIED EINSTEIN		DATE OF COMPUTATION		7/18/2006				
DATE OF SAMPLE		4/21/2001	TIME OF SAMPLE		1430	TEMPERATURE		59.9	SLOPE OF ENERGY GRADIENT		
D ₆₅ =	0.71	mm	D ₃₅ =	0.4	mm	velocity (ft/s) =	2.27	width (ft) =	162	Depth (ft) =	1.9
D _n (ft) =	0.3	ds (ft) =	4.8							0.00011	
SIZE FRACTION IN MILLIMETERS	PERCENT OF MATERIAL SUSPENDED BED	IBQB T/D	QPRIME SUBS(T/D)	Z-VALUES COMPUTED FITTED	COMPUTATIONAL FACTORS F(J) F(I)+1	COMPUTED TOTAL LOAD					
0.001	0.002	0	-9999	0	-9999 0.000	-9999 -9999	0				
0.002	0.004	0	-9999	0	-9999 0.001	-9999 -9999	0				
0.004	0.016	0	-9999	0	-9999 0.003	-9999 -9999	0				
0.016	0.0625	37	0	-9999 137,835	-9999 0.030	1.052 -9999	145.011				
0.0625	0.125	3	0	-9999 11,176	-9999 0.17	1.046 -9999	12.116				
0.125	0.25	27	6	0.655 100,582	0.417 0.417	1.110 180.818	121.22				
0.25	0.5	33	42	12,971 122,934	0.820 0.820	1.767 17.750	230.225				
0.5	1	0	21	18,343 0	-9999 1.276	-9999 4.641	85.131				
1	2	0	6	4,557 0	-9999 1.796	-9999 2.574	11.732				
2	4	0	5	0.200 0	-9999 2.437	-9999 1.934	0.387				
4	8	0	6	0.000 0	-9999 3.264	-9999 1.632	0.000				
8	16	0	8	0	-9999 4.353	-9999 1.451	0				
16	32	0	6	0	-9999 5.795	-9999 1.324	0				
32	64	0	0	-9999 0	-9999 7.849	-9999 -9999	0				
64	128	0	0	-9999 0	-9999 10.258	-9999 -9999	0				
128	256	0	0	-9999 0	-9999 13.645	-9999 -9999	0				
TOTAL						606.335					
OUTPUT 5/22/2001											
METHOD OF COMPUTATION			MODIFIED EINSTEIN		DATE OF COMPUTATION		7/18/2006				
DATE OF SAMPLE		5/22/2001	TIME OF SAMPLE		1430	TEMPERATURE		72.5	SLOPE OF ENERGY GRADIENT		
D ₆₅ =	1.17	mm	D ₃₅ =	0.41	mm	velocity (ft/s) =	2.41	width (ft) =	164	Depth (ft) =	3.6
D _n (ft) =	0.3	ds (ft) =	4.8							0.00011	
SIZE FRACTION IN MILLIMETERS	PERCENT OF MATERIAL SUSPENDED BED	IBQB T/D	QPRIME SUBS(T/D)	Z-VALUES COMPUTED FITTED	COMPUTATIONAL FACTORS F(J) F(I)+1	COMPUTED TOTAL LOAD					
0.001	0.002	58	0	-9999 1352,311	-9999 0.001	1.046 -9999	1414.764				
0.002	0.004	8	0	-9999 186,526	-9999 0.002	1.046 -9999	195.191				
0.004	0.016	9	0	-9999 209,841	-9999 0.010	1.048 -9999	219.897				
0.016	0.0625	15	1	0.010 349,736	-9999 0.069	1.060 17895.94	370.806				
0.0625	0.125	6	3	0.143 139,894	0.287 0.279	1.131 1174.85	158.197				
0.125	0.25	3	8	1.101 69,947	0.412 0.412	1.120 70,795	66.357				
0.25	0.5	1	32	12,226 23,316	1.099 1.059	2.818 7.848	95.888				
0.5	1	0	19	20,531 0	-9999 1.512	-9999 3.041	62.445				
1	2	0	0	-9999 0	-9999 2.007	-9999 -9999	0				
2	4	0	0	-9999 0	-9999 2.594	-9999 -9999	0				
4	8	0	0	-9999 0	-9999 3.323	-9999 -9999	0				
8	16	0	0	-9999 0	-9999 4.243	-9999 -9999	0				
16	32	0	0	-9999 0	-9999 5.411	-9999 -9999	0				
32	64	0	0	-9999 0	-9999 6.897	-9999 -9999	0				
64	128	0	0	-9999 0	-9999 8.790	-9999 -9999	0				
128	256	0	0	-9999 0	-9999 11.203	-9999 -9999	0				
TOTAL						2616.733					
OUTPUT 6/20/2001											
METHOD OF COMPUTATION			MODIFIED EINSTEIN		DATE OF COMPUTATION		7/18/2006				
DATE OF SAMPLE		6/20/2001	TIME OF SAMPLE		1430	TEMPERATURE		51.44	SLOPE OF ENERGY GRADIENT		
D ₆₅ =	0.76	mm	D ₃₅ =	0.38	mm	velocity (ft/s) =	1.78	width (ft) =	92	Depth (ft) =	1.8
D _n (ft) =	0.3	ds (ft) =	4.8							0.00011	
SIZE FRACTION IN MILLIMETERS	PERCENT OF MATERIAL SUSPENDED BED	IBQB T/D	QPRIME SUBS(T/D)	Z-VALUES COMPUTED FITTED	COMPUTATIONAL FACTORS F(J) F(I)+1	COMPUTED TOTAL LOAD					
0.001	0.002	0	-9999	0	-9999 0.002	-9999 -9999	0				
0.002	0.004	0	-9999	0	-9999 0.005	-9999 -9999	0				
0.004	0.016	0	-9999	0	-9999 0.018	-9999 -9999	0				
0.016	0.0625	65	0	-9999 45,125	-9999 0.086	1.064 -9999	48.035				
0.0625	0.125	4	1	0.005 2,777	0.304 0.273	1.128 752.016	3.132				
0.125	0.25	24	8	0.120 16,662	0.425 0.548	1.327 81,758	22.113				
0.25	0.5	7	42	1.776 4,860	1.045 0.901	1.984 12,825	22.774				
0.5	1	0	23	2,750 0	-9999 1.242	-9999 4.913	13.512				
1	2	0	11	0.546 0	-9999 1.503	-9999 3.391	1.691				
2	4	0	6	0.000 0	-9999 1.959	-9999 0.000					
4	8	0	5	0	-9999 2.401	-9999 2.014	0				
8	16	0	4	0	-9999 2.932	-9999 1.768	0				
16	32	0	0	-9999 3.576	-9999 0	-9999 0	0				
32	64	0	0	-9999 4.359	-9999 0	-9999 0	0				
64	128	0	0	-9999 5.313	-9999 0	-9999 0	0				
128	256	0	0	-9999 6.474	-9999 0	-9999 0	0				
TOTAL						111.258					
5/7/2002, 5/7/2002, -9999, FITTED Z-VALUES GENERATED NEGATIVE EXPONENT, NOT CONTINUING... 4/3/2003, 4/3/2003, -9999, FITTED Z-VALUES GENERATED NEGATIVE EXPONENT, NOT CONTINUING...											

OUTPUT 5/12/2003									
METHOD OF COMPUTATION		MODIFIED EINSTEIN		DATE OF COMPUTATION		7/18/2006			
DATE OF SAMPLE		5/12/2003		TIME OF SAMPLE		1430		TEMPERATURE	
$D_{65} = 0.39$ mm		$D_{35} = 0.27$ mm							
velocity (ft/s) = 1.58		width (ft) = 137		Depth (ft) = 0.99					
D_n (ft) = 0.3		D_s (ft) = 4.8							
SIZE FRACTION IN MILLIMETERS									
PERCENT OF MATERIAL SUSPENDED BED		IBQB		QPRIME SUBS(T/D)		Z-VALUES COMPUTED FITTED		COMPUTATIONAL FACTORS F(J) F(I)+1	
T/D									
0.001	0.002	0	0	-9999	0	-9999	0.002	-9999	-9999
0.002	0.004	0	0	-9999	0	-9999	0.025	-9999	-9999
0.004	0.016	0	0	-9999	0	-9999	0.075	-9999	-9999
0.016	0.0625	95	0	-9999	123,249	-9999	0.124	1.075	-9999
0.0625	0.125	1	1	0.011	1,297	0.459	0.457	1,242	148,179
0.125	0.25	3	27	0.844	3,892	0.950	0.957	2,199	10,733
0.25	0.5	1	59	5,218	1,297	1.578	1.571	7,567	3,012
0.5	1	0	12	2,520	0	-9999	2,185	-9999	2,036
1	2	0	1	0.010	0	-9999	2,843	-9999	1,716
2	4	0	0	-9999	0	-9999	3,609	-9999	0
4	8	0	0	-9999	0	-9999	4,153	-9999	0
8	16	0	0	-9999	0	-9999	5,701	-9999	0
16	32	0	0	-9999	0	-9999	7,146	-9999	0
32	64	0	0	-9999	0	-9999	8,955	-9999	0
64	128	0	0	-9999	0	-9999	11,220	-9999	0
128	256	0	0	-9999	0	-9999	14,057	-9999	0
TOTAL									
163.482									
OUTPUT 6/6/2003									
METHOD OF COMPUTATION		MODIFIED EINSTEIN		DATE OF COMPUTATION		7/18/2006			
DATE OF SAMPLE		6/6/2003		TIME OF SAMPLE		1430		TEMPERATURE	
$D_{65} = 0.47$ mm		$D_{35} = 0.33$ mm							
velocity (ft/s) = 1.7		width (ft) = 107		Depth (ft) = 1.3					
D_n (ft) = 0.3		D_s (ft) = 4.8							
SIZE FRACTION IN MILLIMETERS									
PERCENT OF MATERIAL SUSPENDED BED		IBQB		QPRIME SUBS(T/D)		Z-VALUES COMPUTED FITTED		COMPUTATIONAL FACTORS F(J) F(I)+1	
T/D									
0.001	0.002	76	0	-9999	285,977	-9999	0.004	1,047	-9999
0.002	0.004	13	0	-9999	48,917	-9999	0.008	1,048	-9999
0.004	0.016	6	0	-9999	22,577	-9999	0.025	1,051	-9999
0.016	0.0625	0	0	-9999	0	-9999	0.111	-9999	0
0.0625	0.125	1	2	0.013	3,763	0.357	0.334	1,159	391,959
0.125	0.25	2	7	0.130	7,526	0.516	0.444	1,472	15,862
0.25	0.5	2	62	3,558	7,526	1,086	0.983	2,216	0,577
0.5	1	0	22	3,570	0	-9999	1,311	-9999	4,435
1	2	0	5	0.122	0	-9999	1,643	-9999	3,009
2	4	0	2	0.000	0	-9999	2,011	-9999	2,383
4	8	0	0	-9999	0	-9999	2,443	-9999	0
8	16	0	0	-9999	0	-9999	2,959	-9999	0
16	32	0	0	-9999	0	-9999	3,580	-9999	0
32	64	0	0	-9999	0	-9999	4,329	-9999	0
64	128	0	0	-9999	0	-9999	5,235	-9999	0
128	256	0	0	-9999	0	-9999	6,331	-9999	0
TOTAL									
435.678									
OUTPUT 4/15/2004									
METHOD OF COMPUTATION		MODIFIED EINSTEIN		DATE OF COMPUTATION		7/18/2006			
DATE OF SAMPLE		4/15/2004		TIME OF SAMPLE		1430		TEMPERATURE	
$D_{65} = 0.4$ mm		$D_{35} = 0.28$ mm							
velocity (ft/s) = 4.72		width (ft) = 162		Depth (ft) = 2.5					
D_n (ft) = 0.3		D_s (ft) = 4.8							
SIZE FRACTION IN MILLIMETERS									
PERCENT OF MATERIAL SUSPENDED BED		IBQB		QPRIME SUBS(T/D)		Z-VALUES COMPUTED FITTED		COMPUTATIONAL FACTORS F(J) F(I)+1	
T/D									
0.001	0.002	53	0	-9999	12,773,28	-9999	0.013	1,050	-9999
0.002	0.004	8	0	-9999	1928,042	-9999	0.023	1,053	-9999
0.004	0.016	7	0	-9999	1687,037	-9999	0.056	1,060	-9999
0.016	0.0625	8	0	-9999	1928,042	-9999	0.177	1,094	-9999
0.0625	0.125	2	2	1,906	482,011	0.436	0.411	1,217	373,107
0.125	0.25	16	24	64,698	482,011	0.436	0.411	1,217	586,780
0.25	0.5	6	58	4,646,636	1446,032	0.586	0.674	5,298	5895,014
0.5	1	0	13	276,625	0	-9999	1,131	-9999	6,132
1	2	0	1	22,625	0	-9999	1,404	-9999	4,161
2	4	0	1	14,554	0	-9999	1,640	-9999	3,277
4	8	0	0	-9999	0	-9999	1,903	-9999	0
8	16	0	1	0.117	0	-9999	2,204	-9999	2,317
16	32	0	0	-9999	0	-9999	2,549	-9999	0
32	64	0	0	-9999	0	-9999	2,949	-9999	0
64	128	0	0	-9999	0	-9999	3,410	-9999	0
128	256	0	0	-9999	0	-9999	3,943	-9999	0
TOTAL									
33308.270									
OUTPUT 5/24/2004									
METHOD OF COMPUTATION		MODIFIED EINSTEIN		DATE OF COMPUTATION		7/18/2006			
DATE OF SAMPLE		5/24/2004		TIME OF SAMPLE		1430		TEMPERATURE	
$D_{65} = 0.78$ mm		$D_{35} = 0.43$ mm							
velocity (ft/s) = 2.56		width (ft) = 158		Depth (ft) = 4					
D_n (ft) = 0.3		D_s (ft) = 4.8							
SIZE FRACTION IN MILLIMETERS									
PERCENT OF MATERIAL SUSPENDED BED		IBQB		QPRIME SUBS(T/D)		Z-VALUES COMPUTED FITTED		COMPUTATIONAL FACTORS F(J) F(I)+1	
T/D									
0.001	0.002	0	0	-9999	0	-9999	0.000	-9999	0
0.002	0.004	0	0	-9999	0	-9999	0.000	-9999	0
0.004	0.016	0	0	-9999	0	-9999	0.002	-9999	0
0.016	0.0625	51	0	-9999	2342,864	-9999	0.019	1,051	-9999
0.0625	0.125	2	0	-9999	91,877	-9999	0.099	1,070	-9999
0.125	0.25	9	4	0.478	413,447	0.258	0.261	1,126	951,376
0.25	0.5	33	40	13,532	1515,971	0.475	0.502	1,289	121,236
0.5	1	4	33	31,577	183,754	0.919	0.773	1,683	23,297
1	2	1	10	11,078	45,939	0.978	1,087	2,607	7,435
2	4	0	6	0.622	0	-9999	1,479	-9999	3,659
4	8	0	4	0.000	0	-9999	1,983	-9999	2,466
8	16	0	3	0	0	-9999	2,560	-9999	1,927
16	32	0	0	-9999	0	-9999	3,556	-9999	0
32	64	0	0	-9999	0	-9999	4,750	-9999	0
64	128	0	0	-9999	0	-9999	6,344	-9999	0
128	256	0	0	-9999	0	-9999	8,472	-9999	0
TOTAL									

Appendix G –

HEC-RAS Sediment Transport Application Limits

The information presented in the pages below was taken from HEC-RAS v. 3.1.3 (USACE 2005).

Ackers-White (flume):

$$\begin{aligned} 0.04 < d < 7 \text{ mm} \quad 1.0 < s < 2.7 \\ 0.07 < V < 7.1 \text{ fps} \quad 0.01 < D < 1.4 \text{ ft} \\ 0.00006 < S < 0.037 \quad 0.23 < W < 4.0 \text{ ft} \\ 46 < T < 89 \text{ degrees F} \end{aligned}$$

A total load function developed under the assumption that fine sediment transport is best related to the turbulent fluctuations in the water column and coarse sediment transport is best related to the net grain shear with the mean velocity used as the representative variable. The transport function was developed in terms of particle size, mobility and transport. A dimensionless size parameter is used to distinguish between the fine, transitionary, and coarse sediment sizes. Under typical conditions, fine sediments are silts less than 0.04 mm, and coarse sediments are sands greater than 2.5 mm. Since the relationships developed by Ackers-White are applicable only to non-cohesive sands, greater than 0.04 mm, only transitionary and coarse sediments apply. Experiments were conducted with coarse grains up to 4 mm. This function is based on over 1000 flume experiments using uniform or near-uniform sediments with flume depths of up to 1.4 m. A range of bed configurations was used, including plane, rippled, and dune forms, however the equations do not apply to upper phase transport (e.g. anti-dunes) with Froude numbers in excess of 0.8. A hiding adjustment factor was developed for the Ackers-White method by Profitt and Sutherland (1983), and is included in RAS as an option. The hiding factor is an adjustment to include the effects of a masking of the fluid properties felt by smaller particles due to shielding by larger particles. This is typically a factor when the gradation has a relatively large range of particle sizes and would tend to reduce the rate of sediment transport in the smaller grade classes.

Engelund-Hansen (flume):

$$\begin{aligned} 0.19 < dm < 0.93 \text{ mm} \quad 0.65 < V < 6.34 \\ 0.19 < D < 1.33 \text{ fps} \quad 0.000055 < S < 0.019 \text{ ft} \\ 45 < T < 93 \text{ degrees F} \end{aligned}$$

A total load predictor, which gives adequate results for sandy rivers with substantial suspended load. It is based on flume data with sediment sizes between 0.19 and 0.93 mm. It has been extensively tested, and found to be fairly consistent with field data.

Laursen (Copeland) (field):

$$\begin{aligned}0.08 < d_m < 0.7 \text{ mm} \quad 0.068 < V < 7.8 \text{ fps} \\0.67 < D < 54 \text{ ft} \quad 0.0000021 < S < 0.0018 \\63 < W < 3640 \text{ ft} \quad 32 < T < 93 \text{ degrees F}\end{aligned}$$

Laursen (Copeland) (flume):

$$\begin{aligned}0.011 < d_m < 29 \text{ mm} \quad 0.7 < V < 9.4 \text{ fps} \\0.03 < D < 3.6 \text{ ft} \quad 0.00025 < S < 0.025 \\0.25 < W < 6.6 \text{ ft} \quad 46 < T < 83 \text{ degrees F}\end{aligned}$$

A total sediment load predictor, derived from a combination of qualitative analysis, original experiments and supplementary data. Transport of sediments is primarily defined based on the hydraulic characteristics of mean channel velocity, depth of flow and energy gradient, and on the sediment characteristics of gradation and fall velocity. Contributions by Copeland (Copeland, 1989) extend the range of applicability to gravel-sized sediments. The overall range of applicability is 0.011 to 29 mm.

MPM. Meyer-Peter Muller (flume):

$$\begin{aligned}0.4 < d < 29 \text{ mm} \quad 1.25 < s < 4.0 \\1.2 < V < 9.4 \text{ fps} \quad 0.03 < D < 3.9 \text{ ft} \\0.0004 < S < 0.02 \quad 0.5 < W < 6.6 \text{ ft}\end{aligned}$$

BED LOAD ONLY! A bed load transport function based primarily on experimental data. It has been extensively tested and used for rivers with relatively coarse sediment. The transport rate is proportional to the difference between the mean shear stress acting on the grain and the critical shear stress. Applicable particle sizes range from 0.4 to 29 mm with a sediment specific gravity range of 1.25 to in excess of 4.0. This method can be used for well-graded sediments and flow conditions that produce other-than-plane bed forms. The Darcy-Weisbach friction factor is used to define bed resistance. Results may be questionable near the threshold of incipient motion for sand bed channels as demonstrated by Amin and Murphy (1981).

Toffaleti (field):

$0.062 < d < 4 \text{ mm}$ $0.095 < dm < 0.76 \text{ mm}$
 $0.7 < V < 7.8 \text{ fps}$ $0.07 < R < 56.7 \text{ ft}$
 $0.000002 < S < 0.0011$ $63 < W < 3640 \text{ ft}$
 $40 < T < 93 \text{ degrees F}$

Toffaleti (flume):

$0.062 < d < 4 \text{ mm}$ $0.45 < dm < 0.91 \text{ mm}$
 $0.7 < V < 6.3 \text{ fps}$ $0.07 < R < 1.1 \text{ ft}$
 $0.00014 < S < 0.019$ $0.8 < W < 8 \text{ ft}$
 $32 < T < 94 \text{ degrees F}$

A modified-Einstein total load function that breaks the suspended load distribution into vertical zones, replicating two-dimensional sediment movement. Four zones are used to define the sediment distribution. They are the upper zone, the middle zone, the lower zone and the bed zone. Sediment transport is calculated independently for each zone and the summed to arrive at total sediment transport. This method was developed using an exhaustive collection of both flume and field data. The flume experiments used sediment particles with mean diameters ranging from 0.45 to 0.91 mm, however successful applications of the Toffaleti method suggests that mean particle diameters as low as 0.095 mm are acceptable.

Yang (field, sand):

$0.15 < d < 1.7 \text{ mm}$ $0.8 < V < 6.4 \text{ fps}$
 $0.04 < D < 50 \text{ ft}$ $0.000043 < S < 0.028$
 $0.44 < W < 1750$ $32 < T < 94 \text{ degrees F}$

A total load function developed under the premise that unit stream power is the dominant factor in the determination of total sediment concentration. The research is supported by data obtained in both flume experiments and field data under a wide range conditions found in alluvial channels. Principally, the sediment size range is between 0.062 and 7.0 mm with total sediment concentration ranging from 10 ppm to 585,000 ppm. Yang (1984) expanded the applicability of his function to include gravel-sized sediments.